CSIRO PUBLISHING

Invertebrate Systematics, 2012, **26**, 115–192
http://dx.doi.org/10.1071/IS11027

Explosive radiation of the genus *Schizopera* on a small subterranean island in Western Australia (Copepoda : Harpacticoida): unravelling the cases of cryptic speciation, size differentiation and multiple invasions

Tomislav Karanovic[A,C] *and Steven J. B. Cooper*[B]

[A]Department of Life Sciences, Hanyang University, Seoul 133-791, South Korea.
[B]Evolutionary Biology Unit, South Australian Museum, North Terrace, Adelaide, SA 5000; and Australian Centre for Evolutionary Biology and Biodiversity, The University of Adelaide, Adelaide, SA 5005, Australia.
[C]Corresponding author. Email: tomislav.karanovic@utas.edu.au

Abstract. A previously unsurveyed calcrete aquifer in the Yilgarn region of Western Australia revealed an unprecedented diversity of copepods, representing 67% of that previously recorded in this whole region. Especially diverse was the genus *Schizopera*, with up to four morphospecies per bore and a significant size difference between them. Aims of this study were to: (1) survey the extent of this diversity using morphological and molecular tools; (2) derive a molecular phylogeny based on *COI*; and (3) investigate whether high diversity is a result of an explosive radiation, repeated colonisations, or both, size differentiation is a result of parallel evolution or different phylogeny, and whether *Schizopera* is a recent invasion in inland waters. More than 300 samples were analysed and the *COI* fragment successfully amplified by PCR from 43 specimens. Seven species and one subspecies are described as new, and three possible cryptic species were detected. Reconstructed phylogenies reveal that both explosive radiation and multiple colonisations are responsible for this richness, and that *Schizopera* is probably a recent invasion in these habitats. No evidence for parallel evolution was found, interspecific size differentiation being a result of different phylogeny. Sister species have parapatric distributions and show niche partitioning in the area of overlap.

Received 22 June 2011, accepted 2 February 2012, published online 6 August 2012

Introduction

Subterranean waters of Western Australia are becoming known as a significant hot spot for faunal diversity on a global scale (Humphreys 2008; Guzik *et al*. 2011*a*). Arid Western Australia is famous for numerous isolated calcrete aquifers that lie along palaeodrainage channels, and range in diameter from hundreds of metres to tens of kilometres (Humphreys 2001, 2006). Highly porous and carbonate-rich sediments here represent an ideal habitat for various groups of stygofauna (aquatic subterranean fauna), including dytiscid beetles (Watts and Humphreys 2006, 2009; and references therein), amphipods (Finston *et al*. 2007; King *et al*. 2012), isopods (Wilson 2008), bathynellids (Cho *et al*. 2006*a*, 2006*b*), ostracods (Karanovic 2007) and copepods (Karanovic 2004, 2006). Previous genetic and morphological studies suggest that individual calcretes are equivalent to closed island habitats, which have been isolated for millions of years (Cooper *et al*. 2008). The majority of stygobitic species evolved within individual calcretes following independent colonisation by epigean ancestors (Cooper *et al*. 2002, 2007, 2008; Leys *et al*. 2003; Guzik *et al*. 2008; Leys and Watts 2008). Phylogeographic studies of dytiscid beetles (Cooper *et al*. 2002; Leys *et al*. 2003), amphipods (Cooper *et al*. 2007; Bradford *et al*. 2010), isopods (Cooper *et al*. 2008) and bathynellids (Guzik *et al*. 2008) have confirmed the presence of monophyletic groups restricted to single calcretes. The diversity of stygofauna is mostly dependent on the size of the calcrete, and typically includes one to three species from each major group, most of them endemic to that site (Karanovic 2004, 2006, 2007; Finston *et al*. 2007; Leys and Watts 2008). An example of a typical Yilgarn calcrete is that at Sturt Meadows, where multiple studies from a very dense grid of bores (115 bore holes in an area of 3.5 km^2) revealed only two copepod species, one cyclopoid and one harpacticoid (Allford *et al*. 2008; Bradford *et al*. 2010).

In Western Australia it is necessary for any new development that potentially impacts on groundwater to be preceded by biological surveys of groundwater biodiversity (Eberhard *et al*. 2005, 2009). Motivated by the need to assess the likely environmental impacts of economically important natural resources development projects on stygofauna, in the past couple of years many private environmental consulting agencies, as well as individuals from several academic institutions, have collected here and most of the copepod material was entrusted to the senior author for identification. Recent investigations of one of the larger calcretes (~40 km long)

near Yeelirrie pastoral station (Figs 1, 2), in the uppermost reaches of the Carey palaeochannel in the Yilgarn region, revealed an unprecedented diversity of these crustaceans. Using morphological methods we were able to distinguish 21 different species and subspecies from six copepod families, 20 of them stygobionts. This represents 67% of previously recorded copepod diversity in the whole Yilgarn region, and this region was relatively well surveyed (Karanovic 2004). Especially diverse in this newly explored calcrete was the harpacticoid genus *Schizopera* Sars, 1905, which is the subject of this study, with up to four morphospecies per single bore (sampling locality), and normally with at least two. This very high diversity posed a couple of challenges and raised a few questions. First of all, the number of previously known members of this genus from the whole Yilgarn region was five, and they were all allopatric species, restricted to a single calcrete or a group of neighbouring calcretes (Karanovic 2004). This would imply that it is more likely that we are dealing here with a case of an explosive radiation than with repeated colonisations, as the surrounding areas do not have enough diversity to support many different invasions, and all previously known species seemed to be closely related (a notion also reinforced by their allopatric distribution). Investigating the likelihood of these two hypotheses as an explanation for the high species diversity in the Yeelirrie calcrete became one of the primary goals of our study. To do this, we investigated the extent of this diversity and precise species distributions by sampling very intensively in the Yeelirrie area. Employing molecular techniques in addition to traditional morphological ones was also one of the priorities to aid in species delineation and reconstruction of their phylogenetic relationships. Recently, DNA-based species identification methods, referred to as 'DNA barcoding', have been widely employed to estimate levels of species diversity, with the 5′ end of the mitochondrial cytochrome C oxidase subunit 1 (*COI*) gene proposed as the 'barcode' for all animal species (Hebert *et al*. 2003). The advantage of *COI* is that it often shows low levels of genetic variation within species, but high levels of divergence (usually >15% among crustacean species, Lefébure *et al*. 2006) between species. The availability of so-called 'universal' primers developed by Folmer *et al*. (1994) for

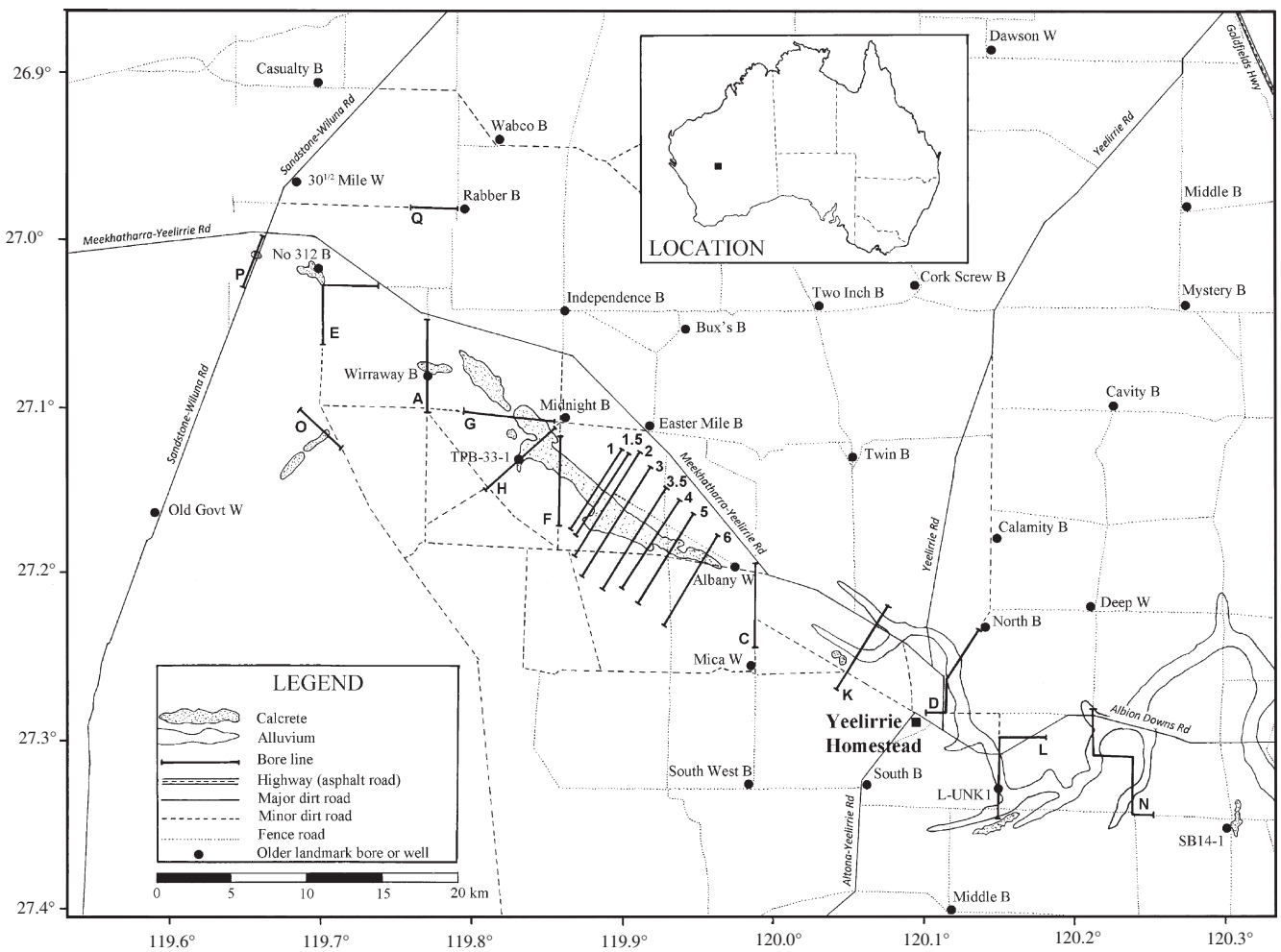

Fig. 1. Map of the area investigated, showing only some of the sampling localities (bores and wells). All other sampling bores lie on the following 21 bore lines (from north-west to south-east): P, Q, O, E, A, G, H, F, 1, 1.5, 2, 3, 3.5, 4, 5, 6, C, K, D, L and N. The water flow in the palaeochannel is also in this direction. Inset shows location of the area in Australia.

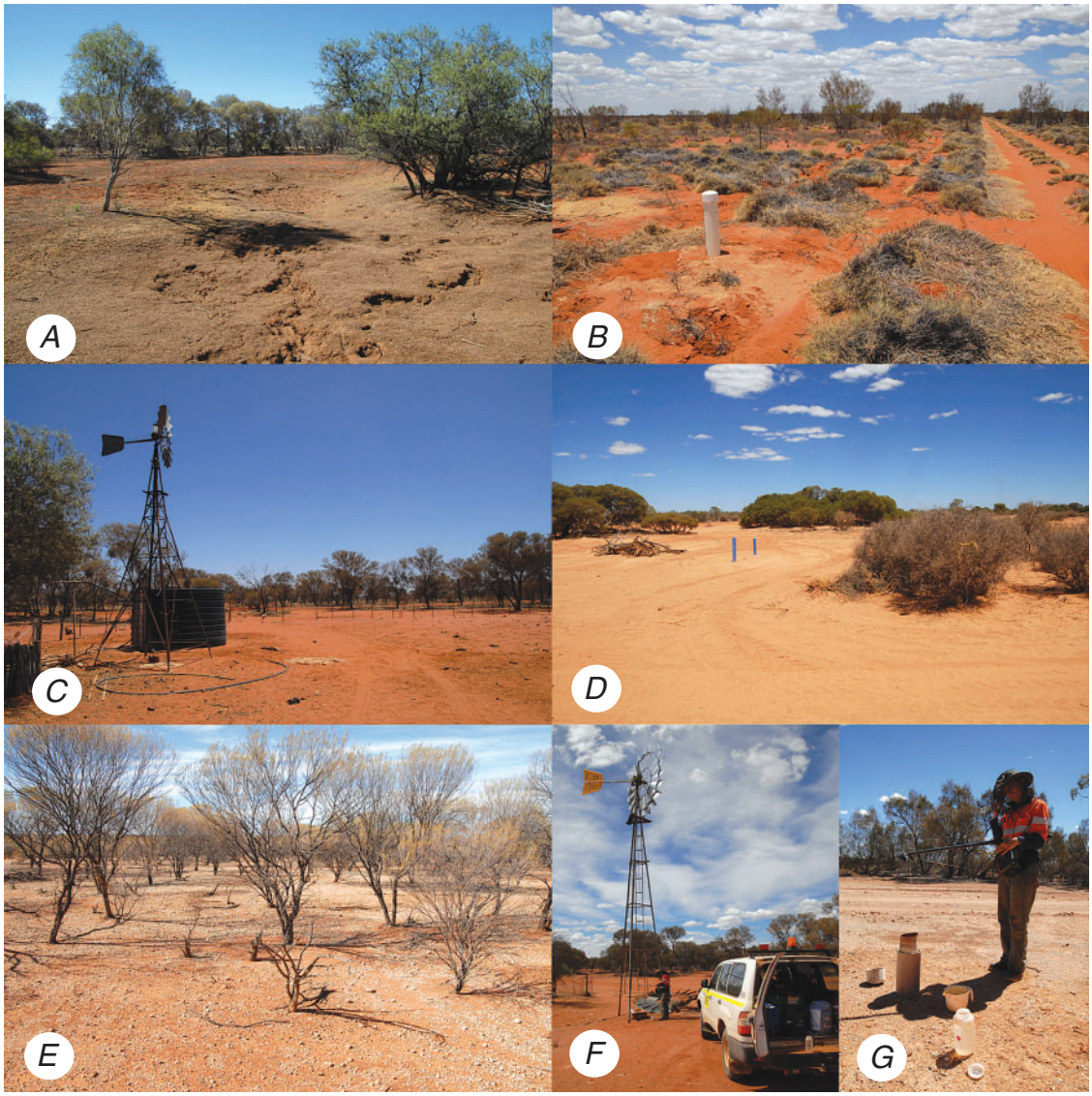

Fig. 2. Selection of different habitats and sampling localities in the Yeelirrie area: (*A*) clay sediments near bore No. 312, on line E. (*B*) Bore specifically made for sampling troglofauna (not stygofauna) on line Q. (*C*) Old pastoral well with a windmill on line L. (*D*) Two bores specifically made for sampling stygofauna on line 2. (*E*) Exposed calcrete sediments on line O. (*F*) Sampling at Wirraway Bore, on line A. (*G*) Sampling at bore YU1, on line F.

PCR amplification of *COI* also greatly facilitates the use of this marker to investigate species boundaries in animals, and these primers have previously been employed successfully to PCR-amplify copepod DNA (Adamowicz *et al*. 2007; Bradford *et al*. 2010; Sakaguchi and Ueda 2010).

Another interesting initial discovery was that most *Schizopera* morphospecies, when found together, significantly differed in size. This is a phenomenon well known in these habitats for diving beetles, where the fauna of a single calcrete typically consists of three species of very different sizes, with 13 cases of sympatric sister species pairs being reported in different calcretes (Leys *et al*. 2003; Leys and Watts 2008). Even sympatric speciation was considered at one stage as a possible explanation (Cooper *et al*. 2002, 2008; Leys *et al*. 2003; Bradford *et al*. 2010); however, evidence for considerable population structuring within calcretes makes it difficult to rule out parapatric or allopatric modes of speciation (Guzik *et al*. 2009, 2011*b*). Although theoretical work suggests that speciation can occur despite initially high gene flow, empirical evidence for sympatric (Savolainen *et al*. 2006; Ryan *et al*. 2007) or parapatric (Foster *et al*. 2007; Quesada *et al*. 2007) speciation remains thin (Berner *et al*. 2009). A possibility that we are dealing with either of the two models in this calcrete made a further investigation of the *Schizopera* species a priority. In copepods, the only well-documented case of closely related sympatric species in subterranean environments with a significant body size difference was that of four *Diacyclops* Kiefer, 1927, congeners in the Pilbara region, where sometimes two species were found together (Karanovic 2006), but never three or four. However, this case was never tested using molecular methods, so many aspects remained elusive.

The presence of at least three different size classes of *Schizopera* in the investigated area, and with at least two morphospecies in each size class, suggested a possibility of interspecific size differentiation as a main evolutionary mechanism here, as well as parallel evolution of similar traits (size in this case). Body size considerably determines many aspects of life history, such as energy balance, resource utilisation, competition, dispersal and reproduction rates (Kubota and Sota 1998; Sota *et al*. 2000; Leyequién *et al*. 2007). Differences among similar species whose distributions overlap geographically are normally accentuated in areas where the species live sympatrically, but are minimised or lost in areas where their distributions do not overlap (Brown and Wilson 1956). This has been considered an important phenomenon in speciation (Mayr 1963, 2001; Nagel and Schluter 1998; Berner *et al*. 2009). The process is driven by competition for limited resources (Bolnick and Fitzpatrick 2007), and in subterranean interstitial environments, size differentiation would enable different closely related species to explore and utilise voids of different size, thus avoiding competition (Gibert *et al*. 1994; Culver and Pipan 2009). The process often results in parallel speciation (Rundle *et al*. 2000). To investigate whether our *Schizopera* ecomorphs are a result of parallel evolution or different phylogeny (and thus colonisation history), we examined all morphospecies from this calcrete for mitochondrial DNA haplotypes. For phylogeny to have a significant influence, populations of the same ecomorph must be more closely related to each other than to populations of different ecomorphs (Rundle *et al*. 2000).

The genus *Schizopera* was established by Sars (1905), with *S. longicauda* Sars, 1905 as the type species. Subsequently, many new species have been described, but a great number of the descriptions are incomplete and/or inadequate, even nearly 100 years after Sars's time. Consequently, together with the normal expansion of generic boundaries resulting from the inclusion of new species, systematics of the genus *Schizopera* became very difficult. Lang (1948, 1965*a*) maintained clarity in the generic diagnosis by noting the presence of a 'transformed spine' on the male third leg exopod as a fundamental characteristic of *Schizopera*, and he also provided a key to 46 valid species and subspecies described until then (Lang 1965*a*). Wells and Rao (1976), in presenting a new species from the Andaman Islands, described the new genus *Eoschizopera*, but unfortunately they also assigned almost all 'doubtful members of the genus *Schizopera*' to this new genus. In the same paper they gave a very useful list of important morphological features for many *Schizopera* species, although not for 22 species and subspecies known at that time. Subsequently, Apostolov (1982) divided another new genus, *Schizoperopsis*, but then he subdivided all three genera into two subgenera on the basis of 2- or 3-segmented first leg endopod. Mielke (1992, 1995) strongly criticised these two attempts to split the genus *Schizopera*, and he rejected both new genera (with all subgenera), because he thought that they were based on symplesiomorphic character states. Willen (2000) incorrectly attributed *Eoschizopera* to Apostolov (1982), listing it without any comments. Karanovic (2004) reassessed the characters of *Eoshizopera* and demonstrated its validity, although abandoning the subgeneric division established by Apostolov (1982). He demonstrated that a two-segmented endopod of the first leg can be a part of intraspecific variability, and thus not a reliable character on the genus-group level. In support of the genus *Eoschizopera* he listed six morphological characters that are different from *Schizopera*, at least three of them being probable synapomorphies. His view was followed by Boxshall and Halsey (2004), Wells (2007) and Huys (2009), with only four species accepted as valid members of the genus. Wells (2007) listed 85 valid species and subspecies in the genus *Schizopera*, omitting only *S. rybnikovi* Chertoprud & Kornev, 2005 from the Caspian Sea (see Chertoprud and Kornev 2005). Only two species have been described subsequently, both from lakes of increased salinity in Uzbekistan (Mirabdullayev and Ginatullina 2007): *S. setulosa* Mirabdullayev & Ginatullina, 2007 and *S. spinulosa* Mirabdullayev & Ginatullina, 2007. The former is unfortunately a homonym of *S. spinulosa* Sars, 1909. Together with eight taxa described in this paper, the genus now numbers 96 species and subspecies, distributed in a variety of marine, brackish and freshwater habitats around the world, which makes it an ideal model for testing hypotheses of multiple invasions of freshwater, which was suggested for copepods generally (Boxshall and Jaume 2000).

In Australia, the first record of the genus *Schizopera* was that of *S. clandestina* (Klie, 1924) by Halse *et al*. (2002), who listed it without any drawings, descriptions or comments, from surface waters of Lake Coyrecup, a small semipermanent saline lake in south-western Western Australia, some 125 km from the nearest coast. This species was originally described by Klie (1923) from German brackish waters of various salinities, and later on reported from many other parts of the world (Lang 1948; Bodin 1997). An incredible range of morphological variability, and several described subspecies (Wells 2007), would suggest that we are probably dealing with a species complex here, and the Australian taxon is unlikely to be that of a species described from German brackish waters. This matter would need a proper taxonomic revision of the complex, with redescription of the type material, as the original description is no longer adequate for modern taxonomic standards in this group (Karanovic 2006). Karanovic (2004) described five species from the Yilgarn region and Karanovic (2006) described another two from the Pilbara region. These two neighbouring Western Australian regions show remarkable differences in most major groups of stygofauna that were well studied. For example, diving beetles are completely absent from the Pilbara region (Watts and Humphreys 2006; Leys and Watts 2008), ostracods show differences at the tribe level (Karanovic 2007), and copepods are mostly different at the genus level (Karanovic 2006), with no shared stygobitic species whatsoever (Humphreys 2008). Even those few shared copepod genera show significant phylogenetic divergences between the two regions, with current members being only remotely related (Karanovic 2010; Karanovic *et al*. 2011). The discovery that Australian regions have different relationships to other Gondwanan areas was already anticipated by Weston and Crisp (1994). Giribet and Edgecombe (2006) showed the importance of looking at small-scale patterns when inferring Gondwanan biogeography for terrestrial invertebrates. Copepod results also challenged assumptions of monophyly of large continental blocks like Australia (Karanovic 2008; Karanovic and Tang 2009), which

was already discussed by Karanovic (2006), who proposed a 'pulsating desert hypothesis' as a novel dynamic model that may explain some of the differences observed. A strong connection between the Pilbara region, tropical Queensland and New Zealand was observed, which even predates Gondwanan regionality (Karanovic and Hancock 2009; Karanovic 2010). The only real connection between these two regions in copepod stygofauna seemed to be the genus *Schizopera*, for which it was hypothesised that it represents a relatively recent invasion from marine interstitial (Karanovic 2006). Testing this hypothesis also by molecular techniques became another aim of this study, for which we managed to collect two species from the Pilbara region, where this genus is relatively rare.

Material and methods

Most samples studied here were collected in the Yeelirrie calcrete (Figs 1, 2), Yilgarn region of Western Australia, as a part of an impact assessment study by a private environmental consulting company, Subterranean Ecology, and entrusted to the senior author for morphological identification. Two as yet undescribed new *Schizopera* species from the Pilbara region of Western Australia were donated by another private environmental consulting company, Bennelongia, which were intended as outgroups for our molecular analysis. The other three outgroups for our molecular phylogenies came from the family Canthocamptidae Brady, 1880: *Cletocamptus deitersi* (Richard, 1897) with *COI* sequence data available from GenBank, *Australocamptus hamondi* Karanovic, 2004 was collected also in the Yeelirrie calcrete (bore line E, bore No 312; see Fig. 1) and *Elaphodella humphreysi* Karanovic, 2006 was collected from several bores near Newman in the Pilbara region of Western Australia. Locality data and number of specimens are listed separately for every Yeelirrie *Schizopera* species, and all type material is deposited in the Western Australian Museum, Perth (WAM). Some additional material is kept as voucher specimens by Subterranean Ecology, but will ultimately be also deposited in the Western Australian Museum.

Samples were collected with haul-nets (mesh size 50 or 150 µm) from groundwater bores. Bores are holes mainly made by mining companies or agricultural enterprises for the purpose of water monitoring and abstraction or mineral exploration. They are usually from 5 to 20 cm in diameter and may be lined entirely, or in part, by PVC tubing (the casing). This tubing may be open only at the bottom, or it may be pierced at one or more levels by holes of various sizes ('slots'). The top may be securely capped or entirely open to the elements. Some bores record the water pressure at a given level in the aquifer (piezometers), while others, equipped with windmills or solar pumps, provide water for pastoral use. Haul-nets are simple plankton nets of a different size suitable for the bore; collars can range from 20 to 150 mm in diameter and are made of stainless steel. Weighted nets (using simple fishing leads) were lowered down into the bore with a bottle screwed on its distal part and then hauled through the water column, usually six times. Samples were preserved in the field in cold 100% ethanol, kept on ice or in a refrigerator, and sorted in a laboratory. Each sample was given a unique four digit laboratory code, and these were used thoughout the investigation, and are also presented in this paper for all material examined (prefix seLN). Note that the same number is also used for our *COI* seqences from different localities and/or sampling occasions. Bores established for hydrogeological work, mineral exploration and water monitoring have prefixes or suffixes of relevance only to that drilling program. These codes are cited in the 'Material examined' for each species to aid specification of the location, although precise coordinates are also provided.

Specimens for morphological observation were dissected and mounted on microscope slides in Faure's medium, which was prepared following the procedure discussed by Stock and von Vaupel Klein (1996), and dissected appendages were then covered by a coverslip. For the urosome or the entire animal two human hairs were mounted between the slide and coverslip, so the parts would not be compressed. By manipulating the coverslip carefully by hand, the whole animal or a particular appendage could be positioned in different aspects, making possible the observation of morphological details. During the examination, water slowly evaporated and appendages eventually remained in a completely dry Faure's medium, ready for long-term depositing. All line drawings were prepared using a drawing tube attached to a Leica MB2500 phase-interference compound microscope, with N-PLAN objectives (Leica Microsystems, Wetzlar, Germany). Specimens that were not drawn were examined in propylene glycol (CH3CH(OH)CH2OH) and, after examination, were again preserved in 100% ethanol. Photographs of whole specimens were taken in propylene glycol with a Leica DFC420 micro-camera attached to a Leica M205C dissecting microscope. The software package Leica Application Suite (LAS), version 3.5.0, was used to create a multifocal montage image. Specimens for the scanning electron micrography were dehydrated in progressive ethanol concentrations, critical-point dried, coated in gold and observed under a LEO 1525 microscope (Carl Zeiss SMT, Oberkochen, Germany) on the in-lens detector, with working distances between 5.9 and 6.1 mm and accelerating voltages of 5 or 10 kV.

Morphological terminology follows Huys and Boxshall (1991), except for caudal ramus setae numbering (not used) and small differences in the spelling of some appendages (antennula, mandibula and maxillula instead of antennule, mandible and maxillule), as an attempt to standardise the terminology for homologous appendages in different crustacean groups. New species are not listed alphabetically; instead, they were presented according to the descending number of perceived plesomorphic morphological features. Descriptions of second to last taxon were shortened by making them comparative, and only the first species is described here in full; the term 'previous species' in that context means the immediately prior species, unless otherwise stated. Biospeleological terminology follows Humphreys (2000).

Specimens for molecular analysis were examined without dissecting under a compound microscope (objective 63× dry) in propylene glycol. After examination they were returned to 100% ethanol. DNA was extracted using the GENTRA method (Puregene) according to the manufacturer's protocol for fresh tissues. Polymerase chain reaction amplifications of a 623-bp fragment from the mitochondrial *COI* gene were generally carried out with the 'universal' primers LCOI490 and HCO2198 (Folmer

et al. 1994). However, the use of these primers proved problematic in many cases and hence additional 'nested' primers were designed by Kathleen Saint (South Australian Museum) from preliminary copepod *COI* sequence data and used in combination with the Folmer *et al*. (1994) primers to improve the PCR amplification efficiency (Table 1). An initial PCR amplification used the combination LCOI490/HCO2198, then 1 μL of product was used to seed nested PCRs in the following combinations: M1323/HCO2198 or M1321/M1322 (see Table 1 for codes). Polymerase chain reaction amplifications were carried out in 25 μL volumes containing 4 mM $MgCl_2$, 0.20 mm dNTPs, 1 × PCR buffer (Applied Biosystems), 6 pmol of each primer and 0.5 U of AmpliTaq Gold (Applied Biosystems, Foster City, CA, USA). Polymerase chain reaction amplification was performed under the following conditions: 94°C for 9 min, then 34 cycles of 94°C for 45 s; annealing 48°C for 45 s; 72°C for 60 s; with a final elongation step at 72°C for 6 min. Polymerase chain reaction products were purified using a vacuum plate method and sequencing was undertaken using the ABI prism Big Dye Terminator Cycle sequencing kit (Applied Biosystems). Sequencing was carried out on an ABI 3700 DNA analyser and sequences were edited and manually aligned in SeqEd version 1.0.3 (Applied Biosystems). For this study, DNA was extracted and the *COI* fragment successfully PCR amplified from 43 copepod specimens (Table 2).

Phylogenetic analyses of the *COI* sequence data were conducted with or without the use of outgroup taxa, and using a combination of different approaches to assess the robustness of the tree topology. A distance approach, using neighbour joining (NJ) and a maximum parsimony (MP) approach were conducted using the program PAUP* version 4.0b10 (Swofford 2002). A maximum likelihood (ML) approach was conducted using the ML program RAxML and the WEB-based RAxML 'black box' (http://phylobench.vital-it.ch/raxml-bb/; Stamatakis *et al*. 2008) provided by the Vital-IT Unit of the Swiss Institute of Bioinformatics. The data were also analysed using a Bayesian inference (BI) approach using MrBayes ver. 3.2 (Huelsenbeck and Ronquist 2001; Ronquist and Huelsenbeck 2003). An HKY-85 (Hasegawa *et al*. 1985) distance model was used for the NJ analyses. Maximum parsimony analyses were conducted using an heuristic search option and default options (TBR branch swapping, ACCTRAN character state optimisation), with the exception of using random stepwise addition repeated 100 times. Neighbour joining and MP bootstrap analyses (Felsenstein 1985) were carried out using 1000 bootstrap pseudoreplicates, employing an heuristic search option as above with random input of taxa and 'max trees' set to 100 for the MP bootstrap analysis. The ML analyses were conducted applying a general time reversible (GTR) model and unequal variation at sites modelled using a gamma distribution. Support for branches was estimated using the bootstrap option in RAxML, using 100 bootstrap pseudoreplicates.

The program MODELTEST (ver. 3.7; Posada and Crandall 1998) with the Akaike information criterion was used to show that a GTR model (Rodríguez *et al*. 1990), with a proportion of invariant sites (I) and unequal rates among sites (G) (Yang 1996), was most appropriate for BI analyses. The BI analysis of *COI* data was carried out using default uninformative priors with four chains run simultaneously for five million generations in two independent runs, sampling trees every 500 generations. After this number of generations, the final standard deviation of split frequencies had reduced to 0.0045 and the potential scale reduction factor (PSRF) was ~1.0 for all parameters, suggesting convergence had been reached. Assessment of effective sample sizes for each parameter estimate was determined using the program Tracer ver. 1.4 (Rambaut and Drummond 2007). The likelihood values converged to relatively stationary values after ~5000 generations. Trees from each MrBayes run were combined and a burn-in of 5000 trees (25% of the total) was chosen, with a >50% posterior probability consensus tree constructed from the remaining 15 002 trees.

Average DNA sequence divergence within groups (morphotaxa) and between groups was estimated using the program MEGA ver. 4 (Kumar *et al*. 2008), with a composite likelihood distance applied under a HKY-85 model of DNA sequence evolution.

Systematics

Subphylum **CRUSTACEA** Brünnich

Class **MAXILLOPODA** Dahl

Subclass **COPEPODA** Milne Edwards

Order **HARPACTICOIDA** Sars

Family **MIRACIIDAE** Dana

Genus ***Schizopera*** Sars

Schizopera analspinulosa, sp. nov.

(Figs 3*A*, 5–11)

Material examined

Name-bearing type. Holotype (WAM C37470), adult ♀ completely dissected on 1 slide in Faure's medium, 18.iii.2010, leg. T. Karanovic and S. Callan (seLN8182).

Table 1. Oligonucleotide primers used to PCR amplify the 5′ end of *COI*

Three additional primers were also developed but were unsuccessful in PCR amplifications of *COI*

Primer code	Primer sequence (5′–3′)	Designed by
LCOI490 (M414)	GGTCAACAAATCATAAAGATATTGG	Folmer *et al*. (1994)
HCO2198 (M423)	TAAACTTCAGGGTGACCAAAAAATCA	Folmer *et al*. (1994)
M1321	TRRNGAYGAYCARRTTTATAATGT	K. Saint
M1322	TCAAAATARRTGYTGRTAWARHAC	K. Saint
M1323	GAYGAYCARRTTTATAATGT	K. Saint

Table 2. List of copepod specimens for which *COI* fragment was successfully amplified

Code	Species	Region	Line	Bore number	Date	GenBank
–	*S.* sp. 1	Pilbara	–	Harding River	?	JQ390555
7081a	*A. hamondi*	Yilgarn	E	312	13 Jan 2010	JN039160
7081b	*A. hamondi*	Yilgarn	E	312	13 Jan 2010	JN039163
7106	*S.* sp. 2	Pilbara	–	FMGSM1585	27 Feb 2010	JQ390556
7122	*A. hamondi*	Yilgarn	E	312	19 Mar 2010	JN039165
7131	*S. leptafurca*	Yilgarn	K	YYHC085B	18 Mar 2010	JQ390557
7304	*S. emphysema*	Yilgarn	2	YYAC1004C	27 Aug 2009	JQ390558
7308	*S. kronosi*	Yilgarn	2	YYAC1007A	27 Aug 2009	JQ390559
7342	*S. akation*	Yilgarn	3.5	YYAC284	12 Nov 2009	JQ390560
7342.1	*S. uranusi*	Yilgarn	3.5	YYAC284	12 Nov 2009	JQ390561
7342.2	*S. uranusi*	Yilgarn	3.5	YYAC284	12 Nov 2009	JQ390562
7360	*S. analspinulosa linel*	Yilgarn	L	LUNK1	12 Jan 2010	JQ390563
7374	*S. uranusi*	Yilgarn	2	YYAC1007	12 Nov 2009	JQ390564
7389	*S. leptafurca*	Yilgarn	3	YYAC118	12 Nov 2009	JQ390565
7417	*S. leptafurca*	Yilgarn	1.5	YYAC35	12 Nov 2009	JQ390566
7417	*S. kronosi*	Yilgarn	1.5	YYAC35	12 Nov 2009	JQ390567
7421.1	*S. leptafurca*	Yilgarn	1.5	YYAC33	12 Nov 2009	JQ390568
7421.2	*S. leptafurca*	Yilgarn	1.5	YYAC33	12 Nov 2009	JQ390569
7433	*S. leptafurca*	Yilgarn	3.5	YYAC328	12 Nov 2009	JQ390570
7439	*S. uranusi* sp. 2	Yilgarn	3.5	YYAC248	12 Nov 2009	JQ390571
7730	*S.* sp. 2	Pilbara	–	FMGSM1585	20 Jan 2010	JQ390572
7991	*E. humphreysi*	Pilbara	–	FMGSM1529	23 Jan 2010	JN039161
8110	*E. humphreysi*	Pilbara	–	FMGSM3644	2 Mar 2010	JN039166
8119	*E. humphreysi*	Pilbara	–	FMGSM3645	1 Mar 2010	JN039173
8302	*S. uranusi*	Yilgarn	1	YYAC0019B	20 Mar 2010	JQ390573
8385	*S. leptafurca*	Yilgarn	5	YYAC0014D	17 Mar 2010	JQ390574
8393	*S. leptafurca*	Yilgarn	3.5	YYAC328	17 Mar 2010	JQ390575
8393	*S. kronosi*	Yilgarn	3.5	YYAC328	17 Mar 2010	JQ390576
8417	*S. uranusi*	Yilgarn	1	YYAC0016A	20 Mar 2010	JQ390577
8417	*S. leptafurca*	Yilgarn	1	YYAC0016A	20 Mar 2010	JQ390578
8427	*S. uranusi*	Yilgarn	F	YYHC0139	17 Mar 2010	JQ390579
8464	*S. leptafurca*	Yilgarn	K	YYHC0049K	20 Mar 2010	JQ390580
8479	*S. uranusi*	Yilgarn	1	YYD26	15 Mar 2010	JQ390581
8479	*S. leptafurca*	Yilgarn	1	YYD26	15 Mar 2010	JQ390582
8479	*S. akation*	Yilgarn	1	YYD26	15 Mar 2010	JQ390583
8496	*S. akolos*	Yilgarn	1	YYD22	15 Mar 2010	JQ390584
8496	*S. akation*	Yilgarn	1	YYD22	15 Mar 2010	JQ390585
8517	*S. analspinulosa* s. str.	Yilgarn	SB14	SB14–1	16 Mar 2010	JQ390586
8517	*S. akation*	Yilgarn	SB14	SB14–1	16 Mar 2010	JQ390587
8527	*A. hamondi*	Yilgarn	E	312	16 Mar 2010	JN039170
8533	*S. analspinulosa linel*	Yilgarn	L	LUNK1	16 Mar 2010	JQ390588
8533	*S. akation*	Yilgarn	L	LUNK1	16 Mar 2010	JQ390589
8538	*S. leptafurca*	Yilgarn	3	YYAC118	21 Mar 2010	JQ390590

Type locality. Australia: Western Australia: Yilgarn region, Yeelirrie station, bore SB14–1, 27.344283°S 120.307708°E (south-eastern corner on Fig. 1).

Additional material examined. All from type locality: allotype (WAM C37471), adult ♂ dissected on 1 slide, 18.iii.2010, leg. T. Karanovic and S. Callan (seLN8182); 8 paratype ♂ + 15 paratype ♀ + 4 paratype copepodids (WAM C37472), together in ethanol, 18.iii.2010, leg. T. Karanovic and S. Callan (seLN8182); 2 paratype ♂ and 2 paratype ♀ on 1 SEM stub (WAM C37473), 18.iii.2010, leg. T. Karanovic and S. Callan (seLN8182); paratype ♀ dissected on 1 slide, 18.iii.2010, leg. T. Karanovic and S. Callan (seLN8182); paratype ♂ dissected on 1 slide, 18.iii.2010, leg. T. Karanovic and S. Callan (seLN8182); 6 ♂ + 2 ♀ + 2 copepodids together in ethanol, 16.iii.2010, leg. T. Karanovic and G. Perina (seLN8517); 1 ♀ destroyed for DNA sequence, 16.iii.2010, leg. T. Karanovic and G. Perina (seLN8517); 1 ♂ + 3 ♀ in ethanol, 11.iii.2009, leg. P. Bell and S. Eberhard (seLN6492); 1 ♀ dissected on 1 slide, 11.iii.2009, leg. P. Bell and S. Eberhard (seLN6492).

Description of female

Data from holotype and several paratypes. Total body length, measured from tip of rostrum to posterior margin of caudal rami (excluding caudal setae), ranges from 402 to 632 µm (413 µm in holotype). Colour of preserved specimen yellowish. Nauplius eye not visible. Habitus (Figs 3*A*, 5*A*, 9*A*, *B*) cylindrical, slender, without distinct demarcation between prosome and urosome; prosome–urosome ratio ~1 (in dorsal view); greatest width at posterior end of cephalothorax. Body length–width ratio ~3.7;

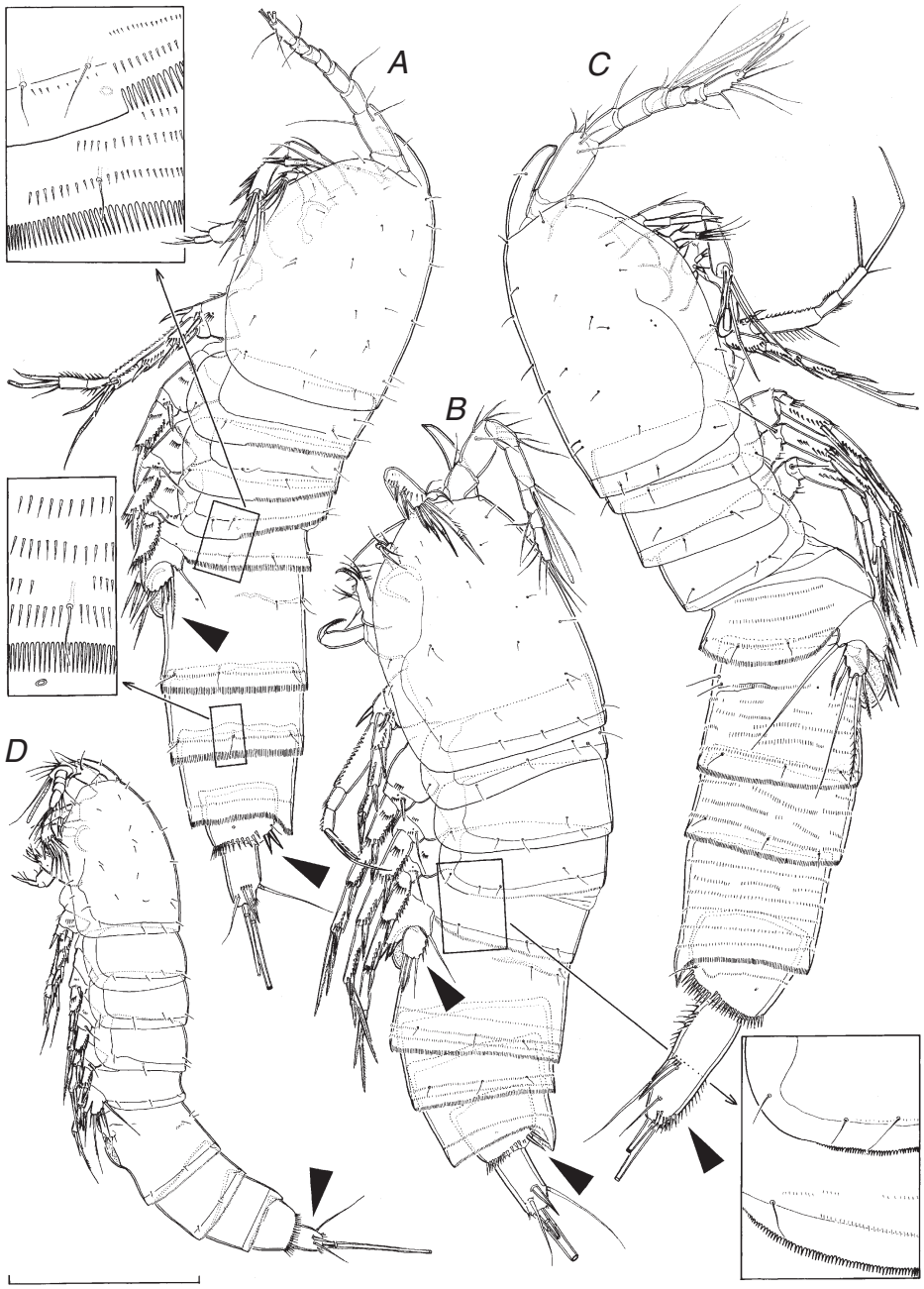

Fig. 3. Female habitus in lateral view of four different species of *Schizopera* G.O. Sars, 1905 (all holotypes). (*A*) *Schizopera analspinulosa*, sp. nov.; (*B*) *S. kronosi*, sp. nov.; (*C*) *S. emphysema*, sp. nov.; (*D*) *S. akolos*, sp. nov. Insets show fine details of body ornamentation; arrows point to most prominent specific characters. Scale bar = 100 μm.

cephalothorax 1.25 times as wide as genital double somite. Free pedigerous somites without pronounced lateral dorsal expansions. Integument relatively strongly chitinised. All somites (except cephalothorax) and caudal rami, besides other ornamentation, with dense cover of minute spinules (insets in Fig. 3*A*, and Figs 5*B*, *C*, 6*B*, *C*, 9*A*–*E*). Rostrum (Figs 7*A*, 9*D*) long and clearly demarcated at base, reaching two-thirds of second antennular segment, linguiform, with blunt tip, about twice as long as wide; ornamented with two sensilla dorsolaterally.

Cephalothorax (Figs 6*A*, 9*D*) ~1.2 times as long as wide in dorsal view (without rostrum); represents 30% of total body length. Surface of cephalothoracic shield and tergites of first three free pedigerous somites with characteristic pattern of large sensilla and small cuticular pores (Figs 3*A*, 5*A*, 6*A*). Two sensilla and two pores at base of rostrum (Fig. 9*D*). Cephalothoracic

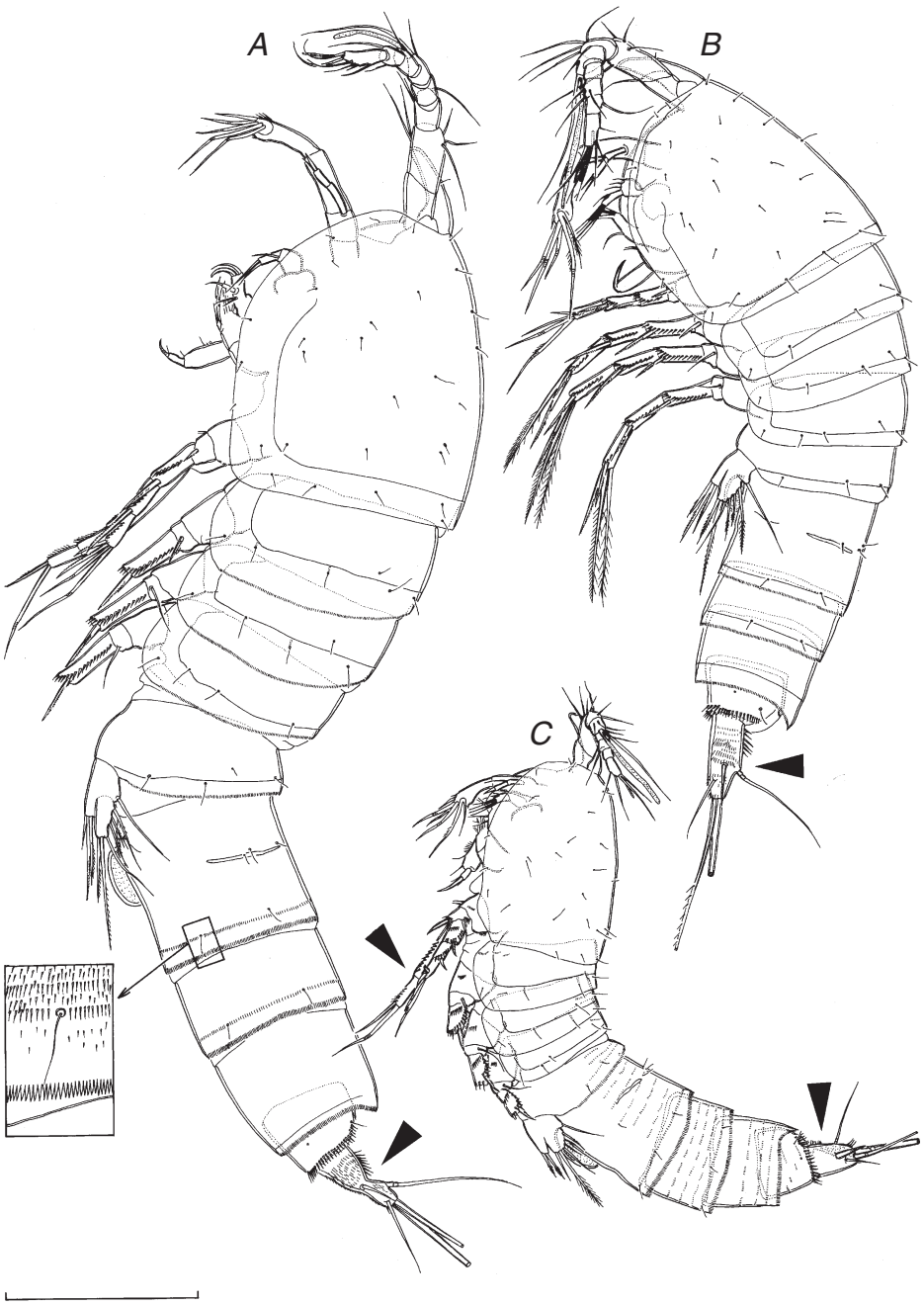

Fig. 4. Female habitus in lateral view of three different species of *Schizopera* G.O. Sars, 1905 (all holotypes). (*A*) *Schizopera leptafurca*, sp. nov.; (*B*) *S. uranusi*, sp. nov.; (*C*) *S. akation*, sp. nov. Inset shows fine details of body ornamentation; arrows point to most prominent specific characters. Scale bar = 100 µm.

shield with additional dense pattern of shallow pits, each with central stria (primordial spinula?) (Fig. 9*D*). Hyaline fringe of cephalothoracic shield smooth and unornamented, those of other prosomites finely serrated dorsally and partly laterally, with smooth ventrolateral corners (Figs 3*A*, 9*A*, *B*). Fifth pedigerous somite (first urosomal) ornamented with four dorsal large sensilla and two lateral sensilla (one on each side), as well as with two cuticular pores ventrolaterally (one on each side), in addition to several irregular rows of numerous minute cuticular spinules; hyaline fringe sharply serrated (Figs 3*A* and upper inset, 5*A*, *B*, 9*A*, *B*).

Genital double somite (Figs 5*A*, *B*, *C*, 9*A*, *B*) ~0.7 times as long as wide (dorsal view), with visible suture internally; ornamented with eight sensilla dorsally (six at midlength, two near posterior margin), two posterior sensilla ventrally, and two posterior sensilla and two midlength pores laterally (one on each side), in addition to numerous rows of minute spinules (which interrupted at midlength, dorsally and laterally (Fig. 9*A*, *B*),

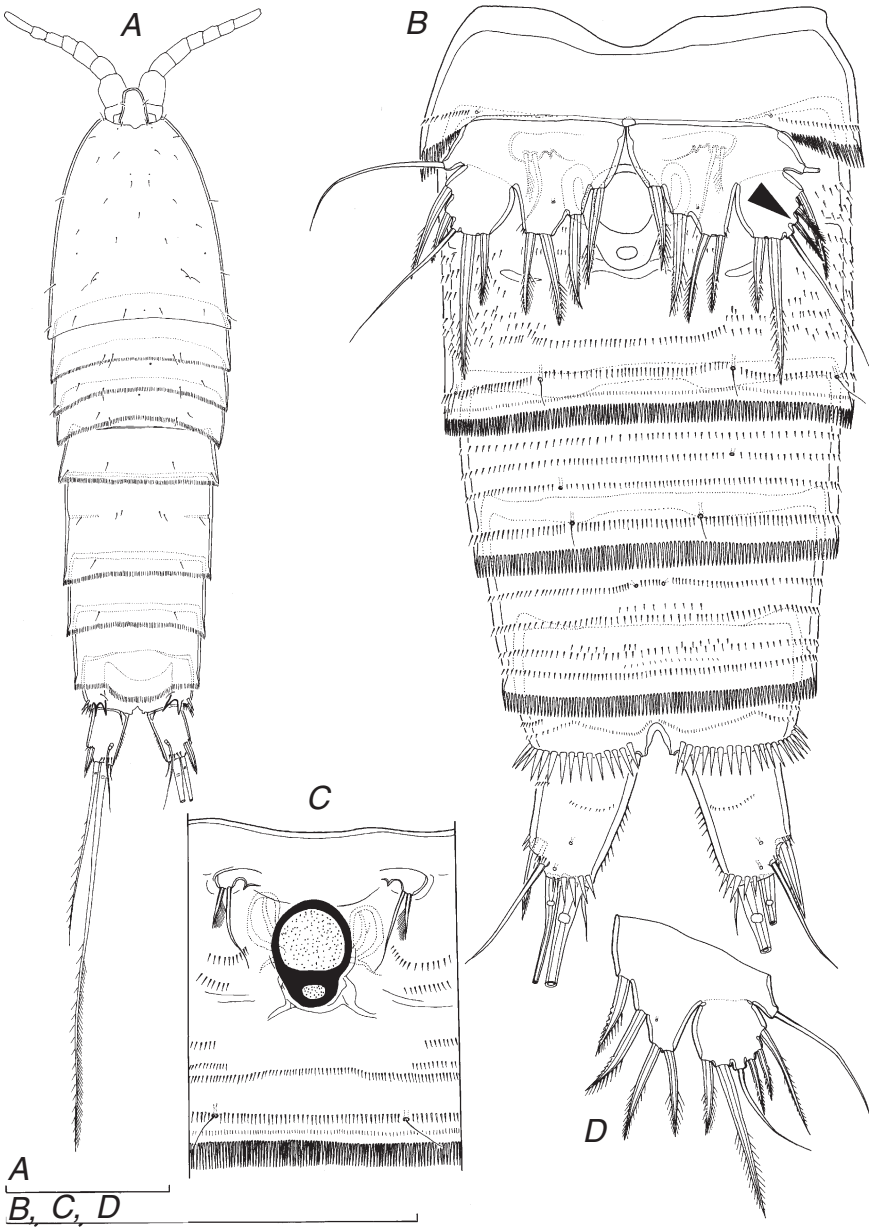

Fig. 5. *Schizopera analspinulosa*, sp. nov. A–C, holotype ♀; D, paratype ♀ I. (*A*) Habitus without minute spinules drawn, dorsal view; (*B*) urosome, ventral view; (*C*) genital field, ventral view (flattened); (*D*) fifth leg, anterior view (dissected and flattened). Arrow points to asymmetry in fifth leg armature. Scale bar = 100 µm.

revealing smooth area that corresponds to internal suture and marks ancestral segmentation); hyaline fringe sharply serrated both ventrally and dorsally. Female genital complex (Fig. 5*C*) typical for genus: single copulatory pore partly covered by epicopulatory bulb (which serves also as copulatory duct), two small seminal receptacles placed inside large, paired genital apertures; apertures with two ventral gonopores, each covered by reduced sixth leg. Epicopulatory bulb large, ovoid, ~1.4 times as long as wide. Seminal receptacles very small, ovoid, reaching to about anterior margin of epicopulatory bulb, ~0.6 times as long as epicopulatory bulb. Third urosomite ornamented with six posterior sensilla (two dorsal, two ventral and two lateral) and two ventral pores at midlength (Fig. 5*B*), in addition to numerous rows of slender spinules of various sizes; hyaline fringe serrated and straight. Preanal somite without sensilla, ornamented with two ventral pores at midlength (Fig. 5*B*) and many rows of minute spinules; hind margin clearly bulging posteriorly in dorsal region, forming very sharply serrated pseudoperculum (Figs 6*B*, 9*E*). Anal somite (Figs 6*B*, *C*, 9*C*, *E*) with convex and very short anal operculum ornamented with transverse row of spinules along posterior margin, and completely hidden beneath pseudoperculum; ornamented with two large sensilla dorsally,

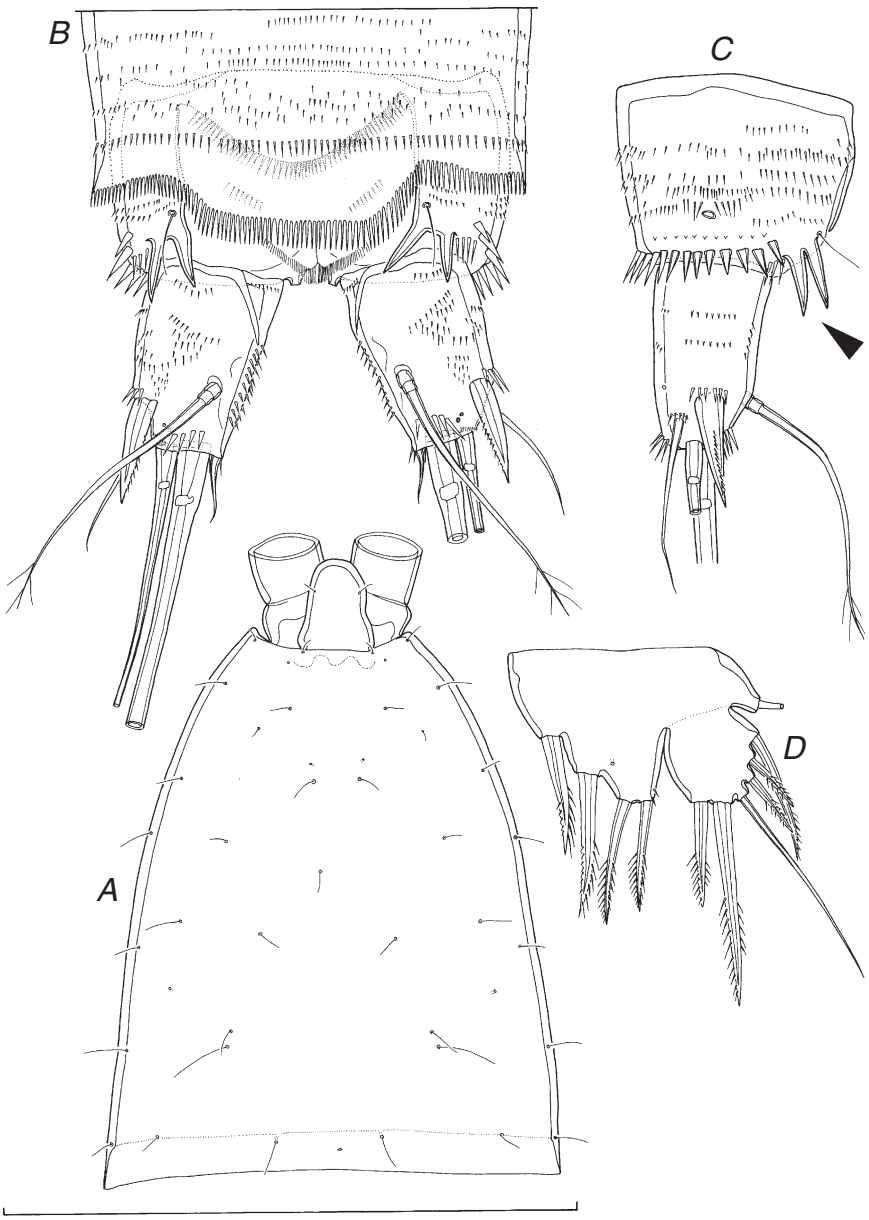

Fig. 6. *Schizopera analspinulosa*, sp. nov., holotype ♀. (*A*) Cephalothoracic shield, dorsal view; (*B*) last two urosomal somites and caudal rami, dorsal view; (*C*) anal somite and left caudal ramus, lateral view; (*D*) fifth leg, anterior view (dissected and flattened). Arrow points to two enlarged posterior dorsal spinules on anal somite. Scale bar = 100 µm.

two lateral cuticular pores, two ventromedian pores and a transverse row of large spinules along posterior margin; two most dorsal of these posterior spinules characteristically enlarged and strongly fused basally to somite (arrowed in Fig. 6*C*). Anal sinus (Figs 6*B*, 9*E*) widely opened and ornamented with two diagonal rows of slender spinules; represents 58% of somite's width.

Caudal rami (Figs 5*B*, 6*B*, *C*, 9*C*, *E*) strongly sclerotised, ~1.5 times as long as greatest width in dorsal view, almost cylindrical (somewhat tapering towards caudal end but with straight inner margin), strongly divergent, with space between them about half of one ramus width; ornamented with two ventral and two dorsal cuticular pores in posterior half, transverse row of several large spinules along posterior margin dorsally and ventrally, and several short rows of minute spinules dorsally, laterally and medially (only one row ventrally); armed with six elements (two lateral, one dorsal and three apical). Dorsal seta slender and apically pinnate, ~1.6 times as long as ramus, inserted at two-thirds of ramus length, triarticulate. Lateral proximal spine stout, inserted at three-quarters of ramus length, 0.6 times as long as ramus. Lateral distal seta very slender, smooth, inserted slightly ventrolaterally at four-fifths of ramus length, ~0.8 times as long as

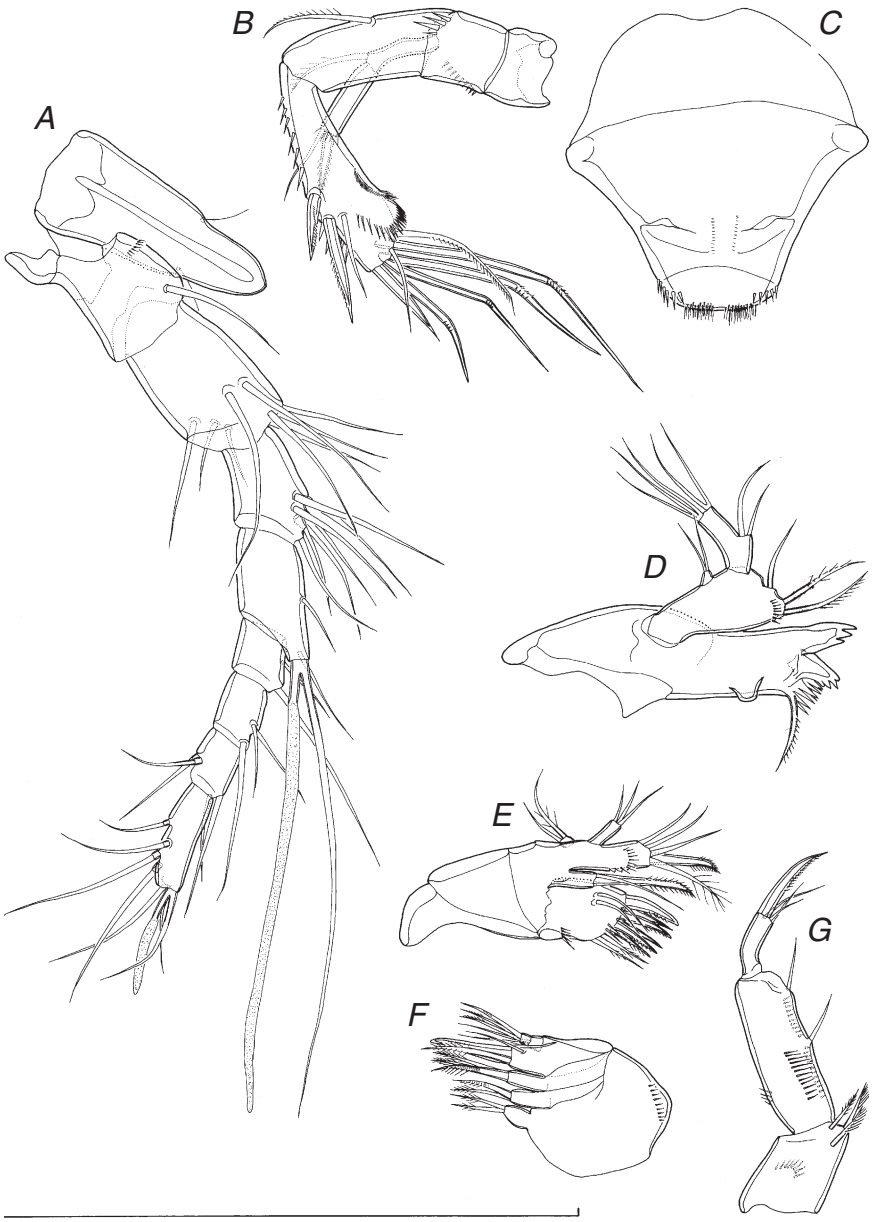

Fig. 7. *Schizopera analspinulosa*, sp. nov., holotype ♀. (*A*) Rostrum and antennula, ventral view; (*B*) antenna, ventral view; (*C*) labrum, ventral (anterior) view; (*D*) mandibula, anterior view; (*E*) maxillula, anterior view; (*F*) maxilla, anterior view; (*G*) maxilliped, anterior view. Scale bar = 100 μm.

ramus. Inner apical seta short and smooth, 0.3 times as long as ramus. Principal apical setae with breaking planes; middle apical seta strongest, bipinnate at distal end, twice as long as unipinnate outer apical seta, and almost 0.6 times as long as body length (Fig. 5*A*).

Antennula (Fig. 7*A*) eight-segmented, ~0.8 times as long as cephalothorax, with short aesthetasc on eighth segment fused to two apical setae, and large aesthetasc on fourth segment reaching significantly beyond tip of appendage and fused basally to equally long seta; setal formula: 1.9.7.3.2.3.4.7. Only two lateral setae on seventh segment and four on eighth segment biarticulate. All setae smooth and slender, and most end apically with pore (except apical and subapical ones), only observable under scanning electron microscope. Length ratio of antennular segments, from proximal end and along caudal margin, 1 : 1.3 : 0.7 : 0.8 : 0.5 : 0.6 : 0.5 : 1. First segment ornamented with short transverse row of small spinules ventromedially, other segments unornamented.

Antenna (Fig. 7*B*) comprising coxa, basis, two-segmented endopod, and much smaller but also two-segmented exopod. Coxa very short, without ornamentation or armature. Basis also short and unarmed, about as long as wide, ornamented with several large spinules distally near inner margin, and diagonal row of smaller spinules on outer margin. First endopodal segment

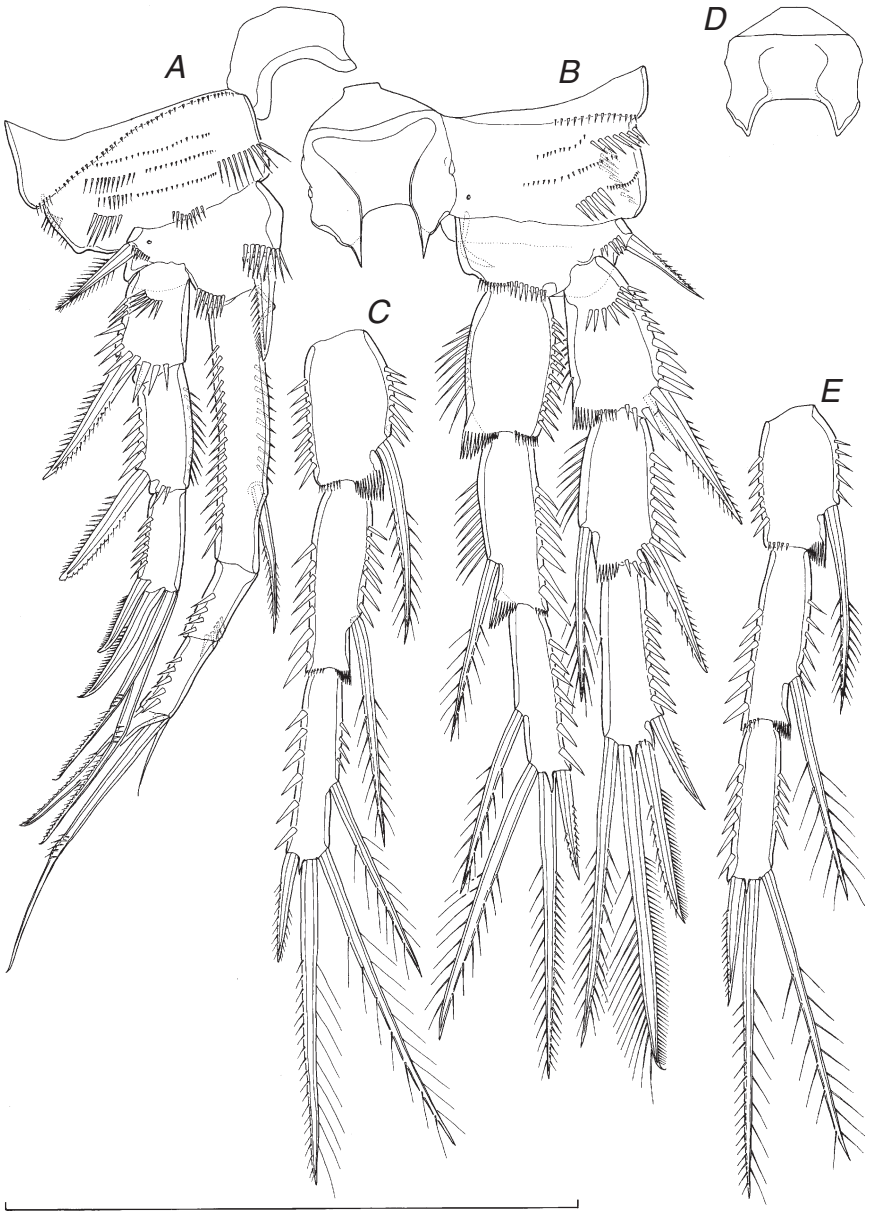

Fig. 8. *Schizopera analspinulosa*, sp. nov., holotype ♀. (*A*) First swimming leg, anterior view; (*B*) second swimming leg, anterior view; (*C*) endopod of third swimming leg, anterior view; (*D*) intercoxal sclerite of fourth swimming leg, anterior view; (*E*) endopod of fourth swimming leg, anterior view. Scale bar = 100 µm.

2.8 times as long as wide and 2.3 times as long as basis, without ornamentation, armed with one unipinnate lateral seta at middle. Second endopodal segment 1.3 times as long as first, more slender proximally, with two surface frills distally; lateral armature consists of two strong spines flanking small seta; apical armature consisting of seven elements: one slender smooth seta, one smooth spine, four prehensile setae, longest one bearing spinules around geniculation and fused basally to another slender, unipinnate seta. Ornamentation of second endopodal segment consists of longitudinal row of large spinules along anterior margin, and diagonal row of large spinules between lateral and apical armature elements. Both exopodal segments of about same length; first segment armed with one unipinnate subapical seta, unornamented; second segment armed apically with one smooth seta and one bipinnate spine of about same length, ornamented with transverse subterminal row of spinules.

Labrum (Fig. 7*C*) large, rigidly sclerotised, with rounded cutting edge, ornamented apically and subapically with spinules; lateral spinules stronger than middle ones.

Mandibula (Fig. 7*D*) with narrow cutting edge of coxa, armed with two complex teeth in ventral part (first tricuspidate, second quadricuspidate), several simple teeth in dorsal part, and one

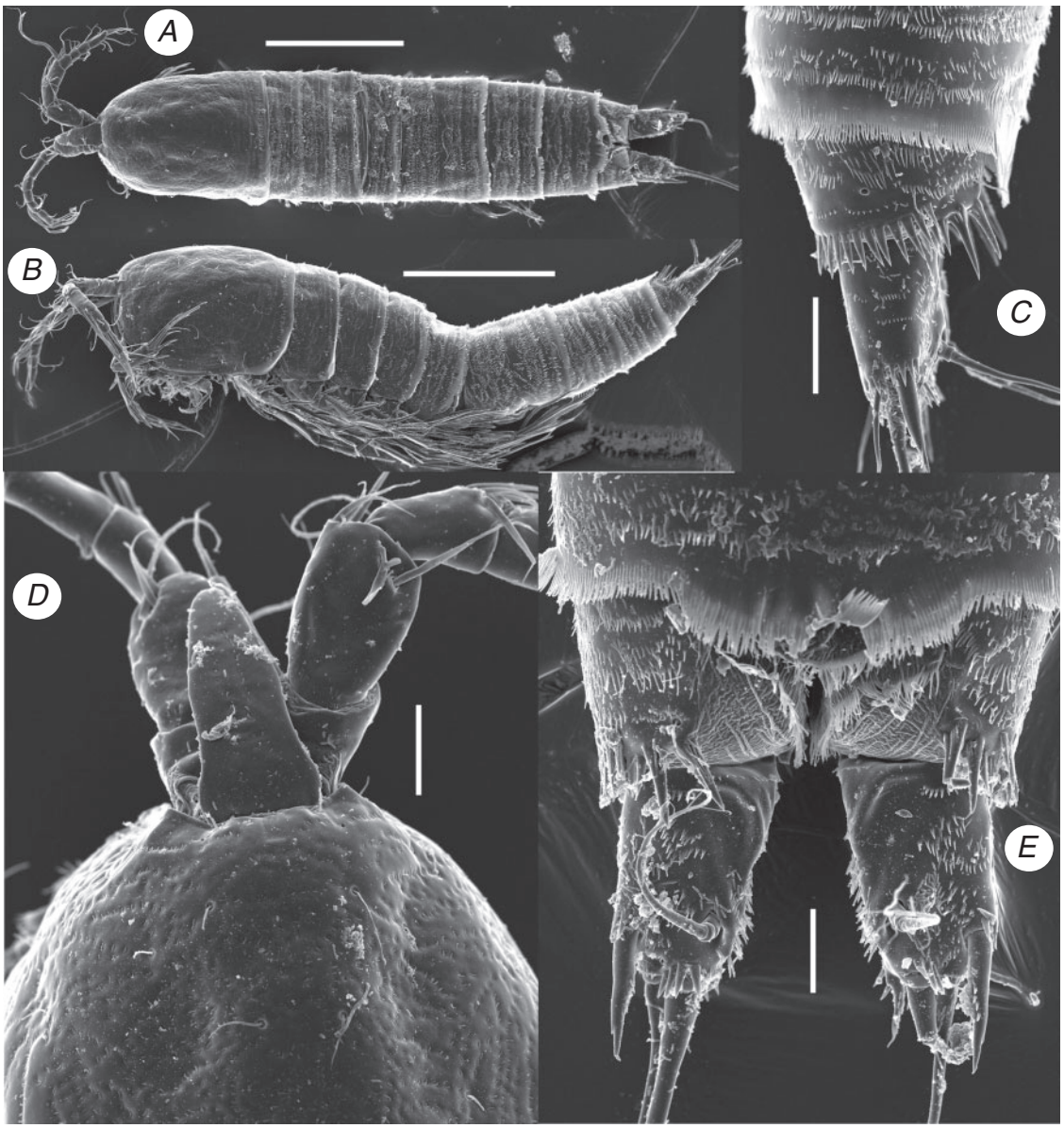

Fig. 9. *Schizopera analspinulosa*, sp. nov., scanning electron micrographs. A, D, and E, paratype ♀ II; B and C, paratype ♀ III. (*A*) Habitus, dorsal view; (*B*) habitus, lateral view; (*C*) last two urosomal somites and left caudal ramus, lateral view; (*D*) anterior part of cephalothorax with rostrum and antenullae, dorsal view; (*E*) last two urosomal somites and caudal rami, dorsal view. Scale bars A, B = 100 μm; C–E = 10 μm.

unipinnate dorsal-most seta. Basis trapeziform plate, about twice as long as wide, armed with three setae along inner margin (one smooth, two unipinnate); ornamented with transverse row of spinules at base of inner setae. Endopod one-segmented, twice as long as wide, armed with two lateral and five apical smooth setae. Exopod very small but distinct segment, armed with two smooth apical setae.

Maxillula (Fig. 7*E*) with large preacoxa, arthrite highly mobile, armed apically with six strong, unipinnate spines, and two bipinnate setae; laterally armed with two slender smooth setae and ornamented with short row of spinules on middle of arthrite. Coxa small, armed with two setae on inner margin; distal seta slender and smooth, proximal seta very strong, spiniform and bipinnate. Basis furnished with one strong, curved and bipinnate spine, and four setae on inner margin, proximal-most seta bipinnate, others smooth. Endopod one-segmented, small, ~2.4 times as long as wide, armed with three apical smooth setae. Exopod also distinct but very small segment, armed with two apical setae (inner seta bipinnate, outer smooth).

Maxilla (Fig. 7*F*) composed of syncoxa, basis and two-segmented endopod. Syncoxa with three endites, each armed with two subequal setae. Basis armed with one apical, claw-like spine (partly fused to basis), one bipinnate and strong apical seta, and one slender and smooth lateral seta. First endopodal segment

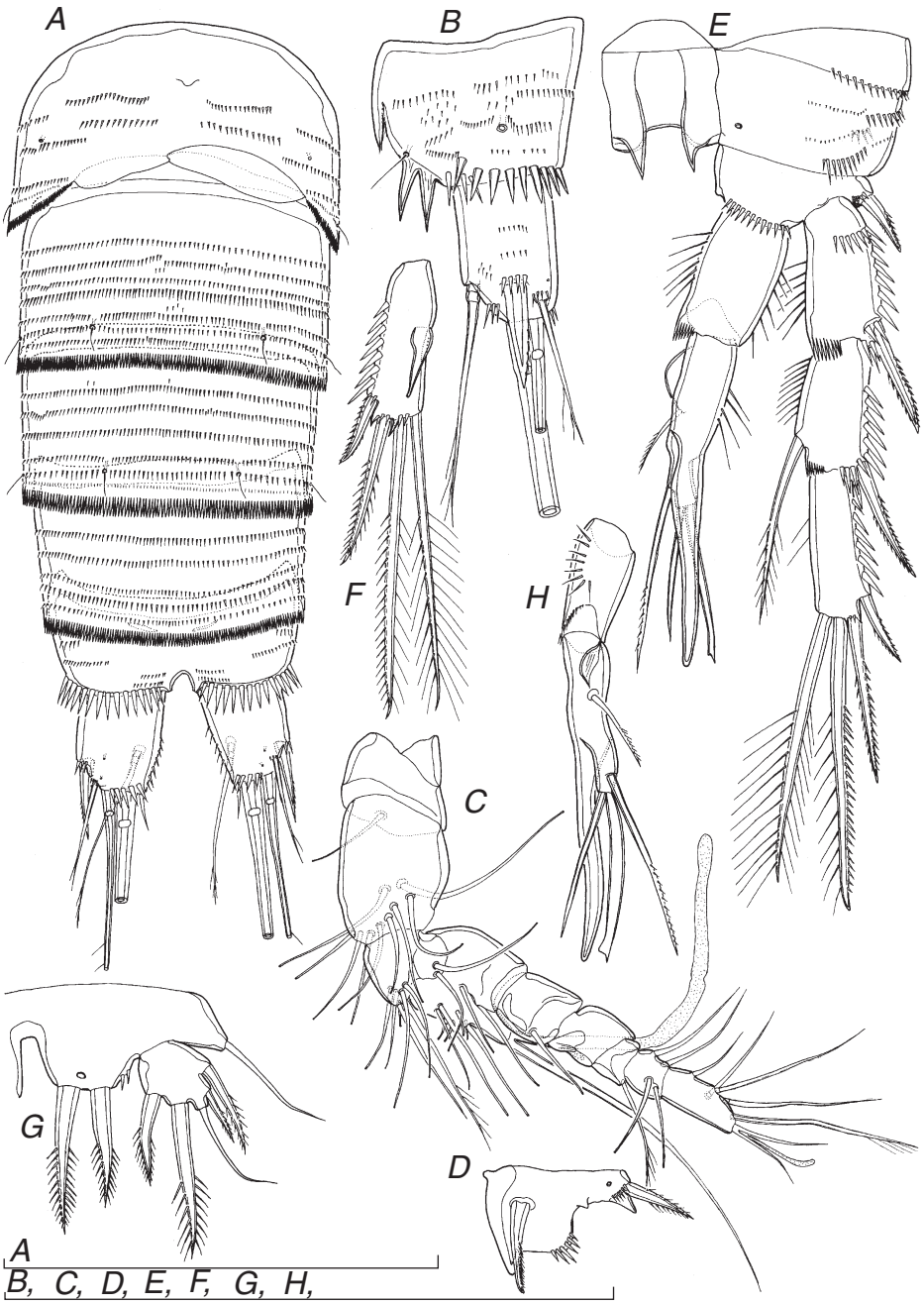

Fig. 10. *Schizopera analspinulosa*, sp. nov. A–G, allotype ♂; H, paratype ♂ I. (*A*) Urosome without fifth pedigerous somite, ventral view; (*B*) anal somite and right caudal ramus, lateral view; (*C*) antennula, dorsoposterior view; (*D*) basis of first swimming leg, anterior view; (*E*) second swimming leg, anterior view; (*F*) third exopodal segment of third swimming leg, anterior view; (*G*) fifth leg, anterior view (dissected and flattened); (*H*) endopod of second swimming leg, ventromedian view (compressed and somewhat deformed). Scale bar = 100 μm.

armed with two smooth and slender setae, second armed with three stronger setae, two unipinnate at distal end. Only ornamentation consists of single row of spinules close to outer margin anteriorly.

Maxilliped (Fig. 7*G*) prehensile, three-segmented, composed of coxobasis and two-segmented endopod. Coxobasis 1.2 times as long as wide, rhomboidal, ornamented with arched row of large spinules on posterior margin, armed with three setae on inner (median) margin (two unipinnate, one bipinnate). First endopodal segment ~2.8 times as long as wide and 1.8 times as long as coxobasis, ornamented with longitudinal row of very large spinules proximally on anterior surface, one longer row of

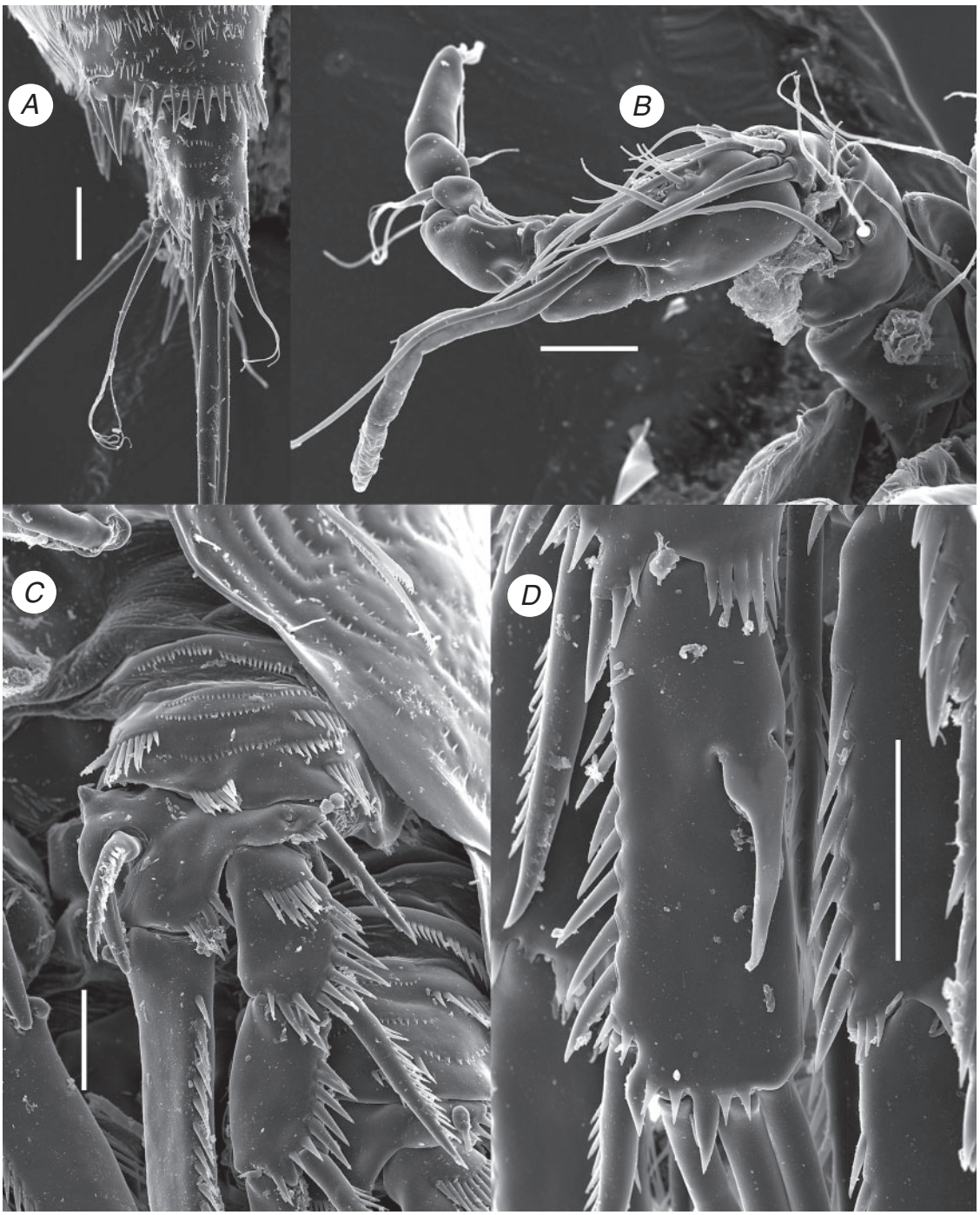

Fig. 11. *Schizopera analspinulosa*, sp. nov., scanning electron micrographs. A, paratype ♂ II; B–D, paratype ♂ III. (*A*) Anal somite and right caudal ramus, lateral view; (*B*) antennula, ventral view; (*C*) proximal part of first swimming leg, anterior view; (*D*) third exopodal segment of third swimming leg, anterior view. Scale bar = 10 μm.

smaller spinules on posterior surface, and one short row of spinules near outer margin proximally; armed with one lateral and one subapical smooth seta. Second endopodal segment only 0.4 times as long as first and 3.3 times as long as wide, armed with one claw-like apical spine and three slender and smooth subapical setae; apical spine 1.4 times as long as second endopodal segment.

All swimming legs (Fig. 8) slender, composed of small triangular preacoxa, large quadrate coxa, smaller basis, three-segmented exopod, and three-segmented endopod. Coxae in all legs connected with intercoxal sclerite. All exopodal and endopodal segments of about same length, except much longer first endopodal segment of first leg.

First swimming leg (Fig. 8*A*) with very small intercoxal sclerite, concave at distal end and unornamented. Preacoxa unarmed, ornamented with posterior row of minute spinules. Coxa also unarmed, but ornamented with several horizontal rows of spinules on anterior surface and two on posterior; anterior spinules grouped into three parallel rows of minute ones, and five groups of large ones (one inner, one distal and three close to outer margin). Basis armed with one inner and one outer strong spine; ornamentation consists of row of spinules at base of each spine, additional row of spines along distal margin, between endopod and exopod, and one cuticular pore near base of outer spine (all on anterior surface). Exopod armed with single outer-distal spine on first and second segments, and with two outer spines and two apical prehensile setae on third segment; all exopodal segments ornamented with strong spinules along outer margin and subdistally, and second segment additionally along inner margin; first exopodal segment with additional arched row of strong spinules on anterior surface proximally; inner prehensile seta on third segment only slightly shorter than entire exopod. Endopod geniculate, with first segment 0.9 times as long as entire exopod, 3.1 times as long as second endopodal segment, and about five times as long as wide; strongly sclerotised beak present proximally on inner margin of first segment, hidden behind inner spine of basis; endopodal armature consists of one strong inner seta on first segment (inserted at about two-thirds), and three setae on third segment (innermost slender and smooth, middle longest and prehensile, outermost spiniform seta (or spine?) 0.6 times as long as middle one); endopodal ornamentation consists of strong spinules along inner margin of all segments, and also along outer margins of first and second segments.

Second swimming leg (Fig. 8*B*) with even smaller preacoxa than in first leg, also unarmed and ornamented only with posterior row of minute spinules. Coxa armed with three horizontal rows of spinules on anterior surface (two groups larger than others), and two diagonal rows of large spinules on posterior surface. Intercoxal sclerite with paired, pointed distal protrusions. Basis armed only with outer spine, ornamented with spinules at base of outer spine and along distal margin at base of endopod. Distal inner corners of first and second exopodal and endopodal segments with hyaline frills. All exopodal and endopodal segments ornamented with strong spinules on outer margins; first and second segments also with less strong spinules along inner margins. Exopod armed with outer-distal spines on first and second segments, inner seta on second segment, two outer spines and two apical setae on third segment; all spines and setae strong, spiniform and bipinnate; outer apical seta on third segment looks like transitional stage between spine and seta, with outer margin furnished with short spinules and inner margin with slender spinules. Endopod armed with single inner seta on second segment, and four elements on third segment: outer-distal short spine, two apical long setae and one inner strong seta (inserted at two-thirds).

Third swimming leg (Fig. 8*C*) very similar to second, except that basis armed with outer slender seta instead of spine, and endopod additionally armed with inner seta on first segment. Also pointed processes on intercoxal sclerite less sharp than in second leg.

Fourth swimming leg (Fig. 8*D*, *E*) very similar to third leg, except that inner seta missing on third endopodal segment, and pointed processes on intercoxal sclerite even less sharp.

Fifth leg (Figs 5*B*, *D*, 6*D*) biramous but exopod fused to baseoendopod on anterior surface (subdivision visible on posterior surface). Baseoendopod with outer basal smooth seta arising from relatively short setophore, without ornamentation at its base. Endopodal lobe trapezoidal, extending almost to posterior margin of exopod, ornamented with small cuticular pore and two small spinules distally, and armed with four very stout, spiniform elements (two inner ones probably spines, two outer ones probably spiniform setae); length ratio of endopodal armature elements, from inner side, 1 : 1.2 : 1 : 0.9. Exopod ovoid, about as long as maximum width, unornamented but armed with five or six elements; two innermost strong and bipinnate, middle one smooth and slender, two or three outermost short, stout and bipinnate; length ratio of exopodal armature elements, from inner side, 1 : 1.9 : 2 : 0.6 : (0.6) : 1.3.

Sixth leg (Fig. 5*D*) indistinct, very small cuticular plate, covering gonopore, armed with one very small spine, fused basally to plate, and two setae; inner seta slender and smooth, ~1.8 times as long as outer seta, plumose along inner margin.

Description of male

Data from allotype and several paratypes. Body length ranges from 375 to 480 µm (405 µm in allotype). Habitus more slender than in female, but also cylindrical, and with similar proportions of prosome–urosome, and cephalothorax–genital somite. Body length–width ratio ~4.2. Ornamentation of prosomites, colour and nauplius eye similar to female.

Genital somite (Fig. 10*A*) twice as wide as long. Single, completely formed, longitudinally placed spermatophore inside first two urosomites in most specimens (not visible in allotype). Abdominal somites similar to female, except that cuticular pores not visible ventrally (Fig. 10*A*). Anal somite (Fig. 10*A*, *B*) very similar to female, including two enlarged dorsal spinules.

Caudal rami (Figs 10*A*, *B*, 11*A*) slightly shorter and less divergent than in female, but with similar armature and ornamentation, except ventral row of minute spinules missing.

Antennula (Figs 10*C*, 11*B*) also as long as cephalothorax, but strongly geniculate and nine-segmented (basically female's sixth segment subdivided), with geniculation between fourth and fifth and seventh and eighth segments. Segments that participate in geniculation strengthened with cuticular plates along anterior surface, largest ones being on sixth segment. Aesthetascs as in female, on fourth and last segments; first one somewhat wider than in female. First two and last two segments similar to female. Setal formula: 1.9.9.10.1.0.1.4.7. Most setae smooth and with pore on top; same setae biarticulated as in female.

Antenna, labrum, mandibula, maxillula, maxilla, maxilliped, exopod and endopod of first swimming leg, exopod of second swimming leg, endopod of third swimming leg, and fourth swimming leg similar to female.

First swimming leg (Figs 10*D*, 11*C*) with modified basis, inner margin of which very rigidly sclerotised, with spiniform, smooth process distally and smaller one proximally. Inner spine on basis smaller than in female, without spinules at its base, inserted more

proximally, and slightly longer than distal spiniform process of basis.

Second swimming leg (Fig. 10*E*, *H*) with transformed endopodal second and third segments. Second segment with part of inner margin protruded as rounded indistinct lobe, without ornamentation on its surface; inner seta shorter than in female, unipinnate and slender. Third segment completely modified; two ancestral apical setae transformed into smooth, spiniform armature elements of about same length; outer one stronger and with abruptly sharpened tip. Ancestral outer spine completely fused to somite, transformed into very strong and smooth thorn, slightly longer than ancestral apical elements. As a result of these transformations, third segment medially cleft. Inner seta on third segment more slender than in female and unipinnate.

Third swimming leg (Figs 10*F*, 11*D*) with very characteristic element on anterior surface of third exopodal segment; this structure swollen at basal part, with pore on top (observable only under scanning electron microscope), inserted at two-fifths and close to inner margin, not reaching distal margin of third segment. Interestingly, structure not clearly demarcated at base; either represents transformed inner armature element, or hugely enlarged tubular pore. First and second exopodal segments of third leg similar to female.

Fifth legs (Fig. 10*G*) with basally fused baseoendopods, ornamented with single pore and two spinules as in female. Endopodal lobe much smaller and shorter, also trapezoidal, extending to middle of exopod in length, armed with two very strong apical spines; inner spine ~1.3 times as long as outer one. Exopod about as long as its maximum width, demarcated basally on both anterior and posterior surface, armed with five elements; fifth element from inner side, sometimes present in female, not observed in male specimens; length ratio of exopodal armature elements, from inner side, 1 : 1.7 : 1.3 : 0.6 : 1.

Sixth legs (Fig. 10*A*) pair of small and short cuticular plates, without armature or ornamentation; left plate wider and larger than right one, and better demarcated at base.

Variability

Female fifth leg exopod can be ornamented with five or six elements (arrowed in Fig. 5*B*). In the holotype (Fig. 5*B*) and one paratype female (Fig. 5*D*) six setae are present on left side, while the right side has five setae. One other dissected paratype female had six setae on exopods of both sixth legs. Minute details of somite ornamentation can vary slightly between specimens (Fig. 9*A*, *B*), but never in such a way that a complete row or a group of spinules would be absent. Caudal rami shape and enlarged spines on anal somite (Figs 6*B*, 9*C*, *E*) are remarkably conservative.

Distribution

This species was found only in the type locality, bore SB14–1 (south-western corner of the area investigated), where it was collected on three separate occasions (Figs 1, 40).

Remarks

Schizopera analspinulosa, sp. nov. differs from all previously described species by its two enlarged spinules on either side of the anal sinus, which are very strongly chitinised and thus strongly refract light, so they are visible even under a dissecting microscope (arrowed in Figs 3*A*, 6*C*). It is closely related to *S. kronosi*, sp. nov. (see below), which also has similar spinules on the anal somite. The two species can be distinguished by several characters. The most obvious one, and the easiest to check, is the size and robustness of the outer exopodal setae on the fifth leg, which can be observed without a need to dissect the specimen (arrowed in Figs 3*A*, *B*, 5*B*, 15*A*, 16*G*). Especially significant is the reduction of the outermost exopodal seta in the latter species. Other differences include numerous reductions in size of the armature elements on the swimming legs and the fifth leg in *S. kronosi* (arrowed in Fig. 16), as well as a convex inner margin of the distal part of caudal rami (arrowed in Fig. 15*B*). This margin is always nearly straight in *S. analspinulosa*. Morphological differences between the two subspecies of *S. analspinulosa* are discussed below, and they are all very small indeed.

Some molecular data suggest that *S. analspinulosa* is relatively closely related to *S. akolos*, sp. nov. (Fig. 39*A*), but the two species could not be more morphologically different (see below). The latter species has many reductions that are probably a result of its diminution. All species from Yeelirrie, except *S. akolos* and *S. akation*, sp. nov. (see below), have two sensilla and two pores at the base of the rostrum and heavily ornamented somites. Somites of *S. akation*, *S. akolos*, and two outgroups from the Pilbara region look rather smooth (see Figs 19, 20, 38*C*, *D*).

Relatively similar caudal rami shape to that of *S. analspinulosa* can be found in the following three species: *S. brusinae* Petkovski, 1954, described from the Adriatic Sea, Croatia; *S. taricheana* Por, 1968, from the Sea of Galilee, Israel; and *S. haitiana* Kiefer, 1934 from Haiti (see Kiefer 1934; Petkovski 1954; Por 1968). This, in our view, is either a result of convergent evolution or (more probably) a plesiomorphic character, as all three species differ from *S. analspinulosa* by many characters. For example, *S. brusinae* has an unusually short outer apical seta on the caudal rami, while *S. taricheana* lacks inner seta on the second endopodal segment of the fourth leg, and *S. haitiana* has a much more reduced baseoendopod of the female fifth leg. All three, as well as all other known species from this genus, lack enlarged dorsal spinules on the anal somite, which is a synapomorphy for *S. analspinulosa* s. str., *S. a. linel* and *S. uranusi*.

Etymology

The new species is named after two characteristically enlarged spinules (cuticular ornamentation elements) on the posterior margin of the anal somite (Fig. 6*C*), which can be observed even under a dissecting microscope (Fig. 3*A*). The name is composed of two Latin adjectives, *anal* (same meaning as in English) and *spinulosus* (i.e. thorny), agreeing in gender with the feminine genus name.

Schizopera analspinulosa linel, ssp. nov.

(Figs 12–14)

Material examined

Name-bearing type. Holotype (WAM C37474), adult ♀ completely dissected on 1 slide in Faure's medium, 18.iii.2010, leg. T. Karanovic and S. Callan (seLN7139).

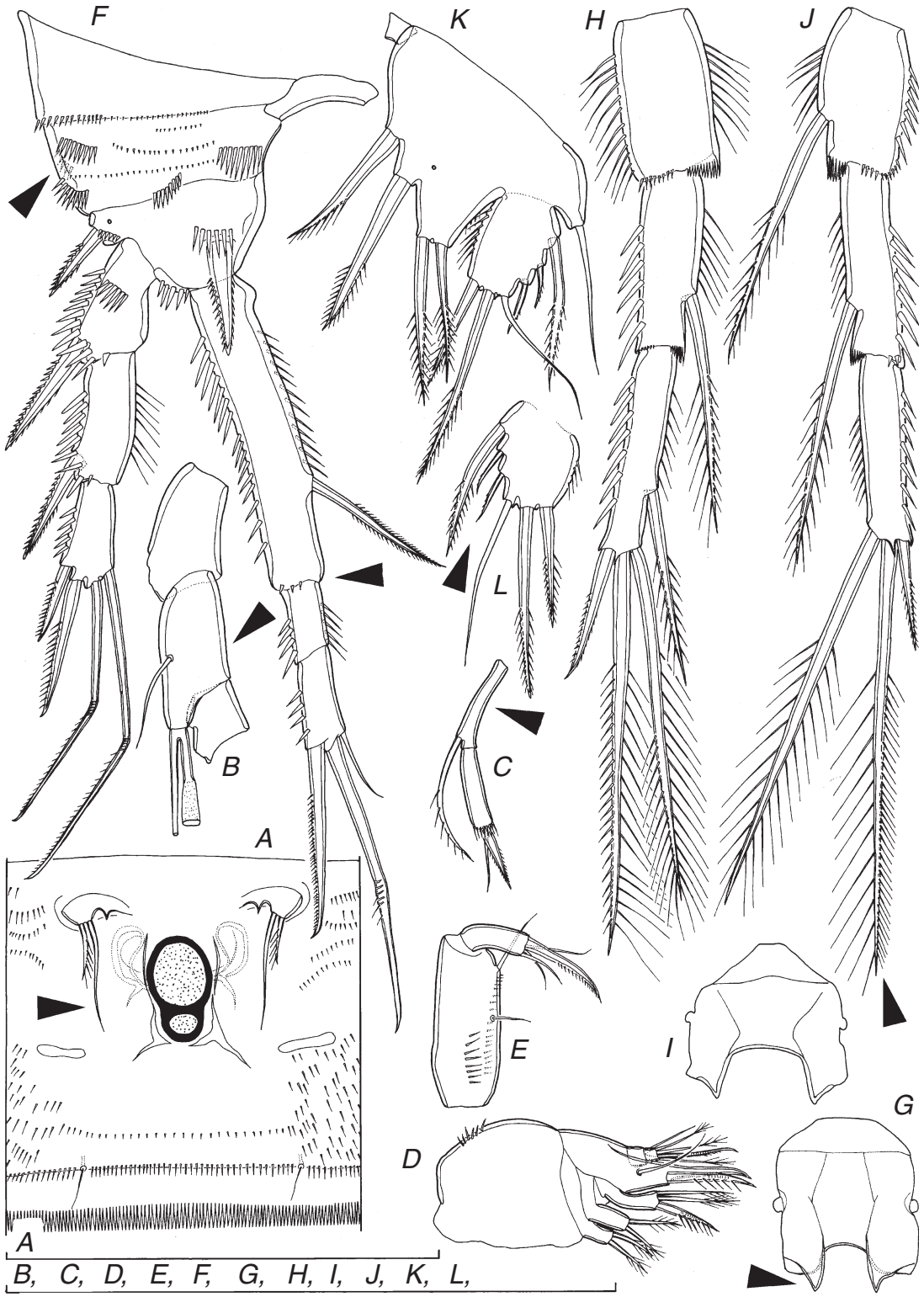

Fig. 12. *Schizopera analspinulosa linel*, ssp. nov., holotype ♀. (*A*) Genital filed, ventral view (flattened); (*B*) third to fifth segments of antennula with incomplete armature, ventral view; (*C*) exopod of antenna, dorsal view; (*D*) maxilla, anterior view; (*E*) distal part of maxilliped, anterior view; (*F*) first swimming leg; (*G*) intercoxal sclerite of second swimming leg, anterior view; (*H*) endopod of second swimming leg, anterior view; (*I*) intercoxal sclerite of fourth swimming leg; (*J*) endopod of fourth swimming leg; (*K*) left fifth leg (dissected and flattened); (*L*) exopod of right fifth leg. Arrows point to most prominent subspecific microcharacters. Scale bar = 100 μm.

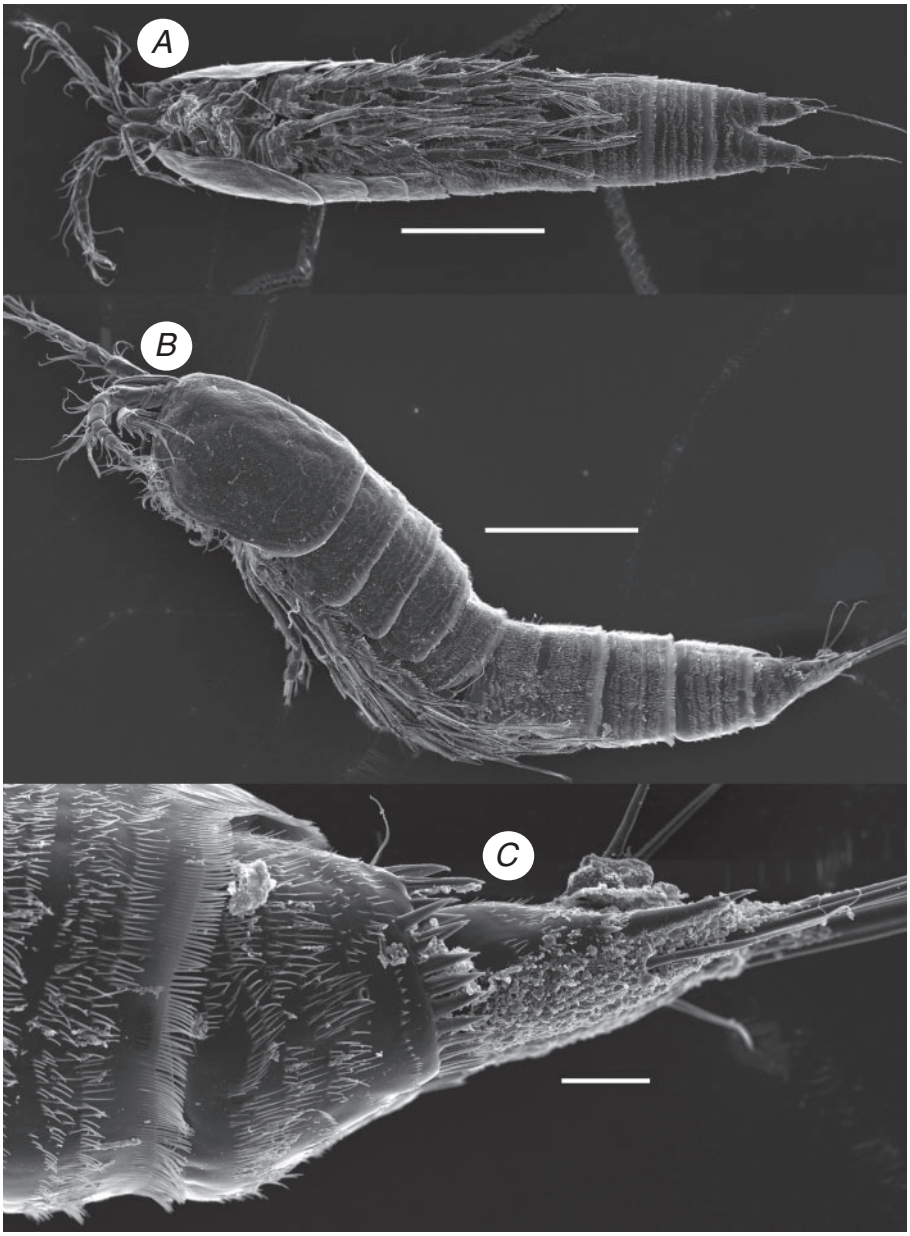

Fig. 13. *Schizopera analspinulosa linel*, ssp. nov., scanning electron micrographs. A, paratype ♀ I; B and C, paratype ♀ II. (*A*) Habitus, ventral view; (*B*) habitus, lateral view; (*C*) last two urosomal somites and left caudal ramus, lateral view. Scale bars A, B = 100 µm; C = 10 µm.

Type locality. Australia: Western Australia: Yilgarn region, Yeelirrie station, bore line L, bore L-UNK1, 27.329832°S 120.150590°E.

Additional material examined. All from type locality: allotype (WAM C37475), adult ♂ dissected on 1 slide, 18.iii.2010, leg. T. Karanovic and S. Callan (seLN7139); 7 paratype ♂ + 4 paratype ♀ + 3 paratype copepodids (WAM C37476), together in ethanol, 18.iii.2010, leg. T. Karanovic and S. Callan (seLN7139); 3 paratype ♂ and 2 paratype ♀ on 1 SEM stub (WAM C37477), 18.iii.2010, leg. T. Karanovic and S. Callan (seLN7139); paratype ♀ dissected on 1 slide, 18.iii.2010, leg. T. Karanovic and S. Callan (seLN7139); paratype ♂ dissected on 1 slide, 18.iii.2010, leg. T. Karanovic and S. Callan (seLN7139); 5 ♂ + 1 ♀ together in ethanol, 16.iii.2010, leg. T. Karanovic and G. Perina (seLN8533); 1 ♀ destroyed for DNA sequence, 16.iii.2010, leg. T. Karanovic and G. Perina (seLN8533); 1 ♀ in ethanol, 14.xi.2009, leg. P. Bell and G. Perina (seLN7315); 1 ♀ destroyed for DNA sequence, 12.i.2010, leg. T. Karanovic and S. Callan (seLN7360).

Description of female

Data from holotype and several paratypes. Total body length, measured from tip of rostrum to posterior margin of caudal rami (excluding caudal setae), ranges from 455 to 610 µm (510 µm in holotype). Colour of preserved specimen yellowish. Nauplius eye not visible. Habitus (Fig. 13*A*, *B*)

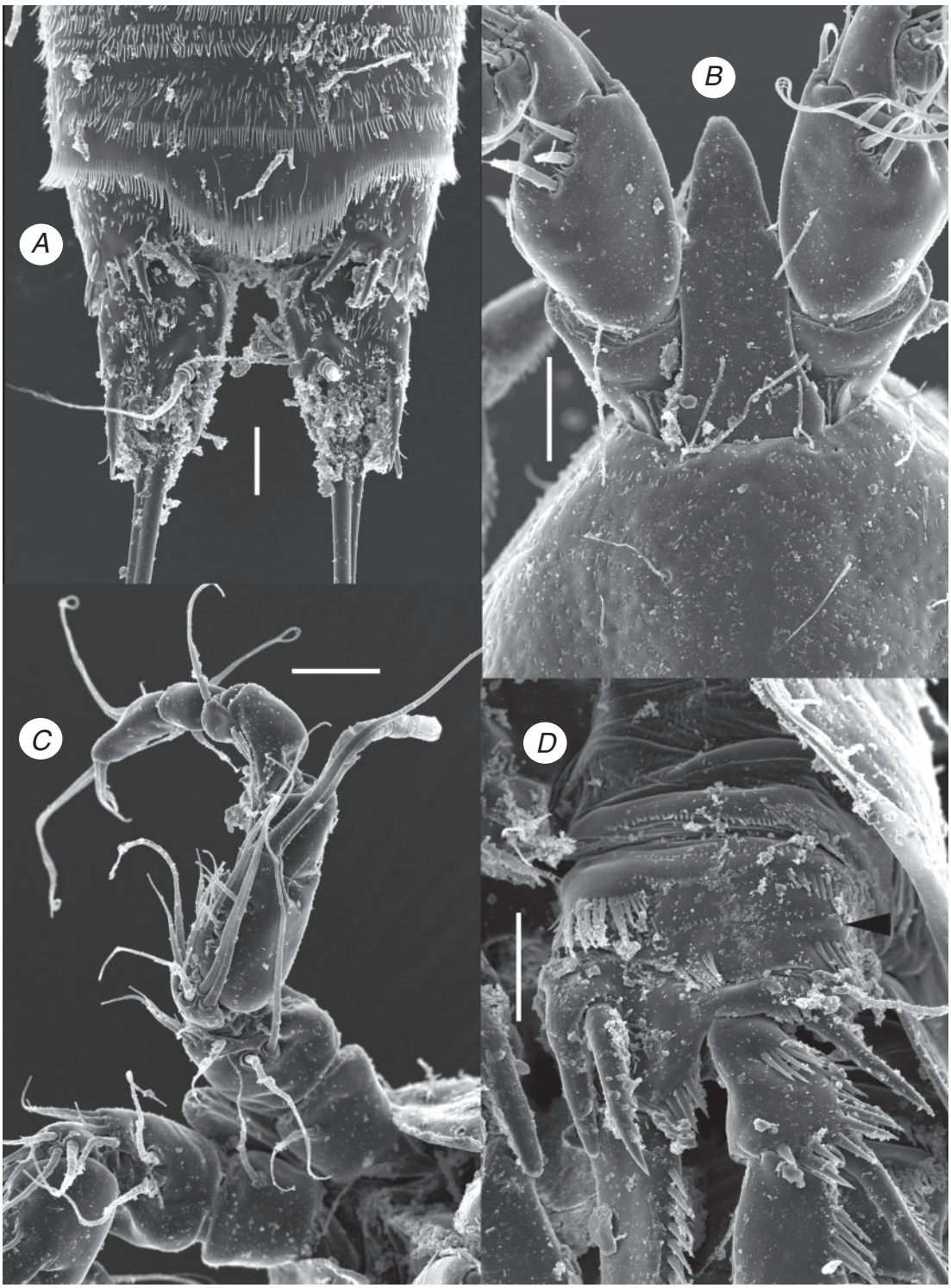

Fig. 14. *Schizopera analspinulosa linel*, ssp. nov., scanning electron micrographs. A and B, paratype ♂ I; C and D, paratype ♂ II. (*A*) Last two urosomal somites and caudal rami, dorsal view; (*B*) anterior part of cephalothorax with rostrum and antennulae, dorsal view; (*C*) left antennula, ventral view; (*D*) proximal part of first swimming leg, anterior view. Scale bars = 10 µm.

cylindrical, somewhat more slender than in nominotypical subspecies, without distinct demarcation between prosome and urosome; prosome–urosome ratio ~1.1 (in dorsal view); greatest width at posterior end of cephalothorax. Body length–width ratio ~4.5; cephalothorax 1.27 times as wide as genital double somite. Free pedigerous somites without pronounced lateral dorsal

expansions. Integument relatively strongly chitinised. All somites (except cephalothorax) and caudal rami, besides other ornamentation, with dense cover of minute spinules (Fig. 13). Rostrum and cephalothoracic shield as in nominotypical species, although cuticular pores at base of rostrum slightly more anterior. Sensilla and pore pattern on all somites also as in nominotypical subspecies, and cephalothoracic shield also with dense pattern of shallow pits, each with central stria. Hyaline fringe of cephalothoracic shield smooth and unornamented, those of other prosomites finely serrated dorsally and partly laterally, with smooth ventrolateral corners, but this smooth area larger than in nominotypical subspecies, especially on third pedigerous somite (Fig. 13*B*). Anal somite with slightly more slender minute spinules on ventral side (Fig. 13*C*).

Genital double somite (Fig. 12*A*) ~0.8 times as long as wide (dorsal view). Epicopulatory bulb large, ovoid, ~1.7 times as long as wide. Seminal receptacles very small, ovoid, but reaching beyond anterior margin of epicopulatory bulb, ~0.55 times as long as epicopulatory bulb. Ornamentation of urosomal somites and serration of hyaline fringes as in nominotypical subspecies.

Caudal rami (Fig. 13*C*) usually very dirty and fine ornamentation hard to distinguish, but no differences observed from nominotypical subspecies.

Antennula with somewhat more elongated fourth segment (arrowed in Fig. 12*B*), as well as first exopodal segment of antenna (arrowed in Fig. 12*C*). Other details of antennula, antenna, labrum, mandibula, maxillula, maxilla (Fig. 12*D*) and maxilliped (Fig. 12*E*) as in nominotypical subspecies.

First swimming leg (Fig. 12*F*) with very small intercoxal sclerite, slightly concave at distal end and unornamented. Coxal ornamentation similar to nominotypical subspecies, both middle group of large spinules on anterior surface missing (arrowed up in Fig. 12*F*). First endopodal segment also longer (arrowed down in Fig. 12*F*), as long as or slightly longer than entire exopod, four times as long as second endopodal segment, and about five times as long as wide.

Second swimming leg (Fig. 12*G*, *H*) with less sharp distal protrusions on intercoxal sclerite (arrowed in Fig. 12*G*), and somewhat more elongated apical setae on third endopodal segment (Fig. 12*H*). Third swimming leg as in nominotypical subspecies.

Fourth swimming leg (Fig. 12*I*, *J*) with somewhat more slender apical setae on third endopodal segment (arrowed in Fig. 12*J*), but with equally blunt protrusions on intercoxal sclerite (Fig. 12*I*).

Fifth leg (Fig. 12*K*, *L*) with slightly more elongated exopod than in nominotypical subspecies, but always armed with six elements and fourth and fifth elements from inner side much smaller and more slender (arrowed in Fig. 12*L*). Latter character very reliable and easily observable even without dissecting specimens. Note: sixth element equally long and strong as in nominotypical subspecies.

Sixth leg (Fig. 12*A*) with longer inner seta (arrowed), ~2.5 times as long as outer seta.

Description of male

Data from allotype and several paratypes. Body length ranges from 410 to 520 µm (475 µm in allotype). Habitus more slender than in female, but also cylindrical, and with similar proportions of prosome–urosome, and cephalothorax–genital somite. Body length–width ratio ~4.7. Ornamentation of prosomites, colour and nauplius eye similar to female. Ornamentation of urosomites also very similar to female and that of nominotypical subspecies, including shape and size of pseudoperculum on preanal somite (Fig. 14*A*). Enlarged spinules next to anal sinus equally well developed. Rostrum (Fig. 14*B*) slightly more elongated than in female, but ornamentation of cephalothoracic shield without any differences.

Caudal rami (Fig. 14*A*) slightly less divergent than in female, but with similar armature and ornamentation.

Antennula (Fig. 14*C*) segmentation and armature as in nominotypical subspecies down to most minute details.

Antenna, labrum, mandibula, maxillula, maxilla, maxilliped, exopod and endopod of first swimming leg, exopod of second swimming leg, endopod of third swimming leg, and fourth swimming leg similar to female.

First swimming leg (Fig. 14*D*) similar to that in nominotypical subspecies, but middle row of large spinules on anterior surface missing (arrowed), just as in female. Endopod of second leg, exopod of third leg, fifth leg, and sixth leg as in nominotypical subspecies.

Variability

Female fifth leg exopod can be more or less elongated (Fig. 12*K*, *L*), but it is always armed with six elements. No other forms of variability observed, except in body size.

Distribution

This subspecies was found only in the type locality, bore L-UNK1 on the bore line L, where it was collected on four separate occasions (Fig. 40).

Remarks

This subspecies differs from the nominotypical subspecies very little morphologically, and the main characters include a more slender habitus (Fig. 13*A*, *B*), absence of the middle group of large spinules on coxa of the first leg (arrowed in Figs 12*F*, 14*D*), and shorter and thinner middle and distal outer setae on the fifth leg exopod (arrowed in Fig. 12*L*). However, these differences are consistent in all specimens examined, and show very little variability. Proportionately longer setae on the swimming legs (arrowed in Fig. 12*J*), as well as the first endopodal segment of the first leg (arrowed in Fig. 12*F*), fourth segment of the antennula (arrowed in Fig. 12*B*), and the first exopodal segment on the antenna (Fig. 12*C*) are probably all related to a more slender habitus, as is the more slender epicopulatory bulb (arrowed in Fig. 12*A*). The only other difference that we found between these two subspecies is the sharpness of the distal processes on the innercoxal sclerite of the second leg (Fig. 12*G*). All other morphological characters are the same, down to the last minute detail of spinules, pores and sensilla ornamentation (compare, for example, Figs 9*B* and 9*C*, 13*B* and 9*D*, 13*C* and 9*E*, 14*B* and 11*B*, 14*A* and 11*C*, 14*C* and 14*D*).

However, the *COI* sequence data suggest a divergence of 15.8% between these two populations (Table 3), and such high divergence values are often indicative of distinct species by

comparison with other crustaceans (Leféb ure *et al*. 2006). We believe that these divergences may have resulted from a long-term isolation of populations of the same species within different geographic regions of the Yeelirrie calcrete (further discussed in the 'Discussion' section below). Also, one should not completely exclude a possibility of existence of additional populations between line L and bore SB14, which may bridge the molecular gap and enable some limited gene flow, even though our sampling at line N failed to produce any specimens (see Fig. 40). However, our sampling was limited by the amount of available bores and wells in calcrete environments, and none were present between the line N and bore SB14, for example. Many other bores and pastoral wells in sediments other than calcrete (alluvial sands, clays etc.) were sampled during this study, but they typically produced no stygofauna.

Etymology

The subspecific name comes from the line of bores where it was collected (Line L). It comprises an arbitrary combination of letters that can be treated as a Latin word, and should be conceived as a noun in apposition to the generic name.

Schizopera kronosi, sp. nov.

(Figs 3*B*, 15, 16)

Material examined

Name-bearing type. Holotype (WAM C37478), adult female, completely dissected on 1 slide in Faure's medium, 17.iii.2010, leg. S. Callan and N. Krawczyk (seLN8393).

Type locality. Australia: Western Australia: Yilgarn region, Yeelirrie station, bore line 3.5, bore YYAC328, 27.175601°S 119.907658°E.

Additional material examined. Paratype ♀ dissected on 1 slide, 17.iii.2010, leg. S. Callan and N. Krawczyk (seLN8393), type locality; paratype ♀ destroyed for DNA sequence, 17.iii.2010, leg. S. Callan and N. Krawczyk (seLN8393), type locality; 1 ♀ destroyed for DNA sequence, 27.viii.2009, leg. P. Bell and S. Callan (seLN7308), bore line 2, bore YYAC1007A, 27.165236°S 119.883142°E; 1 copepodid destroyed for DNA sequence, 12.xi.2009, leg. P. Bell and G. Perina (seLN7417), bore line 1.5, bore YYAC35, 27.166173°S 119.873977°E; 3 ♀ together in ethanol, 18.iii.2010, leg. T. Karanovic and S. Callan (seLN8563), bore line H, bore TPB-33, 27.133739°S 119.827871°E; 1 ♀ in ethanol, 14.i.2010, leg. T. Karanovic and S. Callan (seLN7357), same locality; 1 ovigerous ♀ in ethanol, 18.iii.2010, leg. T. Karanovic and S. Callan (seLN8459), bore line K, bore YYHC0049K, 27.247548°S 120.054862°E; 1 ♂ in ethanol, 20.iii.2010, leg. T. Karanovic and S. Callan (seLN8464), same locality; 1 ♀ in ethanol, 16.iii.2010, leg. S. Callan and N. Krawczyk (seLN8514), bore line 2, bore YYAC1006B, 27.170328°S 119.868867°E; 1 ♀ dissected on 1 slide, 12.xi.2009, leg. P. Bell and G. Perina (seLN7389), bore line 3, bore YYAC118, 27.174573°S 119.889727°E; 1 ♀ in ethanol, 12.i.2010, leg. P. Bell and G. Perina (seLN7701), bore line 5, bore YYAC0014D, 27.185508°S 119.929231°E.

Description of female

Data from holotype and several paratypes. Total body length, measured from tip of rostrum to posterior margin of caudal rami (excluding caudal setae), ranges from 405 to 550 µm (422 µm in holotype). Colour of preserved specimen yellowish. Nauplius eye not visible. Habitus (Fig. 3*A*) cylindrical, but more robust than in previous species, without distinct demarcation between prosome and urosome; prosome–urosome ratio ~1.3 (in dorsal view); greatest width at posterior end of cephalothorax. Body length–width ratio ~3.5; cephalothorax 1.2 times as wide as genital double somite. Free pedigerous somites without pronounced lateral dorsal expansions. Integument relatively strongly chitinised. All somites (except cephalothorax) and caudal rami, besides other ornamentation, with rows of minute spinules, but much less on prosomal somites than in previous species (inset in Fig. 3*B*). Rostrum (Fig. 16*A*) long and clearly demarcated at base, reaching more than two-thirds of second antennular segment, linguiform (in dorsal view) but with sharp tip, about twice as long as wide; ornamented with two sensilla dorsolaterally. Surface of cephalothoracic shield and tergites of first three free pedigerous somites with same pattern of large sensilla and small cuticular pores as in *S. analspinulosa*, but hyaline fringes of second and third pedigerous somites not serrated dorsally or laterally (Fig. 3*B*). Fifth pedigerous somite (first urosomal) ornamented with four dorsal large sensilla and two lateral sensilla (one on each side), as well as with two cuticular pores ventrolaterally (one on each side), in addition to several rows of minute cuticular spinules; hyaline fringe serrated but more finely than in previous species (inset in Fig. 3*B*).

Genital double somite (Fig. 15*A*) ~0.8 times as long as wide (ventral view), with visible lateral suture internally; ornamented with eight sensilla dorsally (six at midlength, two near posterior margin), two posterior sensilla ventrally, and two posterior sensilla and two midlength pores laterally (one on each side), in addition to numerous rows of minute spinules (interrupted at midlength, dorsally and laterally, revealing smooth area that corresponds to internal suture and marks ancestral segmentation); hyaline fringe sharply serrated both ventrally and dorsally. Epicopulatory bulb large, ovoid, ~1.3 times as long as wide. Seminal receptacles relatively large, ovoid, reaching beyond anterior margin of epicopulatory bulb, ~0.7 times as long as epicopulatory bulb. Third urosomite ornamented with six posterior sensilla (two dorsal, two ventral and two lateral) but without ventral pores at midlength (Fig. 15*A*), in addition to numerous rows of slender spinules of various sizes; hyaline fringe serrated and straight. Preanal somite without sensilla, ornamented with two ventral pores at midlength but further apart than in previous species (Fig. 15*A*) and many rows of minute spinules; hind margin clearly bulging posteriorly in dorsal region, forming very sharply serrated pseudoperculum (Fig. 15*B*). Anal somite (Fig. 15*A–C*) with convex and very short anal operculum ornamented with transverse row of spinules along posterior margin; ornamented with two large sensilla dorsally, two large lateral cuticular pores, two ventromedian pores, two transverse rows of slender spinules laterally (one at middle, one in proximal part), and transverse row of large spinules along posterior margin; two most dorsal of those posterior spinules characteristically enlarged and strongly fused basally to somite as in previous species. Anal sinus widely opened and ornamented with two diagonal rows of slender spinules; represents only 48% of somite's width.

Caudal rami (Fig. 15*A–C*) strongly sclerotised, ~1.6 times as long as greatest width in dorsal view, almost cylindrical but tapering towards caudal end, with convex inner margin distally (arrowed in Fig. 15*B*), slightly divergent, with space between

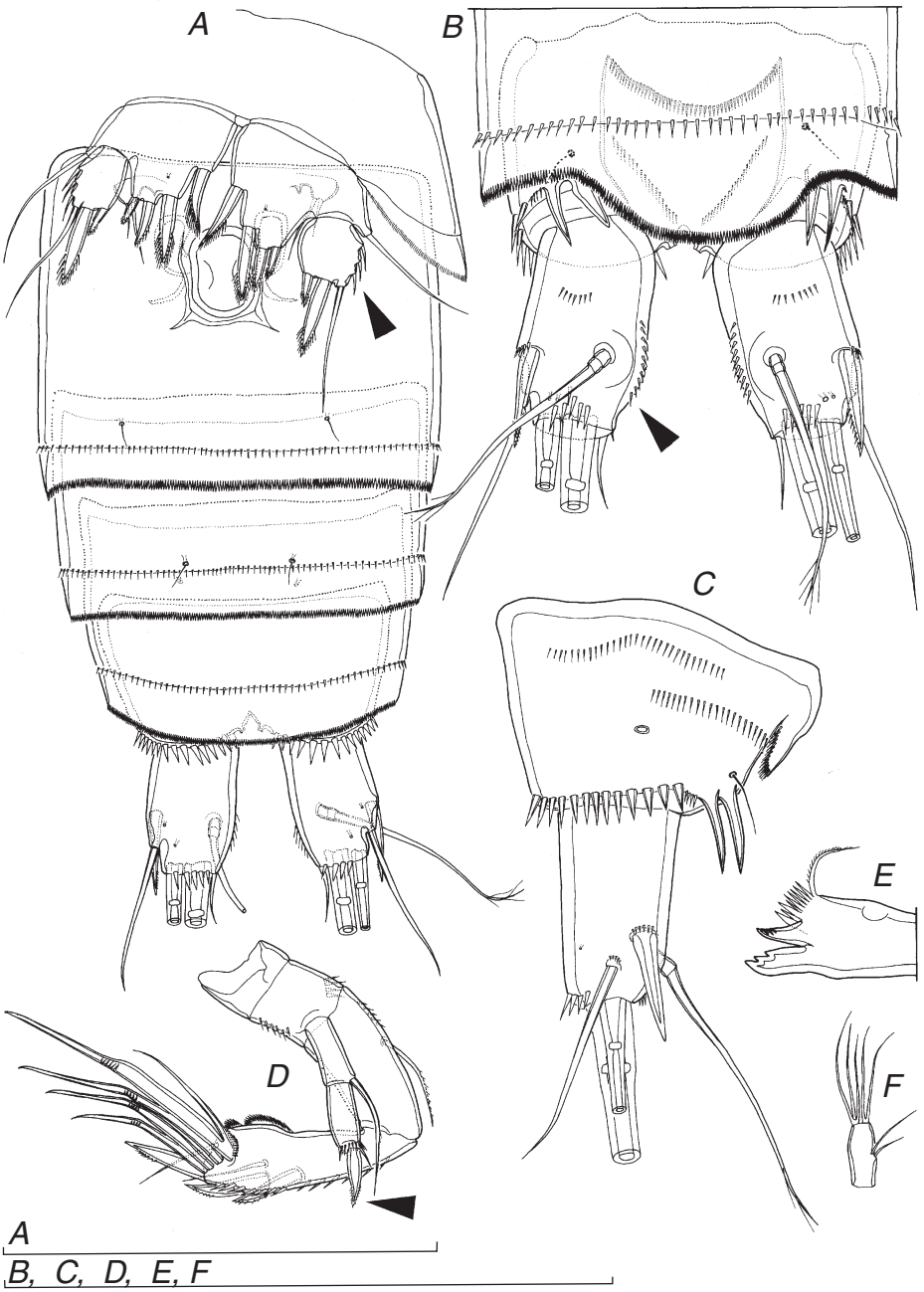

Fig. 15. *Schizopera kronosi*, sp. nov., holotype ♀. (*A*) Urosome with partly detached first somite, ventral view; (*B*) last two urosomal somites and caudal rami, dorsal view; (*C*) anal somite and left caudal ramus, lateral view; (*D*) antenna, dorsal view; (*E*) cutting edge of mandibula, anterior view; (F) endopod of mandibula, anterior view. Note: A, B, and C without minute spinules drawn. Arrows point to characters different from previous species. Scale bars = 100 μm.

them less than half of one ramus width; ornamented with two ventral and two dorsal cuticular pores in posterior half, transverse row of several large spinules along posterior margin dorsally and ventrally, and one short row of minute spinules dorsally and medially (no spinules ventrally, and only several small ones laterally at base of lateral armature); armed with six elements (two lateral, one dorsal and three apical). Dorsal seta slender and apically pinnate, ~1.2 times as long as ramus, inserted at two-thirds of ramus length, triarticulate. Lateral proximal spine stout, inserted at three-quarters of ramus length, 0.5 times as long as ramus. Lateral distal seta very slender, smooth, inserted slightly ventrolaterally at four-fifths of ramus length, about as long as ramus. Inner apical seta short and smooth, 0.3 times as long as ramus. Principal apical setae with breaking planes; middle apical

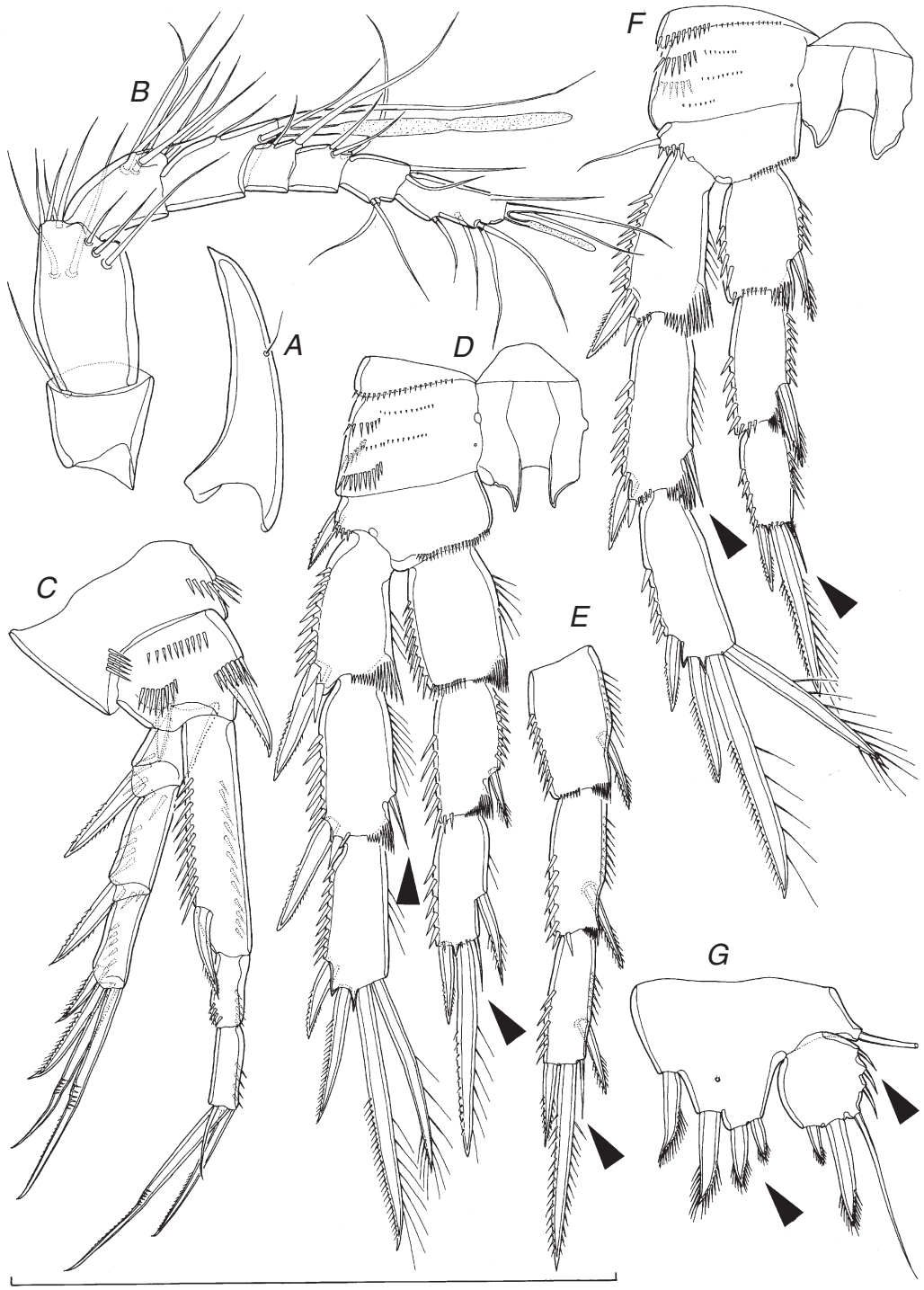

Fig. 16. *Schizopera kronosi*, sp. nov., holotype ♀. (*A*) Rostrum, lateral view; (*B*) antennula, dorsal view; (*C*) first swimming leg, anteroventral (anteromedian) view; (*D*) second swimming leg, anterior view; (*E*) endopod of third swimming leg, anterior view; (*F*) fourth swimming leg, anterior view; (*G*) fifth leg, anterior view. Arrows point to characters different from previous two species. Scale bar = 100 µm.

seta strongest, bipinnate at distal end, twice as long as unipinnate outer apical seta, and ~0.7 times as long as body length.

Antennula (Fig. 16*B*) eight-segmented, unornamented, ~0.7 times as long as cephalothorax, with short aesthetasc on eighth segment, fused to two apical setae, and large aesthetasc on fourth segment, reaching significantly beyond tip of appendage and fused basally to equally long seta; setal formula: 1.9.7.3.2.3.4.7. Only two lateral setae on seventh segment and four on

eighth segment biarticulate. All setae smooth and slender. Length ratio of antennular segments, from proximal end, 1 : 1.3 : 0.7 : 0.7 : 0.4 : 0.4 : 0.5 : 1.

Antenna (Fig. 16*D*) segmentation as in previous species, as well as armature formula and ornamentation; apical spine on second exopodal segment much shorter and bulbous at proximal end (arrowed in Fig. 15*D*); endopodal armature also somewhat shorter and stronger.

Labrum as in previous species.

Mandibula (Fig. 15*E*, *F*) with narrower cutting edge of coxa than in previous species but same armature and ornamentation; endopod slightly less arched but also armed with two lateral and five apical smooth setae.

Maxillula, maxilla and maxilliped with slightly shorter spiniform elements than in previous species, but without any difference in armature or ornamentation.

All swimming legs (Fig. 16*C–F*) with more slender coxa and with shorter and wider endopodal and exopodal segments and all armature; segmentation, armature formula and most ornamentation details as in previous species.

First swimming leg (Fig. 16*C*) mounted in a slightly awkward position but all structures easily observable. Coxa ornamentation as in *S. analspinulosa linel*, i.e. with only two rows of large spinules on anterior surface close to outer margin. Basis with additional row of spinules medially at basal part, making two rows of spinules at base of inner spine. Second exopodal segment without ornamentation on inner margin. First endopodal segment without cuticular beak basally and with much shorter inner seta than in previous species, 0.8 times as long as entire exopod, 3.3 times as long as second endopodal segment, and about four times as long as wide.

Second swimming leg (Fig. 16*D*) with small preacoxa and very narrow coxa, only 1.4 times as wide as long, but ornamented with same rows of spinules as in previous species. Intercoxal sclerite with large and sharp distal protrusions, although not as sharp as in *S. a. analspinulosa*. Basis as in previous species. All exopodal and endopodal segments shorter and wider than in previous species, and all armature elements much shorter; especially reduced in size inner element on second exopodal segment and innermost apical element on third endopodal segment, also smooth and slender (arrowed in Fig. 16*D*).

Third swimming leg (Fig. 16*E*) very similar to second, except that basis armed with outer slender seta instead of spine, and endopod additionally armed with inner seta on first segment. Inner element on second exopodal segment and innermost apical element on third endopodal segment also reduced in size, smooth and slender (latter arrowed in Fig. 16*E*). Pointed processes on intercoxal sclerite less sharp than in second leg, as in previous species.

Fourth swimming leg (Fig. 16*F*) very similar to third leg, except that inner seta missing on third endopodal segment, and pointed processes on intercoxal sclerite even less sharp. Distal group of large spinules on anterior surface of coxa also missing. Inner element on second exopodal segment and innermost apical element on third endopodal segment reduced in size and as in second and third leg, smooth and slender (both arrowed in Fig. 16*F*).

Fifth leg (Fig. 16*G*) biramous, with exopod clearly demarcated from baseoendopod on both anterior and posterior surfaces. Baseoendopod with outer basal smooth seta arising from relatively short setophore, without ornamentation at its base. Endopodal lobe trapezoidal, extending almost to posterior margin of exopod, ornamented only with small cuticular pore at distal part on anterior surface, and armed with four very stout, spiniform elements; two inner elements of about same size, 1.5 times as long as next element and twice as long as outermost element (last two arrowed in Fig. 16*G*); length ratio of endopodal armature elements, from inner side, 1 : 1 : 0.7 : 0.5. Exopod ovoid (almost round), about as long as maximum width, unornamented but armed with six armature elements; two innermost strong and bipinnate, middle one smooth and slender, three outermost very small and smooth; length ratio of exopodal armature elements, from inner side, 1 : 2.4 : 4 : 0.8 : 0.7 : 0.7. Reduced size of outermost exopodal element observable even without dissection and reliable specific character (arrowed in Figs 3*B*, 16*G*).

Sixth leg (Fig. 9*A*) indistinct, very small cuticular plate, covering gonopore, armed with one very small spine, fused basally to plate, and two smooth and slender setae; inner seta 1.8 times as long as outer one.

Male

Unknown.

Variability

Except for the difference in body length, no other variable features were observed. Exopod of the right fifth leg (Fig. 15*A*) that appears to be narrower than the same structure on the left leg is just a consequence of a different angle of observation. As in many other harpacticoid species, most intraspecific differences in body length are a result of the different extension (retraction) of the telescopic body somites (especially urosomites). For example, in the holotype specimen the anal somite is hardly visible outside the preanal one both ventrally and dorsally (Fig. 15*A*, *B*).

Distribution

This species was found, always in very low numbers, on the following bore lines, from north-west to south-east: H, 1.5, 2, 3, 3.5, 5 and K (Fig. 40).

Remarks

Like both of the above described subspecies of *Schizopera analspinulosa*, *S. kronosi* differs from all previously described species by its two enlarged spinules on either side of the anal sinus, which are very strongly chitinised (arrowed in Fig. 3*B*, but see also Fig. 15*B*, *C*). These ornamentation elements are bizarre structures, which seem unlikely to have evolved convergently in these three taxa, especially as all other morphological characters point to a close relationship. The fact that these synapomorphies are not some reductions in subterranean environments, but newly gained features, gives confidence in speculating that these three taxa represent a monophyletic clade. However, the new species can be distinguished from *S. analspinulosa* by several characters. The most obvious one is the size and robustness of the outer exopodal setae on the fifth leg, which can be observed without dissection (arrowed in Figs 3*A*, *B*, 5*B*, 15*A*, 16*G*). Especially significant is the reduction of the outermost exopodal seta in

S. kronosi. Other differences include numerous reductions in size of armature elements on the swimming legs and the fifth leg (arrowed in Fig. 16), and a convex inner margin of the distal part of caudal rami (arrowed in Fig. 15*B*). Although all setae and some spines on the second to fifth legs are shorter than those in *S. analspinulosa*, the innermost apical setae on the ultimate endopodal segments and inner setae on the second exopodal segments of the second to fourth legs are especially reduced in size, and slender and smooth. Prosomal somites of *S. kronosi* are somewhat less ornamented than in *S. analspinulosa* (compare insets in Fig. 3*A*, *B*), but urosomal somites are hardly different at all. In addition to these morphological characters, the *COI* sequence data (Fig. 39; Table 3) suggest divergences between these two taxa in excess of 20%, which are normally indicative of distinct species (Lefébure *et al*. 2006).

Schizopera kronosi is a rare species, but with a relatively wide distribution. It lives in the biggest patch of calcrete sympatrically with five other species, and was frequently found in the same bore with other congeners. It was found alone in only one sample (seLN7701). In four samples it was found together with *S. uranusi* (seLN7308, 8563, 7357 and 8514); in three samples with *S. leptafurca* (seLN8393, 7417 and 8459); and in two samples it was found together with *S. leptafurca* and *S. akation*, sp. nov. (seLN8464 and 7389). In all these samples, dominant species were either *S. uranusi* or *S. leptafurca*, while *S. kronosi* was represented with one or a few specimens. We explore this further and offer some possible explanations in the 'Discussion' section below.

Only one species of *Schizopera* has similarly shaped caudal rami in ventral view to those of *S. kronosi*: *S. baltica* Lang, 1965. It was described from the Baltic Sea, Sweden, by Lang (1965*b*), and can be distinguished from *S. kronosi* by more slender setae on all swimming legs and on the fifth leg, as well as by the absence of enlarged dorsal spinules on the anal somite. It is probable that this species resembles what a marine ancestor of today's *kronosi* +*analspinulosa*+*a. linel* clade looked like, before starting to invade subterranean waters of the Yeelirrie palaeochannel.

Etymology

In Ancient Greek mythology Kronos was the leader of the first generation of Titans, divine descendants of Gaia and Uranus. The specific name is a noun in the genitive singular. The name refers to a close relationship with Uranus, the ancient Greek deity of the sky, which gave name to a planet in our solar system, which in turn gave name to a chemical element, uranium, one of the important mineral deposits in the distribution range of this species.

Schizopera akation, sp. nov.

(Figs 4*C*, 17–21)

Material examined

Name-bearing type. Holotype (WAM C37479), adult female, completely dissected on 1 slide in Faure's medium, 18.iii.2010, leg. T. Karanovic and S. Callan (seLN8182).

Type locality. Australia: Western Australia: Yilgarn region, Yeelirrie station, bore SB14–1, 27.344283°S 120.307708°E (south-eastern corner on Fig. 1).

Additional material examined. Allotype (WAM C37480), adult ♂ dissected on 1 slide, 18.iii.2010, leg. T. Karanovic and S. Callan (seLN8182), type locality; 2 paratype ♂+2 paratype ♀ (WAM C37481), together in ethanol, 18.iii.2010, leg. T. Karanovic and S. Callan (seLN8182), type locality; 1 ♀ destroyed for DNA sequence, 16.iii.2010, leg. T. Karanovic and G. Perina (seLN8517), type locality; 1 ♀ dissected on 1 slide, 11.iii.2009, leg. S. Eberhard and P. Bell (seLN6492), type locality; 1 ♀ in ethanol, 11.iii.2009, leg. S. Eberhard and P. Bell (seLN6492), type locality; 3 ♂+5 ♀ (2 ovigerous) together in ethanol, 16.iii.2010, leg. T. Karanovic and G. Perina (seLN8533), bore line L, bore L-UNK1, 27.329832°S 120.150590°E; 1 ♀ destroyed for DNA sequence, 15.iii.2010, leg. T. Karanovic and G. Perina (seLN8533), same locality; 4 ♂+2 ♀+2 copepodids together in ethanol, 18.iii.2010, leg. T. Karanovic and S. Callan (seLN7139), same locality; 3 ♂+9 ♀ (2 ovigerous) together in ethanol, 15.iii.2010, leg. S. Callan and N. Krawczyk (seLN8496), bore line 1, bore YYD22, 27.167304°S 119.870456°E; 2 ♂+2 ♀ (WAM C37482) on 1 SEM stub, 15.iii.2010, leg. S. Callan and N. Krawczyk (seLN8496), same locality; 1 ♀ destroyed for DNA sequence, 15.iii.2010, leg. S. Callan and N. Krawczyk (seLN8496), same locality; 1 ♂+2 ♀ (1 ovigerous) together in ethanol, 20.iii.2010, leg. T. Karanovic and S. Callan (seLN8411), same locality; 4 ♂+5 ♀ together in ethanol, 1.xi.2009, leg. P. Bell and G. Perina (seLN6610), same locality; 4♀+1 copepodid together in ethanol, 15.iii.2010, leg. S. Callan and N. Krawczyk (seLN8479), bore line 1, bore YYD26, 27.164033°S 119.873196°E; 1 ♀ destroyed for DNA sequence, 15.iii.2010, leg. S. Callan and N. Krawczyk (seLN8479), same locality; 1 ♂+2 ♀+1 copepodid together in etanol, 20.iii.2010, leg. T. Karanovic and S. Callan (seLN8279), same locality; 1 ♀ destroyed for DNA sequence, 12.xi.2009, leg. P. Bell and G. Perina (seLN7342), bore line 3.5, bore YYAC284, 27.173127°S 119.906857°E; 2 ♂+3 ♀ (1 ovigerous) together in ethanol, 15.iii.2010, leg. T. Karanovic and G. Perina (seLN8492), bore line F, bore YU1, 27.142601°S 119.853144°E; 1 ♀ in ethanol, 18.iii.2010, leg. T. Karanovic and S. Callan (seLN8565), same locality; 4 ♂+4 ♀ together in ethanol, 20.iii.2010, leg. T. Karanovic and S. Callan (seLN8464), bore line K, bore YYHC0049K, 27.247548°S 120.054862°E; 3 ♂+1 ♀ together in ethanol, 18.iii.2010, leg. T. Karanovic and S. Callan (seLN7131), bore line K, bore YYHC085B, 27.247824°S 120.054676°E; 6 ♂+3 ♀ together in ethanol, 20.iii.2010, leg. T. Karanovic and S. Callan (seLN8418), same locality; 1 ♀ in ethanol, 21.iii.2010, leg. T. Karanovic and S. Callan (seLN8538), bore line 3, bore YYAC118, 27.174573°S 119.889727°E; 1 ♀ in ethanol, 12.xi.2009, leg. P. Bell and G. Perina (seLN7389), same locality: 1 ♂+3 ♀ (1 ovigerous) together in ethanol, 16.iii.2010, leg. S. Callan and N. Krawczyk (seLN8349), bore line 1, bore YYAC0015A, 27.170329°S 119.868869°E; 3 ♀+2 copepodids together in ethanol, 16.iii.2010, leg. S. Callan and N. Krawczyk (seLN8355), bore line 1, bore YYAC0018C, 27.161503°S 119.874715°E; 2 copepodids in ethanol, 20.iii.2010, leg. T. Karanovic and S. Callan (seLN8302), bore line 1, bore YYAC0019B, 27.159121°S 119.876035°E; 1 ♂+1 ♀ together in ethanol, 21.iii.2010, leg. T. Karanovic and S. Callan (seLN8555), bore line 2, bore YYAC1004C, 27.174665°S 119.877345°E; 2 ♀ in ethanol, 16.iii.2010, leg. S. Callan and N. Krawczyk (seLN8342), bore line 2, bore YYAC1004D, 27.174664°S 119.877343°E; 1 ♀ in ethanol, 11.i.2010, leg. P. Bell and G. Perina (seLN7690), same locality; 2 ♀ in ethanol, 21.iii.2010, leg. T. Karanovic and S. Callan (seLN7126), bore line 1.5, bore YYAC35, 27.166173°S 119.873977°E.

Description of female

Data from holotype, several paratypes, and many specimens from bore YYD22. Total body length, measured from tip of rostrum to posterior margin of caudal rami (excluding caudal setae), ranges from 300 to 463 µm (307 µm in holotype). Colour of preserved specimen yellowish. Nauplius eye not visible. Habitus (Figs 4*C*, 20*A*, *B*) cylindrical, relatively slender, without distinct demarcation between prosome and urosome; prosome–urosome ratio ~1.1 (in dorsal view); greatest width at posterior end of cephalothorax. Body length–width ratio ~4.4;

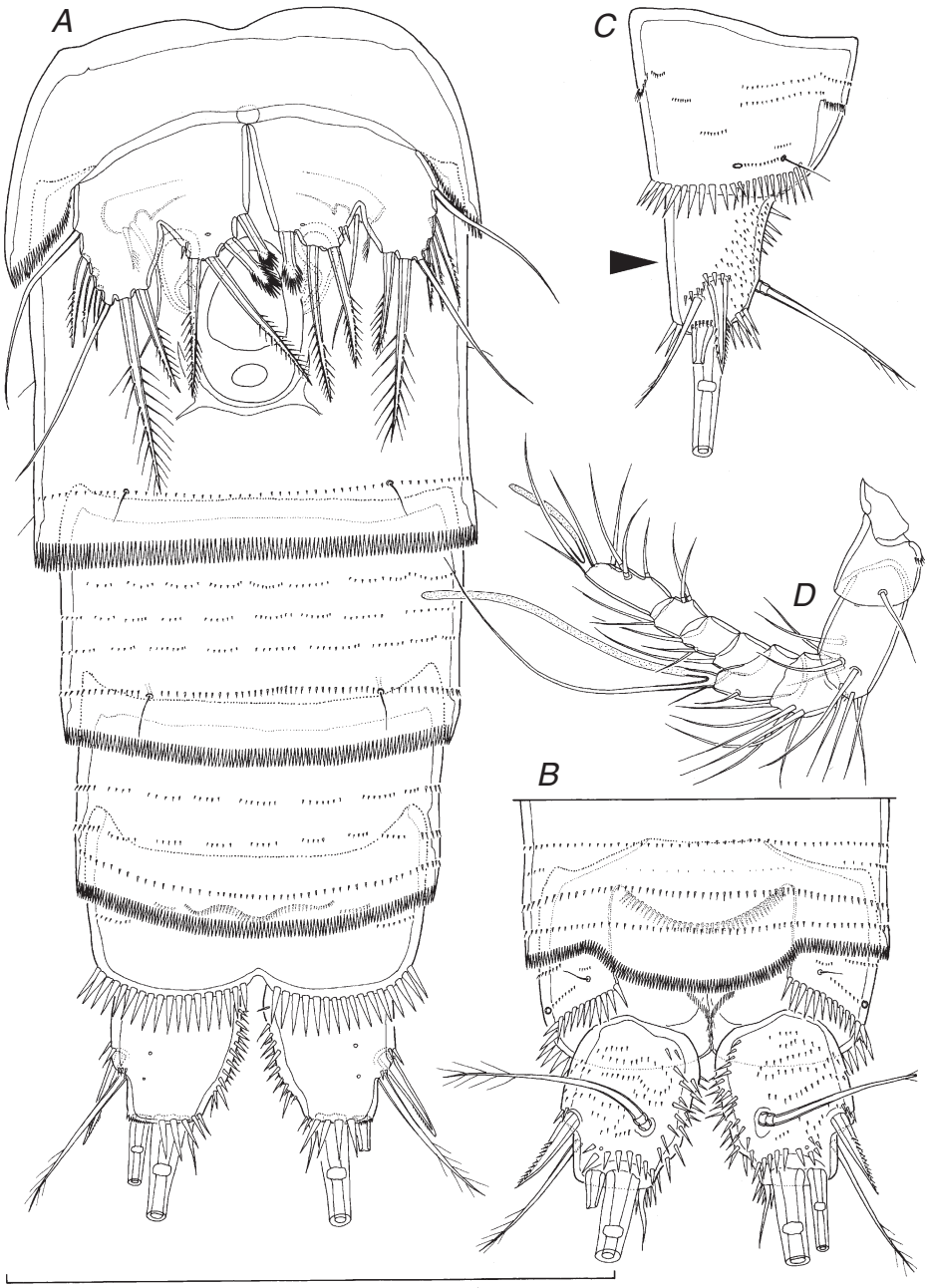

Fig. 17. *Schizopera akation*, sp. nov., holotype ♀. (*A*) Urosome, ventral view; (*B*) last two urosomal somites and caudal rami, dorsal view; (*C*) anal somite and left caudal ramus, lateral view; (*D*) antennula, ventral view. Arrow points to short caudal rami, different from previous two species. Scale bar = 100 µm.

cephalothorax 1.15 times as wide as genital double somite. Free pedigerous somites without pronounced lateral dorsal expansions. Integument relatively strongly chitinised. All somites (except cephalothorax) and caudal rami, besides other ornamentation, with several rows of minute spinules (Figs 4*C*, 19*B*, *C*, 20*A*, *B*), but only a few on prosomites and those on urosomites with wide clean spaces between them. At closer inspection those rows not straight but composed of many small arched components, forming a wavy pattern. Rostrum (Fig. 19*A*) very long and clearly demarcated at base, reaching beyond posterior margin of second antennular segment, linguiform, with blunt tip, about twice as long as wide; ornamented with two sensilla dorsolaterally.

Cephalothorax (Figs 4*C*, 19*A*, 20*A*) ~1.2 times as long as wide in dorsal view (without rostrum); represents 30% of total body length. Surface of cephalothoracic shield and tergites of first three free pedigerous somites with characteristic pattern of large sensilla and small cuticular pores, very similar to the two previous

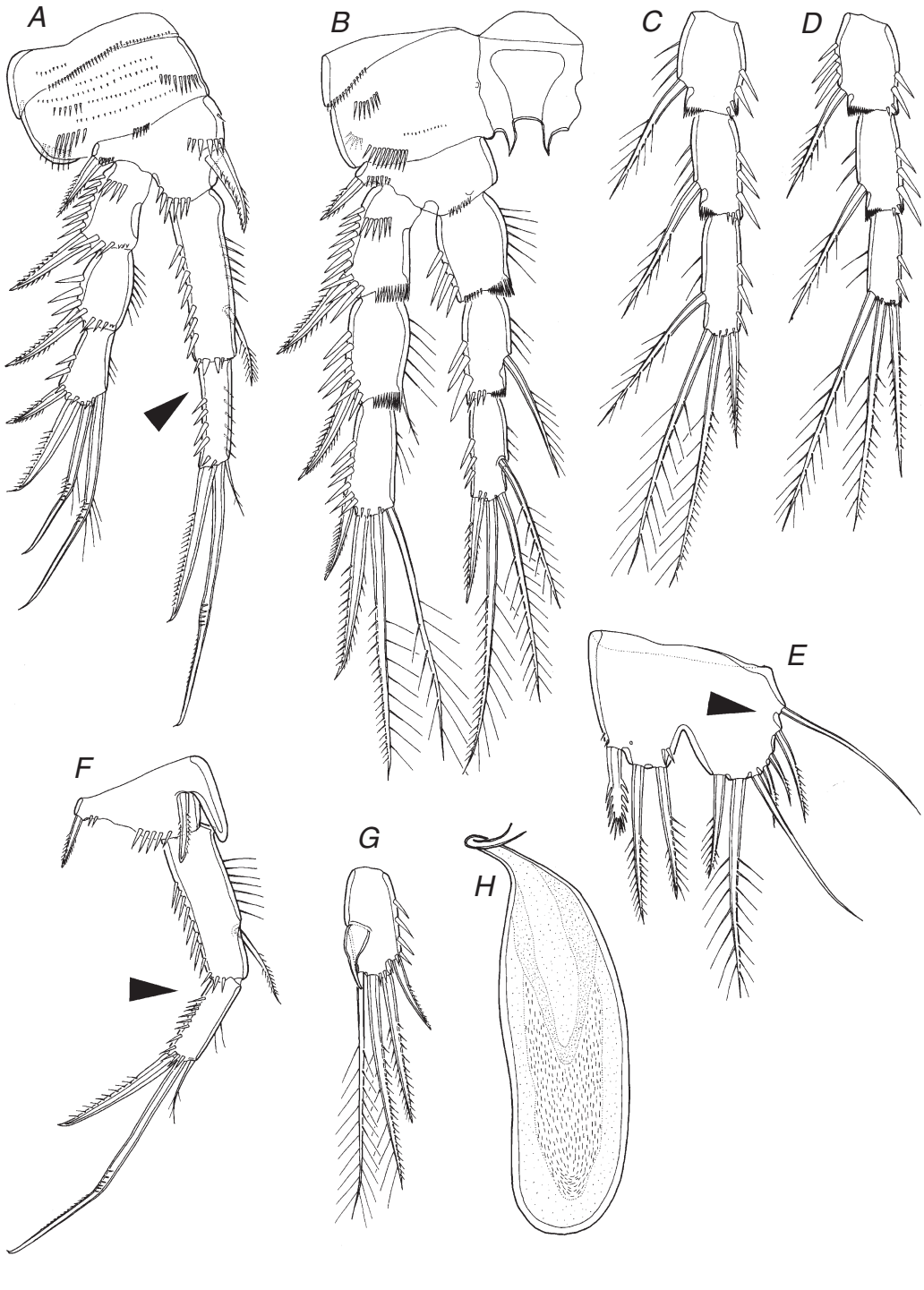

Fig. 18. *Schizopera akation*, sp. nov. A–E, holotype ♀; F–H, allotype ♂. (*A*) First swimming leg, anterior view; (*B*) second swimming leg, anterior view; (*C*) endopod of third swimming leg, anterior view; (*D*) endopod of fourth swimming leg, anterior view (*E*) fifth leg, anterior view; (*F*) basis and endopod of first swimming leg, anterior view; (*G*) third exopodal segment of third swimming leg, anterior view; (*H*) spermatophore, ventral view. Arrows point to characters that are different from previous two species. Scale bar = 100 µm.

species, except small pores at base of rostrum missing (arrowed in Fig. 19*A*). Cephalothoracic shield without pits, very smooth. Hyaline fringe of cephalothoracic shield and all free pedigerous somites smooth and unornamented (Figs 19*D*, 20*A*), those of urosomites finely serrated (Figs 19*B*, *C*, 20*A*, *B*). Fifth pedigerous somite (first urosomal) ornamented with four dorsal large sensilla

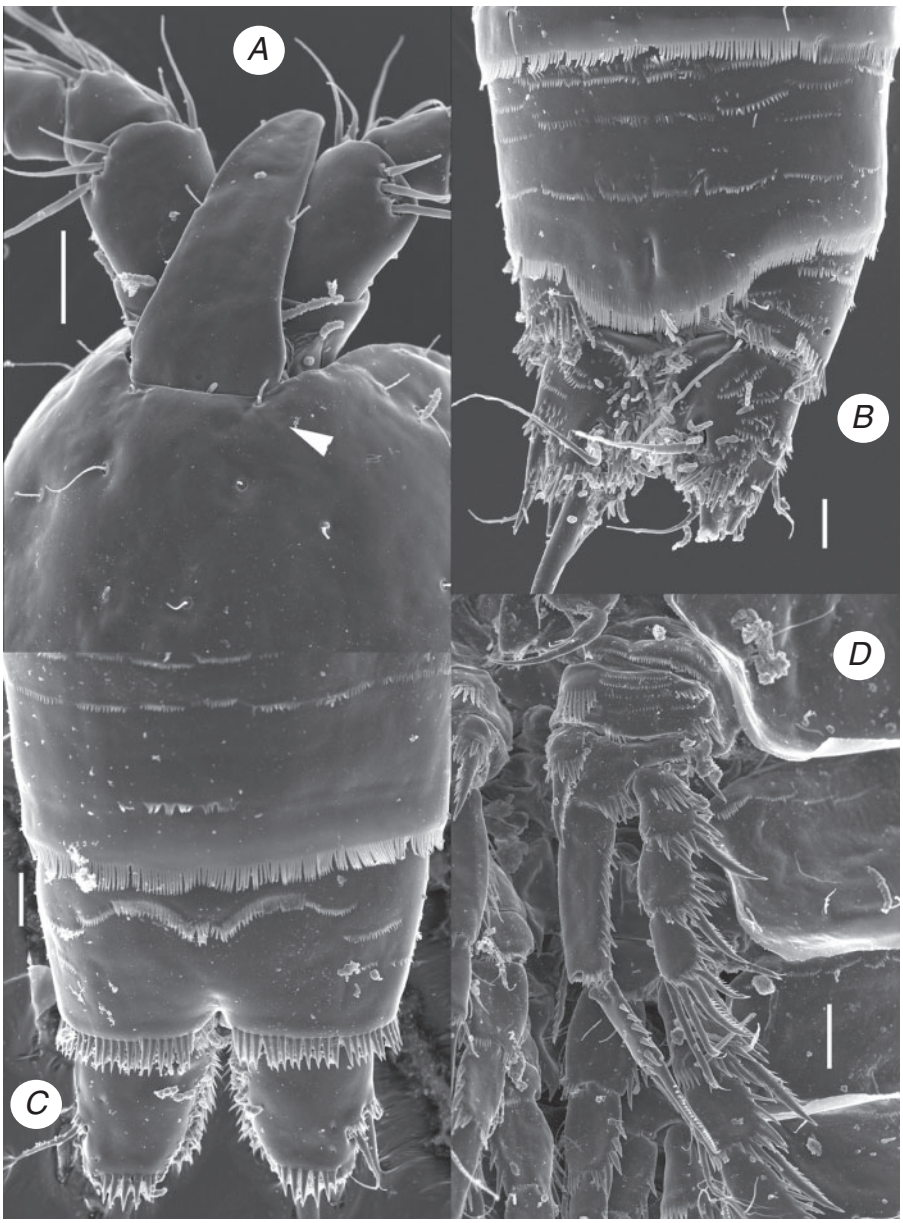

Fig. 19. *Schizopera akation*, sp. nov., scanning electron micrographs. A, B, ♀ I from bore YYD22; C, D, ♀ II from bore YYD22. (*A*) Anterior part of cephalothorax with rostrum and anetnnulae, dorsal view; (*B*) last two urosomal somites and caudal rami, dorsal view; (*C*) last two urosomal somites and caudal rami, ventral view; (*D*) first swimming leg, anterior view. Arrow points to absent cuticular pore on cephalothoracic shield. Scale bars = 10 µm.

and two lateral sensilla (one on each side), in addition to four rows of numerous minute cuticular spinules; hyaline fringe sharply serrated (Figs 17*A*, 20*A*).

Genital double somite (Figs 5*A*, *B*, *C*, 9*A*, *B*) ~0.8 times as long as wide (dorsal view), with visible suture internally; ornamented with eight sensilla dorsally (six at midlength, two near posterior margin), two posterior sensilla ventrally, and two lateral sensilla on each side (one posterior, one at midlength), in addition to seven or eight rows of minute spinules dorsolaterally (Fig. 20*A*), but only a single posterior row ventrally (Figs 17*A*, 20*B*). Female genital complex (Fig. 17*A*) with very large epicopulatory bulb, ovoid, ~1.5 times as long as wide. Seminal receptacles small, pear-shaped, reaching beyond anterior margin of epicopulatory bulb, ~0.6 times as long as epicopulatory bulb. Third urosomite (Figs 17*A*, 20*A*, *B*) ornamented with six posterior sensilla (two dorsal, two ventral and two lateral) and four rows of minute spinules (no ventral pores). Preanal somite with no sensilla or pores, ornamented with three rows of minute spinules; hind margin clearly bulging posteriorly in dorsal region, forming very sharply serrated pseudoperculum (Figs 17*B*, 19*B*). Anal somite (Figs 17*A*, *B*, *C*, 19*B*, *C*) with convex and very short anal operculum ornamented with transverse row of spinules along

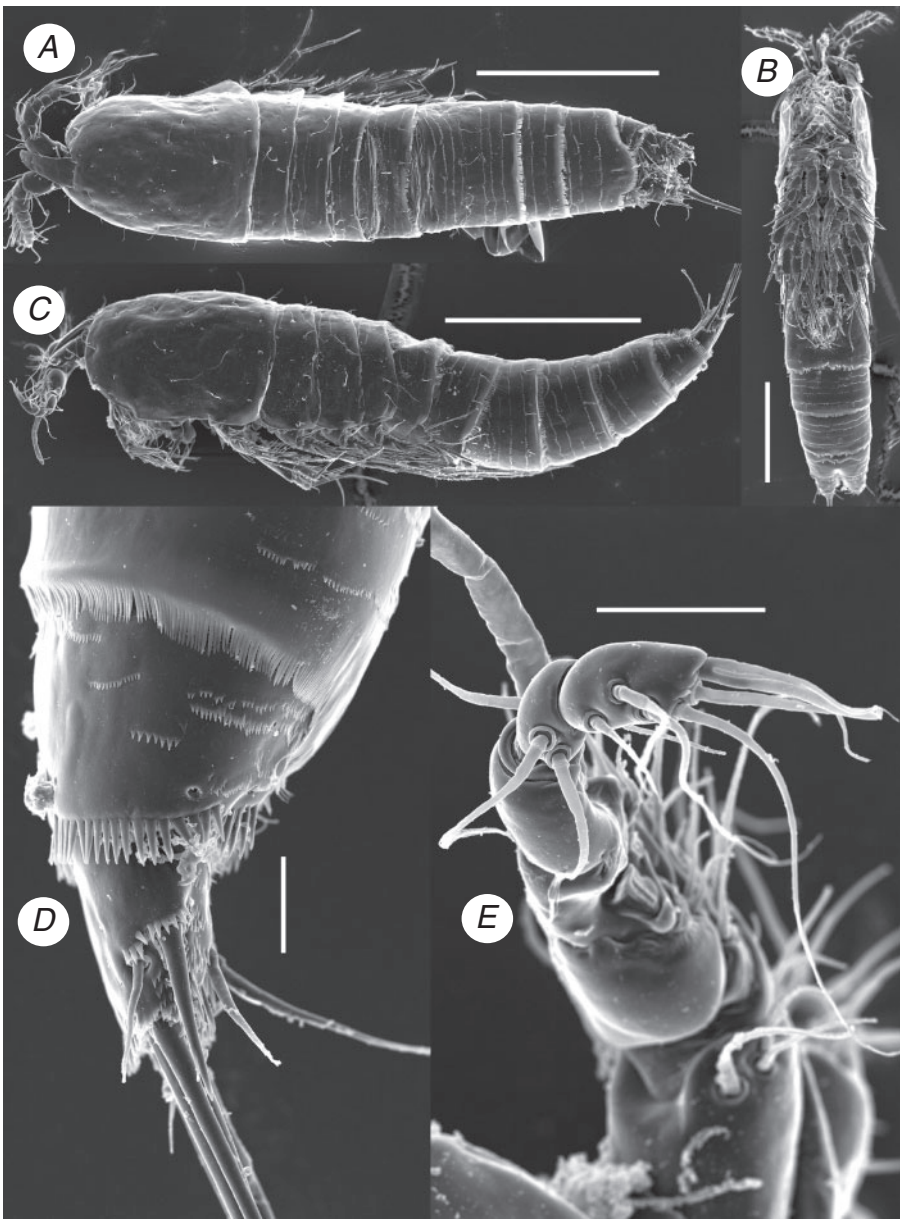

Fig. 20. *Schizopera akation*, sp. nov., scanning electron micrographs. A, ♀I from bore YYD22; B, ♀II from bore YYD22; C-E, ♂ from bore YYD22. (*A*) Habitus, dorsal view; (*B*) habitus, ventral view; (*C*) habitus, lateral view; (*D*) last two urosomal somites and left caudal ramus, lateral view; (*E*) left antennula, lateroapical view. Scale bars: A–C = 100 µm; D, E = 10 µm.

posterior margin; ornamented with two sensilla dorsally, two large lateral cuticular pores, transverse row of large spinules along posterior margin (all of about same length), several shorter rows of minte spinules dorsolaterally, and characteristic bull-horn-shaped row of larger spinules ventrally around midlength. Anal sinus (Figs 17*B*, 19*B*) widely opened and ornamented with two diagonal rows of slender spinules, but always almost completely covered by pseudoperculum; represents 54% of somite's width.

Caudal rami (Figs 17*A–C*, 19*B*, *C*) short, strongly sclerotised, somewhat conical, about as long as greatest width in ventral view, slightly divergent, with very small space between them; ornamented with two ventral and one dorsal cuticular pores in posterior half, transverse row of several large spinules along posterior margin dorsally and ventrally, many large spinules along inner margin, and several short rows of minute spinules dorsally and laterally (none ventrally); armed with six elements (two lateral, one dorsal and three apical). Dorsal seta slender and apically pinnate, ~1.5 times as long as ramus, inserted at two-thirds of ramus length, triarticulate. Lateral proximal spine stout, inserted at three-quarters of ramus length, 0.6 times as long as ramus. Lateral distal seta very slender, apically pinnate, inserted slightly ventrolaterally at four-fifths of ramus length, about as long as ramus. Inner apical seta short and smooth, 0.4 times as

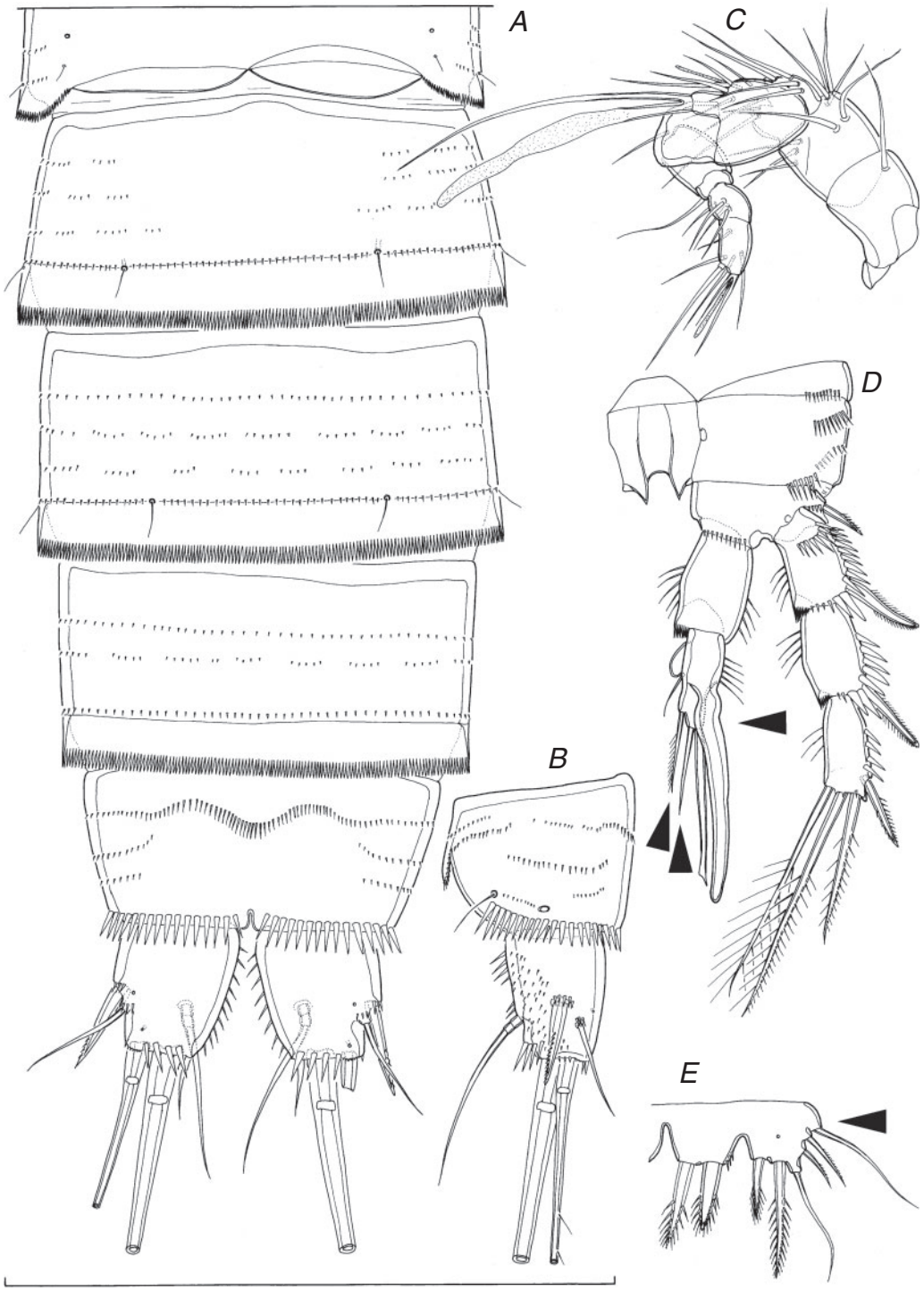

Fig. 21. *Schizopera akation*, sp. nov., allotype ♂. (*A*) Urosome without fifth pedigerous somite, ventral view; (*B*) anal somite and right caudal ramus, lateral view; (*C*) antennula, ventral view; (*D*) second swimming leg, anterior view; (*E*) fifth leg, anterior view. Arrows point to characters different from previous two species. Scale bar = 100 µm.

long as ramus. Principal apical setae with breaking planes; middle apical seta strongest, bipinnate at distal end, twice as long as unipinnate outer apical seta, and 0.6 times as long as body length.

Antennula (Fig. 17*D*) relatively short, eight-segmented, ~0.6 times as long as cephalothorax, with short aesthetasc on eighth segment, fused to two apical setae, and large aesthetasc on fourth segment, reaching significantly beyond tip of appendage and

fused basally to equally long seta; setal formula: 1.9.7.3.2.3.4.7. Only two lateral setae on seventh segment and four on eighth segment biarticulate. All setae smooth and slender, and most end apically with pore (except apical and subapical ones), only observable under scanning electron microscope. Length ratio of antennular segments, from proximal end, 1: 1.1: 0.4: 0.4: 0.4: 0.4: 0.5: 1. First segment ornamented with short transverse row of small spinules ventromedially, other segments unornamented.

Antenna, labrum, mandibula, maxillula, maxilla and maxilliped as in *S. a. analspinulosa*.

All swimming legs (Figs 18*A–D*, 19*D*) slender, composed of small triangular preacoxa, large quadrate coxa, smaller basis and three-segmented exopod; endopod of first swimming leg two-segmented (arrowed in Fig. 18*A*), all other endopods three-segmented. All exopodal and endopodal segments of about same length, except much longer first endopodal segment of first leg.

First swimming leg (Figs 18*A*, 19*D*) with very small intercoxal sclerite, concave at distal end and unornamented. Preacoxa unarmed, ornamented with posterior row of minute spinules. Coxa also unarmed, but ornamented with several horizontal rows of spinules on anterior surface and one on posterior; anterior spinules grouped into four parallel rows of minute ones, and four groups of large ones (one inner, one distal and three close to outer margin). Basis armed with one inner and one outer strong spine; inner spine slightly curved inwards; ornamentation consists of row of spinules at base of each spine, additional row of spines along distal margin, between endopod and exopod, and one cuticular pore near base of outer spine (all on anterior surface). Exopod armature and ornamentation as in *S. a. analspinulosa*. Endopod (arrowed in Fig. 18*A*) geniculate, with first segment 0.7 times as long as entire exopod, 1.6 times as long as second endopodal segment, and ~3.4 times as long as wide; strongly sclerotised beak present proximally on inner margin of first segment, hidden behind inner spine of basis; endopodal armature consists of one strong inner seta on first segment (inserted at about two-thirds), and three setae on second segment (innermost slender and short, middle longest and prehensile, outermost spiniform seta (or spine?), last 0.6 times as long as middle one); endopodal ornamentation consists of strong spinules along inner, outer and distal margins.

Second swimming leg (Fig. 18*B*) armature and ornamentation as in *S. a. analspinulosa*, both terminal segments somewhat less elongated and armature elements more slender.

Third swimming leg (Fig. 18*C*) very similar to second, except that basis armed with outer slender seta instead of spine, and endopod additionally armed with inner seta on first segment. Also pointed processes on intercoxal sclerite less sharp than in second leg.

Fourth swimming leg (Fig. 18*D*) very similar to third leg, except that inner seta missing on third endopodal segment, and pointed processes on intercoxal sclerite even less sharp.

Fifth leg (Figs 17*A*, 18*E*) bilobate, with exopod fused to baseoendopod without any sutures visible (arrowed in Fig. 18*E*). Baseoendopodal outer basal seta almost without setophore, and without ornamentation at its base, smooth. Endopodal lobe trapezoidal, extending almost to posterior margin of exopodal lobe, ornamented with small cuticular pore and several small spinules distally, and armed with three or four very stout, spiniform elements (two inner ones probably spines, two outer ones probably spiniform setae); length ratio of endopodal armature elements, from inner side, 1 : 1 : 2 : 1.8. Exopod simple unornamented lobe, ~0.65 times as long as maximum width, armed with six armature elements; two innermost strong and bipinnate, middle one smooth and slender, three outermost short, stout and unipinnate; length ratio of exopodal armature elements, from inner side, 1 : 2.1 : 1.8 : 0.6 : 0.6 : 0.9.

Sixth leg (Fig. 17*A*) indistinct, very small cuticular plate, covering gonopore, armed with one very small spine fused basally to plate, and two setae; inner seta slender and smooth, almost three times as long as outer seta, plumose along inner margin.

Description of male

Data from allotype, several paratypes and several specimens from bore YYD22. Body length ranges from 310 to 408 µm (340 µm in allotype). Habitus (Fig. 20*C*) slightly more slender than in female, but also cylindrical, and with similar proportions of prosome–urosome, and cephalothorax–genital somite. Body length–width ratio ~4.6. Ornamentation of prosomites, colour and nauplius eye similar to female. Genital somite free, twice as wide as long in dorsal view. Single, completely formed, longitudinally placed spermatophore (Fig. 18*H*) inside first two urosomites in most specimens, about three times as long as wide. Ornamentation of abdominal somites similar to female (Figs 20*C*, 21*A*), except genital somite with two additional pores ventrolaterally. Anal somite (Figs 20*D*, 21*A*, *B*) very similar to female, including bull-horn-shaped row of spinules on ventral surface and details of lateral and dorsal spinules, only slightly more ornamented laterally.

Caudal rami (Figs 20*D*, 21*A*, *B*) slightly less conical than in female, but with similar armature and ornamentation.

Antennula (Figs 20*E*, 21*C*) also ~0.6 times as long as cephalothorax, but strongly geniculate and nine-segmented (basically female's sixth segment subdivided), with geniculation between fourth and fifth and seventh and eighth segments. Segments that participate in geniculation strengthened with cuticular plates along anterior surface, the largest ones being on the sixth segment. Aesthetascs as in female, on fourth and last segments; first one somewhat wider than in female. First two and last two segments similar to female. Setal formula: 1.9.9.10.1.0.1.4.7, but many setae hardly visible without scanning electron microscope. Most setae smooth and with pore on top; same setae biarticulate as in female.

Antenna, labrum, mandibula, maxillula, maxilla, maxilliped, exopod and endopod of first swimming leg, exopod of second swimming leg, endopod of third swimming leg, and fourth swimming leg similar to female.

First swimming leg (Fig. 18*F*) with modified basis, inner margin of which very rigidly sclerotised, with spiniform, smooth process distally. Inner spine on basis smaller than in female, without spinules at its base, inserted more proximally, and slightly longer than distal spiniform process of basis. Endopod two-segmented as in female (arrowed in Fig. 18*F*).

Second swimming leg (Fig. 21*D*) with transformed endopodal second and third segments. Second segment with part of

inner margin protruded as rounded indistinct lobe, without ornamentation on its surface; inner seta much shorter than in female, smooth and slender. Third segment completely modified; two ancestral apical setae transformed into smooth, spiniform armature elements; outer one stronger, with abruptly sharpened tip, and ~1.8 times as long as inner one. Ancestral outer spine completely fused to somite, transformed into very strong and smooth thorn, slightly longer than outer ancestral apical element, and 1.8 times as long as last two endopodal segments combined. As result of these transformations, third segment medially cleft. Inner seta on third segment more slender than in female and unipinnate, about as long as inner apical seta (arrowed in Fig. 21*D*), along with inner apical element and inner side of endopod, showing proportions of outer spine and last two endopodal segments.

Third swimming leg (Fig. 18*G*) with very characteristic element on anterior surface of third exopodal segment; this structure is swollen at basal part, with pore on top (observable only under scanning electron microscope), inserted at three-fifths and close to inner margin, reaching slightly beyond distal margin of third segment. First and second exopodal segments of third leg similar to female.

Fifth legs (Fig. 21*E*) with exopods fused to baseoendopods (arrowed in Fig. 21*E*), and baseoendopods fused basally to each other, ornamented with single pore on exopodal lobe (visble also on Fig. 20*C*) and several spinules on outer margin of endopodal lobe. Endopodal lobe much smaller and shorter than in female, also trapezoidal, extending to middle of exopodal lobe, armed with two very strong apical spines; inner spine ~1.3 times as long as outer one. Exopodal lobe about half as long as its maximum width, armed with five elements; sixth element from inner side not observed in male specimens; length ratio of exopodal armature elements, from inner side, 1 : 1.9 : 1.9 : 0.7 : 1.

Sixth legs (Fig. 21*A*) pair of small and short cuticular plates, without armature or ornamentation; left plate wider and larger than right one, and better demarcated at base.

Variability

Female fifth leg endopodal lobe can be armed with three or four elements even on the same animal (Fig. 17*A*), but most examined specimens showed a four-element condition. The exact position of ventral cuticular pores on the caudal rami can vary sometimes (Fig. 19*C*), but in most cases they are in the caudal half. Our careful examination of microcharacters, as well as re-examination after sequencing results, failed to show any morphological differences between three distinct clades revealed by *COI* data and showing sequence divergences (HKY-85 distances) ranging from 12% to 16.5% (see below).

Distribution

This species was found, usually in low numbers, on the following bore lines, from north-west to south-east: F, 1, 1.5, 2, 3, 3.5, K, L and bore SB14–1 (Fig. 41).

Remarks

This species differs from all other congeners from Yeelirrie by its two-segmented endopod of the first swimming leg (arrowed in Figs 4*C*, 18*A*, *F*, but see also Fig. 19*D*), which can be observed from a lateral view without the need to dissect the specimen. Another important morphological character is the short caudal rami (arrowed in Figs 4*C*, 17*C*), which it only shares in Yeelirrie with *S. akolos*, sp. nov. However, the latter species is smaller, has a much more slender habitus, three-segmented endopod of the first leg, two-segmented endopod of the fourth leg, reduced armature on third and fifth legs, and even shorter caudal rami (see Figs 3*D*, 22, 23). The two species seem to be only remotely related, which is also supported by our molecular analyses (Fig. 39). Interestingly, *S. akation*, sp. nov. has a very light somite ornamentation, just like the two undescribed species from the Pilbara region (*S.* sp. 1 and *S.* sp. 2), which we included in our molecular analysis as potential outgroups (compare, for example, Figs 19, 20, 38*C*, *D*). All three species also lack a pair of cuticular pores at the base of the rostrum (arrowed in Fig. 19*A*), while these pores are present in all Yeelirrie species, except *S. akolos*. This is the first recorded case in copepod crustaceans, which shows that cuticular pores can be phylogenetically significant structures, and they have hardly ever been studied in detail. Even more interesting is the fact that all Yeelirrie species with these pores present have heavily ornamented somites, with multiple rows of large spinules, sometimes resembling a mammalian pelt. All this suggests to us that *S. akation* resulted from a separate colonisation event, and possibly a more recent one as we discuss below. Additional characters that distinguish *S. akation* from other Yeelirrie congeners are evident in the extent of fusion of the fifth leg exopod (arrowed in Figs 18*E*, 21*E*), as well as in the proportion of the armature elements on the sexually dimorphic endopod of the second leg in males (arrowed in Fig. 21*D*).

Schizopera akation is the species with the widest distribution in Yeelirrie, found all the way from bore SB14 in the south-east to bore line F in the north-west (Fig. 41), and it is recorded living sympatrically with all other congeners here. Not surprisingly, sizewise it most likely occupies a separate niche, being significantly smaller than all other species, except *S. akolos*, which is even smaller and much more slender (see Figs 3, 4). Given this wide distribution of *S. akation* in the palaeochannel, it is perhaps not surprising to find a greater intraspecific molecular divergence than within any of the species studied here (Fig. 39). Populations from SB14 (8517) appear to be quite distinct from those from line L (8533), while those from the largest calcrete body to the north-west represent a third group (7342, 8479 and 8496). We discuss the most likely colonisation path of this species in the palaeochannel, and the possibility of these divergences between populations to be a result of long-term isolation within different geographic regions, in the 'Discussion' section below. However, we could not find any morphological differences between these three populations, and if they are indeed reproductively isolated, they would represent proper cryptic species.

The only other Australian *Schizopera* with a two-segmented endopod of the first leg is one specimen of *S. oldcuei* Karanovic, 2004, where this feature is asymmetric, i.e. two-segmented on the left leg and three-segmented on the right leg (Karanovic 2004: 169). This morphological character was used by Apostolov (1982) to subdivide three genera into subgenera, including *Schizopera*. The subdivision was strongly criticised by Mielke (1992) and rejected also by Mielke (1995), Karanovic (2004,

2006), Wells (2007) and Huys (2009), while it was maintained as a practical tool by Bodin (1997). Our molecular data also show that *S. akation* is deeply nested within the investigated clade, and it probably originated from an ancestor with a three-segmented endopod.

Morphologically, *S. akation* is most similar to an as yet undescribed new species from marine interstitial of Shark Bay in Western Australia (T. Karanovic, unpubl. data), which is the coastal part of the Yilgarn region in which Yeelirrie is situated. The similarities include the two-segmented endopod of the first leg, short and strong caudal rami, absence of cuticular pores at base of rostrum, as well as minute details of cuticular ornamentation of all somites. Both species even have three armature elements on the baseoendopod of one female fifth leg and four on the opposite one (as in Fig. 17*A*). The differences are mostly observed in the relative length of the first endopodal segment of first leg, relative size and shape of the epicopulatory bulb, proportions of some armature elements on the swimming legs, as well as a distinct exopod of the fifth leg and a completely fused basis and first endopodal segments of the antenna (forming an allobasis) in the marine species. Given the nature of these differences, it is uncertain whether the marine species is ancestral to the inland one, as the main distinguishing characters are a mixture of more primitive (e.g. exopod of the fifth leg) and more advanced features (e.g. antennal allobasis). Other species with a relatively similar morphology to that of *S. akation* are all marine representatives from the northern parts of Europe: *S. inornata* Noodt, 1954 from a sandy beach on the Baltic Sea, in Sweden; *S. pratensis* Noodt, 1958 from littoral near Kiel, Northern Sea, Germany; *S. arconae* Arlt, 1983 from benthic samples in the central part of the Baltic Sea; and *S. meridionalis listensis* Mielke, 1975 from a sandy beach on the island of Sylt, Northern Sea, Germany (see Noodt 1954, 1958; Mielke 1975; Arlt 1983). They all have short caudal rami, two-segmented endopod of the first swimming legs, and no particular modifications on the caudal rami armature or ornamentation. However, they can be distinguished from our new species, among other things, by the armature of the fifth leg. *Szhizopera arconae* has five elements on the exopod; *S. meridionalis listensis* has five elements on the baseoendopod; *S. inornata* has all four elements on the baseoendopod slender; and *S. pratensis* has all three outer exopodal setae long and slender. Additional differences can be found in the relative length of some armature elements in the swimming legs. All of these four species are unfortunately described from a limited set of morphological characters, so many ornamentation details could not be compared. Many other *Schizopera* species have short caudal rami and a two-segmented endopod of the first swimming leg, but can be distinguished from *S. akation* by several morphological characters. Interestingly, many show modifications and enlargements of the caudal rami armature, especially the proximal lateral and principal apical setae.

Etymology

The new species name *akation* (i.e. dwarf, Gr.) refers to its much smaller size when it was first discovered, living sympatrically with a much larger *S. a. analspinulosa*, sp. nov. in bore SB14. The name is a noun in apposition.

Schizopera akolos, sp. nov.

(Figs 3*D*, 22, 23)

Material examined

Name-bearing type. Holotype (WAM C37483), adult female, completely dissected on 1 slide in Faure's medium, 15.iii.2010, leg. S. Callan and N. Krawczyk (seLN8496).

Type locality. Australia: Western Australia: Yilgarn region, Yeelirrie station, bore line 1, bore YYD22, 27.167304°S 119.870456°E.

Additional material examined. All from type locality: allotype (WAM C37484), adult ♂ dissected on 1 slide, 15.iii.2010, leg. S. Callan and N. Krawczyk (seLN8496); 1 paratype ♀ destroyed for DNA sequence, 15.iii.2010, leg. S. Callan and N. Krawczyk (seLN8496); 1 ♀ in ethanol, 1.ix.2009, leg. P. Bell and S. Callan (seLN6610).

Description of female

Data from holotype and four paratypes. Total body length, measured from tip of rostrum to posterior margin of caudal rami (excluding caudal setae), ranges from 273 to 304 µm (291 µm in holotype). Colour of preserved specimen yellowish to white. Nauplius eye not visible. Habitus (Figs 3*D*, 22*A*) cylindrical, very slender even in lateral view, without distinct demarcation between prosome and urosome; prosome–urosome ratio ~1.3 (in dorsal view); greatest width at posterior end of cephalothorax. Body length–width ratio ~4.5; cephalothorax 1.2 times as wide as genital double somite. Free pedigerous somites without pronounced lateral dorsal expansions. Integument relatively weakly chitinised. All somites (except anal somite and caudal rami) without spinules, ornamented only with sensilla and cuticular pores (Figs 3*D*, 22*A*, 23*A*), preanal somite without any ornamentation at all (Figs 22*A*, *B*, 23*A*). Rostrum (Fig. 22*A*) very long and clearly demarcated at base, reaching posterior margin of second antennular segment, linguiform, with blunt tip, about1.5 times as long as wide; ornamented with two sensilla dorsolaterally.

Cephalothorax (Figs 3*D*, 22*A*) ~1.3 times as long as wide in dorsal view (without rostrum); represents 28% of total body length. Surface of cephalothoracic shield and tergites of first three free pedigerous somites with characteristic pattern of large sensilla and small cuticular pores, very similar to *S. a. analspinulosa* (compare with Fig. 6*A*), except small pores in anterior half missing (including those at base of rostrum), one pair of sensilla at midlength expressed as pores and one pair of pores in posterior half expressed as sensilla; central posterior pore also missing. Cephalothoracic shield without pits, very smooth. Hyaline fringe of cephalothoracic shield and all free pedigerous somites smooth and unornamented (Fig. 22*A*), those of urosomites finely serrated (Figs 22*A*, *B*, 23*A*). Ornamentation of free pedigerous somites with sensilla and pores similar to *S. a. analspinulosa*, except central dorsal pore missing on second pedigerous somite, and one additional pair of sensilla present on second pedigerous somite. Fifth pedigerous somite (first urosomal) ornamented with four dorsal large sensilla and four lateral sensilla (two on each side), hyaline fringe sharply but less deeply serrated (Figs 3*A*, 22*A*).

Genital double somite (Figs 22*A*, 23*A*) ~0.7 times as long as wide (dorsal view), with visible suture internally; ornamented with eight sensilla dorsally (six at midlength, two near posterior

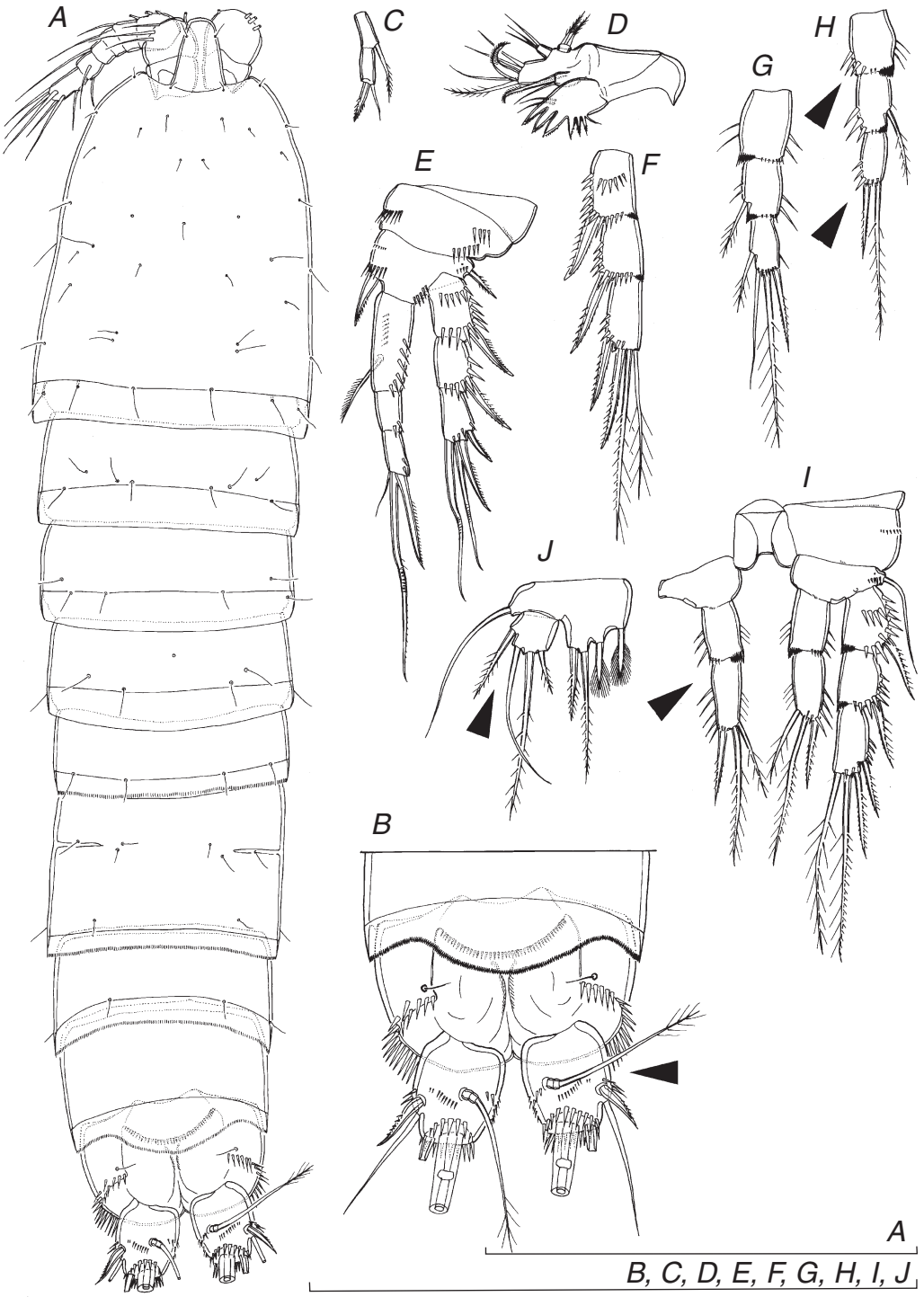

Fig. 22. *Schizopera akolos*, sp. nov., holotype ♀. (*A*) Habitus, dorsal view; (*B*) last two urosomal soomites and caudal rami, dorsal view; (*C*) exopod of antenna, dorsal view; (*D*) maxillula, posterior view; (*E*) first swimming leg, anterior view; (*F*) exopod of second swimming leg, anterior view; (*G*) endopod of second swimming leg, posterior view; (*H*) endopod of third swimming leg, anterior view; (*I*) left fourth swimming leg and endopod of right fourth leg, anterior view; (*J*) fifth leg, anterior view. Arrows point to characters different from previous species. Scale bars = 100 µm.

margin), two posterior sensilla ventrally, and one lateral sensillum on each side close to posterior margin; hyaline fringe sharply serrated, but grooves relatively shallow. Female genital complex (Fig. 23*A*) with large and ovoid epicopulatory bulb, ~1.4 times as long as wide. Seminal receptacles small, kidney-shaped, not reaching anterior margin of epicopulatory bulb, ~0.6 times

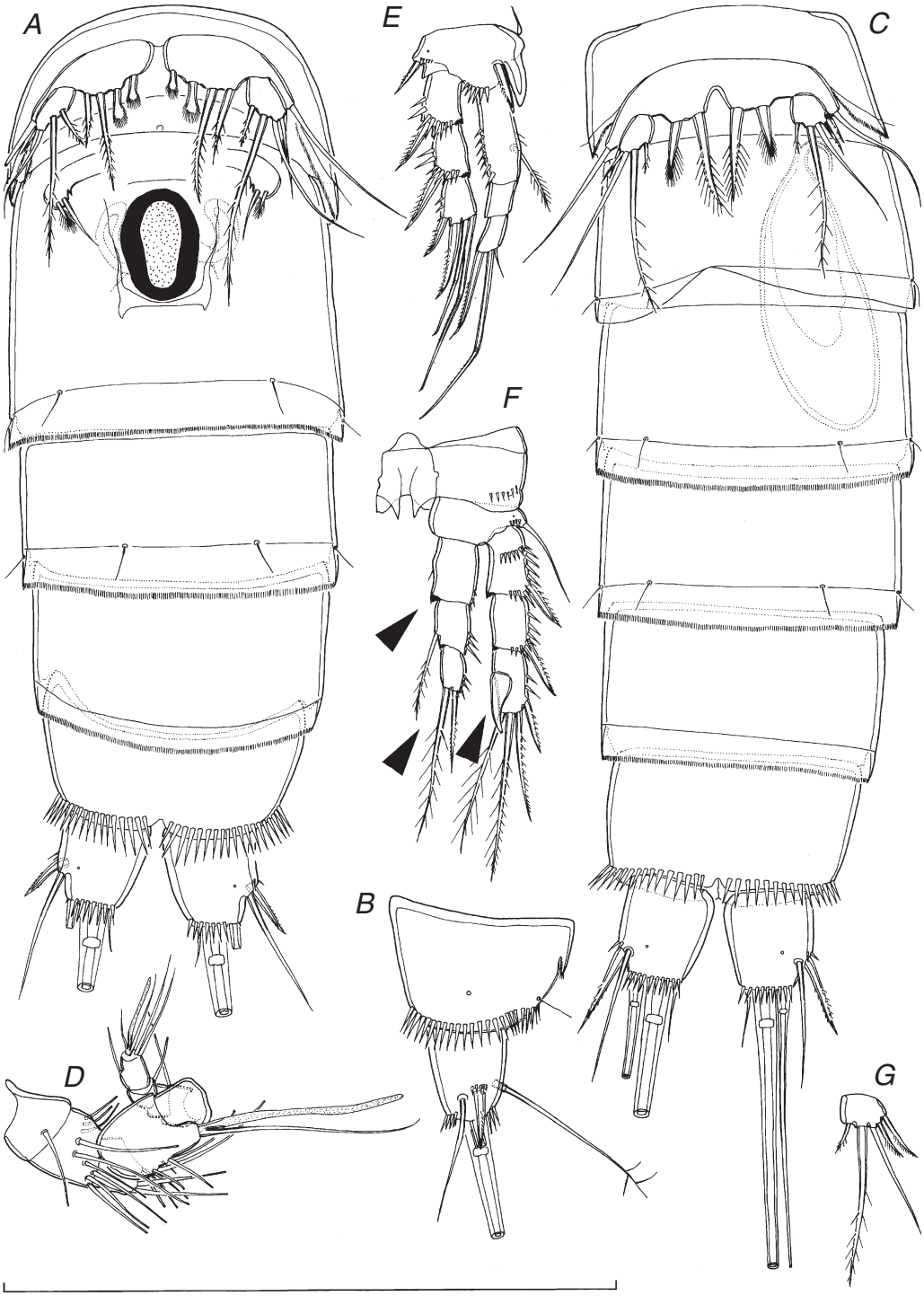

Fig. 23. *Schizopera akolos*, sp. nov., A and B, holotype ♀; C–G, allotype ♂. (*A*) Urosome, ventral view; (*B*) anal somite and left caudal ramus, lateral view; (*C*) urosome, ventral view; (*D*) antennula, ventrolateral view; (*E*) first swimming leg, anterior view; (*F*) third swimming leg, anterior view; (*G*) exopod of fifth leg, anterior view. Arrows point to characters different from previous species. Scale bar = 100 µm.

as long as epicopulatory bulb. Third urosomite (Figs 22*A*, 23*A*) ornamented only with six posterior sensilla (two dorsal, two ventral and two lateral). Preanal somite with no sensilla or pores; hind margin somewhat bulging posteriorly in dorsal region, forming sharply serrated short pseudoperculum (Fig. 22*B*). Anal somite (Figs 22*B*, 23*A*, *B*) with convex and very short anal operculum, ornamented with transverse row of spinules along posterior margin; ornamented with two sensilla

dorsally, two large lateral cuticular pores, and transverse row of large spinules along posterior margin (all of about same length). Anal sinus (Fig. 22*B*) widely opened and ornamented with two diagonal rows of slender spinules; represents 56% of somite's width.

Caudal rami (Figs 22*B*, 23*A*, *B*) short, strongly sclerotised, somewhat conical, about as long as greatest width in ventral view, slightly divergent, with very small space between them; ornamented with one ventral cuticular pore in posterior half, transverse row of several large spinules along posterior margin dorsally and ventrally, and several spinules at base of lateral proximal spine; armed with six elements (two lateral, one dorsal and three apical). Dorsal seta slender and apically pinnate, about twice as long as ramus, inserted at three-fifths of ramus length, triarticulate. Lateral proximal spine stout, inserted at two-thirds of ramus length, 0.7 times as long as ramus. Lateral distal seta very slender, smooth, inserted slightly ventrolaterally at three-quarters of ramus length, about as long as ramus. Inner apical seta short and smooth, 0.4 times as long as ramus. Principal apical setae with breaking planes; middle apical seta strongest, bipinnate at distal end, twice as long as unipinnate outer apical seta, and 0.5 times as long as body length.

Antennula, labrum, mandibula, maxilla and maxilliped as in *S. a. analspinulosa*.

Antenna (Fig. 22*C*) also very similar to that in *S. a. analspinulosa*, except first exopodal segment somewhat less slender.

Maxillula (Fig. 22*D*) with segmentation and armature as in previous three species, except endopod somewhat shorter, spines on preacoxal arthrite more widely spaced and one missing, and no ornamentation visible.

All swimming legs (Fig. 22*E–I*) very short in proportion to rest of body, composed of small triangular preacoxa, large quadrate coxa, smaller basis and three-segmented exopod; endopod of fourth swimming leg two-segmented (arrowed in Fig. 22*I*), all other endopods three-segmented. Exopodal and endopodal segments of about same length in first three legs, endopod of fourth leg much shorter than exopod.

First swimming leg (Fig. 22*E*) with very small intercoxal sclerite, concave at distal end and unornamented. Preacoxa unarmed, ornamented with posterior row of minute spinules. Coxa also unarmed, ornamented with three horizontal rows of large spinules on anterior surface (one close to inner margin and two close to outer margin); no rows of minute spinules. Basis armed with one inner and one outer strong spine; ornamentation consists of row of spinules at base of each spine, one additional row of smaller spinules proximally, parallel to inner row and several spinules along distal margin, between endopod and exopod. Exopodal armature and ornamentation similar to that in *S. a. analspinulosa*, but segments proportionately shorter. Endopod geniculate, with first segment slightly shorter than first two exopodal segments combined, 2.4 times as long as second endopodal segment, and ~2.6 times as long as wide; no sclerotised beak proximally on inner margin; endopodal armature consists of one strong inner seta on first segment (inserted at about two-thirds), and three setae on third segment (innermost slender and smooth, middle longest and prehensile, outermost spiniform seta (or spine?) half as long as middle one); endopodal ornamentation consists of strong spinules along inner margin of all segments, and also along outer margin of first segment.

Second swimming leg (Fig. 22*F*, *G*) armature formula and general ornamentation as in *S. a. analspinulosa*, but segments proportionately shorter and setae much more slender, and inner seta on second segment missing; inner apical seta on third endopodal segment smooth, all others bipinnate; coxa with only two rows of spinules.

Third swimming leg (Fig. 22*H*) very similar to second, except basis armed with outer slender seta instead of spine, and endopod with only two armature elements on third segment (bottom arrow in Fig. 22*H*); first endopodal segment without inner seta on first segment (top arrow in Fig. 22*H*), seta present in all other species presented here. Also, pointed processes on intercoxal sclerite less sharp than in second leg.

Fourth swimming leg (Fig. 22*I*) with exopod very similar to second and third leg, and basis similar to third leg; pointed processes on intercoxal sclerite even less sharp than in third leg; coxa with only one row of minute spinules on anterior surface; endopod two-segmented (arrowed in Fig. 22*I*), reaching only posterior margin of second exopodal segment, without armature on first segment, with three elements on second segment apically; inner apical seta on second endopodal segment about as long as outer spiniform seta (or spine?), and only half as long as middle apical seta.

Fifth leg (Fig. 22*J*) biramous, with exopod clearly demarcated on both anterior and posterior surfaces. Baseoendopod with outer basal smooth seta arising from relatively short setophore, without ornamentation at its base. Endopodal lobe trapezoidal, extending almost to posterior margin of exopod, unornamented, armed with four very stout, spiniform elements (two inner ones probably spines, two outer ones probably spiniform setae); length ratio of endopodal armature elements, from inner side, 1 : 1 : 2.7 : 1.5. Exopod pentagonal, about as long as maximum width, unornamented, armed with only four elements: two innermost strong and bipinnate, next one smooth and slender, outermost element stout and bipinnate; length ratio of exopodal armature elements, from inner side, 1 : 3.9 : 3.3 : 1.8.

Sixth leg (Fig. 22*A*) indistinct, very small cuticular plate covering gonopore, armed with one very small spine fused basally to plate and two setae; inner seta slender and smooth, twice as long as plumose outer seta.

Description of male

Data from allotype. Body length 297 µm. Habitus slightly more slender than in female, but also cylindrical, and with similar proportions of prosome–urosome, and cephalothorax–genital somite. Body length–width ratio ~4.8. Ornamentation of prosomites, colour and nauplius eye similar to female. Genital somite free, twice as wide as long in dorsal view. Single, completely formed, longitudinally placed spermatophore (Fig. 23*C*) inside second and third urosomites, ~2.4 times as long as wide. Ornamentation of abdominal somites similar to female (Fig. 23*C*), except additional pair of lateral sensilla on genital somite posteriorly. Anal somite (Fig. 23*C*) very similar to female, but with slightly smaller ventral posterior spinules.

Caudal rami (Fig. 23*C*) slightly more cylindrical in ventral view than in female, but with similar armature and ornamentation.

Antennula (Fig. 23*D*) short and very strongly geniculate, nine-segmented, with geniculation between fourth and fifth and seventh and eighth segments. Aesthetascs as in female, on fourth and last segments; first one somewhat longer than in female. First two and last two segments similar to female. Setal formula: 1.9.4.8.1.0.1.4.5, but many setae hardly visible and some possibly missed. All setae smooth and most with pore on top; same setae biarticulate as in female.

Antenna, labrum, mandibula, maxillula, maxilla, maxilliped, exopod and endopod of first swimming leg, exopod of second swimming leg, endopod of third swimming leg (same reductions in armature arrowed in Fig. 23*F*), and fourth swimming leg similar to female.

First swimming leg (Fig. 23*E*) with modified basis, inner margin of basis very rigidly sclerotised, with spiniform, smooth process distally. Inner spine on basis same size as in female, but without spinules at its base and inserted more proximally; inner spine only slightly longer than distal spiniform process of basis. Endopod three-segmented as in female.

Second swimming leg as in *S. a. analspinulosa*, with transformed endopodal second and third segments, but not mounted satisfactorily enough to allow drawing.

Third swimming leg (Fig. 23*F*) with characteristic element on anterior surface of third exopodal segment; this structure proportionately larger than in any other species described here, swollen at basal part, with pore on top, inserted at two-fifths and close to inner margin, reaching well beyond distal margin of third segment. First and second exopodal segments of third leg similar to female.

Fifth legs (Fig. 23*C*, *G*) with exopods also not fused to baseoendopods, but baseoendopods fused basally to each other, unornamented. Endopodal lobe much smaller and shorter than in female, also trapezoidal, extending to middle of exopod, armed with two very strong apical spines (or spiniform setae?); inner spine ~1.9 times as long as outer one. Exopod ~0.7 times as long as its maximum width, armed with five elements; length ratio of exopodal armature elements, from inner side, 1 : 5 : 3.8 : 1.3 : 1.6.

Sixth legs (Fig. 23*C*) completely fused to somite, without armature or ornamentation; only sign of their presence is a medial cleft, slightly moved to right side (indicating larger ancestral left plate).

Variability

Length ratio of the female fifth leg exopod armature can be somewhat variable (Fig. 23*A*), but no other forms of variability were observed. All examined specimens have a two-segmented endopod of the fourth swimming leg on both sides (Fig. 22*I*).

Distribution

This species was found only in the type locality, bore YYD22 on bore line 1, where it was collected on two separate occasions.

Remarks

This species differs from all Australian congeners by its two-segmented endopod of the fourth swimming leg (arrowed in Fig. 22*I*), in addition to its minute size, reductions in the armature of the third, fourth and fifth legs, and extremely short caudal rami. The two-segmented endopod of the fourth leg was used by Apostolov (1982) to define a newly erected genus, *Schizoperopsis* Apostolov, 1982. In the same publication Apostolov (1982) subdivided this genus into two subgenera based on the segmentation of the first leg endopod, the character he used also to subdivide two other genera separated from *Schizopera* Sars, 1905. Mielke (1992) strongly criticised this revision, and rejected *Schizoperopsis* as not being based on proven synapomorphies. He did a very provisional phylogenetic analysis of this group of harpacticoids, based on 15 characters and on the genus level, not on the species level. It is apparent from his cladogram, although he did not explain it, that he considered *Schizoperopsis* as one of the terminal clades of the larger *Schizopera* tree, and that its acceptance would render *Schizopera* as a paraphyletic taxon. Mielke's (1992) rejection of *Schizoperopsis* and its two subgenera was followed by Mielke (1995), Wells (2007) and Huys (2009), while it was maintained as a practical tool by Bodin (1997), and given in the list of valid genera by Boxshall and Halsey (2004). Karanovic (2004) also rejected the subgeneric division, but stated that the genus may be valid. However, he gave no arguments for this. Here we argue that the genus should be synonymised with *Schizopera*, as first proposed by Mielke (1992), as a closer examination of morphological characters shows that it represents a polyphyletic taxon.

Besides *S. akolos*, sp. nov., there are four other currently known members of *Schizopera* with a two-segmented endopod of the fourth leg: *S. arenicola* Chappuis & Serban, 1953 from the Romanian coast of the Black Sea; *S. gauldi* Chappuis & Rouch, 1961 from a sandy beach in Accra, Ghana; *S. nichollsi* Soyer, 1974 from Kerguelen Island, Southern Ocean; and *S. varnensis* Apostolov, 1972 from the Bulgarian coast of the Black Sea (see Chappuis and Serban 1953; Chappuis and Rouch 1961; Apostolov 1972; Soyer 1974). The only morphological character that unites them is the segmentation of the fourth leg endopod, while the following characters differ between species: ornamentation of the caudal rami (extra rows of spinules dorsally in *S. nichollsi*); armature of the caudal rami (proximal lateral seta enlarged in *S. arenicola* and *S. gauldi*); segmentation of the first leg endopod (two-segmented in *S. gauldi*, three-segmented in other species); armature of the first endopodal segment of the first leg (inner seta absent in *S. gauldi*, present in other species); armature of the second leg endopod (formula 0.1.4 in *S. akolos* and *S. nichollsi*, 0.1.3 in *S. varnensis*, 0.0.3 in *S. arenicola* and 0.0.2 in *S. gauldi*); armature of the third leg endopod (formula 1.1.3 in *S. nichollsi*, 1.1.2 in *S. varnensis*, 0.1.2 in *S. akolos*, 0.0.3 in *S. arenicola* and 0.0.2 in *S. gauldi*); armature of the fourth leg endopod (formula 1.3 in *S. gauldi*, 1.2 in *S. nichollsi*, 0.3 in *S. akolos*, and 0.2 in *S. arenicola* and *S. varnensis*); armature of the female fifth leg exopod (six elements in *S. nichollsi* and *S. varnensis*, five in *S. arenicola* and *S. gauldi* and four in *S. akolos*); armature of the female fifth leg baseoendopod (three elements in *S. gauldi*, four in other species). Our new species has no close relatives among these four species, and we suggest they all originated independently from more primitive *Szhizopera* species with a three-segmented endopod of the fourth leg, each one developing its own set of reductions. Note that all previously described Australian, and

most other species from around the world, have exactly the same armature formula of the swimming legs.

The phylogenetic position of *S. akolos* is unclear from the molecular data (Fig. 39). Different analyses put it either as a sister clade to *S.* sp. 2 from the Pilbara region, or the *kronosi* +*analspinulosa* s. str.+*analspinulosa linel* clade. The support for both is rather weak, and *S. akolos* is probably a separate colonisation event in the Yeerlirrie calcrete. It is a rare species, collected on two separate occasions in a single bore, despite the fact that we actively looked for it in the last two sampling rounds because of its small size.

The fact that *S. akolos* is nested inside the *Schizopera* clade based on *COI* data, can be used as an additional support for the rejection of the genus *Szhizoperopsis*.

Etymology

The new species name *akolos* (i.e. bit, morsel, Gr.) refers to its minute size even when compared to the very small *S. akation*, sp. nov., with which it was found to live sympatrically. The name is a noun in apposition.

Schizopera emphysema, sp. nov.

(Figs 3*C*, 24–27)

Material examined

Name-bearing type. Holotype (WAM C37485), adult female, completely dissected on 1 slide in Faure's medium, 27.viii.2009, leg. P. Bell and S. Callan (seLN7304).

Type locality. Australia: Western Australia: Yilgarn region, Yeelirrie station, line 2, bore YYAC1004C, 27.174665°S 119.877345°E.

Additional material examined. All from type locality: allotype (WAM C37486), adult ♂ dissected on 1 slide, 21.iii.2010, leg. T. Karanovic and S. Callan (seLN8555); 1 paratype ♂ in ethanol, 21.iii.2010, leg. T. Karanovic and S. Callan (seLN8555); 2 paratype ♂ + 1 paratype copepodid (WAM C37487) together in ethanol, 16.iii.2010, leg. S. Callan and N. Krawczyk (seLN8526); 1 copepodid destroyed for DNA sequence, 27.viii.2009, leg. P. Bell and S. Callan (seLN7304).

Description of female

Data from holotype. Total body length, measured from tip of rostrum to posterior margin of caudal rami (excluding caudal setae) 524 µm. Colour of preserved specimen yellowish. Nauplius eye not visible. Habitus (Fig. 3*C*) cylindrical, slender, without distinct demarcation between prosome and urosome; prosome–urosome ratio ~0.9 (in dorsal view); greatest width at posterior end of cephalothorax. Body length–width ratio ~4.9; cephalothorax 1.2 times as wide as genital double somite. Free pedigerous somites without pronounced lateral dorsal expansions. Integument relatively strongly chitinised. Prosomites ornamented only with sensilla and cuticular pores, with smooth integument and no pits; all urosomites and caudal rami, besides other ornamentation, with numerous parallel rows of minute spinules (Fig. 3*C*), although not as dense as in *S. analspinulosa* or next two species. Rostrum (Fig. 3*C*) long and clearly demarcated at base, reaching two-thirds of second antennular segment, linguiform, with blunt tip, about twice as long as wide; ornamented with two sensilla dorsolaterally.

Cephalothorax (Fig. 3*C*) ~1.2 times as long as wide in dorsal view (without rostrum); represents 30% of total body length. Surface of cephalothoracic shield and tergites of first three free pedigerous somites with characteristic pattern of large sensilla and small cuticular pores, exactly as in *S. a. analspinulosa* in dorsal view (see Fig. 6*A*), while two lateral sensilla expressed as pores at midlength laterally and two sensilla closer to each other next to these (Fig. 3*C*). Two sensilla and two pores at base of rostrum. Cephalothoracic shield and free prosomites without cuticular pits or spinules; hyaline fringes smooth and unornamented (Fig. 3*C*). Fifth pedigerous somite (first urosomal) ornamented with four dorsal large sensilla and two lateral sensilla (one on each side), as well as with two cuticular pores ventrolaterally (one on each side), in addition to three rows of numerous minute cuticular spinules; hyaline fringe sharply serrated (Figs 3*C*, 24*A*)

Genital double somite (Figs 3*C*, 24*A*) ~0.8 times as long as wide (dorsal view), with visible suture internally; ornamented with eight sensilla dorsally (six at midlength, two near posterior margin), two posterior sensilla ventrally, and two posterior sensilla and two midlength pores laterally (one on each side), in addition to several rows of minute spinules dorsally and laterally, and much less ventrally; hyaline fringe sharply serrated both ventrally and dorsally. Female genital complex with elongated, large and ovoid epicopulatory bulb, ~1.8 times as long as wide. Seminal receptacles small, ovoid, reaching anterior margin of epicopulatory bulb, ~0.6 times as long as epicopulatory bulb. Third urosomite ornamented with six posterior sensilla (two dorsal, two ventral and two lateral) and two ventral pores at midlength (Fig. 24*A*), in addition to four irregular but roughly parallel rows of slender spinules; hyaline fringe serrated and straight. Preanal somite (Fig. 24*A*, *C*) without sensilla or pores, ornamented with several irregular rows of slender spinules (rows in dorsal view broken into smaller crescentic components, forming a wavy pattern); hind margin clearly bulging posteriorly in dorsal region, forming very sharply serrated pseudoperculum (Fig. 24*C*). Anal somite (Fig. 24*A*, *B*, *C*) with convex and relatively short anal operculum, ornamented with transverse row of spinules along posterior margin; ornamented with two large sensilla dorsally, two lateral cuticular pores (one on each side), two ventromedian pores, one dorsolateral row of minute spinules at midlength, one bull-horn-shaped row of spinules ventrally, and transverse row of large spinules along posterior margin; all posterior spinules of about same size. Anal sinus (Fig. 24*C*) widely opened, unornamented, almost completely covered with pseudoperculum; represents 55% of somite's width.

Caudal rami (Fig. 24*A*, *B*, *C*) strongly sclerotised, very long, inflated almost along entire length (arrowed in Fig. 24*B*, *C*), 2.8 times as long as wide in dorsal view, and 1.2 times as long as anal somite, almost parallel, with space between them less than half of one ramus width; ornamented with two ventral and two dorsal cuticular pores in posterior half, transverse row of several large spinules along posterior margin ventrally (none dorsally), two parallel rows of large spinules along dorsal margin, and several short rows of minute spinules ventrally and medially (only one row ventrally); armed with six elements (two lateral,

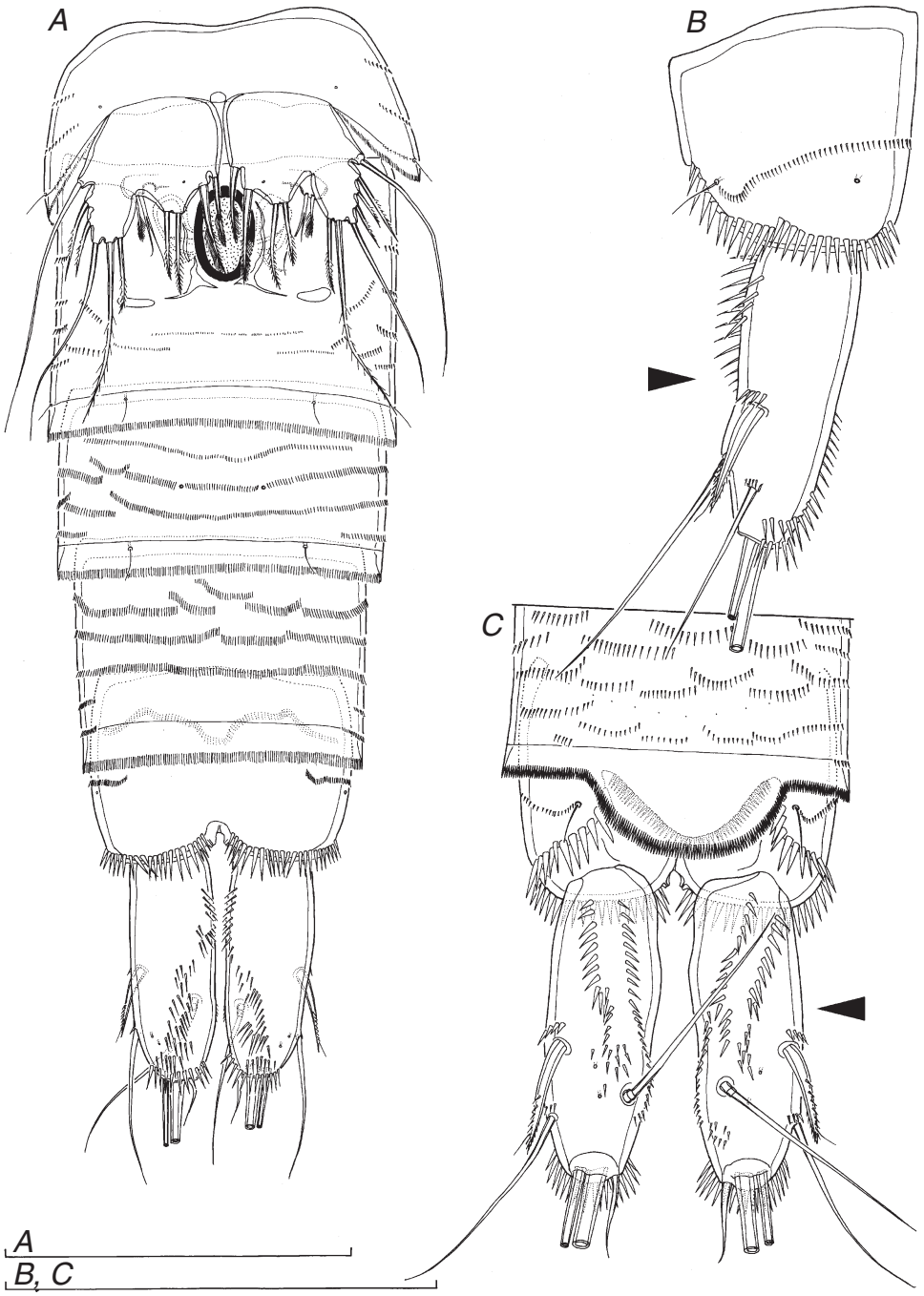

Fig. 24. *Schizopera emphysema*, sp. nov., holotype ♀. (*A*) Urosome, ventral view; (*B*) anal somite and right caudal ramus, lateral view; (*C*) last two urosomal somites and caudal rami, dorsal view. Arrows point to inflated caudal rami, different from previous species. Scale bars = 100 µm.

one dorsal and three apical). Dorsal seta slender and smooth, ~0.9 times as long as ramus, inserted at three-quarters of ramus length, triarticulate. Lateral proximal spine stout, inserted slightly posterior to midlength, only 0.4 times as long as ramus. Lateral distal seta very slender, smooth, inserted slightly ventrolaterally at five-sixths of ramus length, ~0.6 times as long as ramus. Inner apical seta short and smooth, 0.25 times as long as ramus. Principal apical setae without breaking planes; middle apical seta strongest, bipinnate at distal end, 1.6 times as long as unipinnate outer apical seta, and almost 0.6 times as long as body length.

Antennula (Figs 3*C*, 25*A*) eight-segmented, only slightly shorter than cephalothorax, with short aesthetasc on eighth segment, fused to two apical setae, and large aesthetasc on fourth segment, reaching significantly beyond tip of appendage and fused basally to equally long seta; setal

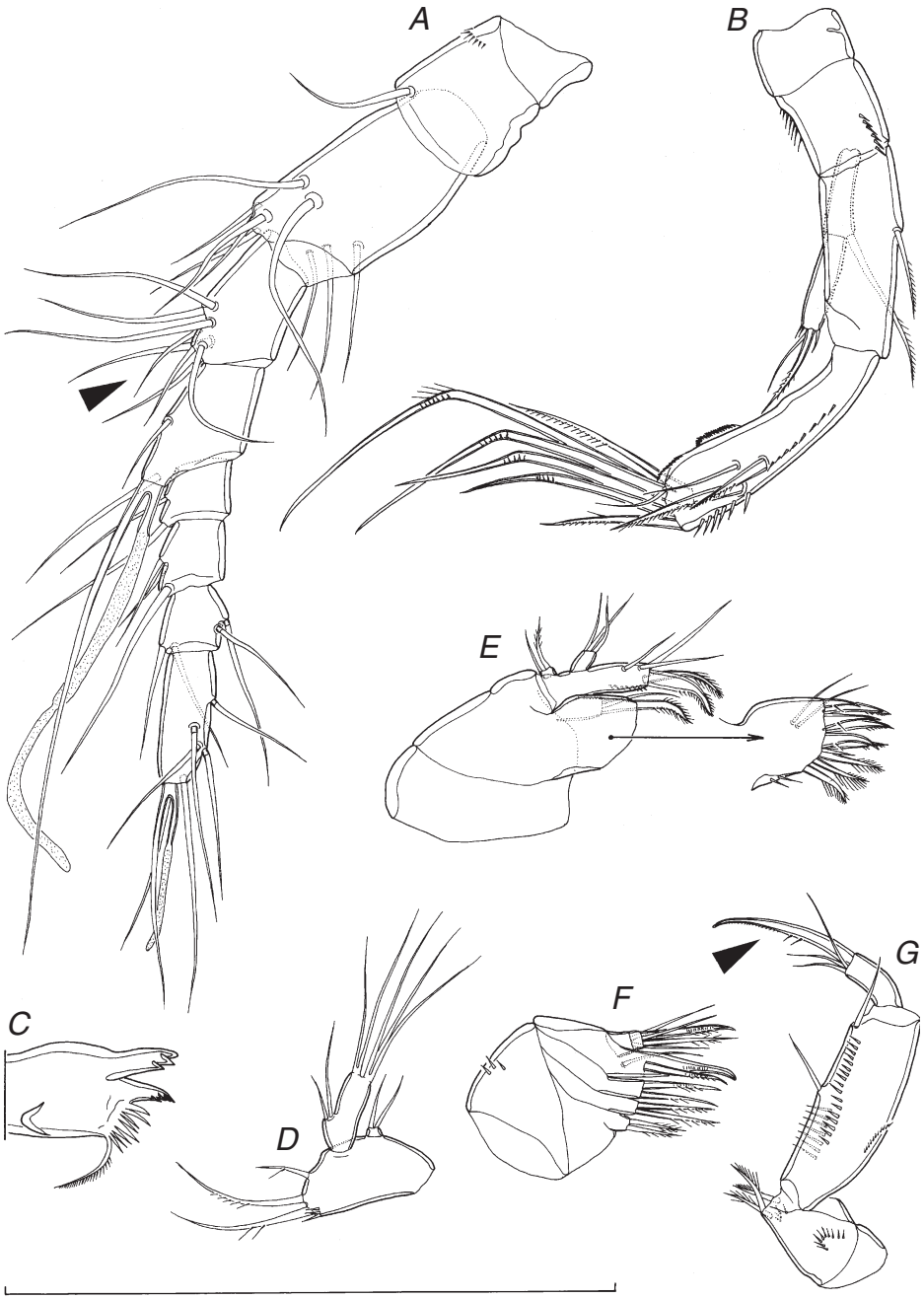

Fig. 25. *Schizopera emphysema*, sp. nov., holotype ♀. (*A*) Antennula, ventral view; (*B*) antenna, ventral view; (*C*) cutting edge of mandibula, anterior view; (*D*) mandibular palp, anterior view; (*E*) maxillula, posterior view; (*F*) maxilla, anterior view; (*G*) maxilliped, posterior view. Arrows point to characters different from previous species. Scale bar = 100 µm.

formula: 1.9.8.3.2.3.4.7, as in *S. analspinulosa* except for one additional seta on third segment (arrowed in Fig. 25*A*). Only two lateral setae on seventh segment and four on eighth segment biarticulate. All setae smooth and slender. Length ratio of antennular segments, from proximal end, 1 : 2.3 : 1 : 1 : 0.6 : 0.6 : 0.6 : 1.4. First segment ornamented with short transverse row of small spinules ventromedially, other segments unornamented.

Antenna (Fig. 25*B*) segmentation, armature, and even basic ornamentation as in *S. a. analspinulosa*, but more elongated and with more slender armature elements; seta on first exopodal segment also proportionately longer.

Labrum as in *S. a. analspinulosa*.

Mandibula (Fig. 25*C*, *D*) also very similar to that in *S. a. analspinulosa*, only with slightly more elongated complex teeth on cutting edge of coxa (Fig. 25*C*), and shorter basis (Fig. 25*D*).

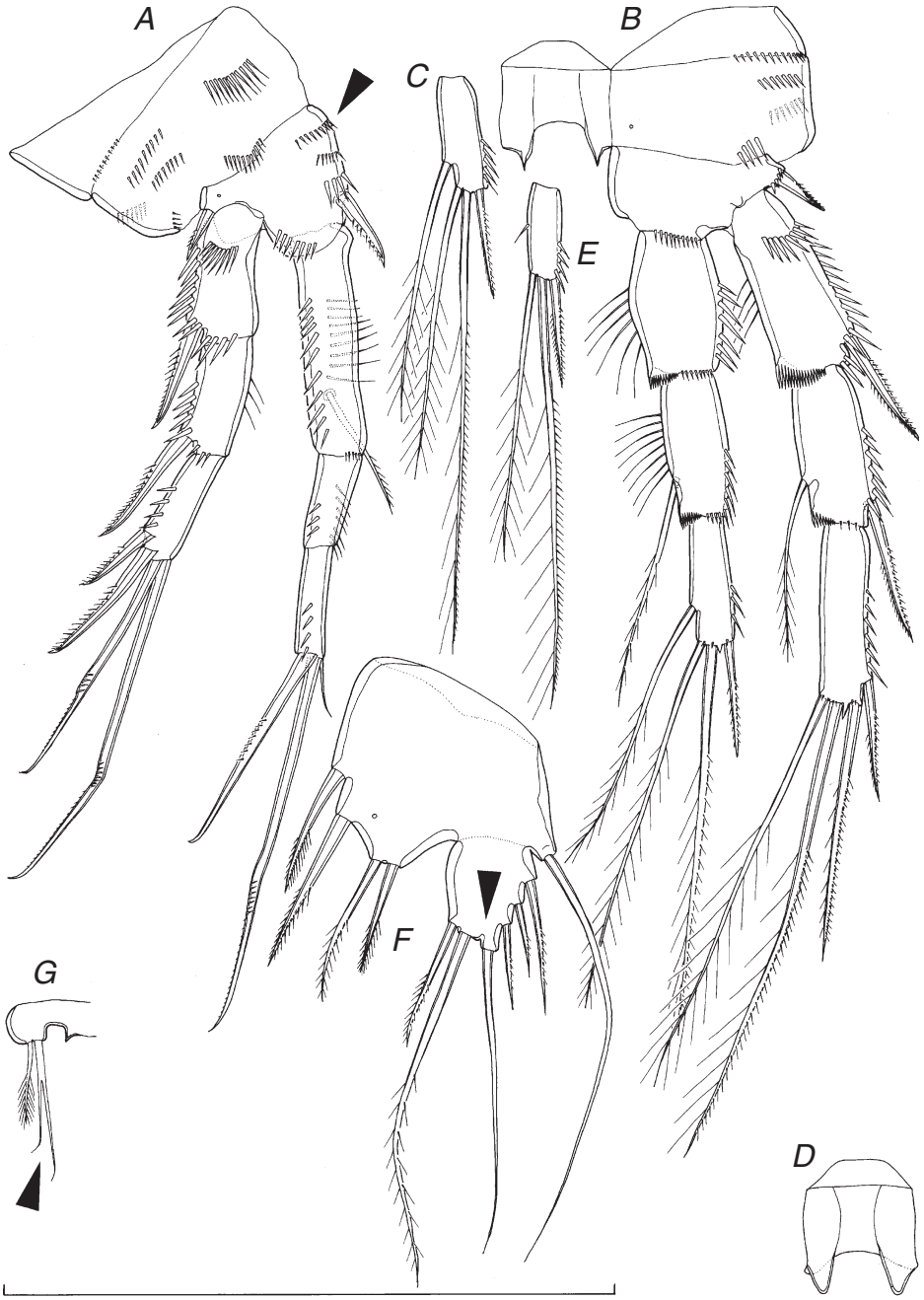

Fig. 26. *Schizopera emphysema*, sp. nov., holotype ♀. (*A*) First swimming leg, anterior view; (*B*) second swimming leg, anterior view; (*C*) third endopodal segment of third swimming leg, anterior view; (*D*) intercoxal sclerite of fourth swimming leg, anterior view; (*E*) third endopodal segment of fourth swimming leg, anterior view; (*F*) fifth leg, anterior view; (*G*) sixth leg, anterior (ventral) view. Arrows point to characters different from previous species. Scale bar = 100 µm.

Maxillula (Fig. 25*E*) with large preacoxa, arthrite highly mobile, armed apically with six strong, unipinnate spines, and three bipinnate setae; laterally armed with two slender smooth setae and ornamented with two slender spinules on middle of arthrite. Coxa, basis and exopod very similar to those in *S. a. analspinulosa*, while endopod slightly shorter.

Maxilla (Fig. 25*F*) also very similar to that in *S. a. analspinulosa*, only with somewhat stronger spinules near outer margin of syncoxa.

Maxilliped (Fig. 25*G* segmentation, armature, and even basic ornamentation as in *S. a. analspinulosa*, but with proportionately much longer claw-like apical spine on second endopodal segment

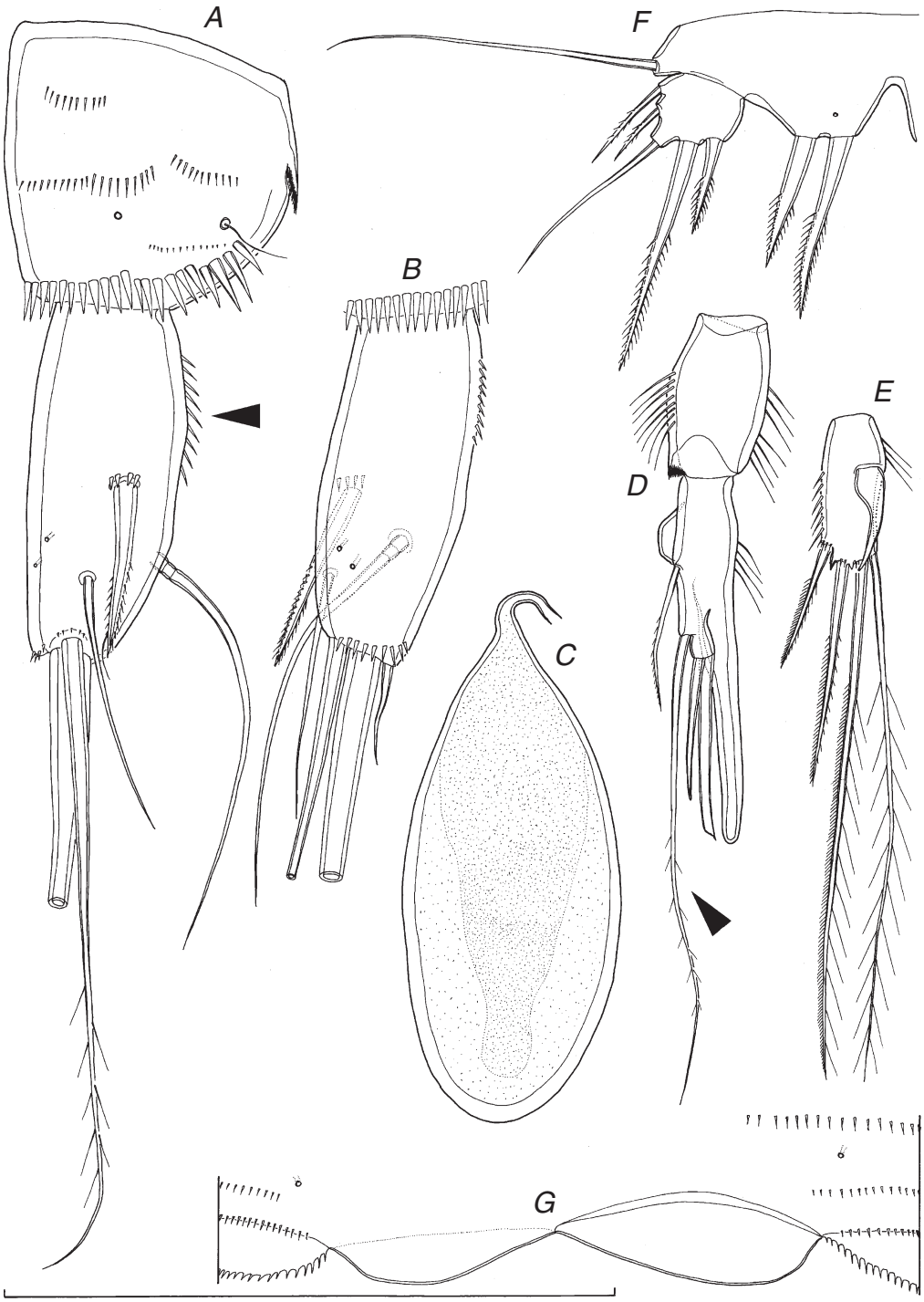

Fig. 27. *Schizopera emphysema*, sp. nov., allotype ♂. (*A*) Anal somite and left caudal ramus, lateral view; (*B*) right caudal ramus, ventral view; (*C*) spermatophore, ventral view; (*D*) endopod of third swimming leg, posterior view; (*E*) third exopodal segment of third swimming leg; (*F*) fifth leg, anterior view; (*G*) sixth legs, ventral view. Arrows point to characters different from previous species. Scale bar = 100 µm.

(arrowed in Fig. 25*G*); spinules on outer margin of first endopodal segment smaller and more numerous.

All swimming legs (Fig. 26*A–E*) slender and long, segmentation and armature formula as in *S. a. analspinulosa*, but with much more slender armature elements and somewhat shorter endopods; composed of small triangular preacoxa, large quadrate coxa, smaller basis, three-segmented exopod, and three-segmented endopod. Coxae in all legs connected with intercoxal

sclerites. All exopodal and endopodal segments of similar length, except much longer first endopodal segment of first leg.

First swimming leg (Fig. 26*A*) with very small intercoxal sclerite, concave at distal end and unornamented. Preacoxa unarmed, ornamented with short posterior row of minute spinules. Coxa also unarmed, ornamented with four horizontal short rows of large spinules on anterior surface (one inner, one distal and two close to outer margin) and one on posterior; no parallel rows of minute spinules. Basis armed with one inner and one outer strong spine; ornamentation consists of row of spinules at base of each spine, two additional rows of spinules close to inner margin and parallel to that at base of inner spine (proximal one arrowed in Fig. 26*A*), one row of large spinules along distal margin (between endopod and exopod), and one cuticular pore near base of outer spine (all on anterior surface). Exopodal armature and ornamentation as in *S. a. analspinulosa.* Endopod geniculate, with first segment slightly shorter than first two exopodal segments combined, 2.5 times as long as second endopodal segment, and about four times as long as wide; strongly sclerotised beak present proximally on inner margin of first segment, hidden behind inner spine of basis; endopodal armature and ornamentation as in *S. a. analspinulosa*, except inner seta on first segment much more slender (but not longer; ~0.6 times as long as first endopodal segment).

Second swimming leg (Fig. 26*B*) with even smaller preacoxa than in first leg, also unarmed and ornamented only with posterior row of minute spinules. Coxa armed with two short horizontal rows of large spinules on anterior surface, and one row of large spinules on posterior surface. Intercoxal sclerite with paired, pointed distal protrusions, although not as long as in *S. a. analspinulosa*. Basis armed only with outer spine, ornamented with spinules at base of outer spine and along distal margin at base of endopod. Distal inner corners of first and second exopodal and endopodal segments with hyaline frills. All exopodal and endopodal segments ornamented with strong spinules on outer margins; first exopodal and first and second endopodal segments also with less strong spinules along inner margins. Exopod armed with outer-distal spines on first and second segments, inner seta on second segment, two outer spines and two apical setae on third segment; all setae slender and bipinnate, those on terminal segments much longer than in *S. a. analspinulosa*; outer apical seta on third exopodal segment looks like transitional stage between spine and seta, with outer margin furnished with short spinules and inner margin with slender spinules. Endopod armed with single inner seta on second segment, and four elements on third segment: outer-distal short spine, two apical long setae, and one inner slender seta (inserted at two-thirds); inner apical seta as long as middle seta.

Third swimming leg (Fig. 26*C*) very similar to second, except that basis armed with outer slender seta instead of spine, and endopod additionally armed with inner seta on first segment. Also pointed processes on intercoxal sclerite less sharp than in second leg. All setae slender; inner apical seta on third endopodal segment only ~0.6 times as long as middle seta.

Fourth swimming leg (Fig. 26*D, E*) very similar to third leg, except that inner seta missing on third endopodal segment (Fig. 26*E*), and pointed processes on intercoxal sclerite even less sharp (Fig. 26*D*); inner apical seta on third endopodal segment also only ~0.6 times as long as middle seta.

Fifth leg (Figs 24*A*, 26*F*) biramous but exopod fused to baseoendopod on anterior surface (subdivision visible on posterior surface). Baseoendopod with outer basal smooth seta arising from relatively short setophore, without ornamentation at its base. Endopodal lobe trapezoidal, extending almost to midlength of exopod, ornamented only with small cuticular pore, armed with four stout, spiniform elements (two inner ones probably spines, two outer ones probably spiniform setae); length ratio of endopodal armature elements, from inner side, 1 : 1.3 : 1.2 : 0.9. Exopod pentagonal, with middle part produced distally (arrowed in Fig. 26*F*), 1.2 times as long as maximum width, unornamented but armed with five or six elements; two innermost bipinnate, middle one smooth and slender, two or three outermost short, relatively stout and unipinnate; length ratio of exopodal armature elements, from inner side, 1 : 2.7 : 2.3 : 0.6 : (0.6) : 1.

Sixth leg (Fig. 26*G*) indistinct, very small cuticular plate, covering gonopore, armed with one very small spine, fused basally to plate, and two setae; inner seta characteristically bifid (arrowed in Fig. 26*G*), ~1.6 times as long as plumose outer seta.

Description of male

Data from allotype and two paratypes. Body length ranges from 484 to 516 µm (516 µm in allotype). Habitus slightly more slender than in female, but also cylindrical, and with similar proportions of prosome–urosome, and cephalothorax–genital somite. Body length–width ratio about 5.0. Ornamentation of prosomites, colour and nauplius eye similar to female.

Genital somite twice as wide as long. Single, completely formed, longitudinally placed spermatophore (Fig. 27*C*) inside first two urosomites in all specimens, ~2.2 times as long as wide. Abdominal somites similar to female, except that cuticular pores not visible ventrally. Anal somite (Fig. 27*A*) similar to female, but additionally ornamented with three short rows of minute spinules laterally.

Caudal rami (Fig. 27*A*, *B*) slightly more inflated than in female (arrowed in Fig. 27*A*) and with principal outer seta bipinnate; both principal setae also without breaking planes.

Antennula very similar to that in *S. a. analspinulosa*.

Antenna, labrum, mandibula, maxillula, maxilla, maxilliped, exopod and endopod of first swimming leg, exopod of second swimming leg, endopod of third swimming leg, and fourth swimming leg similar to female.

First swimming leg with modified basis, inner margin of basis very rigidly sclerotised, with spiniform, smooth process distally, and smaller one proximally. Inner spine on basis smaller than in female, without spinules at its base, inserted more proximally, and slightly longer than distal spiniform process of basis.

Second swimming leg (Fig. 27*D*) with transformed endopodal second and third segments. Second segment with part of inner margin protruded into rounded indistinct lobe, without ornamentation on its surface; inner seta shorter than in female and unipinnate. Third segment completely modified; two ancestral apical setae transformed into smooth, spiniform armature elements, outer one stronger and with abruptly sharpened tip, ~1.3 times as long as inner apical one; inner

seta (arrowed in Fig. 27*D*) very long, slender and bipinnate, 2.5 times as long as outer apical seta. Ancestral outer spine completely fused to somite, transformed into very strong and smooth thorn slightly longer than ancestral apical elements, and about as long as last two endopodal segments combined. As a result of these transformations, third segment medially cleft.

Third swimming leg (Fig. 27*E*) with very characteristic element on anterior surface of third exopodal segment; this structure is swollen at basal part, with pore on top, inserted at two-fifths and close to inner margin, reaching slightly beyond distal margin of third segment, proportionately much larger than in *S. a. analspinulosa*; also apical setae on third exopodal segment proportionately longer. First and second exopodal segments of third leg similar to female.

Fifth legs (Fig. 27*F*) with basally fused baseoendopods, ornamented with single pore and two spinules as in female. Endopodal lobe much smaller and shorter, also trapezoidal, extending to middle of exopod in length, armed with two very strong apical spines; inner spine ~1.4 times as long as outer one. Exopod about as long as its maximum width, demarcated basally on both anterior and posterior surface, armed with five elements; fifth element from inner side not observed in male specimens, sometimes present in females; length ratio of exopodal armature elements, from inner side, 1 : 2.5 : 2 : 0.7 : 1.

Sixth legs (Fig. 27*G*) pair of small and short cuticular plates, without armature or ornamentation; left plate wider and larger than right one, and better demarcated at base.

Variability

Fifth leg exopod in the holotype female is armed with five elements on the right side and six elements on the left side (Fig. 24*A*).

Distribution

This species was found only in the type locality, bore YYAC1004C on bore line 1, where it was collected on three separate occasions (Fig. 41). Interestingly, three other bores that are situated only a few metres from this one (YYAC1004A, B and D) have never produced any animals of this species, although some produced other copepod species found in YYAC1004C.

Remarks

This species can be distinguished from all other Australian congeners by its characteristically modified caudal rami, which are long and bulbous (i.e. have an inflated look; arrowed in Fig. 24*B*, *C*). Absence of enlarged dorsal spinules on the anal somite distinguishes it additionally from *S. kronosi*, sp. nov. and *S. analspinulosa*, sp. nov., while the segmentation of the swimmings legs distinguishes it from *S. akation*, sp. nov. and *S. akolos*, sp. nov. Densely ornamented somites and cuticular pore pattern would put *S. emphysema*, sp. nov. close to *S. leptafurca*, sp. nov. and *S. uranusi*, sp. nov., and this is mostly supported by molecular data (Fig. 39). Also, they all have three rows of spinules at base of inner spine on the first leg basis in female (arrowed in Figs 26*A*, 30*A*, 35*C*), and principal apical setae on the caudal rami without breaking planes. It is interesting that all three species are large forms, living sympatrically (ranges of the latter two overlap only partly), and that the most obvious differences are found in the caudal rami, appendages responsible for sexual recognition. The only other Australian species of *Schizopera* with inflated caudal rami is an as yet undescribed marine interstitial species from Walpole, south-western Western Australia, more than 900 km south-west from the Yeelirrie calcrete (T. Karanovic, unpubl. data). However, this species lacks an inner seta on the second endopodal segment of second to fourth legs, has a longer first endopodal segment of the first leg, and a very different looking armature of the caudal rami, with proximal lateral seta very short and spiniform, distal lateral seta very short and slender, and dorsal seta inserted at midlength. The inflated look in these two species probably originated convergently.

Five other species of *Schizopera* have caudal rami with a more or less inflated look: *S. anomala* Coull, 1971 from littoral habitats of North Carolina, USA; *S. bradyi* Soyer, 1974 from Kerguelen Island, Southern Ocean; *S. longifurcata* Chappuis, 1955 from sandy beaches of Lake Tanganyika and Lake Nyasa, Africa; and two species from sandy beaches of the Bay of Biscay in France: *S. parvula* Noodt, 1955 and *S. minuta* Noodt, 1955 (see Chappuis 1955; Noodt 1955; Fryer 1956; Coull 1971; Soyer 1974). The first species was so incompletely described that we cannot even be sure it belongs to the genus *Schizopera*. However, all five differ from *S. emphysema* by several morphological characters, many of them related to the shape and position of different armature elements on the inflated caudal rami, showing that the inflated condition most likely originated convergently in probably all six taxa.

Other Australian species also differ from *S. emphysema* by several morphological characters, although the five species described from the Yilgarn region by Karanovic (2004) are more closely related than those from the Pilbara region (Karanovic 2006). All five previously described species from the Yilgarn have a dense coat of slender spinules on their somites and caudal rami, at least one row of long spinules along the inner margin of the caudal rami, as well as a very long inner seta on the third endopodal segment of the male second leg (arrowed in Fig. 27*D*). The last character is unknown in *S. oldcuei* Karanovic, 2004 as males have not been found yet. However, none of them, or any other *Schizopera*, have two parallel rows of spinules along the dorsal margin (see Fig. 24*C*), which is clearly one of the autapomorphic features of *S. emphysema*. Another autapomorphic feature of the new species is a bifid inner seta on the female sixth leg (arrowed in Fig. 26*G*), although this minute character may have been easily overlooked in some early descriptions. Five previously described species from the Yilgarn region can additionally be distinguished from *S. emphysema* by the size and shape of their caudal rami, as well as some other morphological details. For example, *S. oldcuei* has a very short outer principal apical seta on the caudal rami, and (together with *S. uramurdahi* Karanovic, 2004) breaking planes on both caudal principal apical setae. *Schizopera depotspringsi* Karanovic, 2004 has a much longer first endopodal segment of the first leg, and only five elements on the female fifth leg exopod. *Schizopera austindownsi* Karanovic, 2004 has a narrower baseoendopod and shorter exopod of the female fifth leg, while *S. jundeei* Karanovic, 2004 has the proximal lateral (spiniform) seta inserted more posteriorly than the dorsal seta.

Etymology

The new species is named after its characteristically inflated caudal rami. The name *emphysema* (i.e. something inflated, swollen, Gr.) is a noun in apposition.

Schizopera leptafurca, sp. nov.

(Figs 4*A*, 28–33)

Material examined

Name-bearing type. Holotype (WAM C37488), adult female, completely dissected on 1 slide in Faure's medium, 16.iii.2010, leg. S. Callan and N. Krawczyk (seLN8360).

Type locality. Australia: Western Australia: Yilgarn region, Yeelirrie station, line 1.5, bore YYAC33, 27.169565°S 119.871815°E.

Additional material examined. Allotype (WAM C37489), adult ♂ dissected on 1 slide, 16.iii.2010, leg. S. Callan and N. Krawczyk (seLN8360), type locality; 2 paratype ♂+2 paratype ♀ (WAM C37490) together on 1 SEM stub, 16.iii.2010, leg. S. Callan and N. Krawczyk (seLN8360), type locality; 1 paratype ♀ dissected on 1 slide, 16.iii.2010, leg. S. Callan and N. Krawczyk (seLN8360), type locality; 1 paratype ♂ dissected on 1 slide, 16.iii.2010, leg. S. Callan and N. Krawczyk (seLN8360), type locality; 15 paratype ♂+25 paratype ♀+15 paratype copepodids (WAM C37491) together in ethanol, 16.iii.2010, leg. S. Callan and N. Krawczyk (seLN8360), type locality; 20 ♂+10 ♀+12 copepodids together in ethanol, 12.xi.2009, leg. P. Bell and G. Perina (seLN7421), type locality; 2 ♀ destroyed for DNA sequence, 12.xi.2009, leg. P. Bell and G. Perina (seLN7421), type locality; 70 ♂+100 ♀+30 copepodids, 21.iii.2010, leg. T. Karanovic and S. Callan (seLN8305), type locality; 1 ♀ destroyed for DNA sequence, 12.xi.2009, leg. P. Bell and G. Perina (seLN7417), bore line 1.5, bore YYAC35, 27.166173°S 119.873977°E; 1 ♂+1 ♀ together in ethanol, 16.iii.2010, leg. S. Callan and N. Krawczyk (seLN8366), same locality; 2 ♂+6 ♀ together in ethanol, 21.iii.2010, leg. T. Karanovic and S. Callan (seLN7126), same locality; 3 ♂+10 females, 11.i.2010, leg. P. Bell and G. Perina (seLN7645), same locality; 4 ♂+1 copepodid together in ethanol, 12.xi.2009, leg. P. Bell and G. Perina (seLN7389), bore line 3, bore YYAC118, 27.174573°S 119.889727°E; 1 ♀ destroyed for DNA sequence, 12.xi.2009, leg. P. Bell and G. Perina (seLN7389), same locality; 4 ♂+4 ♀+2 copepodids together in ethanol, 21.iii.2010, leg. T. Karanovic and S. Callan (seLN8538), same locality; 1 ♀ destroyed for DNA sequence, 21.iii.2010, leg. T. Karanovic and S. Callan (seLN8538), same locality; 1 ♂ in ethanol, 16.iii.2010, leg. S. Callan and N. Krawczyk (seLN8369), same locality; 1 ♂+3 ♀ together in ethanol, 12.xi.2009, leg. P. Bell and G. Perina (seLN7433), bore line 3.5, bore YYAC328, 27.175601°S 119.907658°E; 1 ♀ destroyed for DNA sequence, 12.xi.2009, leg. P. Bell and G. Perina (seLN7433), same locality; 1 ♀ in ethanol, 11.i.2010, leg. P. Bell and G. Perina (seLN7685), same locality; 1 ♂ destroyed for DNA sequence, 17.iii.2010, leg. T. Karanovic and S. Callan (seLN8393), same locality; 3 ♂+1 ♀ together in ethanol, 20.iii.2010, leg. T. Karanovic and S. Callan (seLN8417), bore line 1, bore YYAC0016A, 27.170328°S 119.868867°E; 1 ♂ destroyed for DNA sequence, 20.iii.2010, leg. T. Karanovic and S. Callan (seLN8417), same locality; 2 ♂+2 ♀ together in ethanol, 20.viii.2009, leg. P. Bell and S. Callan (seLN6597), same locality; 10 ♂+14 ♀+5 copepodids together in ethanol, 15.iii.2010, leg. S. Callan and N. Krawczyk (seLN8479), bore line 1, bore YYD26, 27.164033°S 119.873196°E; 1 ♀ destroyed for DNA sequence, 15.iii.2010, leg. S. Callan and N. Krawczyk (seLN8479), same locality; 20 ♂+60 ♀+13 copepodids together in ethanol, 20.iii.2010, leg. T. Karanovic and S. Callan (seLN8297), same locality; 22 ♂+15 ♀+20 copepodids together in ethanol, 1.ix.2009, leg. P. Bell and S. Callan (seLN6605), same locality; 1 ♂+2 ♀ together in ethanol, 31.viii.2009, leg. P. Bell and S. Callan (seLN7289), same locality; 1 ♂ in ethanol, 17.iii.2010, leg. T. Karanovic and S. Callan (seLN8385), bore line 5, bore YYAC0014D, 27.185508°S 119.929231°; 1 ♂ destroyed for DNA sequence, 17.iii.2010, leg. T. Karanovic and S. Callan (seLN8385), same locality; 1 ♀ destroyed for DNA sequence, 18.iii.2010, leg. T. Karanovic and S. Callan (seLN7131), bore line K, bore YYHC085B, 27.247824°S 120.054676°E; 3 ♂+7 ♀+4 copepodids together in ethanol, 20.iii.2010, leg. T. Karanovic and S. Callan (seLN8418), same locality; 2 ♂+9 ♀+1 copepodid together in ethanol, 20.iii.2010, leg. T. Karanovic and S. Callan (seLN8464), bore line K, bore YYHC0049K, 27.247548°S 120.054862°E; 1 ♀ destroyed for DNA sequence, 20.iii.2010, leg. T. Karanovic and S. Callan (seLN8464), same locality; 4 ♀ in ethanol, 18.iii.2010, leg. T. Karanovic and S. Callan (seLN8459), same locality; 3 ♂+6 ♀ together in ethanol, 15.iii.2010, leg. S. Callan and N. Krawczyk (seLN8496), bore line 1, bore YYD22, 27.167304°S 119.870456°E; 1 ♀ in ethanol, 20.iii.2010, leg. T. Karanovic and S. Callan (seLN8411), same locality; 1 ♂+2 ♀ together in ethanol, leg. P. Bell and G. Perina (seLN6610), same locality; 1 ♂ in ethanol, 20.iii.2010, leg. T. Karanovic and S. Callan (seLN8302), bore line 1, bore YYAC0019B, 27.159121°S 119.876035°E; 1 ♂+2 ♀ together in ethanol, 16.iii.2010, leg. S. Callan and N. Krawczyk (seLN8356), bore line 1, bore YYAC24, 27.164034°S 119.873195°E; 2 ♂+1 copepodid together in ethanol, 16.iii.2010, leg. S. Callan and N. Krawczyk (seLN8526), bore line 2, bore YYAC1004C, 27.174665°S 119.877345°E; 4 ♂+5 ♀+4 copepodids together in ethanol, 12.i.2010, leg. P. Bell and G. Perina (seLN7351), same locality; 11 ♂+10 ♀+10 copepodids together in ethanol, 21.iii.2010, leg. T. Karanovic and S. Callan (seLN8555), same locality; 4 ♀+2 copepodids together in ethanol, 16.iii.2010, leg. S. Callan and N. Krawczyk (seLN8342), bore line 2, bore YYAC1004D, 27.174664°S 119.877343°E; 1 ♂+1 copepodid together in ethanol, 12.xi.2010, leg. P. Bell and G. Perina (seLN6651), same locality; 1 ♀+1 copepodid together in ethanol, 12.xi.2009, leg. P. Bell and G. Perina (seLN7369), bore line 1, bore YYAC0018C, 27.161503°S 119.874715°E; 1 ♂+1 ♀ together in ethanol, 11.i.2010, leg. P. Bell and G. Perina (seLN7688), bore line 1, bore YYAC0015A, 27.170329°S 119.868869°E; 1 ♀+2 copepodids together in ethanol, hight flow pump, 30.viii.2009, leg. P. Bell and S. Callan (seLN6589), bore line 5, bore YYAC0014A, 27.185507°S 119.929233°; 6 ♂+1 ♀ together in ethanol, slow flow pump, 30.viii.2009, leg. P. Bell and S. Callan (seLN6591), same locality; 3 ♂+1 ♀+1 copepodid together in ethanol, hauling, 30.viii.2009, leg. P. Bell and S. Callan (seLN6599), same locality.

Description of female

Data from holotype and several paratypes. Total body length, measured from tip of rostrum to posterior margin of caudal rami (excluding caudal setae), ranges from 485 to 725 µm (557 µm in holotype). Colour of preserved specimens yellowish. Nauplius eye not visible. Habitus (Figs 4*A*, 31*A*) cylindrical, slender, without distinct demarcation between prosome and urosome; prosome–urosome ratio ~1.3 (in dorsal view); greatest width at posterior end of cephalothorax. Body length–width ratio ~4.5; cephalothorax 1.3 times as wide as genital double somite. Free pedigerous somites without pronounced lateral dorsal expansions. Integument relatively weakly chitinised. All somites and caudal rami, besides other ornamentation, with dense cover of minute spinules (inset in Fig. 4*A*, and Figs 28*B*, *C*, *D*, 29*A*, 31*A*, *B*, *D*). Rostrum (Figs 28*D*, 29*B*, 31*E*) long and clearly demarcated at base, reaching one-third of second antennular segment, linguiform, with blunt tip, about twice as

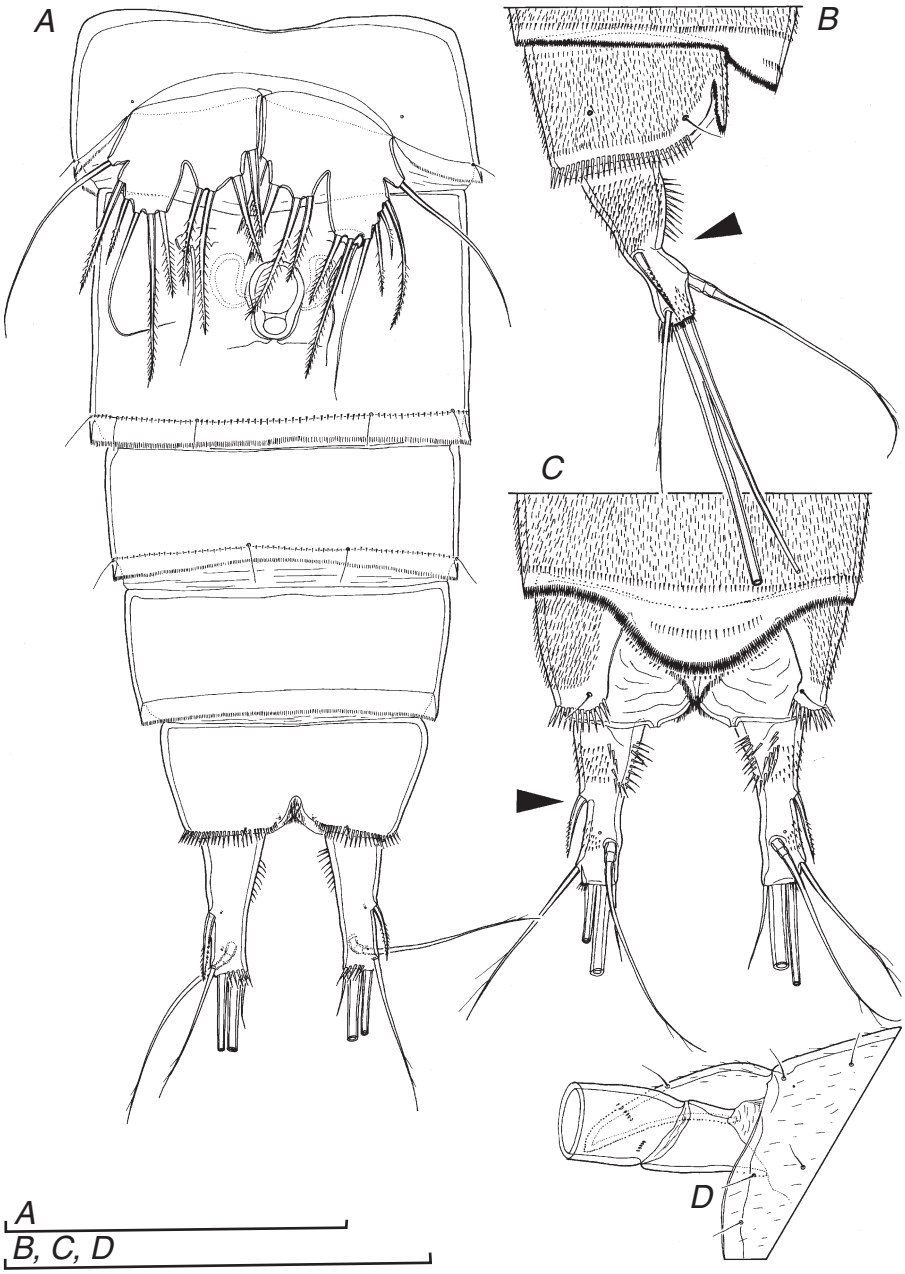

Fig. 28. *Schizopera leptafurca*, sp. nov., holotype ♀. (*A*) Urosome without minute spinules drawn, ventral view; (*B*) last two urosomal somites and left caudal ramus, lateral view; (*C*) last two urosomal somites and caudal rami, dorsal view; (*D*) rostrum and anterior part of cephalothorax, lateral view. Arrows point to constricted caudal rami, different from previous species. Scale bars = 100 µm.

long as wide; ornamented with two sensilla dorsolaterally, and with several slender spinules dorsally.

Cephalothorax (Figs 4*A*, 28*D*, 31*E*) ~1.2 times as long as wide in dorsal view (without rostrum); represents 30% of total body length. Surface of cephalothoracic shield and tergites of first three free pedigerous somites with characteristic pattern of large sensilla and small cuticular pores, very similar to that in *S. a. analspinulosa*, except central dorsal sensilla and posterior dorsal pore missing, and two additional sensilla visible in lateral view. Two sensilla and two pores at base of rostrum (Fig. 28*D*). Cephalothoracic shield without cuticular pits. Hyaline fringe of cephalothoracic shield smooth and unornamented, those of other prosomites finely serrated dorsally and partly laterally, with smooth ventrolateral corners (Fig. 4*A*); sensilla pattern as in *S. a. analspinulosa*. Fifth pedigerous somite (first urosomal) ornamented with four dorsal large sensilla and four lateral

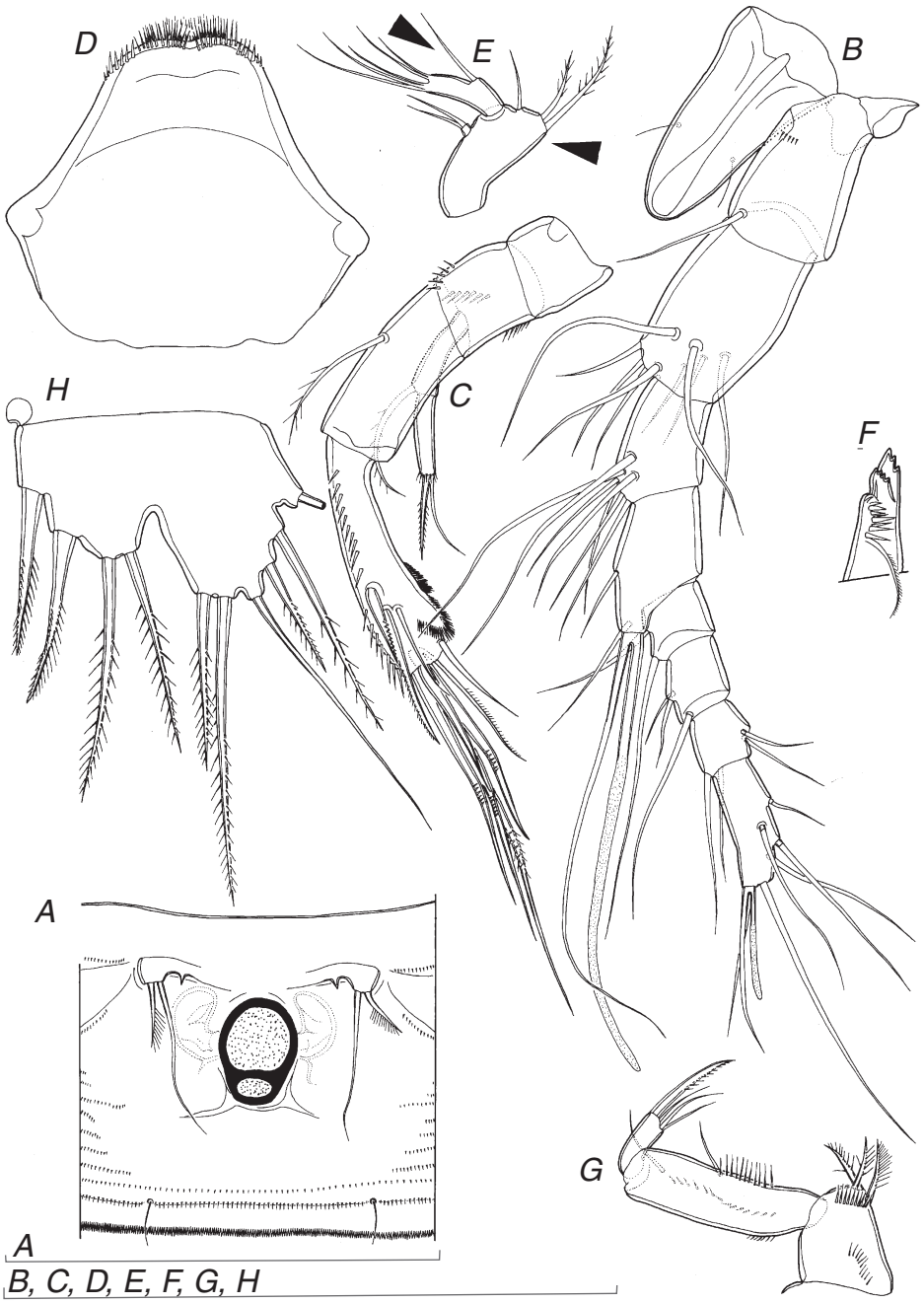

Fig. 29. *Schizopera leptafurca*, sp. nov., holotype ♀. (*A*) Genital field, ventral view (flattened); (*B*) rostrum and antennula, ventral view; (*C*) antenna, ventral view; (*D*) labrum, ventral (anterior) view; (*E*) mandibular palp, anterior view; (*F*) cutting edge of mandibula, dorsal view; (*G*) maxilliped, posterior view; (*H*) fifth leg, posterior view and flattened. Scale bars = 100 µm.

sensilla (two on each side), as well as with two cuticular pores and two sensilla ventrolaterally (one pore and one sensillum on each side), in addition to several irregular rows of numerous minute cuticular spinules; hyaline fringe sharply serrated.

Genital double somite (Figs 4*A*, 28*A*, 29*A*) ~0.7 times as long as wide (dorsal view), with visible suture internally; ornamented with eight sensilla dorsally (six at midlength, two near posterior margin), two posterior sensilla ventrally, and two posterior sensilla laterally (one on each side), in addition to numerous rows of minute spinules (inset in Fig. 4*A*); hyaline fringe sharply serrated both ventrally and dorsally. Female genital complex (Fig. 29*A*) with epicopulatory bulb large, ovoid, ~1.4 times as long as wide, swollen in anterior half. Seminal receptacles very small, kidney-shaped, reaching beyond anterior margin of epicopulatory bulb, ~0.6 times as long as epicopulatory bulb. Third urosomite (Figs 28*A*, 31*A*) ornamented with six posterior

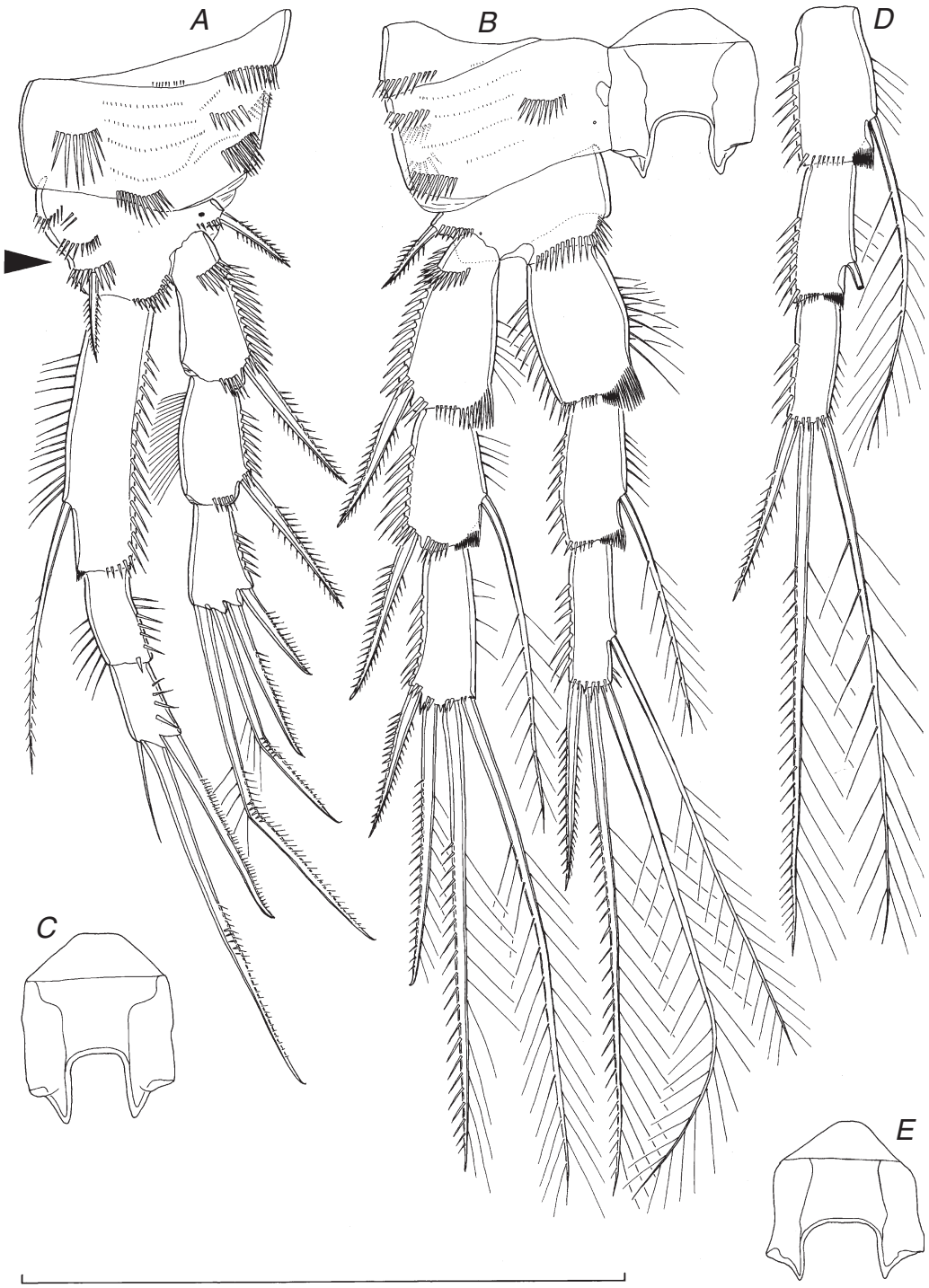

Fig. 30. *Schizopera leptafurca*, sp. nov., holotype ♀. (*A*) First swimming leg, anterior view; (*B*) second swimming leg, anterior view; (*C*) intercoxal sclerite of third swimming leg, anterior view; (*D*) endopod of fourth leg, anterior view; (*E*) intercoxal sclerite of fourth swimming leg, anterior view. Arrow points to additional rows of large spinules, different from previous species. Scale bar = 100 µm.

sensilla (two dorsal, two ventral and two lateral), in addition to numerous rows of slender spinules of various sizes; hyaline fringe serrated and straight. Preanal somite (Figs 28*A–C*, 31*A*) without sensilla or pores, ornamented with many rows of minute spinules; hind margin clearly bulging posteriorly in dorsal region, forming very sharply serrated pseudoperculum (Figs 28*C*, 31*D*). Anal somite (Figs 28*A–C*, 31*B*, *D*) with convex and very short anal operculum, ornamented with transverse row of spinules along

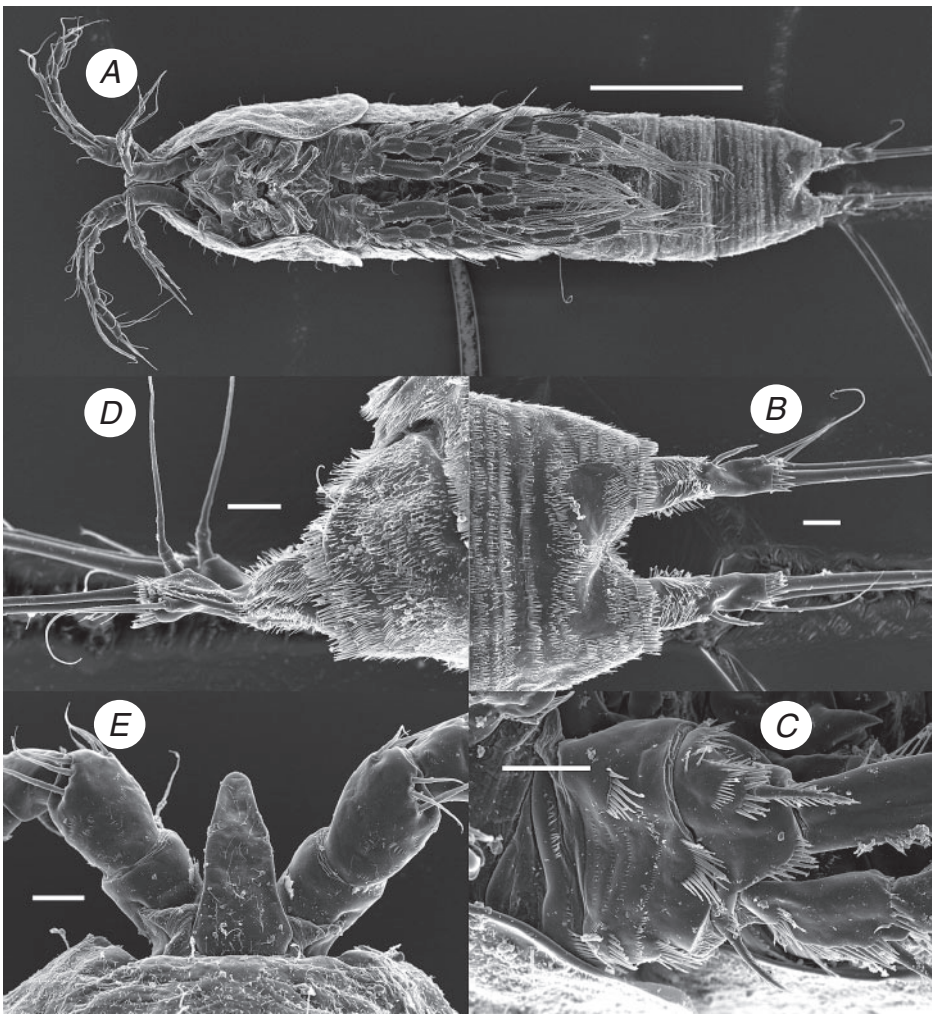

Fig. 31. *Schizopera leptafurca*, sp. nov., scanning electron micrographs. A–C, paratype ♀ I; D, paratype ♀ II; E, paratype ♀ III. (*A*) Habitus, ventral view; (*B*) anal somite and caudal rami, ventral view; (*C*) proximal part of first swimming leg, anterior view; (*D*) anal somite and caudal rami, lateral view; (*E*) anterior part of cephalothorax with rostrum and antennulae, dorsal view. Scale bars A = 100 µm; B–E = 10 µm.

posterior margin; ornamented with two large sensilla dorsally, two lateral cuticular pores, two ventromedian pores, transverse row of large spinules along posterior margin (all of similar length), in addition to many rows of small spinules; two circular areas on anal somite ventrally without spinules, forming characterstic infinity shape (Fig. 31*B*). Anal sinus (Fig. 28*C*) widely opened and ornamented with two diagonal rows of slender spinules, in addition to numerous smaller hairs, not well covered by pseudoperculum (also Fig. 31*D*), widening posteriorly, represents 66% of somite's width in posterior half.

Caudal rami (Figs 28*A–C*, 31*B*, *D*) strongly sclerotised, slender, longer than anal somite, constricted at middle from lateral view, 2.5 times as long as greatest width, with slightly concave inner margin, almost parallel, with space between them more than one ramus width; ornamented with two ventral and one dorsal cuticular pores in posterior half, transverse row of several large spinules along posterior margin ventrally and laterally, many large spinules in anterior half dorsomedially, and many minute and/or slender spinules ventrally in anterior half, and laterally in anterior and posterior part, with a smooth area in central (constricted) part; armed with six elements (two lateral, one dorsal and three apical). Dorsal seta slender and apically pinnate, ~1.7 times as long as ramus, inserted at three-quarters of ramus length, triarticulate. Lateral proximal spine stout, inserted at midlength (in constricted zone) of ramus length (arrowed in Fig. 28*C*), less than half as long as ramus. Lateral distal seta very slender, smooth, inserted slightly ventrolaterally at five-sixths of ramus length, as long as or slightly longer than ramus. Inner apical seta short and smooth, 0.4 times as long as ramus in ventral view. Principal apical setae without breaking planes; middle apical seta strongest, bipinnate at distal end, twice as long as unipinnate outer apical seta, and almost 0.6 times as long as body length.

Antennula (Figs 29*B*, 31*E*) eight-segmented, ~0.8 times as long as cephalothorax, with short aesthetasc on eighth segment, fused to two apical setae, and long but slender aesthetasc on fourth segment, reaching significantly beyond tip of appendage

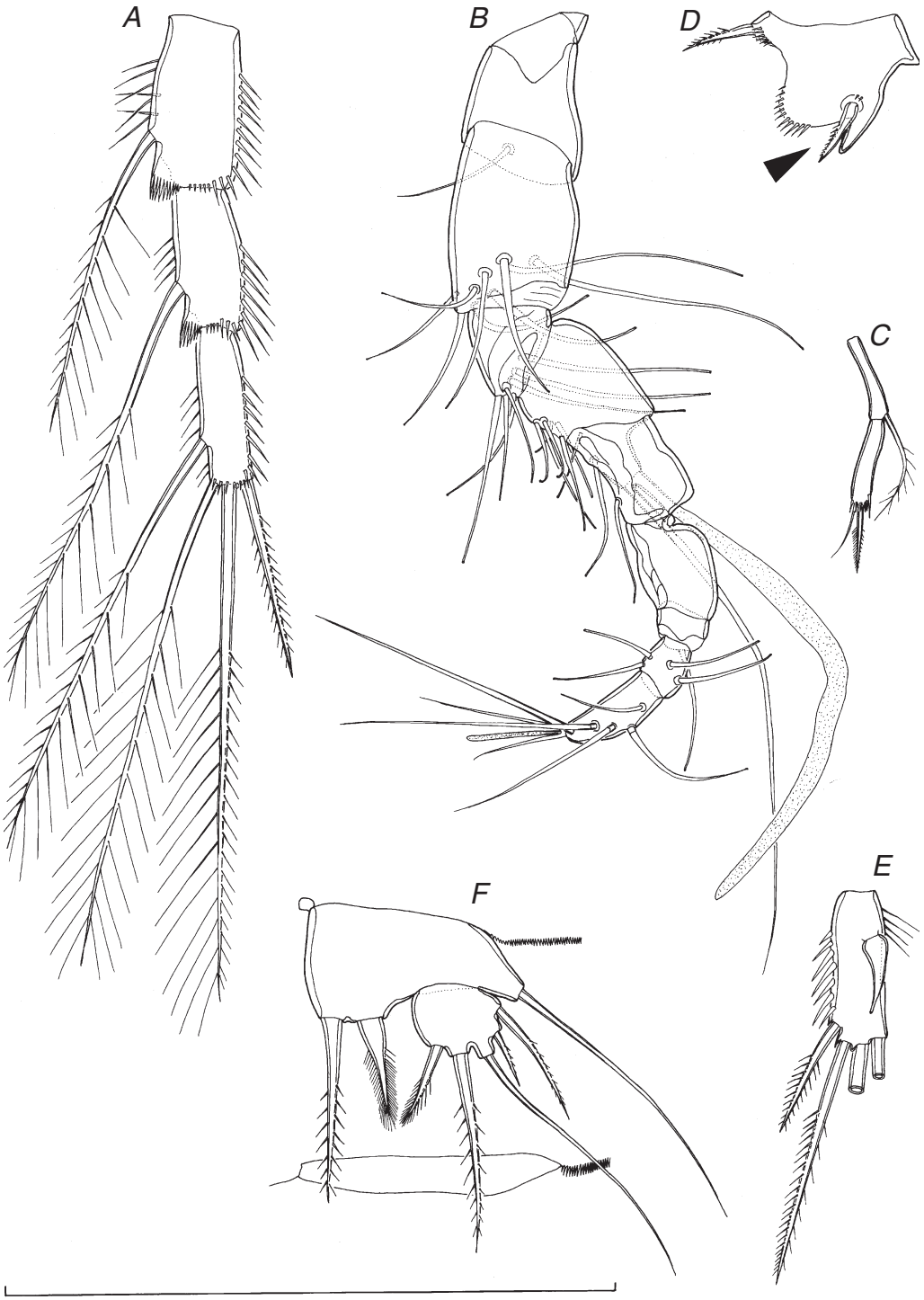

Fig. 32. *Schizopera leptafurca*, sp. nov. A, holotype ♀.; B–F, allotype ♂. (*A*) Endopod of third swimming leg, anterior view; (*B*) antennula, dorsal view; (*C*) exopod of antenna, dorsal view; (*D*) basis of first swimming leg, anterior viewl; (*E*) third exopodal segment of third swimming leg, anterior view; (*F*) left fifth and sixth legs (undissected), ventrolateral view. Arrow points to a relatively small and more distally inserted spine, different from previous species. Scale bar = 100 µm.

and fused basally to equally long seta; setal formula: 1.9.7.3.2.3.4.7. Only two lateral setae on seventh segment and four on eighth segment biarticulate. All setae smooth and slender, and most end apically with pore (except apical and subapical ones). Length ratio of antennular segments, from proximal end, 1 : 1.3 : 0.6 : 0.7 : 0.4 : 0.5 : 0.4 : 0.9. First segment ornamented

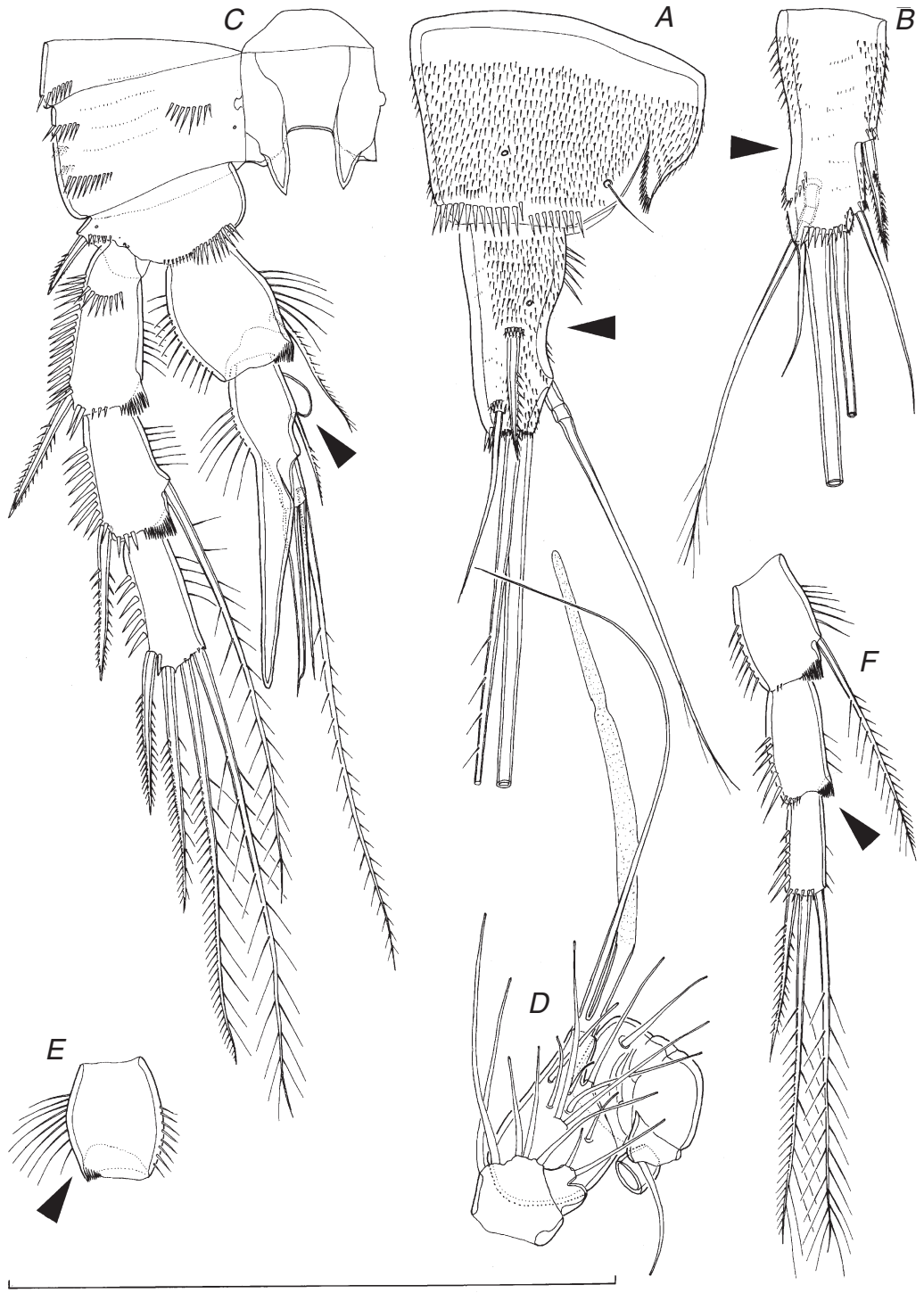

Fig. 33. *Schizopera leptafurca*, sp. nov. A–C, allotype ♂.; D–F, paratype ♂. (*A*) Anal somite and left caudal ramus, lateral view; (*B*) left caudal ramus, ventral view; (*C*) second swimming leg, anterior view; (*D*) middle part of antennula, anterior view; (*E*) first endopodal segment of second swimming leg, anterior view; (*F*) endopod of fourth swimming leg, anterior view. Arrows in A, B and C point to characters different from previous species; arrows in E and F point to intraspecific variable characters. Scale bar = 100 µm.

with short transverse row of small spinules ventromedially; second segment with several rows of striae in different orientation; other segments unornamented.

Antenna (Fig. 29*C*) very similar to that of *S. a. analspinulosa*, only slightly more elongated and with proportionately shorter exopod.

Labrum (Fig. 29*D*) large, rigidly sclerotised, with rounded cutting edge, ornamented apically and subapically with spinules; lateral spinules stronger than middle ones; very similar to that of *S. a. analspinulosa*.

Mandibula (Fig. 29*E*, *F*) with narrow cutting edge of coxa armed with two complex teeth in ventral part (first tricuspidate, second quadricuspidate), several simple teeth in dorsal part, and one unipinnate dorsal-most seta. Basis trapeziform plate, about twice as long as wide, armed with three setae along inner margin (one smooth, two unipinnate); no ornamentation at base of setae (lower arrow in Fig. 29*E*). Endopod one-segmented, twice as long as wide, armed with one lateral (upper arrow in Fig. 29*E*) and five apical smooth setae. Exopod very small but distinct segment, armed with two smooth apical setae.

Maxillula and maxilla without any difference from those in *S. a. analspinulosa*.

Maxilliped (Fig. 29*G*) also very similar to that of *S. a. analspinulosa*, but with additional transverse row of spinules on posterior surface of coxobasis at base of inner setae. Apical strong spine on second endopodal segment also ~1.4 times as long as segment, i.e. much shorter than that in *S. emphysema.*

All swimming legs (Figs 30, 31*C*) slender and long, segmentation and armature formula as in *S. a. analspinulosa*, but with much more slender armature elements and slightly shorter endopods; composed of small triangular preacoxa, large quadrate coxa, smaller basis, three-segmented exopod, and three-segmented endopod. Coxae in all legs connected with intercoxal sclerites. All exopodal and endopodal segments of similar length, except much longer first endopodal segment of first leg.

First swimming leg (Figs 30*A*, 31*C*) with very small intercoxal sclerite, concave at distal end and unornamented. Preacoxa unarmed, ornamented with posterior row of minute spinules on anterior surface and larger spinules closer to outer margin. Coxa also unarmed, but ornamented with several horizontal rows of spinules on anterior surface and two on posterior; anterior spinules grouped into four parallel rows of minute ones, and four groups of large ones (one inner, one distal and two close to outer margin). Basis armed with one inner and one outer strong spine; ornamentation consists of row of spinules at base of each spine, two additional rows of spinules close to inner margin and parallel to that at base of inner spine (proximal one arrowed in Fig. 30*A*), one row of large spinules along distal margin (between endopod and exopod), and one cuticular pore near base of outer spine (all on anterior surface). Exopodal armature and ornamentation as in *S. a. analspinulosa* but all armature elements somewhat longer and more slender. Endopod geniculate, with first segment as long as first two exopodal segments combined, 2.8 times as long as second endopodal segment, and 3.8 times as long as wide; no sclerotised beak on inner margin of first segment; endopodal armature and ornamentation as in *S. a. analspinulosa*, except inner seta on first segment much longer and more slender, about as long as first exopodal segment.

Second swimming leg (Fig. 30*B*) with even smaller preacoxa than in first leg, also unarmed and ornamented only with posterior row of minute spinules. Coxa armed with four horizontal rows of spinules on anterior surface (three groups larger than others), and two diagonal rows of large spinules on posterior surface. Intercoxal sclerite with paired, pointed, distal protrusions, although not as sharp as in *S. a. analspinulosa*. Basis armed only with outer spine, ornamented with spinules at base of outer spine and along distal margin at base of endopod. Distal inner corners of first and second exopodal and endopodal segments with hyaline frills. All exopodal and endopodal segments ornamented with strong spinules on outer margins; and all, except third endopodal, also with somewhat more slender spinules along inner margins. Exopod armed with outer-distal spines on first and second segments, inner seta on second segment, two outer spines and two apical setae on third segment; all setae slender and bipinnate, those on terminal segments much longer than in *S. a. analspinulosa*; outer apical seta on third exopodal segment looks like transitional stage between spine and seta, with outer margin furnished with short spinules and inner margin with slender spinules. Endopod armed with single inner seta on second segment, and four elements on third segment: outer-distal short spine, two apical long setae, and one inner slender seta (inserted at two-thirds); inner apical seta slightly longer than middle seta.

Third swimming leg (Figs 30*C*, 32*A*) very similar to second, except that basis armed with outer slender seta instead of spine, and endopod additionally armed with inner seta on first segment. Pointed processes on intercoxal sclerite not less sharp than in second leg. All setae slender; inner apical seta on third endopodal segment about as long as middle seta.

Fourth swimming leg (Fig. 30*D*, *E*) very similar to third leg, except that inner seta missing on third endopodal segment (Fig. 30*D*), and pointed processes on intercoxal sclerite slightly shorter (Fig. 30*E*); inner apical seta on third endopodal segment as long as middle seta.

Fifth leg (Figs 28*A*, 29*H*) bilobate, with exopod fused to baseoendopod on both anterior and posterior surfaces. Baseoendopod with outer basal smooth seta arising from relatively short setophore, without ornamentation at its base. Endopodal lobe trapezoidal, extending almost to midlength of exopod, unornamented, armed with four stout, spiniform elements (two inner ones probably spines, two outer ones probably spiniform setae); length ratio of endopodal armature elements, from inner side, 1 : 1.3 : 1.7 : 1.5. Exopodal lobe pentagonal, about as long as maximum width, unornamented but armed with five or six elements; two innermost bipinnate, middle one smooth and slender, two or three outermost short, relatively stout and unipinnate; length ratio of exopodal armature elements, from inner side, 1 : 1.8 : 1.7 : 0.7 : 0.6 : 1.3.

Sixth leg (Fig. 29*A*) indistinct, very small cuticular plate covering gonopore, armed with one very small spine fused basally to plate and two setae; inner seta smooth and ~2.4 times as long as outer seta, unipinnate along inner margin.

Description of male

Data from allotype and several paratypes. Body length ranges from 458 to 670 µm (513 µm in allotype). Habitus more slender than in female, but also cylindrical, and with similar proportions of prosome–urosome, and cephalothorax–genital somite. Body length–width ratio ~4.7. Ornamentation of prosomites, colour and nauplius eye similar to female.

Genital somite twice as wide as long. Single, completely formed, longitudinally placed spermatophore inside first two

urosomites in most specimens (not visible in allotype). Abdominal somites similar to female, including absence of ventral cuticular pores. Anal somite (Fig. 33*A*) very similar to female.

Caudal rami (Fig. 33*A*, *B*) slightly shorter than anal somite, less slender and much less constricted at midlength, with only small saddle present dorsally (arrowed in Fig. 33*A*), 2.1 times as long as wide in ventral view, but also with concave inner margin as in female (arrowed in Fig. 33*B*), with similar armature and ornamentation, except few more spinules present in caudal part ventrally and additional large cuticular pore visible in anterior part laterally (not visible in female).

Antennula (Figs 32*B*, 33*D*) also as long as cephalothorax, but strongly geniculate and nine-segmented (basically female's sixth segment subdivided), with geniculation between fourth and fifth and seventh and eighth segments. Segments that participate in geniculation strengthened with cuticular plates along anterior surface, largest ones being on sixth segment. Aesthetascs as in female, on fourth and last segments; first one much wider than in female. First two and last two segments similar to female. Setal formula: 1.9.7.9.1.0.1.4.7. Most setae smooth and with pore on top; same setae biarticulate as in female.

Antenna (Fig. 32*C*), labrum, mandibula, maxillula, maxilla, maxilliped, exopod and endopod of first swimming leg, exopod of second swimming leg, endopod of third swimming leg, and fourth swimming leg (Fig. 33*F*) similar to female.

First swimming leg (Fig. 32*D*) with modified basis, inner margin of basis very rigidly sclerotised, with spiniform, smooth process distally, and smaller one proximally. Inner spine on basis smaller than in female (arrowed in Fig. 32*D*), without spinules at its base, inserted more proximally, and only slightly longer than distal spiniform process of basis.

Second swimming leg (Fig. 33*C*, *E*) with or without (arrowed in Fig. 33*E*) seta on first endopodal segment, and with transformed second and third segments. Second segment with part of inner margin protruded into rounded indistinct lobe, without ornamentation on its surface and pointed distally (arrowed in Fig. 33*C*); inner seta shorter than in female, unipinnate and slender. Third segment completely modified; two ancestral apical setae transformed into smooth, spiniform armature elements, outer one stronger and with abruptly sharpened tip, about as long as inner apical one; inner seta very long, slender and bipinnate, 2.8 times as long as outer apical seta. Ancestral outer spine completely fused to somite, transformed into very strong and smooth thorn slightly longer than ancestral apical elements, and slightly longer than last two endopodal segments combined. As a result of these transformations, third segment medially cleft.

Third swimming leg (Fig. 32*E*) with very characteristic element on anterior surface of third exopodal segment; this structure swollen at basal part, with pore on top, inserted at two-fifths and close to inner margin, not reaching distal margin of third segment. First and second exopodal segments of third leg similar to female.

Fifth leg (Fig. 32*F*) with baseoendopods not basally fused, with free exopod (clearly demarcated at base both on anterior and posterior surfaces), unornamented. Endopodal lobe much smaller and shorter, also trapezoidal, extending to one-third of exopod in length, armed with two very strong apical spines; inner spine ~1.9 times as long as outer one. Exopod about as long as its maximum width, armed with five elements; fifth element from inner side not observed in male specimens, sometimes present in females; length ratio of exopodal armature elements, from inner side, 1 : 2.3 : 3.3 : 0.7 : 1.5.

Sixth legs (Fig. 32*F*) pair of small and short cuticular plates, without any armature or ornamentation; left plate wider and larger than right one, and better demarcated at base.

Variability

Female fifth leg exopod can be ornamented with five or six elements (Fig. 28*A*). Most examined females have a situation as in the holotype, with six elements on the left side and five on the right. A few were observed with six elements on both sides, and even fewer with five elements on both sides. Only one female was observed with six elements on the right side and five on the left. One paratype male was observed without a seta on the second endopodal segment of the fourth leg (arrowed in Fig. 33*F*). Many males were observed without a seta on the first endopodal segment of the second swimming leg (arrowed in Fig. 33*E*). The number of setae on the antennula is a very stable character, both in male (Figs 32*B*, 33*F*) and female.

Distribution

This species was found, usually in great numbers, on the following bore lines, from north-west to south-east: 1, 1.5, 2, 3, 3.5, 5 and K (Fig. 42).

Remarks

Constricted caudal rami (arrowed in Fig. 28*B*) are an autapomorphic feature of *S. leptafurca*, sp. nov. in the genus *Schizopera*, and, as far as we know, not previously observed in any other copepod. Absence of enlarged dorsal spinules on the anal somite distinguishes it additionally from *S. kronosi*, sp. nov. and *S. analspinulosa*, sp. nov., while the segmentation of the swimmings legs distinguishes it from *S. akation*, sp. nov. and *S. akolos*, sp. nov. Densely ornamented somites and cuticular pore pattern are characters shared with *S. emphysema*, sp. nov. and *S. uranusi*, sp. nov., and this clade (*emphysema*+*uranusi* +*leptafurca*) is also supported by molecular data (Fig. 39). All three species have three rows of spinules at base of inner spine of the first leg basis in female and principal apical setae on the caudal rami without breaking planes. Additional morphological differences from previously described congeners from the Yilgarn region are very similar to those of *S. emphysema* (see the 'Remarks' section for the previous species). Molecular data show that *S. leptafurca* is most closely related to *S. uranusi* (Fig. 39), with the average pairwise distances being 15.4% between them, while those between *S. leptafurca* and *S. emphysema* are 21.6% (Table 3). Apart from a different caudal rami shape, there are hardly any other significant morphological differences between these two sister species. Several morphological microcharacters can be used additionally to distinguish them, such as: presence and density of slender spinules on the anterior part of cephalothorax, rostrum and second antennular segments (compare Figs 31*E* and 36*B*), shape of the rostrum (Figs 29*B*, 34*D*), shape of the receptacula seminis (Figs 29*A*, 34*C*), number of lateral armature elements on

the mandibular endopod (Figs 29*E*, 34*F*), sharpness of the intercoxal sclerites between second and third legs (Figs 30*B*, *C*, 35*D*, *E*), ornamentation of the first leg basis in male (Figs 32*D*, 37*D*), and relative length of the inner seta on the female sixth leg (Figs 29*A*, 34*A*); note all these are arrowed in *S. uranusi*. The first character shows that cuticular pits and striae are probably homologous structures with spinules, and gives an exciting insight into formation of the latter. If one carefully studies the ornamentation of cephalothorax and free prosomites on the SEM photos presented in this paper, it is clear that the same place in one species will have just pits, pits with striae in another, while the third one will have spinules. Also, this formation can be observed progressively from the anterior to the posterior part of the body.

Another fact that supports a close relationship of *S. leptafurca* and *S. uranusi* is that their distributional ranges overlap only partly (Fig. 42), suggesting a relatively recent sympatry after the speciation process. We also suggest that this secondary contact may have triggered the evolution of the bizarre caudal rami shapes, which is further discussed in the 'Discussion' section below, as is a possible active upstream colonisation of the calcrete along the palaeochannel.

The average pairwise distances among *COI* sequences within the *S. leptafurca* clade are much larger (nearly 2%) than those within the *S. uranusi* clade (0.5%) (Fig. 39; Table 3).

However, this is an artefact of the sequencing effort, as samples for *S. leptafurca* were from a broader area, from line K (sequences 7131 and 8464) to line 1 (sequences 8417 and 8479), while those of *S. uranusi* encompass a much smaller area (from lines F to 3.5) (Figs 39, 42; Table 2).

Etymology

The new species is named after its characteristically constricted caudal rami in lateral view in females. The specific name is composed of the Greek adjective *leptos* (thin, slender) and the Latin noun *furca* (fork; a term sometimes also used for caudal rami in copepods). It should be treated as a noun in apposition.

Schizopera uranusi, sp. nov.

(Figs 4*B*, 34–37, 38*A*, *B*)

Material examined

Name-bearing type. Holotype (WAM C37492), adult female, completely dissected on 1 slide in Faure's medium, 21.iii.2010, leg. T. Karanovic and S. Callan (seLN8546).

Type locality. Australia: Western Australia: Yilgarn region, Yeelirrie station, line 2, bore YYAC1007A, 27.165236°S 119.883142°E.

Additional material examined. Allotype (WAM C37493), adult ♂ dissected on 1 slide, 21.iii.2010, leg. T. Karanovic and S. Callan (seLN8546), type locality; 2 paratype ♂+3 paratype ♀ (WAM C37494) together on 1 SEM stub, 21.iii.2010, leg. T. Karanovic and S. Callan (seLN8546), type locality; 1 paratype ♀ dissected on 1 slide, 21.iii.2010, leg. T. Karanovic and S. Callan (seLN8546), type locality; 1 paratype ♂ dissected on 1 slide, 21.iii.2010, leg. T. Karanovic and S. Callan (seLN8546), type locality; 17 paratype ♂+24 paratype ♀+13 paratype copepodids (WAM C37495) together in ethanol, 21.iii.2010, leg. T. Karanovic and S. Callan (seLN8546), type locality; 2 ♂+4 copepodids together in ethanol, 12.xi.2009, leg. P. Bell and G. Perina (seLN7374), type locality; 1 ♀ destroyed for DNA sequence, 12.xi.2009, leg. P. Bell and G. Perina (seLN7374), type locality; 2 ♂+3 ♀+1 copepodid together in ethanol, 16.iii.2010, leg. S. Callan and N. Krawczyk (seLN8524), type locality; 1 ♀ in ethanol, 16.iii.2010, leg. S. Callan and N. Krawczyk (seLN8345), type locality; 12 ♂+6 ♀+11 copepodids, 27.viii.2009, leg. P. Bell and S. Callan (seLN7308), type locality; 2 ♂+2 ♀+1 copepodid together in ethanol, 12.xi.2009, leg. P. Bell and G. Perina (seLN7342), bore line 3.5, bore YYAC284, 27.173127°S 119.906857°E; 2 ♀ destroyed for DNA sequence, 12.xi.2009, leg. P. Bell and G. Perina (seLN7342), same locality; 1 copepodid in ethanol, 11.i.2010, leg. P. Bell and G. Perina (seLN7647), same locality; 9 ♂+15 ♀+11 copepodids together in ethanol, 20.iii.2010, leg. T. Karanovic and S. Callan (seLN8302), bore line 1, bore YYAC0019B, 27.159121°S 119.876035°E; 1 ♀ destroyed for DNA sequence, 20.iii.2010, leg. T. Karanovic and S. Callan (seLN8302), same locality; 1 ♀ in ethanol, 30.viii.2009, leg. P. Bell and S. Callan (seLN6588), same locality; 1 ♂+1 ♀ together in ethanol, 15.iii.2010, leg. S. Callan and N. Krawczyk (seLN8479), bore line 1, bore YYD26, 27.164033°S 119.873196°E; 1 ♀ destroyed for DNA sequence, 15.iii.2010, leg. S. Callan and N. Krawczyk (seLN8479), same locality; 2 ♂+1 ♀+3 copepodids in alcohol, 1.ix.2009, leg. P. Bell and S. Callan (seLN6605), same locality; 2 ♂+2 ♀ together in ethanol, 20.iii.2010, T. Karanovic and S. Callan (seLN8417), bore line 1, bore YYAC0016A, 27.170328°S 119.868867°E; 1 ♀ destroyed for DNA sequence, 20.iii.2010, leg. T. Karanovic and S. Callan (seLN8417), same locality; 1 ♀+1 copepodid together in ethanol, 30.viii.2009, leg. P. Bell and S. Callan (seLN6597), same locality; 1 ♀ in ethanol, 17.iii.2010, leg. T. Karanovic and G. Perina (seLN8427), bore line F, bore YYHC0139, 27.138090°S 119.853130°E; 1 ♀ destroyed for DNA sequence, 17.iii.2010, leg. T. Karanovic and G. Perina (seLN8427), same locality; 1 ♂+1 ♀+3 copepodids together in ethanol, 12.xi.2009, leg. P. Bell and G. Perina (seLN7439), bore line 3.5, bore YYAC248, 27.172225°S 119.905149°E; 1 ♀ destroyed for DNA sequence, 12.xi.2009, leg. P. Bell and G. Perina (seLN7439), same locality; 1 ♀ in ethanol, 17.iii.2010, leg. T. Karanovic and G. Perina (seLN8394(, bore line O, bore YYHC0125A, 27.124455°S 119.696322°E; 2 copepodids in ethanol, 15.iii.2010, leg. T. Karanovic and G. Perina (seLN8509), bore line H, bore TPB-33, 27.133739°S 119.827871°E; 2 ♂+1 ♀+1 copepodid together in ethanol, 18.iii.2010, leg. T. Karanovic and S. Callan (seLN8563), same locality; 2 ♀ (1 ovigerous) in ethanol, 14.i.2010, leg. T. Karanovic and S. Callan (seLN7357), same locality; 6 ♂+4 ♀ together in ethanol, 1.ix.2009, leg. P. Bell and S. Callan (seLN7303), same locality; 10 ♂+40 ♀+4 copepodids together in ethanol, 15.iii.2010, leg. T. Karanovic and G. Perina (seLN8492), bore line F, bore YU1, 27.142601°S 119.853144°E; 7 ♂+15 ♀+5 copepodids together in ethanol, 18.iii.2010, leg. T. Karanovic and S. Callan (seLN8565), same locality; 16 ♂+5 ♀ together in ethanol, 1.ix.2009, leg. P. Bell and S. Callan (seLN6613), same locality; 1 ♀ in ethanol, 16.iii.2010, leg. S. Callan and N. Krawczyk (seLN8355), bore line 1, bore YYAC0018C, 27.161503°S 119.874715°E; 1 copepodid in ethanol, 12.xi.2009, leg. P. Bell and G. Perina (seLN7369), same locality; 1 ♀ in ethanol, 16.iii.2010, leg. S. Callan and N. Krawczyk (seLN8514), bore line 2, bore YYAC1006B, 27.169324°S 119.879312°E; 8 ♂+1 ♀+4 copepodids together in ethanol, 21.iii.2010, leg. T. Karanovic and S. Callan (seLN8553), same locality; 1 ♂ in ethanol, 28.viii.2009, leg. P. Bell and S. Callan (seLN7297), same locality; 4 ♀+2 copepodids together in ethanol, 28.viii.2009, leg. P. Bell and S. Callan (seLN7299), same locality; 1 ♂+1 ♀ together in ethanol, 28.viii.2009, leg. P. Bell and S. Callan (seLN7296), same locality; 1 male, 16.iii.2010, leg. S. Callan and N. Krawczyk (seLN8366), bore line 1.5, bore YYAC35, 27.166173°S 119.873977°E; 3 ♀ in ethanol, 21.iii.2010, leg. T. Karanovic and S. Callan (seLN7126), same locality; 1 ♀+1 copepodid together in ethanol, 11.i.2010, leg. P. Bell and G. Perina (seLN7645), same

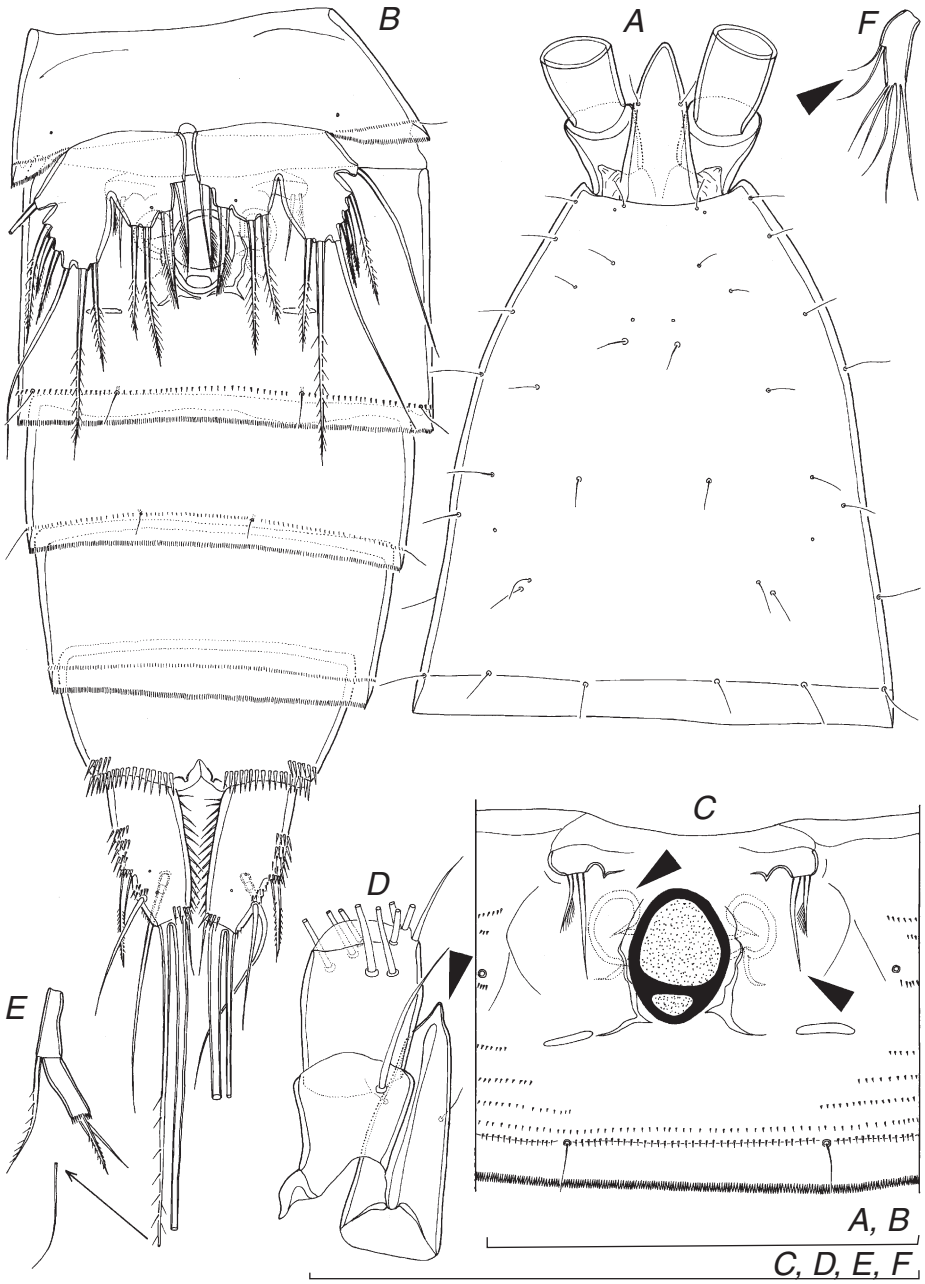

Fig. 34. *Schizopera uranusi*, sp. nov., holotype ♀. (*A*) Cephalothorachic shield with rostrum, dorsal view; (*B*) urosome without minute spinules drawn, ventral view; (*C*) genital field, ventral view; (*D*) rostrum and first two antennular segments, ventral view; (*E*) exopod of antenna, dorsal view. Arrows point to characters different from previous species. Scale bars = 100 µm.

locality; 1 ♀ dissected on 1 slide, 11.i.2010, leg. P. Bell and G. Perina (seLN7645), same locality.

Description of female

Data from holotype and several paratypes. Total body length, measured from tip of rostrum to posterior margin of caudal rami (excluding caudal setae), ranges from 335 to 485 µm (396 µm in holotype). Colour of preserved specimens yellowish. Nauplius eye not visible. Habitus (Figs 4*B*, 36*A*) cylindrical, slender, without distinct demarcation between prosome and urosome; prosome–urosome ratio ~1.2 (in dorsal view); greatest width at posterior end of cephalothorax. Body length–width ratio ~4.2; cephalothorax 1.2 times as wide as genital double somite. Free pedigerous somites without pronounced lateral dorsal expansions. Integument relatively weakly chitinised. All somites and caudal rami, besides other ornamentation, with dense cover of minute spinules (Figs 35*A*, *B*, 36). Rostrum (Figs 34*A*, *D*, 36*B*) long and clearly demarcated at base,

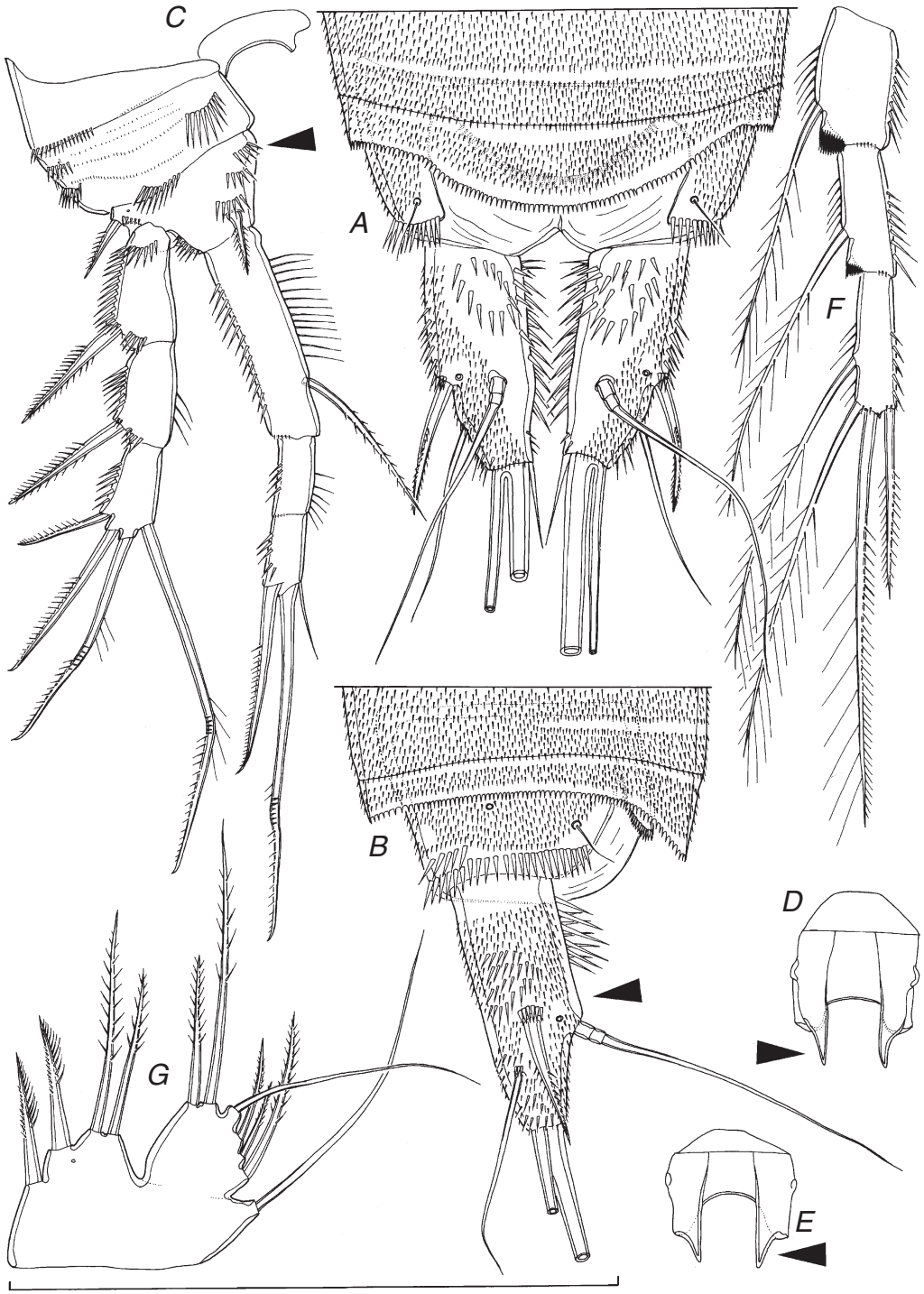

Fig. 35. *Schizopera uranusi*, sp. nov., holotype ♀. (*A*) Last two urosomal somites and caudal rami, dorsal view; (*B*) last two urosomal somites and left caudal ramus, lateral view; (*C*) first swimming leg, anterior view; (*D*) intercoxal sclerite of second swimming leg, anterior view; (*E*) intercoxal sclerite of third swimming leg, anterior view; (*F*) endopod of third swimming leg, anterior view; (*G*) fifth leg, anterior view. Arrows point to characters different from previous species. Scale bar = 100 µm.

reaching midlength of second antennular segment, linguiform, with sharp tip (arrowed in Fig. 34*D*), about twice as long as wide; ornamented with two sensilla dorsolaterally, and bunch of slender spinules dorsally in caudal part.

Cephalothorax (Figs 34*A*, 36*B*) ~1.1 times as long as wide in dorsal view (without rostrum); represents around 32% of total body length. Surface of cephalothoracic shield and tergites of first three free pedigerous somites with characteristic pattern of

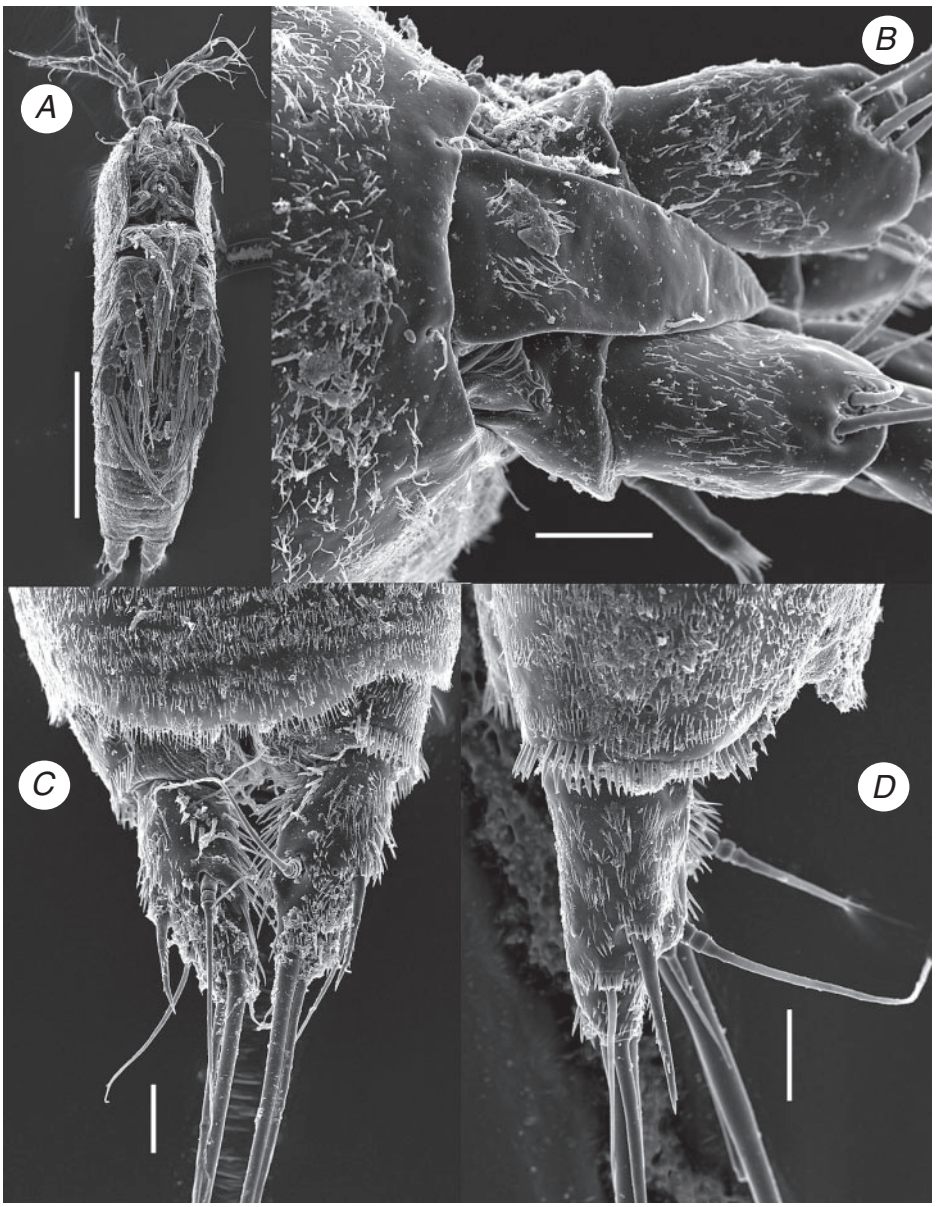

Fig. 36. *Schizopera uranusi*, sp. nov., scanning electron micrographs. A, paratype ♀ I; B and C, paratype ♀ II; D, paratype ♀ III. (*A*) Habitus, ventral view; (*B*) anterior part of cephalothorax with rostrum and antennulae, dorsal view; (*C*) anal somite and caudal rami, dorsal view; (*D*) anal somite and left caudal ramus, lateral view. Scale bars: A = 100 µm; B–D = 10 µm.

large sensilla and small cuticular pores, very similar to that in *S. a. analspinulosa*, except central dorsal sensilla and posterior dorsal pore missing, and two additional sensilla visible in lateral view. Two sensilla and two pores at base of rostrum (Figs 34*A*, 36*B*). Cephalothoracic shield without cuticular pits, but densly ornamented with delicate spinules, looking almost like mammalian pelt. Hyaline fringe of cephalothoracic shield smooth and unornamented, as well as those of other prosomites (Fig. 4*B*); sensilla pattern as in *S. a. analspinulosa*. Fifth pedigerous somite (first urosomal) ornamented with four dorsal large sensilla and four lateral sensilla (two on each side), as well as with two cuticular pores and two sensilla ventrolaterally (one pore and one sensillum on each side; Fig. 34*B*), in addition to several irregular rows of numerous minute cuticular spinules; hyaline fringe sharply serrated.

Genital double somite (Figs 4*B*, 34*B*, *C*) ~0.7 times as long as wide (dorsal view), with visible suture internally; ornamented with eight sensilla dorsally (six at midlength, two near posterior margin), two posterior sensilla ventrally, and two posterior sensilla laterally (one on each side), in addition to numerous rows of minute spinules; hyaline fringe sharply serrated both ventrally and dorsally. Female genital complex (Fig. 34*C*) with epicopulatory bulb large, ovoid, ~1.3 times as long as wide, swollen at midlength. Seminal receptacles very small, kidney-

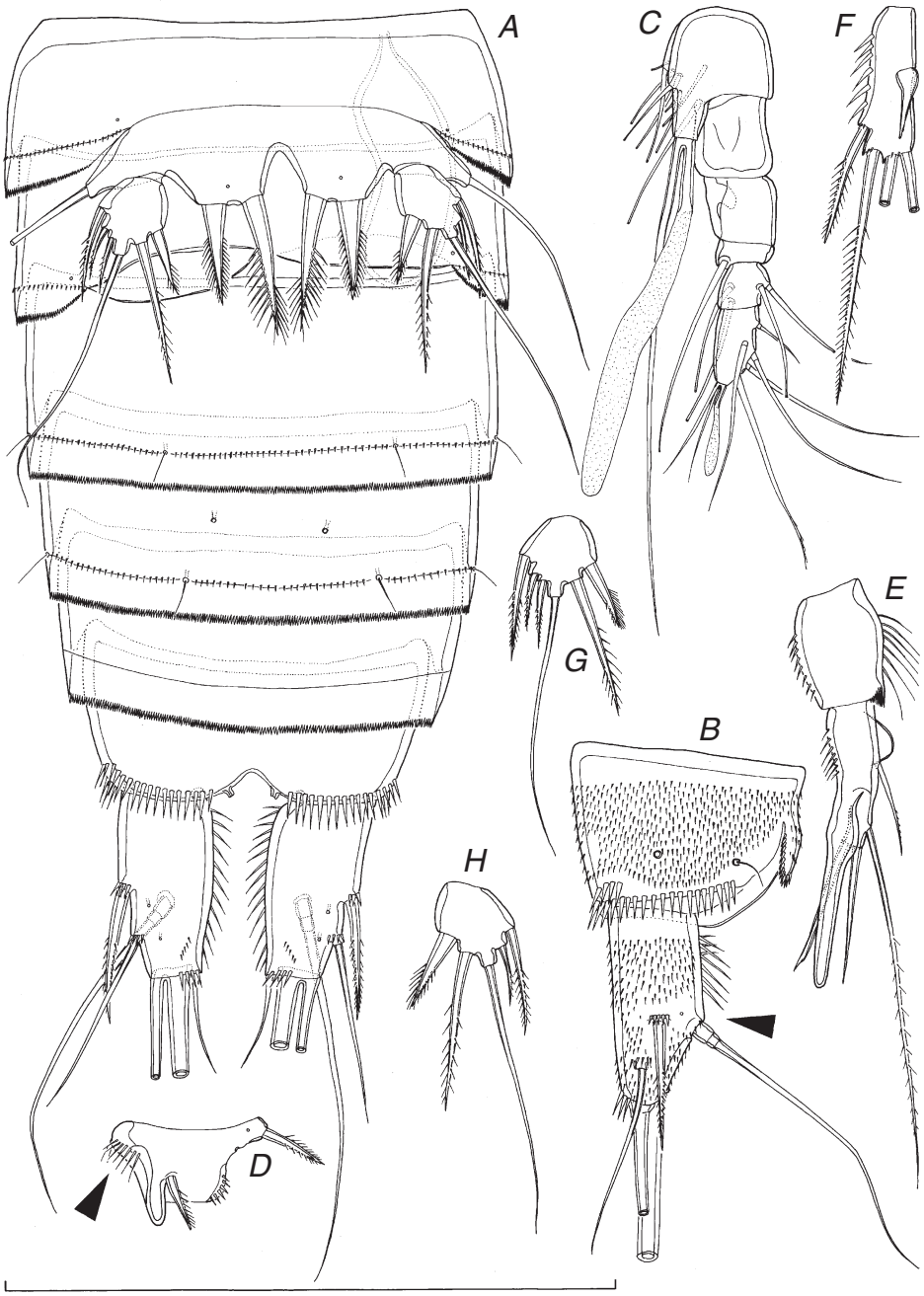

Fig. 37. *Schizopera uranusi*, sp. nov., allotype ♂. (*A*) Urosome without minute spinules drawn, ventral view; (*B*) anal somite and left caudal ramus, lateral view; (*C*) distal part of antennula, ventral view; (*D*) basis of first swimming leg, anterior view; (*E*) endopod of second swimming leg, anterior view; (*F*) third exopodal segment of third swimming leg, anterior view; (*G*) exopod of right fifth leg, anterior view; (*H*) exopod of left fifth leg, anterior view. Arrows point to characters different from previous species. Scale bars = 100 µm.

shaped, reaching anterior margin of epicopulatory bulb, about half as long as epicopulatory bulb, with bulbous anterior parts (arrowed in Fig. 34*C*) oriented towards epicopulatory bulb. Third urosomite (Fig. 34*B*) ornamented with six posterior sensilla (two dorsal, two ventral and two lateral), in addition to numerous rows of slender spinules of various sizes; hyaline fringe serrated and straight. Preanal somite (Figs 34*B*, 35*A*, *B*, 36*C*) without sensilla or pores, ornamented with many rows of minute spinules; hind margin clearly bulging posteriorly in dorsal region, forming very sharply serrated, short pseudoperculum (Figs 35*A*, 36*C*). Anal somite (Figs 34*B*, 35*A*, *B*, 36*C*, *D*) with convex and very short anal operculum, ornamented with transverse row of spinules along posterior margin; ornamented with two large sensilla dorsally, two lateral cuticular pores,

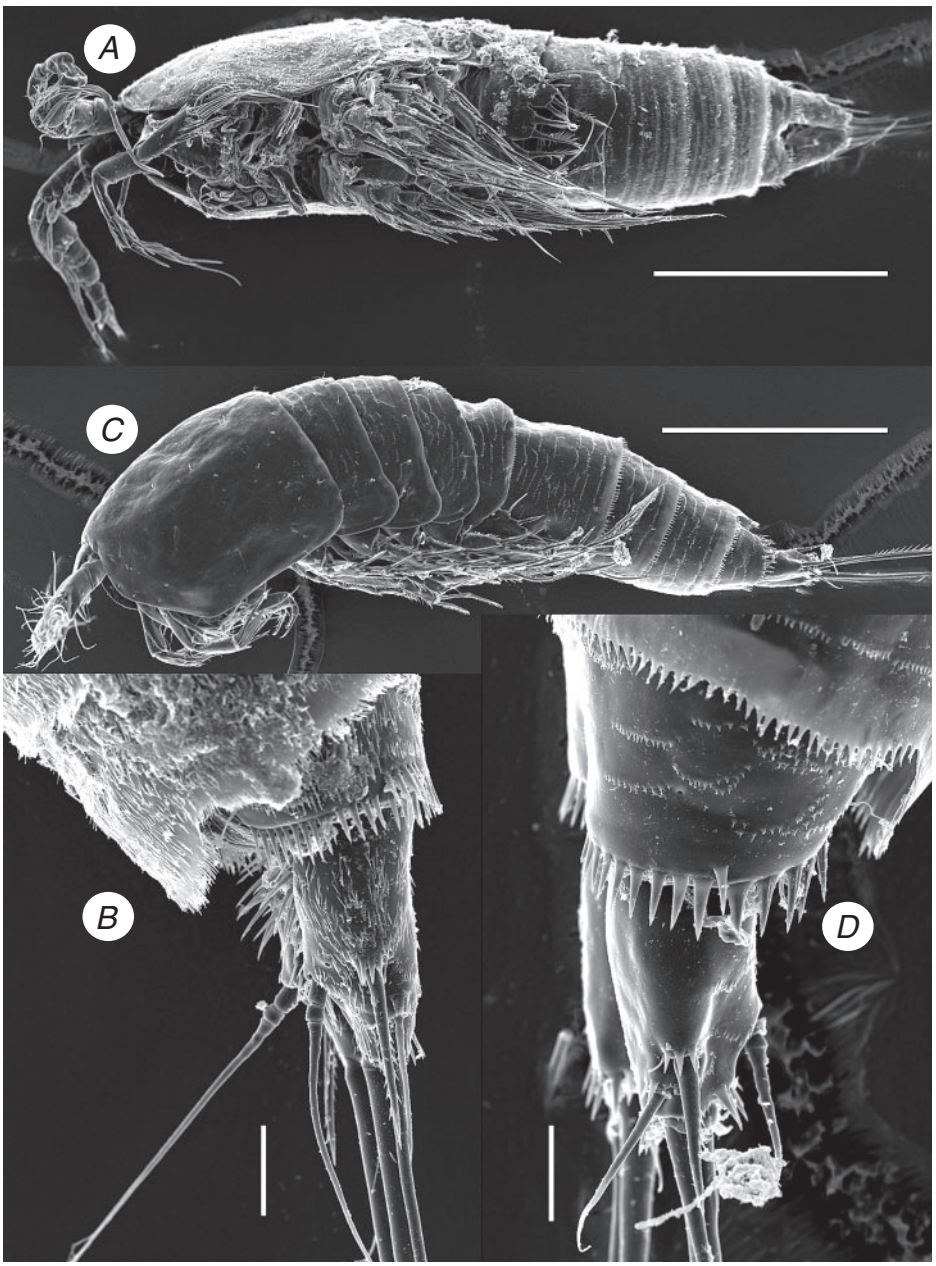

Fig. 38. Scanning electron micrographs of two species: A and B, *Schizopera uranusi*, sp. nov. A, paratype ♂ I; B, paratype ♂ II; C and D *Schizopera* sp. 1 from Harding River, Pilbara region. (*A*) Habitus, ventral view; (*B*) last two urosomal somites and caudal rami, dorsolateral view; (*C*) habitus, lateral view; (*D*) anal somite and caudal rami, ventrolateral view. Scale bars A, C = 100 µm; B, D = 10 µm.

two ventromedian pores, transverse row of large spinules along posterior margin (all of similar length), another short and parallel row of large spinules ventrolaterally, in addition to many rows of small spinules; two small circular areas on anal somite ventrally without spinules, but much smaller than in *S. leptafurca*. Anal sinus (Figs 35*A*, 36*C*) widely opened and ornamented with two diagonal rows of slender spinules, not well covered by pseudoperculum, widest at midlength, represents 66% of somite's width.

Caudal rami (Figs 34*B*, 35*A*, *B*, 36*C*, *D*) strongly sclerotised, relatively slender, longer than anal somite, with cylindrical anterior part and conical posterior part (tapering after dorsal and proximal lateral elements; arrowed in Fig. 35*B*), without constrictions, 2.5 times as long as greatest width, with straight inner margin, converging posteriorly, with space between rami less than half of one ramus width; ornamented with two ventral and one dorsal cuticular pores in posterior half, transverse row of several large spinules along posterior margin ventrally and

laterally, many large spinules in anterior half dorsomedially, and many minute and/or slender spinules dorsally, laterally, with narrow smooth area only in dorsal view; armed with six elements (two lateral, one dorsal and three apical). Dorsal seta slender and smooth, ~1.4 times as long as ramus, inserted at three-fifths of ramus length, triarticulate. Lateral proximal spine stout, inserted also at three-fifths of ramus length, half as long as ramus. Lateral distal seta very slender, smooth, inserted slightly ventrolaterally at four-fifths of ramus length, slightly shorter than ramus. Inner apical seta short and smooth, 0.4 times as long as ramus in ventral view. Principal apical setae on caudal rami fused basally and without breaking planes; middle apical seta strongest, bipinnate at distal end, 1.6 times as long as unipinnate outer apical seta, and about half as long as body length.

Antennula (Figs 34*D*, 36*B*) eight-segmented, ~0.8 times as long as cephalothorax, with short aesthetasc on eighth segment, fused to two apical setae, and long but slender aesthetasc on fourth segment, reaching significantly beyond tip of appendage and fused basally to equally long seta; setal formula: 1.9.7.3.2.3.4.7. Only two lateral setae on seventh segment and four on eighth segment biarticulate. All setae smooth and slender, and most end apically with pore (except apical and subapical ones). Length ratio of antennular segments, from proximal end, 1 : 1.2 : 0.6 : 0.7 : 0.4 : 0.5 : 0.4 : 0.9. First segment unornamented (no short transverse row of small spinules ventromedially); second segment with several rows of hair-like spinules; other segments unornamented.

Antenna (Fig. 34*E*) very similar to that of *S. a. analspinulosa*, only slightly more elongated and with proportionately shorter exopod.

Labrum very similar to that in *S. a. analspinulosa*.

Mandibula (Fig. 34*F*) with two lateral setae on endopod (arrowed in Fig. 34*F*), very similar to that in *S. a. analspinulosa.*

Maxillula, maxilla and maxilliped without any difference from those in *S. a. analspinulosa* or those in *S. leptafurca.*

All swimming legs (Fig. 35*C–F*) slender and long, segmentation and armature formula as in *S. a. analspinulosa*, but with much more slender armature elements and slightly shorter endopods. Ornamentation and armature proportions with hardly any difference from those in *S. leptafurca*.

First swimming leg (Fig. 35*C*) with very small intercoxal sclerite, concave at distal end and unornamented. Preacoxa unarmed, ornamented with posterior row of spinules on anterior surface. Coxa also unarmed, but ornamented with several horizontal rows of spinules on anterior surface and two on posterior; anterior spinules grouped into four parallel rows of minute ones, and four groups of large ones (one inner, one distal and two close to outer margin). Basis armed with one inner and one outer strong spine; ornamentation consists of row of spinules at base of each spine, two additional rows of spinules close to inner margin and parallel to that at base of inner spine, one row of large spinules along distal margin (between endopod and exopod), and one cuticular pore near base of outer spine (all on anterior surface). Exopodal armature and ornamentation as in *S. a. analspinulosa* but all armature elements somewhat longer and more slender. Endopod geniculate, with first segment as long as first two exopodal segments combined, 2.8 times as long as second endopodal segment, and 3.8 times as long as wide; small and blunt sclerotised beak on inner margin of first segment; endopodal armature and ornamentation as in *S. a. analspinulosa*, except inner seta on first segment much longer and more slender, ~0.9 times as long as first exopodal segment.

Second swimming leg (Fig. 35*D*) without any difference from that in *S. leptafurca*, except intercoxal sclerite with longer and sharper distal protrusions (arrowed in Fig. 35*D*).

Third swimming leg (Fig. 35*E*, *F*) very similar to second, except that basis armed with outer slender seta instead of spine, and endopod additionally armed with inner seta on first segment. Pointed processes on intercoxal sclerite less sharp than in second leg, but much longer than those in *S. leptafurca*. All setae slender; inner apical seta on third endopodal segment slightly shorter than middle seta.

Fourth swimming leg very similar to third leg, except that inner seta missing on third endopodal segment and pointed processes on intercoxal sclerite slightly shorter; inner apical seta on third endopodal segment about as long as middle seta.

Fifth leg (Figs 34*B*, 35*G*) bilobate, with exopod fused to baseoendopod on anterior surface and also partly on posterior surface. Baseoendopod with outer basal smooth seta arising from relatively short setophore, without ornamentation at its base. Endopodal lobe trapezoidal, extending almost to midlength of exopod, ornamented with single pore, armed with four stout, spiniform elements (two inner ones probably spines, two outer ones probably spiniform setae); length ratio of endopodal armature elements, from inner side, 1 : 1 : 1.7 : 1.3. Exopodal lobe pentagonal, about as long as maximum width, unornamented but armed with six elements; two innermost bipinnate, middle one smooth and slender, three outermost short, relatively stout and unipinnate; length ratio of exopodal armature elements, from inner side, 1 : 1.9 : 1.7 : 0.7 : 0.5 : 1.2.

Sixth leg (Fig. 34*C*) indistinct, very small cuticular plate covering gonopore, armed with one very small spine fused basally to plate and two setae; inner seta (arrowed in Fig. 34*C*) smooth and ~1.6 times as long as outer seta, unipinnate along inner margin.

Description of male

Data from allotype and several paratypes. Body length ranges from 330 to 398 µm (357 µm in allotype). Habitus hardly more slender than in female, also cylindrical, and with similar proportions of prosome–urosome, and cephalothorax–genital somite. Body length–width ratio ~4.3. Ornamentation of prosomites, colour and nauplius eye similar to female.

Genital somite (Figs 37*A*, 38*A*) more than twice as wide as long. Single, completely formed, longitudinally placed spermatophore inside first two urosomites, 2.7 times as long as wide. Abdominal somites (Fig. 37*A*) similar to female, except for additional pair of pores on fourth urosomite ventrally. Anal somite (Figs 37*A*, *B*, 38*B*) very similar to female, including additional short row of large spinules ventrolaterally, parallel to posterior row.

Caudal rami (Figs 37*A*, *B*, 38*B*) slightly shorter than in female, but with same armature, ornamentation and similar proportions.

Antennula (Fig. 37*C*) also as long as cephalothorax, geniculate and nine-segmented (basically female's sixth segment subdivided), with geniculation between fourth and fifth and

seventh and eighth segments. Segments that participate in geniculation strengthened with cuticular plates along anterior surface, largest ones on sixth segment. Aesthetascs as in female, on fourth and last segments; first one much wider than in female. First two and last two segments similar to female. Setal formula: 1.9.7.10.1.0.1.4.7. Most setae smooth and with pore on top; same setae biarticulate as in female.

Antenna, labrum, mandibula, maxillula, maxilla, maxilliped, exopod and endopod of first swimming leg, exopod of second swimming leg, endopod of third swimming leg, and fourth swimming leg similar to female.

First swimming leg (Fig. 37*D*) with modified basis, inner margin of basis very rigidly sclerotised, with spiniform, smooth process distally; no proximal process medially and inner margin ornamented with diagonal row of large spinules (arrowed in Fig. 37*D*). Inner spine on basis smaller than in female, without spinules at its base, inserted more proximally, and longer than distal spiniform process of basis.

Second swimming leg (Fig. 37*E*) without seta on first endopodal segment, and with transformed second and third segments. Second segment with part of inner margin protruded into rounded indistinct lobe, without ornamentation on its surface; inner seta shorter than in female, unipinnate and slender. Third segment completely modified; two ancestral apical setae transformed into smooth, spiniform armature elements, outer one stronger and with abruptly sharpened tip, about as long as inner apical one; inner seta very long, slender and bipinnate, 2.7 times as long as outer apical seta. Ancestral outer spine completely fused to somite, transformed into very strong and smooth thorn slightly longer than ancestral apical elements, and about as long as last two endopodal segments combined. As a result of these transformations, third segment medially cleft.

Third swimming leg (Fig. 37*F*) with characteristic element on anterior surface of third exopodal segment; this structure swollen at basal part, with pore on top, inserted at three-sevenths and close to inner margin, not reaching distal margin of third segment. First and second exopodal segments of third leg similar to female.

Fifth leg (Fig. 37*A*, *G*, *H*) with baseoendopods basally fused, with free exopod (clearly demarcated at base on both anterior and posterior surfaces), ornamented with single pore, as in female. Endopodal lobe much smaller and shorter, also trapezoidal, extending to one-third of exopod in length, armed with two very strong apical spines; inner spine ~1.4 times as long as outer one. Exopod about as long as its maximum width, armed with five or six elements; fifth element from inner side always present in females, sometimes missing in male specimens; length ratio of exopodal armature elements, from inner side, 1 : 2 : 3.5 : 0.8 : 1.4.

Sixth legs (Fig. 37*A*) pair of small and short cuticular plates, without any armature or ornamentation; right plate wider and larger than left one, and better demarcated at base.

Variability

Male fifth leg exopod can be ornamented with five or six elements (Fig. 37*A*, *G*, *H*). Most examined males have five elements on both legs. One paratype was observed with six elements on both legs, and the allotype has six elements on the right side and five on the left. It is interesting that the allotype also has the right sixth leg more developed, while all other species examined here and most other specimens of *S. uranusi* as well have the left sixth leg more developed. Although we know that in harpactoids only one of the primordial testis and vas deferens develop to maturity and that this usually (70% of species) is the left one (Huys and Boxshall 1991), and the 'functional sixth leg' (i.e. the better developed one, usually also hinged to somite, not fused) covers the gonopore and thus will be on the right or left, dependant on which of the testes and vas deferens pair develops, we know very little about the intra- or interspecific variability of this character. This could be an interesting study to pursue further in the genus *Schizopera.*

Distribution

This species was found, usually in great numbers, on the following bore lines, from north-west to south-east: O, H, F, 1, 1.5, 2, and 3.5 (Fig. 42).

Remarks

As mentioned in the 'Remarks' section for *S. leptafurca*, sp. nov. (see above), this is the sister species of *S. uranusi*, sp. nov., which is supported by both molecular and morphological data. The main morphological differences between the two were also discussed above and will not be repeated here. Most of them are arrowed in Figs 34–37. The shape of the caudal rami is certainly less bizarre in *S. uranusi* than in *S. leptafurca*, being closer to what one may perceive as a more common shape in the genus. However, it is very different from any of the shapes observed in other Yeelirrie species. A somewhat similar shape can be found in *S. depotspringsi* Karanovic, 2004, which also lives in the Yilgarn region, but the dorsal seta is inserted more posteriorly in this species and caudal rami are proportionately smaller, in addition to some other morphological differences in the first and fifth legs, which distinguish these two species. Another species with a relatively similar caudal rami shape is *S. oldcuei* Karanovic, 2004, although in this species the outer principal seta is very small (see Karanovic 2004). The only other congener with a relatively similar caudal rami shape is *S. pseudojugurtha* Borutzky, 1972, from the interstitial habitat of the Lake Issyk-Kul in Kyrgyzstan (Borutzky 1972), but in this species the caudal rami have a slightly more inflated look and the proximal lateral seta is smaller. Absence of enlarged dorsal spinules on the anal somite distinguishes *S. uranusi* additionally from *S. kronosi*, sp. nov. and *S. analspinulosa*, sp. nov., and the segmentation of the swimmings legs from *S. akation*, sp. nov. and *S. akolos*, sp. nov. Somite ornamentation is very similar to that found in *S. emphysema*, sp. nov. and *S. leptafurca*, and this clade is also supported by molecular data (Fig. 39). All three species have three rows of spinules at the base of the inner spine on the first leg basis in females (arrowed in Figs 26*A*, 30*A*, 35*C*), and principal apical setae on the caudal rami without breaking planes (Figs 24*C*, 28*C*, 35*B*). They are all large species, living sympatrically, and with most obvious morphological differences in the caudal rami shape.

Etymology

The name refers to Uranus, the ancient Greek deity of the sky, who gave name to a planet in our solar system, which in turn gave name

to the chemical element uranium, one of the important mineral deposits in the distribution range of this species, which was experimentally mined at Yeelirrie in the 1970s. The specific name is a noun in the genitive singular.

Molecular results

DNA was extracted and the *COI* fragment successfully PCR-amplified from 43 copepod specimens (Table 2) using a nested combination of primers given in Table 1. All the sequences were translated into protein using MEGA and were shown to have no evidence of stop codons, ambiguities or insertions–deletions indicative of non-functional copies of *COI*. BLAST analyses of GenBank revealed that the obtained sequences are copepod in origin and not contaminants, and one of the GenBank *COI* sequences (AF315010.1) from the species *Cletocamptus deitersi* (Richard, 1897) was included in our phylogenetic analyses.

Average pairwise distances between morphotaxa were found to be very high, with the lowest divergence (15.4%) between *S. leptafurca* and *S. uranusi* (Table 3). There was evidence (Table 1) for multiple divergent (12.3% average sequence divergence; 12–16.5% divergence between haplotypes) lineages within the species *S. akation*. The question remains as to whether these lineages represent the presence of further cryptic species or are just divergent mtDNA sequences within a species.

All the analyses (Fig. 39) supported the presence of at least 11 genetically divergent lineages and all nine of the multisample lineages were supported with very high bootstrap values, >97% for NJ and MP analyses, >87% for ML, and 100% posterior probabilities for BI analyses.

A sister group relationship of *S. uranusi* with *S. leptafurca* was strongly supported, and monophyly of a group comprising *S. uranusi*, *S. leptafurca*, *S. emphysema* and Pilbara Harding River *S.* sp. 1 was moderately supported (found in MP, ML and BI trees, the latter showing a high posterior probability of 0.99; Fig. 39*B*). There is also a strongly supported sister group relationship of *S. analspinulosa* s. str. and *S. analspinulosa linel*, found in all trees (bootstrap support >93%, posterior probability 0.94). There were some differences in the topology of trees from the different methods, particularly the inter-relationships of taxa branching from basal nodes in the tree. These uncertainties are reflected in the BI 50% posterior probability tree. Although the MP and NJ trees depict a monophyletic group comprising *S. kronosi*, *S. analspinulosa* s. str. and *S. analspinulosa linel*, bootstrap values and posterior probabilities for this arrangement were very low (<50%). This lack of support is likely to be the result of the low phylogenetic resolution of the *COI* gene in basal nodes of the trees, possibly due to saturation at third codon positions. Our ML analysis showed a modest support (60%) for a sister relationship of the *S. akation* clade and all other *Schizopera* species (not shown in Fig. 39), but this was not recovered in other analyses.

The one specimen that did not match our morphospecies (7439; preliminary identified as *S. uranusi*) formed a separate lineage and is likely to represent another uncharacterised species of *Schizopera*.

Discussion

Distribution patterns and relative abundances

Seven species and one subspecies are described as new: *S. analspinulosa* s. str., sp. nov., *S. analspinulosa linel*, ssp. nov., *S. kronosi*, sp. nov., *S. akation*, sp. nov., *S. akolos*, sp. nov., *S. emphysema*, sp. nov., *S. leptafurca*, sp. nov., and *S. uranusi*, sp. nov. All taxa, except *S. akation*, are short range endemics and stygobionts. *Schizopera analspinulosa* s. str., *S. a. linel* and *S. kronosi* were found to be allopatric taxa (Fig. 40). One bore line was sampled between each population (lines D and N), and no specimens were found, which gives us confidence in assuming that they are also disjunct populations. All three taxa have unusual, highly enlarged, dorsal-most two spinules on the anal somite (see Figs 6*C*, 14*A*, 15*C*), and their morphology suggests that they are more closely related to each other than to any other *Schizopera* species. Their monophyly was also reconstructed in the NJ and MP molecular phylogenies (Fig. 39*A*), although the bootstrap values and posterior probabilities for this arrangement were very low (<50%). While *S. analspinulosa* s. str. and *S. a. linel* were only collected from a single bore each, *S. kronosi* is relatively widely distributed (from line H to line K, more than 25 km). However, all three can be considered short range endemics by any standards (Harvey 2002; Eberhard *et al*. 2009). The *COI* sequence data suggest a divergence of 15.8% between *S. analspinulosa* s.

Table 3. Average pairwise maximum likelihood distances (HKY-85 model) among *COI* sequences between each morphospecies (lower diagonal) and within morphospecies (diagonal)

Species	1	2	3	4	5	6	7	8	9	10	11	12	13
1. *A. hamondi*	0.000												
2. Pilbara *E. humphreysi*	0.276	0.046											
3. Pilbara Harding R *S.* sp. 1	0.413	0.440	–										
4. Pilbara Solomons *S.* sp. 2	0.364	0.381	0.328	0.000									
5. *S. akation*	0.358	0.416	0.336	0.282	0.123								
6. *S. akolos*	0.425	0.429	0.314	0.247	0.345	–							
7. *S. analspinulosa* s. str.	0.336	0.390	0.317	0.349	0.315	0.259	–						
8. *S. analspinulosa linel*	0.331	0.371	0.337	0.311	0.324	0.262	0.158	0.000					
9. *S. emphysema*	0.392	0.430	0.284	0.314	0.341	0.318	0.297	0.304	–				
10. *S. kronosi*	0.296	0.390	0.275	0.278	0.261	0.222	0.233	0.216	0.250	0.008			
11. *S. leptafurca*	0.376	0.392	0.294	0.356	0.348	0.274	0.267	0.275	0.216	0.236	0.019		
12. *S. uranusi*	0.333	0.374	0.239	0.268	0.322	0.263	0.261	0.281	0.190	0.243	0.154	0.005	
13. 7439 *S. uranusi* sp.	0.357	0.310	0.272	0.253	0.313	0.233	0.235	0.209	0.258	0.210	0.239	0.215	–

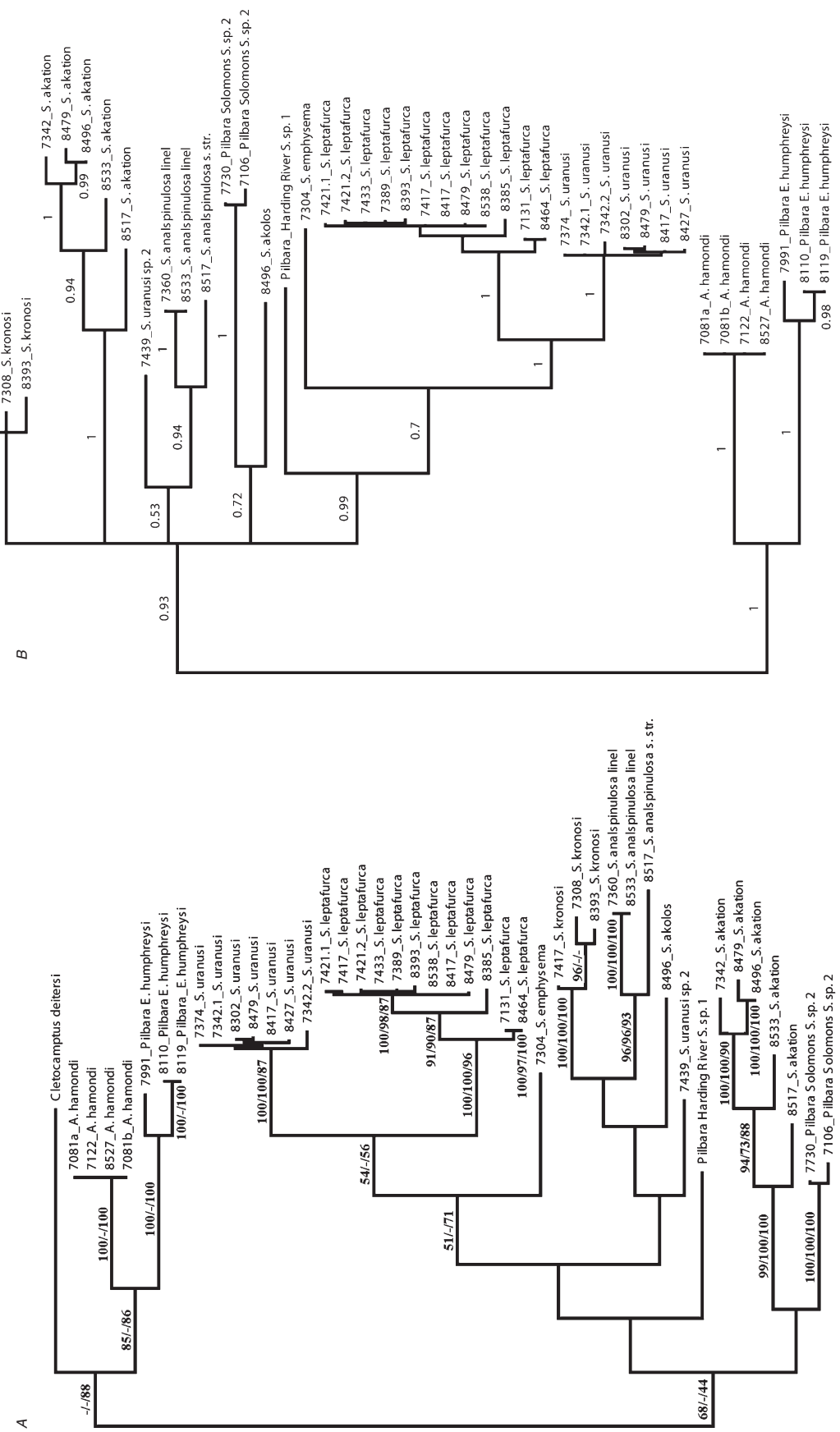

Fig. 39. Two different cladograms based on *COI* sequences of eight new *Schizopera* from Yeelirrie, two as yet undescribed new species from the Pilbara region (*S.* sp. 1 and *S.* sp. 2) and three outgroups taxa: *Cletocamptus deitersi* (Richard, 1897) [GeneBank], *Australocamptus hamondi* Karanovic, 2004 collected also in the Yeelirrie calcrete (bore line E, bore No 312; see Fig. 1) and *Elaphodella humphreysi* Karanovic, 2006 from the Pilbara region. (A) Neighbour Joining tree with numbers on the branches representing bootstrap values above 50% for three different methods (NJ/MP/ML); note that MP analysis resulted in 72 equally parsimonius trees and was done with a midpoint root (no outgroup); (B) MrBayes 50% posterior probability tree, with posterior probabilities shown above the branches.

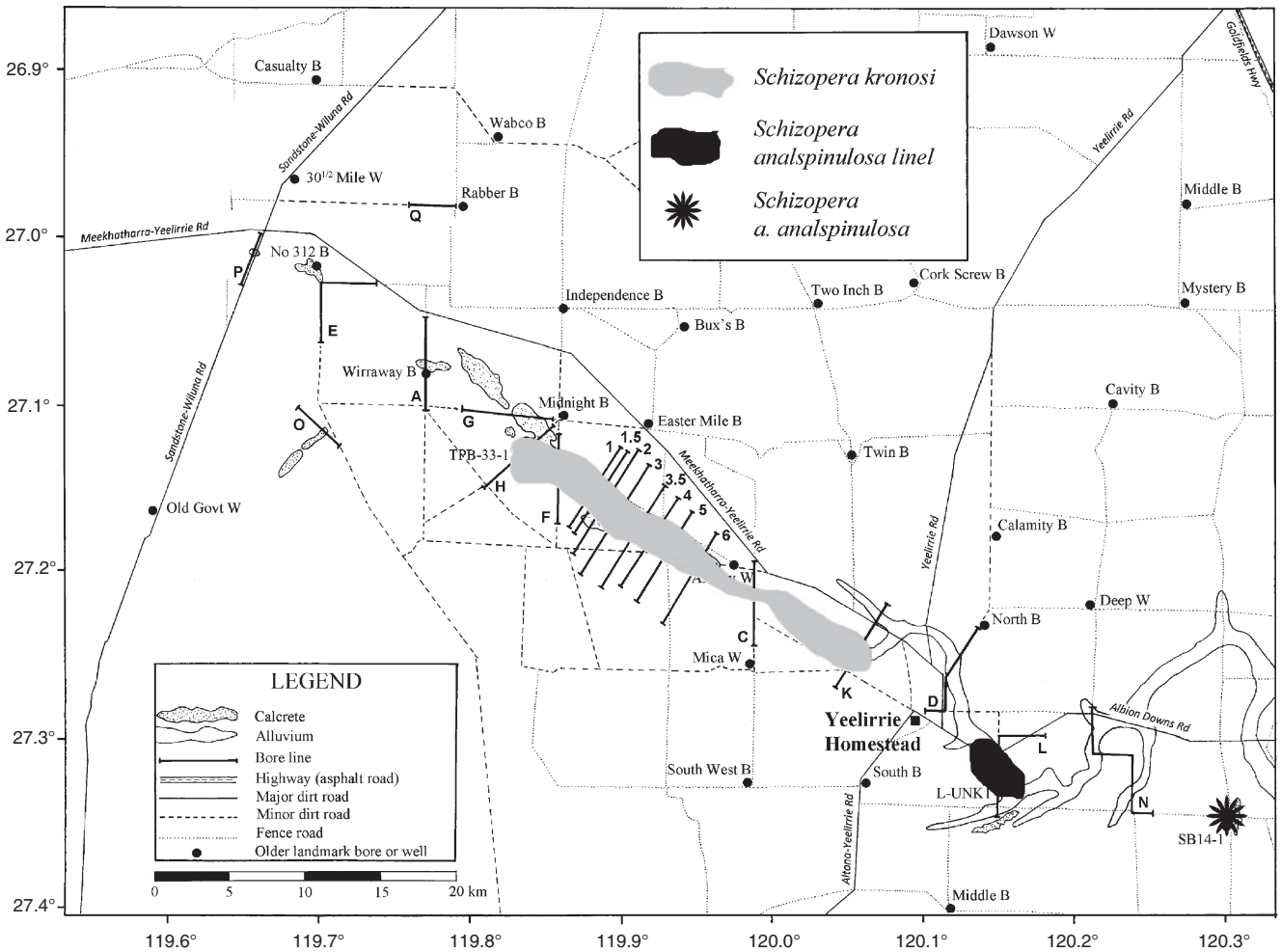

Fig. 40. Presumed distributional ranges of two *Schizopera* species and one subspecies described in this paper: grey surface, *S. kronosi* (recorded on bore lines H, 1.5, 2, 3, 3.5, 5 and K); black surface, *S. analspinulosa linel* (collected in one bore on bore line L); black star, *S. analspinulosa analspinulosa* (collected only in bore SB14–1).

str. and *S. a. linel* (Table 3), and such high divergence values are often indicative of distinct species by comparison with other crustaceans (see Lefébure *et al*. 2006). However, we prefer the hypothesis that these divergences have resulted from a long-term isolation of populations of the same species within different geographic regions of the Yeelirrie calcrete, as the morphological differences are much smaller between them than between either one of them and *S. kronosi*, and all three clades (populations) are allopatric and separated by relatively large distances (Fig. 40). In fact, the two subspecies of *S. analspinulosa* are further apart geographically (almost 20 km) than *S. kronosi* and *S. analspinulosa linel* are (~12 km), but the morphological differences are much greater between the latter two, as are the divergence values in *COI* data (Fig. 39; Table 3).

Interestingly, *S. kronosi* is a very rare species, although with a relatively wide distribution. It lives in the biggest patch of calcrete sympatrically with five other species, and was frequently found in the same bore with other congeners. In four samples it was found together with *S. uranusi*, in three with *S. leptafurca*, and in two samples with *S. leptafurca* and *S. akation*. In all these samples dominant species are either *S. uranusi* or *S. leptafurca*, while *S. kronosi* is represented with one or a few specimens. A possible explanation for this would be that *S. leptafurca* and *S. uranusi* probably evolved in the upper reaches of this palaeochannel (less salinity) and they are better adapted to these conditions. On the other hand, *S. kronosi* could be a member of an older clade, which once flourished here (perhaps during periods of a drier climate and more saline subterranean waters), but is now being replaced with these newly evolved forms. That is possibly why *S. analspinulosa* and *S. analspinulosa linel* are still dominant harpacticoids in their respective habitats, which are in the lower reaches of the palaeochannel, and free from the *leptafurca+uranusi +emphysema* clade. Another possible explanation for the low abundance of *S. kronosi* is related to its size and is discussed further below, but many other possibilities should not be dismissed (trophic differences, different life histories etc.).

Another two rare species are the very small *S. akolos* and the very large *S. emphysema* (Fig. 41), both collected repeatedly from a single bore only. The fact that *S. akolos* is very rare means that

either we did not sample adequately its prime habitat (possibly the smallest crevices in the calcrete), or that this species is a relict here that has largely been replaced by invasions of other more recent arrivals or newly *in situ* evolved forms. It is interesting to note that *S. akolos* lives sympatrically in bore YYD22 with *S. akation*, which is also a small species (although not as small as *S. akolos*). We did actively look for these two species in the last two sampling rounds because of their small size. *Schizopera emphysema* was found only in the type locality, bore YYAC1004C on the bore line 1 (Fig. 41), where it was collected on three separate occasions. Interestingly, three other bores that are situated only a few metres from this one (YYAC1004A, B and D) have never produced any animals of this species, although some produced other copepod species found in YYAC1004C. Water chemistry shows no significant differences between these bores, but they are slotted at different depths, so one has to assume that bore YYAC1004C intercepted a larger cavity in this calcrete, which is a suitable habitat for this large species. *Schizopera akation* was also never very numerous throughout its very wide distributional range (Fig. 41), although this species showed some large divergences in *COI* sequences between different populations and possibly represents a complex of three cryptic species (see below).

Schizopera leptafurca and *S. uranusi* are a sister species pair in the Yeelirrie calcrete, with the average pairwise divergence in *COI* gene being only 15.4% (Table 3), and morphological differences being limited to several microcharacters and different caudal rami shape (see above). However, a detailed sampling in this calcrete showed that their distributional ranges overlap only partly (Fig. 42), suggesting a relatively recent parapatry after an allopatric speciation event. Each species has a range that is longer than 20 km, while they overlap only in an area less than 5 km long (less than 20%). Even in those bore lines where they can be found sympatrically there is a clear tendency of ecological separation, with *S. leptafurca* being a more dominant species in the lower elevation part of the calcrete, in waters of increased salinity. If we analyse samples from a single bore line, these two species are hardly ever present in equal or similar numbers. In the bores that are at a lower elevation and higher salinity, *S. leptafurca* was present with ~100 specimens, while only a few specimens of *S. uranusi* could be found. At higher elevations of the calcrete, where salinity is lower, this situation was reversed.

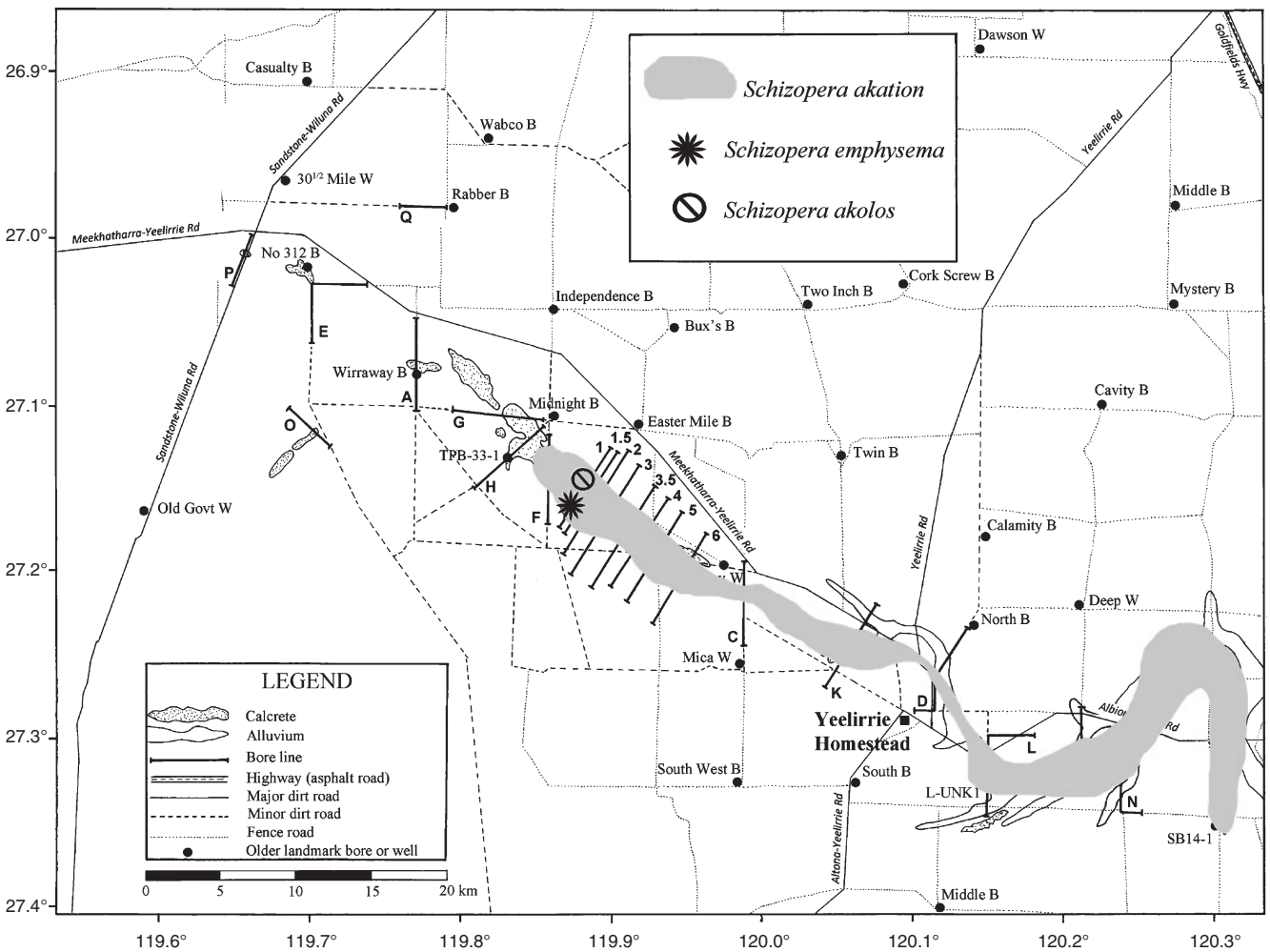

Fig. 41. Presumed distributional ranges of three *Schizopera* species described in this paper: grey surface, *S. akation* (recorded on bore lines F, 1, 1.5, 2, 3, 3.5, K, L and bore SB14–1); black star, *S. emphysema* (collected only in one bore on bore line 1); slashed circle, *S. akolos* (also collected in only one bore on bore line 1).

This difference suggests that they are ecologically separated. Not surprisingly, the rest of the range of *S. leptafurca* is downstream along the palaeochannel, in waters of more increased salinity (ending on line K), while *S. uranusi* lives in upper reaches of this palaeochannel, in waters that are more fresh (between lines 3.5 and O) (Fig. 42).

Yeelirrie and Western Australian stygofaunal regions

Mitochondrial DNA sequence data from *COI* (Fig. 39) confirmed all Yeelirrie morphospecies and revealed the possible presence of several additional cryptic species, which suggests an unprecedented copepod diversity for such a small area. Ongoing morphological and molecular studies on other major groups in this calcrete show them to be much less diverse, containing the usual number of one to three species and with divergence values of *COI* in the order of 5% across the whole Yeelirrie area, which would suggest different ages and colonisation histories for different groups. For example, amphipods are represented with a single new species of *Phreatochiltonia* Zeidler, 1991 (family Chiltoniidae) (T. Finston, pers. comm.), ostracods with a single new species from the genus *Candonopsis* Vavra, 1891 (family Candonidae) (I. Karanovic, pers. comm.), syncarids have two new species from the genus *Atopobathynella* Schminke, 1973 (family Parabathynellidae) and one from the family Bathynellidae (T. Finston, pers. comm.), while diving beetles have two new species from the genus *Limbodessus* Guignot, 1939 and one from the genus *Paroster* Sharp, 1882 (family Dytiscidae) (C. Watts, pers. comm.). Copepod species discovered in the Yeelirrie calcrete represent 67% of previously recorded diversity in the whole Yilgarn region, and this region was relatively well surveyed (Karanovic 2004). As for the genus *Schizopera*, this proportion is even bigger (160% of previously known number of species from the whole region). This phenomenon suggests a possibility of an explosive radiation, which is discussed further below. Detailed hydrological and geological studies, as well as fine level distribution of different species, revealed that what was initially perceived as a single calcrete is in reality a very complex and patchy

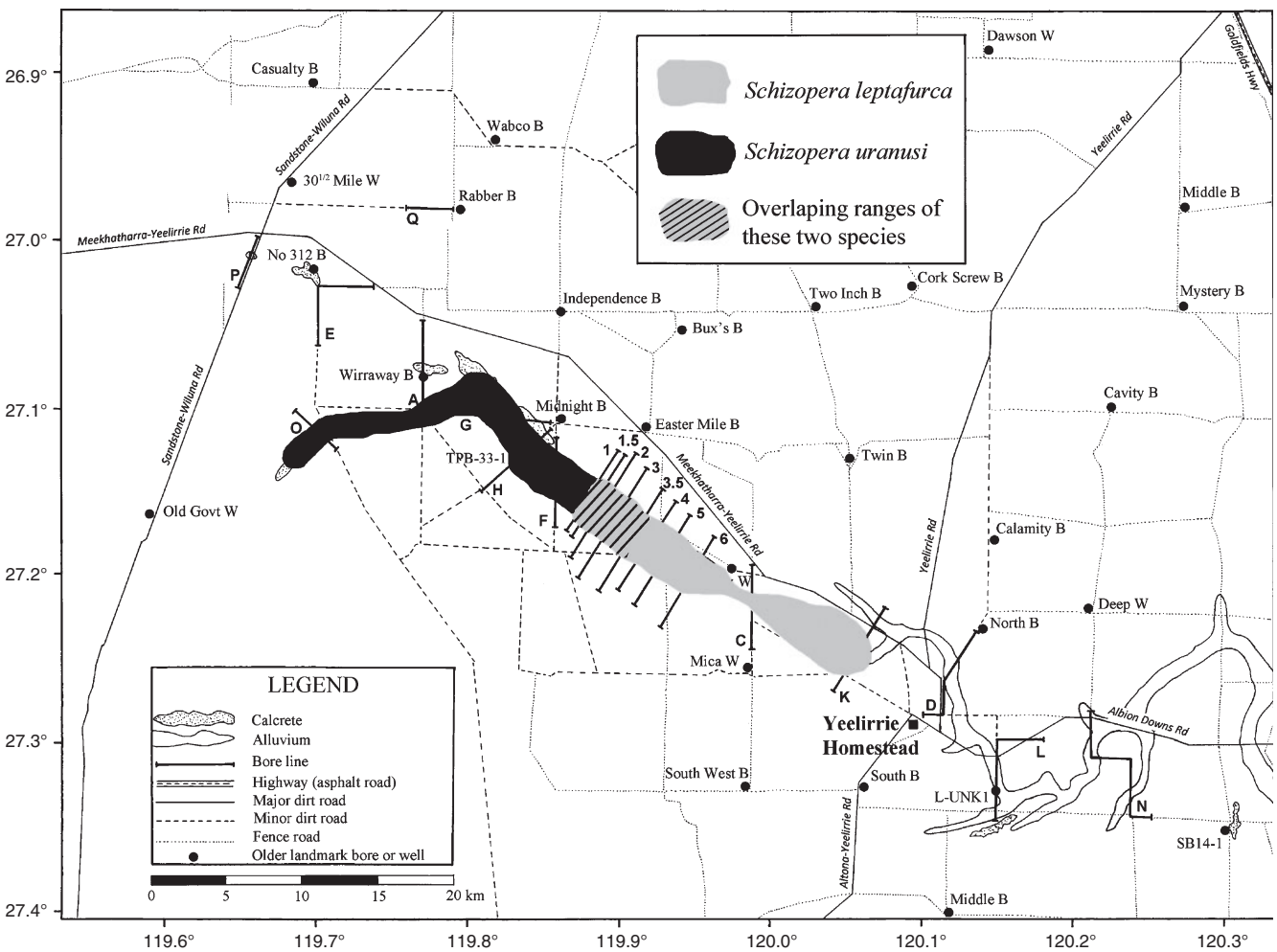

Fig. 42. Presumed distributional ranges of two *Schizopera* species described in this paper: grey surface, *S. leptafurca* (recorded on bore lines 1, 1.5, 2, 3, 3.5, 5 and K), black surface, *S. uranusi* (recorded on bore lines O, H, F, 1, 1.5, 2 and 3.5); black and grey surface, overlapping ranges of these two species.

habitat (S. Eberhard, pers. comm.). This translates into high speciation potential and is probably responsible for the high copepod diversity, in combination with fresher waters in the upper reaches of the Carey palaeochannel and their role in a long accumulation history. Some copepod lineages here, like the harpacticoid genus *Parastenocaris* Kessler, 1913, probably postdate the Permo-Carboniferous glaciation (≤300 million years; see Karanovic 2004, 2006).

Reconstructed phylogenies based on the *COI* gene (Fig. 39) showed that two species from the Pilbara region (*S.* sp. 1 and *S.* sp. 2) are not closely related, despite their similar morphology. We explain this morphology as plesiomorphic, as it is also shared with the Yeelirrie *S. akation* and many other marine members of this genus (T. Karanovic, unpubl. data). All three species have relatively smooth somites, with only several rows of minute spinules and not very deeply serrated hyaline fringes (Figs 19, 20, 38*C, D*). However, all three species are only remotely related based on *COI* data and different methods reconstruct their phylogenies differently (Fig. 39). However, none of them suggest that there are two separate clades for the two separate regions (Yilgarn and Pilbara). This finding provides support for the previously published hypothesis (Karanovic 2006) that *Schizopera* is a relatively recent invasion (possibly <6 Ma) in inland waters of Australia from marine environments, and the only copepod genus with a strong connection between these areas, which is an exception to the general pattern observed. As mentioned in the 'Introduction' section, these two neighbouring Western Australian regions show remarkable differences in most major groups of stygofauna, including copepods (Karanovic 2006, 2010; Karanovic and Hancock 2009), ostracods (Karanovic 2007) and diving beetles (Watts and Humphreys 2006; Leys and Watts 2008).

Cryptic species and 'cryptic' species

One unresolved sequence, which could be a contamination (i.e. a 'cryptic' species), is '7439_S_uranusi sp. 2' (see Fig. 39). This specimen was thoroughly checked on a compound microscope, at 630× magnification in propylene glycol. All important morphological characters of *S. uranusi* were confirmed, including the somite ornamentation, caudal rami shape, and swimming legs armature and segmentation. However, this specimen clusters with the *S. analspinulosa* clade, and not at all with other specimens of *S. uranusi.* Only further sampling and sequencing may help to answer whether we are dealing with a cryptic species here. So far we have not been able to find any other matching sequences in our subsequent sampling trips.

Another candidate for cryptic species in this area is *S. akation*. This species was found, usually in low numbers, on the following bore lines, from north-west to south-east: F, 1, 1.5, 2, 3, 3.5, K, L and bore SB14–1 (Fig. 41). Given its wide distribution in the palaeochannel, it is perhaps not surprising to find a greater molecular divergence than within any of the other species studied here (Fig. 39). The question remains as to whether these lineages represent cryptic species or are just divergent mtDNA sequences within a species. This question could potentially be resolved by further analyses of nuclear markers. Populations from the bore SB14 (8517) appear to be quite distinct from those from line L (8533), while those from the largest calcrete body to the north-west represent a third group (7342, 8479 and 8496). Notably, the first population appears to be the most plesiomorphic (it is basal to two other lineages on our tree) and lives much further downstream in the palaochannel, while the last one is also a terminal clade and lives most upstream in the palaochannel (Fig. 41). This possibly reflects a colonisation pathway from a marine ancestor that was invading interstitial freshwaters, dispersing slowly and actively upstream, but more genes would have to be studied to test this hypothesis.

In this paper we argue in favour of these divergences in the *S. akation* clade resulting from long-term isolation of populations of the same species within different geographic regions of the Yeelirrie system of calcretes. Intensive sampling between these three areas may reveal intermediate populations, with smaller genetic divergences, which would mean that some limited gene flow is still possible. However, in the absence of these data, such high divergences, as recorded in these three populations, often indicate distinct species by comparison with other crustaceans (Leféb ure *et al*. 2006). We could not find any morphological differences between these three populations of *S. akation*, even in the most minute microcharacters, as we found in the two subspecies of *S. analspinulosa*. If these populations are indeed reproductively isolated, they would represent true cryptic species.

It is now well established that morphologically cryptic species occur in most animal groups (Bickford *et al*. 2007; Pfenninger and Schwenk 2007). However, it is clear that groups with well-studied taxonomy and individuals of large size show this phenomenon much less. For example, Hebert *et al*. (2004) discovered only four possible cryptic species of North American birds, after barcoding 260 species. It is symptomatic that a majority of cryptic species in the subterranean fauna of Western Australia are present among amphipod crustaceans (Finston *et al*. 2007; Bradford *et al*. 2010), a group that has not been well studied morphologically. Three 'cryptic' species from the Sturt Meadows, for example, are not even sister clades, i.e. 'they are more closely related to other Yilgarn and non-Yilgarn amphipods than to each other' (Bradford *et al*. 2010), and recent analyses show that they are morphologically distinct and, therefore, not cryptic (King *et al*. 2012). *Schizopera* species from Yeelirrie show that significant morphological differences are found even between the most closely related sister species (*S. leptafurca* and *S. uranusi*), when they live together. We suggest that a combined morphological and molecular approach (Will *et al*. 2005) results in a much more thorough study, as recently shown for harpacticoid copepods from the genus *Kinnecaris* Jakobi, 1972 by Karanovic and Cooper (2011).

Size differentiation

In most cases where we had two *Schizopera* species living in the same bore, there was a significant difference in size (see Figs 43, 45, 46). This phenomenon is relatively common in Western Australian subterranean waters for diving beetles (Leys and Watts 2008; Watts and Humphreys 2009; and references therein). In copepods, the only well-documented case (Karanovic 2006) of closely related sympatric species in subterranean environments with a significant body size difference was in the cyclopoid genus *Diacyclops* Kiefer, 1927

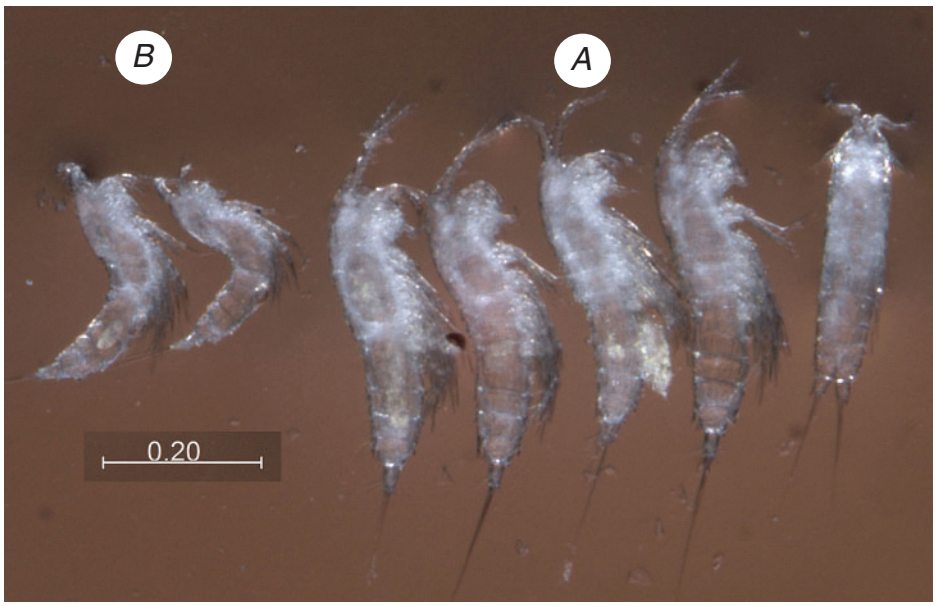

Fig. 43. First two discovered *Schizopera* Sars, 1905 species in Yeelirrie from bore SB14, with a significant size difference. (*A*) *Schizopera analspinulosa* s. str., sp. nov., one ♂ and four ♀ (one ovigerous); (*B*) *S. akation*, sp. nov., two ♀. Scale bar = 0.2 mm.

in the Pilbara region (Fig. 44). However, this case was never tested using molecular methods, so many aspects remained elusive.

Our initial morphological study in Yeelirrie suggested an explosive radiation of the genus *Schizopera*, and size differentiation as the main driving evolutionary force was considered as a working hypothesis. Different species from the same genus living sympatrically, while being in distinct size classes, suggest the possibility of niche partitioning and provide a potential case of sympatric speciation, and because the empirical evidence for sympatric or parapatric speciation remains thin (see the 'Introduction' section above), our work was of potential interest for considering these fundamental scientific questions.

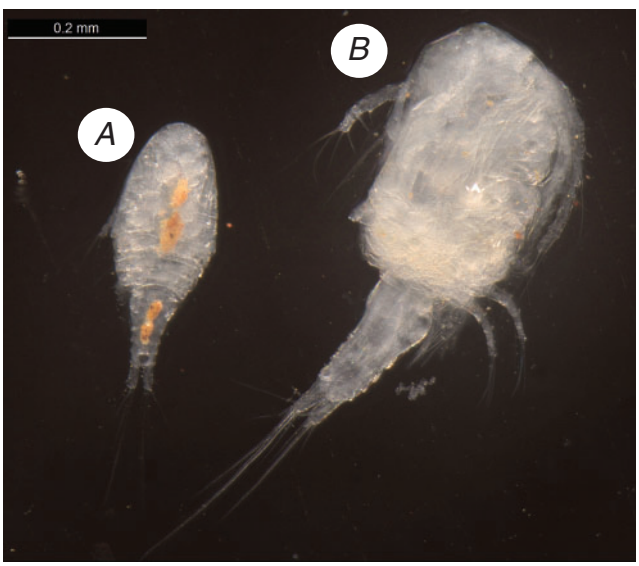

Fig. 44. Two closely related and sympatric *Diacyclops* Kiefer, 1927 species from the Pilbara region with a significant size difference. (*A*) *Diacyclops humphreysi humphreysi* Pesce & De Laurentiis, 1996; (*B*) *D. scanloni* Karanovic, 2006, with somewhat squashed prosome. Scale bar = 0.2 mm.

Schizopera analspinulosa s. str. and *S. akation* are sympatric in bore SB14 (Fig. 43). The latter has the widest distribution in Yeelirrie, and was recorded sympatrically with all other congeners. Sizewise it occupies a separate niche, being significantly smaller than all other species, except *S. akolos*, which is the smallest. These two species were found together with a much larger *S. leptafurca* in bore YYD22 (Fig. 45). *Schizopera akation* was frequently found with *S. leptafurca* and *S. uranusi*, both of which are large species (Fig. 4). As mentioned above, the rare *S. kronosi* was found only once alone. The difference in size probably helps these species in niche partitioning, and enables them to live sympatrically in the same habitat, and we hypothesise here that the small population size of *S. kronosi* in the main patch of calcrete is partly also related to its size. In this part of the palaeochannel live five other *Schizopera* species: *Schizopera akation* and *S. akolos* are much smaller forms, with significantly shorter caudal rami; *S. leptafurca* and *S. emphysema* are much larger, with also much longer caudal rami and heavier ornamentation of somites, while *S. uranusi* is similar in size to *S. kronosi* and probably competes directly with it. We think that *S. uranusi* may share a similar niche to *S. kronosi*, which may be responsible for the small population size of the latter species.

However, sometimes we found *Schizopera* species in the same bore that did not differ in size significantly. Bore YYD26 is a good example (Fig. 46), with a small *S. akation* and two large species, *S. leptafurca* and *S. uranusi*, along with four other copepod species. The latter two species are parapatric,

Fig. 45. Seven sympatric copepod species from bore YYD22 (bore line 1). (*A*) Senior author sampling from the bore; (*B*) *Halicyclops* sp., adult ♂; (*C*) *Schizopera leptafurca*, sp. nov, adult ♀; (*D*) *S. akation*, sp. nov., ovigerous ♀; (*E*) *S. akolos*, sp. nov., adult ♀; (*F*) *Nitocra* sp., ovigerous ♀; (*G*) *Pseudectinosoma* sp., adult ♀; (*H*) *Kinnecaris uranusi* Karanovic & Cooper, 2011, adult ♀.

with strong niche partitioning (see above), and they are morphologically very similar in most characters, if not for their transformed caudal rami. Interestingly, there was no evidence for character displacement here, i.e. differences were not accentuated in regions where these species co-occur nor were they minimised or lost where the species' distributions do not overlap.

Reconstructed phylogenies (Fig. 39) suggest that there is no evidence for parallel evolution in the genus *Schizopera*, as the interspecific size differentiation is a result of different phylogeny (i.e. they originated from ancestors that were already different in size). Sister species *S. leptafurca* and *S. uranusi* hardly differ in size, while *S. akation*, which can frequently be found to live with them (Figs 45, 46), belongs to a distantly related clade. The latter is not even closely related to *S. analspinulsa*, with which it lives sympatrically in the lower reaches of the palaochannel (Figs 40, 41). The very rare and large *S. emphysema* is relatively closely related to *S. leptafurca*, which is also a large species (Figs 3, 4), and yet they both live sympatrically in the same bore, along with the small and unrelated *S. akation*. Instead of the size differentiation in the *leptafurca+uranusi+emphysema* clade, we observe a different phenomenon: their caudal rami have a

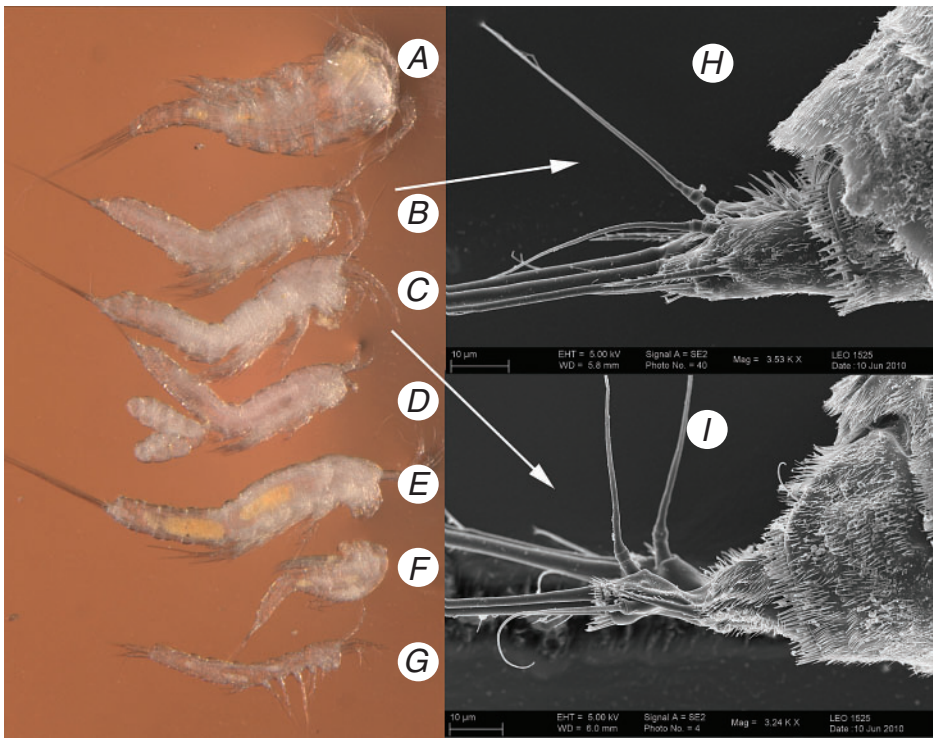

Fig. 46. Seven sympatric copepod species from bore YYD26 (bore line 1). (*A*) *Halicyclops* sp., adult ♀; (*B*) *Schizopera uranusi*, sp. nov., adult ♀; (*C*) *S. leptafurca*, sp. nov, adult ♀; (*D*) *S. akation*, sp. nov., ovigerous ♀; (*E*) *Nitocra* sp., adult ♀; (*F*) *Pseudectinosoma* sp., adult ♀; (*G*) *Kinnecaris uranusi* Karanovic & Cooper, 2011, adult ♀; (*H*) SEM micrograph of *S. uranusi* caudal rami, lateral view; (*I*) SEM micrograph of *S. leptafurca* caudal rami, lateral view.

completely different shape. Those of *S. leptafurca* are constricted in the middle (Figs 31*D*, 46), those of *S. emphysema* are inflated (Fig. 24*B*), while those of *S. uranusi* (Figs 36*D*, 46) are cylindrical in the anterior half and conical in the posterior half. This differentiation in the caudal rami shape is very important in harpacticoid copepods, because these structures are responsible for species sexual recognition. In these animals a male grabs a female by the caudal rami with its antennulae at the start of the copulation process (Lang 1948; Dahms 1988; Huys and Boxshall 1991; Glatzel and Schminke 1996). This is especially significant in subterranean environments, where several closely related species live together, and where there may be a limited possibility for species recognition using chemical signals (due to the physical barriers to diffusion in a crevicular environment). In these habitats, of course, there is no possibility for species recognition using optical signals, as there is no natural light and all these species are blind.

All three closely related species that live sympatrically in the main patch of calcrete (*S. leptafurca*, *S. uranusi* and *S. emphysema*) probably evolved by microallopatric processes. The supporting evidence can be found in the current parapatric distributions of *S. leptafurca* and *S. uranusi* (Fig. 42), which are the two most closely related species (Fig. 39). Even in those bore lines where they can be sympatric there is a clear tendency for ecological separation, with *S. leptafurca* being dominant in bores with increased salinity. This suggests a relatively recent parapatry after an allopatric speciation event. Both molecular and morphological data suggest that these two sister species evolved quite recently (maybe Pliocene, given the divergence level of 15% and assuming a 2.3% divergence rate per million years) from a common ancestor with a disjunct distribution, possibly during a period of decreased humidity. *Schizopera uranusi* probably originated in one of the smaller calcretes in the upper reaches of the palaeochannel, such as the one where bore line O is situated. *Schizopera leptafurca* possibly originated from a population of the ancestral species that survived in the lower part of the main Yeelirrie calcrete. During a subsequent period of increased humidity these two (now reproductively isolated) species may have expanded their ranges and came into secondary contact, somewhere between bores 1 and 3.5. It is interesting that the two most divergent *COI* sequences of *S. leptafurca* (7131 and 8464) come from the southernmost part of the distributional range (line K), the sequence 8385 comes from the central part (line 5), while all the terminal and less divergent sequences come from the northernmost part (lines 1, 1.5, 3 and 3.5) (Fig. 39; Table 2). This is a pattern already observed and discussed above in the *akation* and *analspinulosa+kronosi* clades, and would imply an active upstream colonisation of the calcrete along the palaeochannel, supporting the hypothesis of allopatric speciation, but these patterns are based on analyses of a single genetic locus and require further investigation using additional nuclear markers. However, they are not surprising for a genus with a predominantly marine distribution, and only two large flocks of freshwater species: one in subterranean waters of Western Australia

(Karanovic 2004, 2006), and another in the ancient Lake Tanganyika (Sars 1909; Gurney 1928; Lang 1948; Rouch and Chappuis 1960).

Explosive radiation

The initial hypothesis of an explosive radiation is only partly supported by this study. Detailed morphological and molecular analyses of closely related clades (Fig. 39) suggest a complex story of some radiation, multiple invasions, cryptic speciation among allopatric populations, and differentiation of the characters most responsible for species sexual recognition. Some species are more closely related to congeners from a different region, which strongly implies different colonisation events (see below). At least members of three clades probably evolved in the Yeelirrie area: the *analspinulosa+a. linel+kronosi* clade, the *akation* clade, and the e*mphysema+leptafurca+ uranusi* clade.

Molecular data show that *S. leptafurca* is most closely related to *S. uranusi* (Fig. 39), with the average pairwise distances being 15.4% between them, while those between *S. leptafurca* and *S. emphysema* are 21.6% (Table 3). Apart from a different caudal rami shape, there are very few morphological differences between these three sister species, which suggests relatively recent speciation from a common ancestor (see above).

Three major terminals in the *akation* clade show 12.3% average sequence divergence, and between 12 and 16.5% divergence between haplotypes (Fig. 39; Table 3). Whether they are distinct species or not, the phylogenetic analyses indicate that these populations evolved *in situ* and are allopatric in their distribution (Table 2). In conclusion, we can say that molecular and morphological data provide evidence that this clade underwent an explosive evolution (*sensu* Romer 1960; Hennig 1966) in the Yeelirrie palaeochannel. This term, as opposed to explosive radiation, refers to an explosive diversification without change in morphology.

The MP and NJ trees depict a monophyletic group comprising *S. kronosi*, *S. analspinulosa* s. str. and *S. analspinulosa linel*, but bootstrap values and posterior probabilities for this arrangement were very low <50%. Morphological characters also support the monophyly of *kronosi+analspinulosa* s. str.+*analspinulosa linel*. In particular, the three taxa share enlarged dorsal-most spinules on the anal somite (Figs 6*C*, 9*C*, *E*, 13*C*, 14*A*, 15*C*), which are novel structures, not previously recorded in this genus anywhere. This clade also probably evolved *in situ* and all three taxa are still allopatric (Fig. 40). It is interesting to note that *COI* data suggest a sister relationship between the *S. kronosi* clade from three different localities and the *S. analspinulosa* clade, while the morphological data would suggest *S. analspinulosa* s. str. as the most plesiomorphic form. This would be an interesting case to study further using multiple genes and comparing molecular and morphological phylogenies. The *COI* sequence data suggest a divergence of 15.8% between two subspecies of *S. analspinulosa* (Table 3), and such high divergence values are often indicative of distinct species by comparison with other crustaceans (see Lefébure *et al*. 2006), but the morphological differences are very small (juveniles would be impossible to distinguish). Until further genetic data can be obtained, we prefer the hypothesis that these divergences have resulted from long-term isolation of populations of the same species within different geographic regions of the Yeelirrie calcrete.

Multiple invasions

Our molecular data are still preliminary and we do not have a solid phylogenetic framework of copepods from the Yilgarn region. Nevertheless, reconstructed phylogenies based on *COI* (Fig. 39) suggest that there were at least three (probably four, judged by morphology) independent invasions, either from surface water ancestors or from the marine interstitial: *S. akation*, *S. akolos*, the *leptafurca+uranusi+emphysema* clade, and the *analspinulosa* s. str.+*analpinulosa linel+kronosi* clade. Phylogenetic relationships between these four Yeelirrie clades are not stronger than relationships with two clades from the Pilbara region (some 700 km north from the area investigated), which is reflected in the differences in topology of trees from the different methods, particularly the inter-relationships of taxa branching from basal nodes in the tree. These uncertainties are reflected in the BI results. We perceive all these six *Schizopera* clades (four from Yeelirrie and two from the Pilbara) as only relatively remotely related, although belonging to the same genus.

Surface water is scarce in the Yilgarn region at the moment (Sanders 1973; Beard 1976), given the very arid climate (average annual rainfall of ~200 mm). However, during past periods of increased humidity (e.g. the Miocene or early Pliocene; Holmgren *et al*. 2006; Byrne *et al*. 2008) it is possible that some *Schizopera* species lived in surface water lakes of increased salinity, colonising the subterranean waters as the climate got progressively drier (Martin 2006).

Invasions from marine interstitial by active migration along the palaeochannel is also a possibility, especially because we discovered two new *Schizopera* species in this environment in Western Australia (T. Karanovic, unpubl. data), one of which is morphologically quite similar to *S. akation. Schizopera akation* (or *S. akation*-complex; see above) has the widest distribution in the palaeochannel (Fig. 41), and its reconstructed phylogeny (Fig. 39) possibly reflects its colonisation path, from a marine ancestor that was invading interstitial freshwaters, dispersing slowly and actively upstream. Today the most plesiomorphic form lives most downstream in the palaeochannel (bore SB14), while the terminal clade lives most upstream.

A very similar trend was observed in the distributional range of *S. leptafurca* (Figs 39, 42; see above).

Schizopera akolos has no close relatives in Yeelirrie, or anywhere else in Australia, and also probably represents a separate colonisation event. We believe this species originated from an invasion of a marine interstitial species. We base this hypothesis on its very small size (see Fig. 45) and many reductions in the armature of the swimming legs and ornamentation of somites (see above), all of which would suggest a long evolutionary history in subterranean environments. Various phylogenetic analyses put this species either as a sister clade to the *analspinulosa* s. str.+*analspinulosa linel+kronosi* clade (Fig. 39*A*), or to an as yet undescribed new species from the Pilbara region (*S.* sp. 2) (Fig. 39*B*), but support for both is rather weak. Morphology also holds no clues, but the absence of dorsal pores on the base of the rostrum would put this species with the more plesiomorphic *S. akation*, *S.* sp. 1 and *S.* sp. 2.

However, groupings made on symplesiomophies can only result in paraphyletic clades (Hennig 1966), which is not a sound taxonomic practice. We were only successful at sequencing one specimen of *S. akolos* unfortunately, but this is a very rare species in the Yeelirrie calcrete, found in a single bore.

In the *analspinulosa* s. str.+*analpinulosa linel*+*kronosi* clade a trend in the reduction of outer armature elements on the fifth leg exopod is clearly visible from south-east to north-west, with those in *S. analspinulosa* s. str. being all robust (Fig. 6*D*), middle and distal ones more reduced in *S. a. linel* (Fig. 12*L*), and all three being reduced in size in *S. kronosi* (Fig. 16*G*). This morphological evidence may also suggest an upstream invasion along the palaeochannel, but our molecular data do not support it (Fig. 39).

Seasonal dynamics in subterranean habitats

It is almost common knowledge that stygobitic animals exhibit a reduction or loss of eyes and pigments and have enhanced non-optic sense organs, and species that inhabit interstitial spaces are most often vermiform (Culver *et al*. 1995). It is also a widely accepted view that many convergent physiological adaptations also occur, especially lower metabolic rates, loss of circadian periodicity and seasonal dynamics (Gibert *et al*. 1994; Langecker 2000). They lack resting stages, have fewer young and live longer than their surface relatives (Coineau 2000). Case studies of subterranean animals in Europe have revealed, for example, that embryonic development in the single egg of a bathynellid can take up to nine months (Coineau 2001). Case studies on population dynamics and seasonal variability of stygobitic copepods in France and Slovenia (Lescher-Moutoué 1973; Pipan and Brancelj 2003, 2004) confirmed a generally accepted view that these ecosystems are indeed very stable, slow to recover, and intrinsically vulnerable to anthropogenic effects (Culver and Pipan 2009). This notion was applied to Australian subterranean environments uncritically (Humphreys 2001, 2008), although with some puzzling observations concerning the long persistence of stygofauna in subterranean habitats through geological eras and massive climatic changes. That is why we were so surprised to see pronounced differences in our stygofauna survey results in Yeelirrie in different months, despite very stable environmental conditions. Although most of the results are still awaiting publication, and in this paper we are only discussing one harpacticoid genus, it may be interesting to mention some observations.

Schizopera analspinulosa s. str. was collected from the same bore (SB14) on three separate occasions, once in March 2009 and twice in March 2010, but was absent in January 2010. In Jaunary 2010 all harpacticoids were absent from this bore, and they include *Szhizopera akation* and an as yet undescribed new species from each of the following three genera: *Kinnecaris* Jakobi, 1972, *Nitokra* Boeck, 1865 and *Pseudectinosoma* Kunz, 1935. In January 2010, the only copepod in the bore SB14–1 was *Halicyclops eberhardi* De Laurentiis, Pesce & Humphreys, 2001. This bore was not exceptional, as many other localities produced very few or no *Schizopera* specimens (which can be checked from the list of material examined for each species above), despite an enormous sampling effort and very small changes (if any) in the water level and salinity when compared with our field trip in November 2009. There were no significant rain events in Yeelirrie between January and March 2010, and the water level was even slightly lower and salinity generally slightly higher across the area. In contrast, we discovered a large diversity and density of copepods in the March sampling round, and most of the specimens studied in this paper actually come from this field trip. This would imply very strong seasonal dynamics in this subterranean community, which is a novel concept for these ecosystems.

Key to Australian species of the genus *Schizopera*

This key is based on female characters, because males of *S. kronosi*, *S. oldcuei* Karanovic, 2004 and *S. weelumurra* Karanovic, 2006 are as yet unknown. The record of *S. clandestina* (Klie, 1924) by Halse *et al*. (2002) needs to be verified, as this species was only listed, without any drawings, descriptions or comments. Therefore, this species is not included in the key. All other species were described from Western Australian subterranean water, five from the Yilgarn region by Karanovic (2004), and two from the Pilbara region by Karanovic (2006).

1. Urosomite and caudal rami ornamented with dense cover of long spinules (e.g. Figs 13, 36) 5
   - Somite ornamentation reduced 2
2. Preanal somites without spinules; endopod of fourth leg 2-segmented ..... *S. akolos*, sp. nov.
   - Urosomites ornamented with 2–4 rows of minute triangular spinules (e.g. Figs 20, 38*C*, *D*); endopod of fourth leg 3-segmented 3
3. Caudal rami without large spinules along inner margin 4
   - Caudal rami with large spinules along inner margin ..... *S. akation*, sp. nov.
4. Third endopodal segment of first, second, and third leg without inner seta ..... *S. roberiverensis* Karanovic, 2006
   - This segment with inner seta present ..... *S. weelumurra* Karanovic, 2006
5. Two dorsal-most spinules on anal somite enlarged 6
   - All spinules on anal somite of about same size 8
6. Inner apical setae on third endopodal segment of second, third and fourth legs well developed 7
   - These setae very small and smooth ..... *S. kronosi*, sp. nov.
7. Coxa of first leg with 3 outer groups of large spinules on anterior surface; two distal outer elements on fifth leg exopod as strong as proximal one ..... *S. a. analspinulosa*, sp. nov.
   - Only 2 groups of large spinules on coxa of first leg; two distal outer elements on fifth leg exopod much more slender than proximal one ..... *S. analspinulosa linel*, ssp. nov.
8. Caudal rami widest at anterior margin (where attached to somite) 9
   - Caudal rami widest at middle, with inflated appearance ..... *S. emphysema*, sp. nov.
9. Caudal rami conical or cylindrical 10
   - Caudal rami constricted at middle ..... *S. leptafurca*, sp. nov.
10. Caudal rami less than four times as long as wide 11
    - Caudal rami more than four times as long as wide ..... *S. jundeei* Karanovic, 2004
11. Outer apical seta on caudal rami much longer than ramus 12
    - This seta about as long as ramus ..... *S. oldcuei* Karanovic, 2004
12. Caudal rami more than twice as long as wide 13
    - Caudal rami less than twice as long as wide 14
13. Caudal rami almost cylindrical, with proximal outer and dorsal setae at two-thirds of ramus length ..... *S. uramurdahi* Karanovic, 2004
    - Caudal rami more conical, with proximal outer and dorsal setae at midlength ..... *S. uranusi*, sp. nov.

14. Caudal rami slender when compared with anal somite, ~1.7 times as long as wide; baseoendopod of fifth leg ovoid, exopod armed with five elements ..... *S. depotspringsi* Karanovic, 2004
- Caudal rami broad, 1.4 times as long as wide; baseoendopod of the fifth leg triangular, exopod armed with six elements .... *S. austindownsi* Karanovic, 2004

Acknowledgments

The authors are deeply indebted to Stefan Eberhard, Subterranean Ecology Environmental Services, for entrusting the morphological identification of this material to the senior author and molecular analysis to the junior author. Renate Walter, from the Zoologisches Museum Hamburg, is kindly acknowledged for the help in preparation of the SEM photographs. The following staff of Subterranean Ecology is acknowledged for their help in the field, as well as for sorting the samples: Giulia Perina, Natalie Krawczyk, Peter Bell and Shae Callan. We also are very grateful to Tessa Bradford and Kathleen Saint (South Australian Museum) for carrying out the PCR and sequencing analyses, and Saint is also greatly acknowledged for developing nested primers that were used in combination with universal primers for *COI* gene amplification. Financial support to the senior author came from Brain Pool and NIBR grants (both in Korea) and Subterranean Ecology, while the necessary facilities were provided by the Zoologisches Museum in Hamburg and Hanyang University in Seoul. Financial support for *COI* sequencing was also provided by Subterranean Ecology. Cooper's work was supported by an ARC Linkage grant LP 100200494. Two anonymous reviewers are greatly acknowledged for many constructive remarks.

References

Adamowicz, S. J., Manu-Marque, S., Hebert, P. D. N., and Purvis, A. (2007). Molecular systematics and patterns of morphological evolution in the Centropagidae (Copepoda: Calanoida) of Argentina. *Biological Journal of the Linnean Society. Linnean Society of London* **90**, 279–292. doi:10.1111/j.1095-8312.2007.00723.x

Allford, A., Cooper, S. J. B., Humphreys, W. F., and Austin, A. D. (2008). Diversity and distribution of groundwater fauna in a limestone aquifer: does sampling alter the story? *Invertebrate Systematics* **22**, 127–138. doi:10.1071/IS07058

Apostolov, A. (1972). Catalogue des Copépodes harpacticoides marins de la Mer Noire. *Zoologischer Anzeiger* **188**, 202–254.

Apostolov, A. (1982). Genres et sous-genres nouveaux de la famille Diosaccidae Sars et Cylindropsyllidae Sars, Lang (Copepoda, Harpacticoidea). *Acta Zoologica Bulgarica* **19**, 37–42.

Arlt, G. (1983). Taxonomy and ecology of some harpacticoids (Crustacea, Copepoda) in the Baltic Sea and Kattegat. *Zoologische Jahrbücher. Abteilung für Systematik* **110**, 45–85.

Beard, J. S. (1976). 'Vegetation survey of Western Australia, Murchison.' (University of Western Australia Press: Perth, WA.)

Berner, D., Grandchamp, A.-C., and Hendry, A. P. (2009). Variable progress toward ecological speciation in parapatry: stickleback across eight lake-stream transitions. *Evolution* **63**, 1740–1753. doi:10.1111/j.1558-5646.2009.00665.x

Bickford, D., Lohman, D. J., and Sodhi, N. S. (2007). Cryptic species as a window on diversity and conservation. *Trends in Ecology & Evolution* **22**, 148–155. doi:10.1016/j.tree.2006.11.004

Bodin, P. (1997). Catalogue of the new marine Harpacticoid Copepods (1997 edn). *Documents de travail de l'Institut royal des Sciences naturelles de Belgique* **89**, 1–304.

Bolnick, D. I., and Fitzpatrick, B. M. (2007). Sympatric speciation: models and empirical evidence. *Annual Review of Ecology Evolution and Systematics* **38**, 459–487. doi:10.1146/annurev.ecolsys.38.091206.095804

Borutzky, E. W. (1972). Copepoda Harpacticoida from subterranean water of the shore of Issyk-Kul and Southern Kisilkum. *Trudy Zoologicheskogo Instituta Leningrad* **51**, 98–119. [in Russian]

Boxshall, G. A., and Halsey, S. H. (2004). 'An Introduction to Copepod Diversity.' (The Ray Society: London.)

Boxshall, G. A., and Jaume, D. (2000). Making waves: the repeated colonization of freshwater by copepod crustaceans. *Advances in Ecological Research* **31**, 61–79. doi:10.1016/S0065-2504(00)31007-8

Bradford, T., Adams, M., Humphreys, W. F., Austin, A. D., and Cooper, S. J. B. (2010). DNA barcoding of stygofauna uncovers cryptic amphipod diversity in a calcrete aquifer in Western Australia's arid zone. *Molecular Ecology Resources* **10**, 41–50. doi:10.1111/j.1755-0998.2009.02706.x

Brown, W. L., and Wilson, E. O. (1956). Character displacement. *Systematic Zoology* **5**, 49–64. doi:10.2307/2411924

Byrne, M., Yeates, D. K., Joseph, L., Kearney, M., Bowler, J., Williams, M. A., Cooper, S. J. B., Donnellan, S. C., Keogh, S., Leijs, R., Melville, J., Murphy, D., Porch, N., and Wyrwoll, K.-H. (2008). Birth of a biome: synthesizing environmental and molecular studies of the assembly and maintenance of the Australian arid zone biota. *Molecular Ecology* **17**, 4398–4417. doi:10.1111/j.1365-294X.2008.03899.x

Chappuis, P. A. (1955). Harpacticoides psammiques du Lac Tanganika. *Revue de Zoologie et de Botanique Africaines* **51**, 68–80.

Chappuis, P.-A., and Rouch, R. (1961). Harpacticides psammiques d'une plage près d'Accra (Ghana). *Vie et Milieu* **11**, 605–614.

Chappuis, P. A., and Serban, M. (1953). Copépodes de la nappe phréatique de la plage d'Agigea près Constanza. *Notes Biospéologiqus* **8**, 91–102.

Chertoprud, E. S., and Kornev, P. N. (2005). On the harpacticoid fauna of the Caspian Sea, including the description of *Schizopera rybnikovi* sp. n. (Copepoda: Harpacticoida: Diosaccidae). *Arthropoda Selecta* **14**, 281–289.

Cho, J.-L., Humphreys, W. F., and Lee, S.-D. (2006*a*). Phylogenetic relationships within the genus *Atopobathynella* Schminke, 1973 (Bathynellacea, Parabathynellidae): with the description of six new species from Western Australia. *Invertebrate Systematics* **20**, 9–41. doi:10.1071/IS05019

Cho, J.-L., Park, J.-G., and Ranga Reddy, Y. (2006*b*). *Brevisomabathynella* gen. nov. with two new species from Western Australia (Bathynellacea, Syncarida): the first definitive evidence of predation in Parabathynellidae. *Zootaxa* **1247**, 25–42.

Coineau, N. (2000). Adaptations to interstitial groundwater life. In 'Ecosystems of the World, 30: Subterranean Ecosystems'. (Eds H. Wilkens, D. C. Culver and W. F. Humphreys.) pp. 189–210. (Elsevier: Amsterdam.)

Coineau, N. (2001). Syncarida. In 'Encyclopedia Biospeologica'. (Eds C. Juberthie and V. Decu.) pp. 863–876. (Societé de Biospéologica and Acdémie Roumanie: Moulis and Bucharest.)

Cooper, S. J. B., Hinze, S., Leys, R., Watts, C. H. S., and Humphreys, W. F. (2002). Islands under the desert: molecular systematics and evolutionary origin of stygobitic water beetles (Coleoptera: Dytiscidae) from central Western Australia. *Invertebrate Systematics* **16**, 589–598. doi:10.1071/IT01039

Cooper, S. J. B., Bradbury, J. H., Saint, K. M., Leys, R., Austin, A. D., and Humphreys, W. F. (2007). Subterranean archipelago in the Australian arid zone: mitochondrial DNA phylogeography of amphipods from central Western Australia. *Molecular Ecology* **16**, 1533–1544. doi:10.1111/j.1365-294X.2007.03261.x

Cooper, S. J. B., Saint, K. M., Taiti, S., Austin, A. D., and Humphreys, W. F. (2008). Subterranean archipelago: mitochondrial DNA phylogeography of stygobitic isopods (Oniscidea: *Halniscus*) from the Yilgarn region of Western Australia. *Invertebrate Systematics* **22**, 195–203. doi:10.1071/IS07039

Coull, B. C. (1971). Meiobenthic Harpacticoida (Crustacea, Copepoda) from the North Carolina continental shelf. *Cahiers de Biologie Marine* **12**, 195–237.

Culver, D., and Pipan, T. (2009). 'The Biology of Caves and Other Subterranean Habitats.' (Oxford University Press: Oxford.)

Culver, D. C., Kane, T., and Fong, D. W. (1995). 'Adaptation and Natural Seection in Caves: The Evolution of *Gammarus minus*.' (Harvard University Press: Cambridge.)

Dahms, H. U. (1988). Development of functional adaptation to clasping behaviour in harpacticoid copepods (Copepoda, Harpacticoida). *Hydrobiologia* **167/168**, 505–513. doi:10.1007/BF00026345

Eberhard, S. M., Halse, S. A., and Humphreys, W. F. (2005). Stygofauna in the Pilbara region, north-west Australia: a review. *Journal of the Royal Society of Western Australia* **88**, 167–176.

Eberhard, S. M., Halse, S. A., Williams, M. R., Scanlon, M. D., Cocking, J., and Barron, H. J. (2009). Exploring the relationship between sampling efficiency and short-range endemism for groundwater fauna in the Pilbara region, Western Australia. *Freshwater Biology* **54**, 885–901. doi:10.1111/j.1365-2427.2007.01863.x

Felsenstein, J. (1985). Confidence limits on phylogenies: an approach using the bootstrap. *Evolution* **39**, 783–791. doi:10.2307/2408678

Finston, T. L., Johnson, M. S., Humphreys, W. F., Eberhard, S., and Halse, S. (2007). Cryptic speciation in two widespread subterranean amphipod genera reflects historical drainage patterns in an ancient landscape. *Molecular Ecology* **16**, 355–365. doi:10.1111/j.1365-294X.2006.03123.x

Folmer, O., Black, M., Hoeh, W., Lutz, R., and Vrijenoek, R. (1994). DNA primers for amplification of mitochondrial cytochrome c oxidase subunit 1 from diverse metazoan invertebrates. *Molecular Marine Biology and Biotechnology* **3**, 294–299.

Foster, S. A., McKinnin, G. E., Steane, D. A., Potts, B. M., and Vaillancourt, R. E. (2007). Parallel evolution of dwarf ecotypes in the forest tree *Eucalyptus globulus*. *New Phytologist* **175**, 370–380. doi:10.1111/j.1469-8137.2007.02077.x

Fryer, G. (1956). New species of cyclopoid and harpacticoid copepods from sandy beaches of Lake Nyasa. *Annals & Magazine of Natural History* **9**, 225–249. doi:10.1080/00222935608655810

Gibert, J., Danielopol, D. L., and Stanford, J. A. (1994). 'Groundwater Ecology.' (Academic Press: London.)

Giribet, G., and Edgecombe, G. D. (2006). The importance of looking at small-scale patterns when inferring Gondwanan biogeography: a case study of the centipede *Paralamyctes* (Chilopoda, Lithobiomorpha, Henicopidae). *Biological Journal of the Linnean Society. Linnean Society of London* **89**, 65–78. doi:10.1111/j.1095-8312.2006.00658.x

Glatzel, T., and Schminke, H. K. (1996). Mating behaviour of the groundwater copepod *Parastenocaris phyllura* Kiefer, 1938 (Copepoda: Harpacticoida). *Contributions to Zoology (Amsterdam, Netherlands)* **66**, 103–108.

Gurney, R. (1928). Some Copepoda from Tanganyika collected by Mr S.R.B. Pask. *Proceedings of the Zoological Society of London* **22**, 317–332.

Guzik, M. T., Abrams, K. M., Cooper, S. J. B., Humphreys, W. F., Cho, J.-L., and Austin, A. D. (2008). Phylogeography of the ancient Parabathynellidae (Crustacea: Bathynellacea) from the Yilgarn region of Western Australia. *Invertebrate Systematics* **22**, 205–216. doi:10.1071/IS07040

Guzik, M. T., Cooper, S. J. B., Humphreys, W. F., and Austin, A. D. (2009). Fine-scale comparative phylogeography of a sympatric sister species triplet of subterranean diving beetles from a single calcrete aquifer in Western Australia. *Molecular Ecology* **18**, 3683–3698. doi:10.1111/j.1365-294X.2009.04296.x

Guzik, M. T., Austin, A. D., Cooper, S. J. B., Harvey, M. S., Humphreys, W. F., Bradford, T., Eberhard, S. M., King, R. A., Leys, R., Muirhead, K. A., and Tomlinson, M. (2011*a*). Is the Australian subterranean fauna uniquely diverse? *Invertebrate Systematics* **24**, 407–418. doi:10.1071/IS10038

Guzik, M. T., Cooper, S. J. B., Humphreys, W. F., Ong, S., Kawakami, T., and Austin, A. D. (2011*b*). Evidence for population fragmentation within a subterranean aquatic habitat in the Western Australian desert. *Heredity* **107**, 215–230. doi:10.1038/hdy.2011.6

Halse, S. A., Cale, D. J., Jasinska, E. J., and Shiel, R. J. (2002). Monitoring change in aquatic invertebrate biodiversity: sample size, faunal elements and analytical methods. *Aquatic Ecology* **36**, 395–410. doi:10.1023/A:1016563001530

Harvey, M. S. (2002). Short-range endemism amongst the Australian fauna: examples from non-marine environments. *Invertebrate Systematics* **16**, 555–570. doi:10.1071/IS02009

Hasegawa, M., Kishino, H., and Yano, T. (1985). Dating of the human-ape splitting by a molecular clock of mitochondrial DNA. *Journal of Molecular Evolution* **22**, 160–174. doi:10.1007/BF02101694

Hebert, P. D. N., Cywinska, A., Ball, S. L., and deWaard, J. R. (2003). Biological identifications through DNA barcodes. *Proceedings of the Royal Society of London* **270**, 313–321. doi:10.1098/rspb.2002.2218

Hebert, P. D. N., Stoeckle, M. Y., Zemlak, T. S., and Francis, C. M. (2004). Identification of birds through DNA barcodes. *PLoS Biology* **2**, 1657–1663. doi:10.1371/journal.pbio.0020312

Hennig, W. (1966). 'Phylogenetic Systematics.' (University of Illinois Press: Champaign, IL, USA.)

Holmgren, M., Stapp, P., Dickman, C. R., Gracia, C., Graham, S., Gutiérrez, J. R., Hice, C., Jaksic, F., Kelt, D. A., Letnic, M., Lima, M., López, B. C., Meserve, P. L., Milstead, W. B., Polis, G. A., Previtali, M. A., Richter, M., Sabate, S., and Squeo, F. A. (2006). Extreme climatic events shape arid and semiarid ecosystems. *Frontiers in Ecology and the Environment* **4**, 87–95. doi:10.1890/1540-9295(2006)004[0087:ECESAA]2.0.CO;2

Huelsenbeck, J. P., and Ronquist, F. (2001). MRBAYES: Bayesian inference of phylogeny. *Bioinformatics (Oxford, England)* **17**, 754–755. doi:10.1093/bioinformatics/17.8.754

Humphreys, W. F. (2000). Background and glossary. In 'Ecosystems of the World, 30: Subterranean Ecosystems'. (Eds H. Wilkens, D. C. Culver and W. F. Humphreys.) pp. 3–14. (Elsevier: Amsterdam.)

Humphreys, W. F. (2001). Groundwater calcrete aquifers in the Australian arid zone: the context to an unfolding plethora of stygal biodiversity. *Records of the Western Australian Museum* (Suppl. 64), 63–83.

Humphreys, W. F. (2006). Aquifers: the ultimate groundwater-dependent ecosystems. *Australian Journal of Botany* **54**, 115–132. doi:10.1071/BT04151

Humphreys, W. F. (2008). Rising from Down Under: developments in subterranean biodiversity in Australia from a groundwater perspective. *Invertebrate Systematics* **22**, 85–101. doi:10.1071/IS07016

Huys, R. (2009). Unresolved cases of type fixation, synonymy and homonymy in harpacticoid copepod nomenclature (Crustacea: Copepoda). *Zootaxa* **2183**, 1–99.

Huys, R., and Boxshall, G. A. (1991). 'Copepod Evolution.' (The Ray Society: London.)

Karanovic, T. (2004). Subterranean Copepoda from arid Western Australia. *Crustaceana Monographs* **3**, 1–366.

Karanovic, T. (2006). Subterranean copepods (Crustacea, Copepoda) from the Pilbara region in Western Australia. *Records of the Western Australian Museum* (Suppl. 70), 1–239.

Karanovic, I. (2007). Candoninae ostracods from the Pilbara region in Western Australia. *Crustaceana Monographs* **7**, 1–432.

Karanovic, T. (2008). Marine interstitial Poecilostomatoida and Cyclopoida (Copepoda) of Australia. *Crustaceana Monographs* **9**, 1–331.

Karanovic, T. (2010). First record of the harpacticoid genus *Nitocrellopsis* (Copepoda, Ameiridae) in Australia, with descriptions of three new species. *International Journal of Limnology* **46**, 249–280. doi:10.1051/limn/2010021

Karanovic, T., and Cooper, S. J. B. (2011). Molecular and morphological evidence for short range endemism in the *Kinnecaris solitaria* complex (Copepoda: Parastenocarididae), with description of seven new species. *Zootaxa* **3026**, 1–64.

Karanovic, T., and Hancock, P. (2009). On the diagnostic characters of the genus *Stygonitocrella* (Copepoda, Harpacticoida), with descriptions of seven new species from Australian subterranean waters. *Zootaxa* **2324**, 1–85.

Karanovic, T., and Tang, D. (2009). A new species of the copepod genus *Australoeucyclops* (Crustacea: Cyclopoida: Eucyclopinae) from Western Australia shows the role of aridity in habitat shift and colonization of ground water. *Records of the Western Australian Museum* **25**, 247–263.

Karanovic, T., Eberhard, S. M., and Murdoch, A. (2011). A cladistic analysis and taxonomic revision of Australian *Metacyclops* and *Goniocyclops*, with description of four new species and three new genera (Copepoda, Cyclopoida). *Crustaceana* **84**, 1–67. doi:10.1163/001121610X546698

Kiefer, F. (1934). Neue Ruderfusskrebse von der Insel Haiti. *Zoologischer Anzeiger* **108**, 227–233.

King, R. A., Bradford, T., Austin, A. D., Humphreys, W. F., and Cooper, S. J. B. (2012). Divergent molecular lineages and not-so-cryptic species: the first descriptions of stygobitic chiltoniid amphipods (Talitroidea: Chiltoniidae) from Western Australia. *Journal of Crustacean Biology* **32**, 465–488.

Klie, W. (1923). Über eine neue Brackwasserart der Harpacticoiden-Gattung *Amphiascus. Archiv fuer Hydrobiologie* **14**, 335–339.

Kubota, K., and Sota, T. (1998). Hybridization and speciation in the carabid beetles of the subgenus *Ohomopterus* (Coleoptera, Carabidae, genus *Carabus*). *Researches on Population Ecology* **40**, 213–222. doi:10.1007/BF02763406

Kumar, S., Dudley, J., Nei, M., and Tamura, K. (2008). MEGA: a biologist-centric software for evolutionary analysis of DNA and protein sequences. *Briefings in Bioinformatics* **9**, 299–306. doi:10.1093/bib/bbn017

Lang, K. (1948). 'Monographie der Harpacticiden, A-B.' (Nordiska Bokhandeln: Lund, Sweden.)

Lang, K. (1965*a*). Copepoda Harpacticoida from the Californian Pacific Coast. *Kungliga Svenska Vetensk-Akademiens Handlingar, Fjarde Serien. Almquist and Wiksell, Stockholm* **10**, 1–560.

Lang, K. (1965*b*). Copepoda Harpacticoidea aus dem Kustengrundwasser dicht bei dem Askölaboratorium. *Arkiv för Zoologi* **18**, 73–83.

Langecker, T. G. (2000). The effect of continous darkness on cave ecology and cavernicolous evolution. In 'Ecosystems of the World, 30: Subterranean Ecosystems'. (Eds H. Wilkens, D. C. Culver and W. F. Humphreys.) pp. 135–157. (Elsevier: Amsterdam.)

Lefébure, T., Douady, C. J., Gouy, M., and Gibert, J. (2006). Relationship between morphological taxonomy and molecular divergence within Crustacea: proposal of a molecular threshold to help species delimination. *Molecular Phylogenetics and Evolution* **40**, 435–447. doi:10.1016/j.ympev.2006.03.014

Lescher-Moutoué, F. (1973). Sur la biologie et l'écologie des copepods cyclopides hypogés (Crustacés). *Annales de Spéléologie* **28**, 429–674.

Leyequién, E., de Boer, W. F., and Cleef, A. (2007). Influence of body size on coexistence of bird species. *Ecological Research* **22**, 735–741. doi:10.1007/s11284-006-0311-6

Leys, R., and Watts, C. H. (2008). Systematics and evolution of the Australian subterranean hydroporine diving beetles (Dytiscidae), with notes on *Carabhydrus*. *Invertebrate Systematics* **22**, 217–225. doi:10.1071/IS07034

Leys, R., Watts, C. H. S., Cooper, S. J. B., and Humphreys, W. F. (2003). Evolution of subterranean diving beetles (Coleoptera: Dytiscidae: Hydroporini, Bidessini) in the arid zone of Australia. *Evolution* **57**, 2819–2834.

Martin, H. A. (2006). Cenozoic climatic change and the development of the arid vegetation in Australia. *Journal of Arid Environments* **66**, 533–563. doi:10.1016/j.jaridenv.2006.01.009

Mayr, E. (1963). 'Animal Species and Evolution.' (Harvard University Press: Cambridge, MA, USA.)

Mayr, E. (2001). 'What Evolution Is.' (Basic Books: New York, NY, USA.)

Mielke, W. (1975). Systematik der Copepoda eines Sandstrandes der Nordseeinsel Sylt. *Mikrofauna des Meeresbodens* **52**, 1–134.

Mielke, W. (1992). Description of some benthic Copepoda from Chile and a discussion on the relationships of *Paraschizopera* and *Schizopera* (Diosaccidae). *Microfauna Marina* **7**, 79–100.

Mielke, W. (1995). Species of the taxon *Schizopera* (Copepoda) from the Pacific coast of Costa Rica. *Microfauna Marina* **10**, 89–116.

Mirabdullayev, I. M., and Ginatullina, E. N. (2007). The genus *Schizopera* (Copepoda, Harpacticoida) in Uzbekistan (central Asia). *Vestnik Zoologii* **41**, 305–313.

Nagel, L., and Schluter, D. (1998). Body size, natural selection, and speciation in stickleback. *Evolution* **52**, 209–218. doi:10.2307/2410936

Noodt, W. (1954). Sandstrand-Copepoden von der schwedischen Ostküste. Kungl. *Fysiografiska Sallskapets I Lund Forhandlingar* **24**, 1–8.

Noodt, W. (1955). Harpacticiden (Crust. Cop.) aus dem Sandstrand der französischen Biscaya-Küste. *Kieler Meeresforschungen* **11**, 86–109.

Noodt, W. (1958). *Schizopera pratensis* n. sp. von Salzwiesen der deutschen Meeresküste (Crustacea, Copepoda). *Kieler Meeresforschungen* **14**, 223–225.

Petkovski, T. K. (1954). Harpacticiden des Grundwassers unserer Meeresküste. *Acta Musei Macedonici Scientiarum Naturalium* **2**, 93–123.

Pfenninger, M., and Schwenk, K. (2007). Cryptic animal species are homogeneously distributed among taxa and biogeographical regions. *BMC Evolutionary Biology* **7**, 121–127. doi:10.1186/1471-2148-7-121

Pipan, T., and Brancelj, A. (2003). Fauna of epikarst – Copepoda (Crustacea) in percolation water of caves in Slovenia. *Annales Series Historia Naturalis (Koper)* **13**, 223–228.

Pipan, T., and Brancelj, A. (2004). Distribution patterns of copepods (Crustacea: Copepoda) in percolation water of the Postojnska Jama cave system (Slovenia). *Zoological Studies* **43**, 206–210.

Por, F. D. (1968). The benthic Copepoda of Lake Tiberias and of some inflowing springs. *Israel Journal of Zoology* **17**, 31–50.

Posada, D., and Crandall, K. A. (1998). Modeltest: testing the model of DNA substitution. *Bioinformatics (Oxford, England)* **14**, 817–818. doi:10.1093/bioinformatics/14.9.817

Quesada, H., Posada, D., Caballero, A., Moran, P., and Rolan-Alvarez, E. (2007). Phylogenetic evidence for multiple sympatric ecological diversification in a marine snail. *Evolution* **61**, 1600–1612. doi:10.1111/j.1558-5646.2007.00135.x

Rambaut, A., and Drummond, A. J. (2007). Tracer: MCMC Trace Analysis Package. Available at http://tree.bio.ed.ac.uk/software/tracer/ [verified June 2012]

Rodríguez, F., Oliver, J. F., Marín, A., and Medina, J. R. (1990). The general stochastic model of nucleotide substitutions. *Journal of Theoretical Biology* **142**, 485–501. doi:10.1016/S0022-5193(05)80104-3

Romer, A. S. (1960). Explosive evolution. *Zoologische Jahrbucher* **88**, 79–90.

Ronquist, F., and Huelsenbeck, J. P. (2003). MRBAYES 3: Bayesian phylogenetic inference under mixed models. *Bioinformatics (Oxford, England)* **19**, 1572–1574. doi:10.1093/bioinformatics/btg180

Rouch, R., and Chappuis, P. A. (1960). Sur quelques Copépodes Harpacticoides du lac Tanganika. *Revue de Zoologie et de Botanique Africaines* **61**, 283–286.

Rundle, H. D., Nagel, L., Wenrick Boughman, J., and Schluter, D. (2000). Natural selection and parallel speciation in sympatric stricklbacks. *Science* **287**, 306–308. doi:10.1126/science.287.5451.306

Ryan, P. G., Bloomer, P., Moloney, C. L., Grant, T. J., and Delport, W. (2007). Ecological speciation in south Atlantic island finches. *Science* **315**, 1420–1423. doi:10.1126/science.1138829

Sakaguchi, S. O., and Ueda, H. (2010). A new species of *Pseudodiaptomus* (Copepoda: Calanoida) from Japan, with notes on closely related *P. inopinus* Bruckhardt, 1913 from Kyushu Island. *Zootaxa* **2623**, 52–68.

Sanders, C. C. (1973). Hydrogeology of a calcrete deposit on Paroo Station, Wiluna, and surrounding areas. *Western Australian Geological Survey Annual Report* **1973**, 15–26.

Sars, G. O. (1905). Pacifische Plankton-Crustaceen; Ergebnisse einer Reise nach dem Pacific Schauinsland 1896–1897, II. Brackwasser-Crustaceen von den Chatham-Inseln. *Zoologische Jahrbücher. Abteilung für Systematik* **21**, 371–414.

Sars, G. O. (1909). Zoological results of the third Tanganyika expedition, report on the Copepoda. *Proceedings of the Zoological Society of London* **1909**, 31–77.

Savolainen, V., Anstett, M. C., Lexer, C., Hutton, I., Clarkson, J. J., Norup, M. V., Powell, M. P., Springate, D., Salamin, N., and Baker, W. J. (2006). Sympatric speciation in palms on an oceanic island. *Nature* **441**, 210–213. doi:10.1038/nature04566

Sota, T., Takami, Y., Kubota, K., Ujiie, M., and Ishikawa, R. (2000). Interspecific body size differentiation in species assemblages of the carabid subgenus *Ohomopterus* in Japan. *Population Ecology* **42**, 279–291. doi:10.1007/PL00012006

Soyer, J. (1974). Harpacticoïdes (Crustacés Copépodes) de l'archipel de Kerguelen, 1. Quelques forms mésopsammiques. *Bulletin du Muséum National d'Historie Naturelle. Zoologie* **168**, 1169–1222.

Stamatakis, A., Hoover, P., and Rougemont, J. (2008). A rapid bootstrap algorithm for the RAxML web-servers. *Systematic Biology* **57**, 758–771. doi:10.1080/10635150802429642

Stock, J. K., and von Vaupel Klein, J. C. (1996). Mounting media revisited: the suitability of Reyne's fluid for small crustaceans. *Crustaceana* **69**, 794–798. doi:10.1163/156854096X00826

Swofford, D. L. (2002). 'PAUP*. Phylogenetic Analysis Using Parsimony (* and Other Methods). Version 4.0b10.' (Sinauer Associates: Sunderland, MA, USA.)

Watts, C. H. S., and Humphreys, W. F. (2006). Twenty-six new Dytiscidae (Coleoptera) of the genera *Limbodessus* Guignot and *Nirripirti* Watts and Humphreys from underground waters in Australia. *Transaction of the Royal Society of South Australia* **130**, 123–185.

Watts, C. H. S., and Humphreys, W. F. (2009). Fourteen new Dytiscidae (Coleoptera) of the genera *Limbodessus* Guignot, *Paroster* Sharp and *Exocelina* Broun, from underground waters in Australia. *Transactions of the Royal Society of South Australia* **133**, 62–107.

Wells, J. B. J. (2007). An annotated checklist and keys to the species of Copepoda Harpacticoida. *Zootaxa* **1568**, 1–872.

Wells, J. B. J., and Rao, G. C. (1976). The relationship of the genus *Schizopera* Sars within the family Diosaccidae (Copepoda: Harpacticoida). *Zoological Journal of the Linnean Society* **58**, 79–90. doi:10.1111/j.1096-3642.1976.tb00821.x

Weston, P. H., and Crisp, M. D. (1994). Cladistic biogeography of waratahs (Proteaceae: Embothrieae) and their allies across the Pacific. *Australian Systematic Botany* **7**, 225–249. doi:10.1071/SB9940225

Will, K. W., Mishler, B. D., and Wheeler, Q. D. (2005). The perils of DNA barcoding and the need for integrative taxonomy. *Systematic Biology* **54**, 844–851. doi:10.1080/10635150500354878

Willen, E. (2000). 'Phylogeny of the Thalestridimorpha Lang, 1944 (Crustacea, Copepoda).' (Cuvillier Verlag: Goettingen.)

Wilson, G. D. F. (2008). Gondwanan groundwater: subterranean connections of Australian phreatoicidean isopods to India and New Zealand. *Invertebrate Systematics* **22**, 301–310. doi:10.1071/IS07030

Yang, Z. (1996). Among-site rate variation and its impact on phylogenetic analyses. *Trends in Ecology & Evolution* **11**, 367–372. doi:10.1016/0169-5347(96)10041-0